Herring River Hydrodynamic Modeling

Final Comprehensive Report

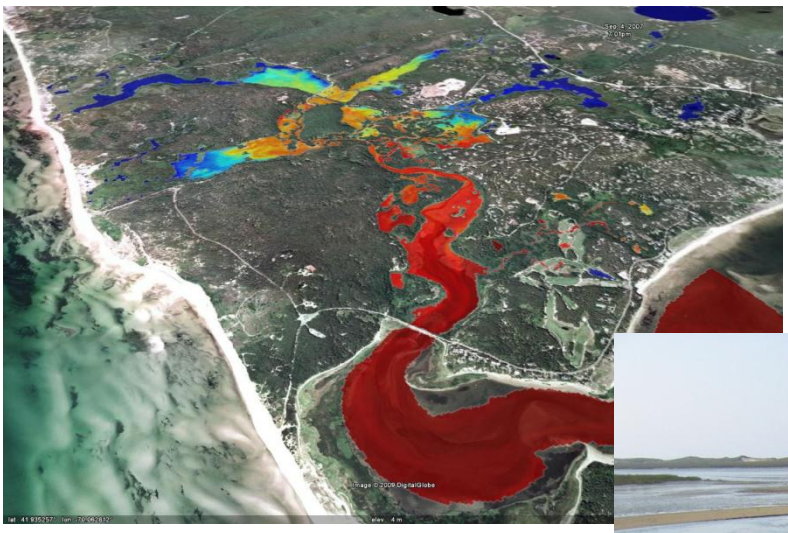

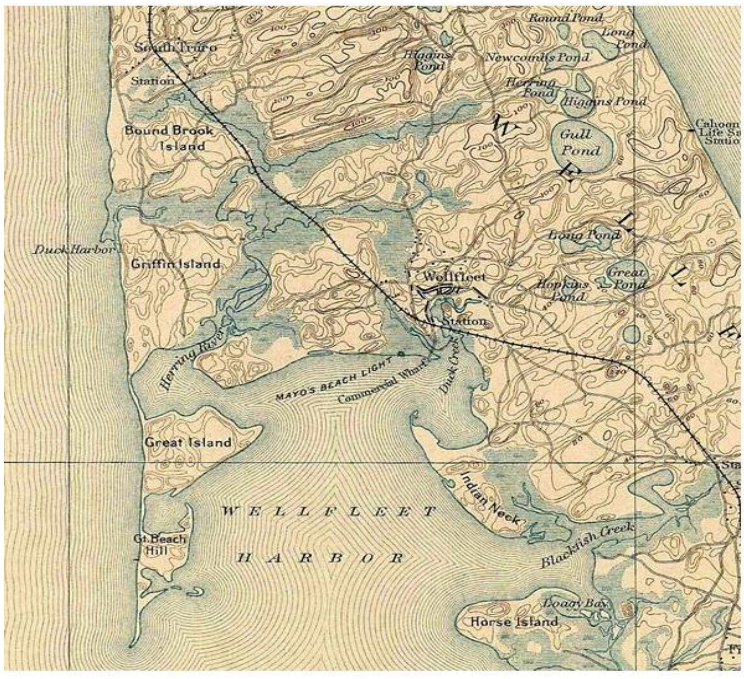

Table of Contents

List of Figures

List of Tables

EXECUTIVE SUMMARY

ES.1 - INTRODUCTION

The Herring River is a 1000+ acre estuary system located on Outer Cape Cod. A majority of the system is located in Wellfleet, Massachusetts and is physically separated from Wellfleet Harbor by a compound dike system at the Chequessett Neck Road crossing. The system is hydraulically connected to Wellfleet Harbor through the dike by three 6-foot wide box culverts, each with a flow control structure (Figure ES-1). One culvert has an adjustable sluice gate, which is currently set to be partially open two (2) feet and allows bi-directional tidal flow. The remaining two culverts have tidal flap gates, which are designed to permit flow only during an ebbing (outgoing) tide. Tidal exchange between the tidal marsh and harbor is severely restricted by the dike and culvert system. Herring River has been tidally restricted for over a century, which has resulted in significant degradation of the ecological functions and values of the marsh.

Figure ES-1. Dike structure at the Chequessett Neck Road crossing.

Prior to the dike construction in 1909, Herring River was connected to Wellfleet Harbor through a natural inlet at Chequessett Neck. The marsh system consisted of nearly 1,100 acres of thriving coastal wetlands, including a productive herring run, shellfishery, and tidal marsh habitats. The dike construction, intended to control mosquitoes and create additional developable land area, significantly degraded the natural marsh ecosystem. Today, after 100 years of influence, as well as numerous other anthropogenic impacts (e.g., upstream culverts, railroad crossings, ditch creation, etc.), hundreds of acres of intertidal tidal marsh have been degraded. This transition has eliminated habitat for estuarine flora and fauna. On-site monitoring has documented reduced tidal amplitudes, minimal salinity levels, loss of marsh vegetation, degraded fish and wildlife habitat, decomposition and subsidence of soils/sediments, and colonization by invasive species.

The Herring River Restoration Committee (HRRC), a multi-agency group appointed by the Cape Cod National Seashore and the Towns of Wellfleet and Truro, has recognized the environmental and socioeconomic benefits of restoring this tidally restricted and degraded wetland system, and is currently developing a comprehensive restoration project/plan that is geared towards identification of restoration actions and adaptive management strategies that will improve the

system through a monitored and adjustable approach. As part of the restoration effort, the HRRC requested the development of a comprehensive hydrodynamic model that could be used to assess existing conditions within the estuarine system, as well as evaluate a range of alternatives and their potential impacts. The model was required to be sufficiently flexible to integrate with the adaptive management approach, capable of simulating the complexities of the Herring River system (e.g., marsh surface wetting and drying, salinity levels, a range of flow control structures, etc.). Working with the Towns of Wellfleet and Truro, the HRRC contracted with the Woods Hole Group (WHG) to identify and develop the hydrodynamic model for the Herring River system.

The hydrodynamic modeling effort is a major component of the restoration plan that will address numerous concerns associated with re-establishing increased tidal exchange, as well as provide the necessary information to design an appropriate system of dikes, culverts, and road crossings. The purpose of this report is to provide details on the development and implementation of the hydrodynamic model for the Herring River System. It is expected that as the restoration plan continues to progress, the model could also be used to assess final design alternatives, refine the adaptive management approach, address additional physical mechanisms as needed, provide visualizations of the proposed alternatives, and provide an adaptive tool for integration of monitoring results.

ES.2 – MODEL SCOPING AND SELECTION

The overall goal of the Herring River Restoration Project is to create a productive, natural environment that will sustain itself with improved water quality and a strengthened ecosystem by restoring tidal flow to the estuary. While it would be desirable to allow the Herring River estuary to simply resume its previous natural state of unimpeded tidal flow, human and environmental constraints pose limitations on the extent to which the natural tidal flow can be restored. The success of the project will largely depend on the successful implementation of a comprehensive restoration plan, which addresses all the important issues related to those limitations. Hydrodynamic modeling is a central piece in developing this plan as it allows for the evaluation of specific questions about potential changes to surface water flow, velocities, water surface elevation, and salinity levels within the estuary.

Following an eel kill in the fall of 1980, which drew attention to the poor and declining water quality in the Herring River upstream of the dike, a significant amount of literature was generated documenting studies conducted within the area. These studies indicated the detrimental impact caused by the diking of the system and called for tidal restoration in order to revitalize the ecosystem. This led to the development of some hydrodynamic model efforts to assess the Herring River System. Overall and not surprisingly, the previous modeling efforts demonstrated that larger openings in the dike would cause increases to the mean tidal elevation and the tidal range. Increasing the opening would also increase the saltwater penetration distance. These modeling efforts provided a good initial evaluation of potential restoration options for Herring River.

The model developed by the WHG as part of this scope of work further advances the hydrodynamic understanding throughout the entire Herring River estuarine system. The model more precisely represents the geometry of the estuary (including its plan form); it considers

variable frictional effects throughout the estuary; it allows for flooding, drying, and ponding of water; it produces accurate current velocities and water surface elevations throughout the estuary; and it properly represents the physics of mixing for a wide range of forcing conditions.

The Herring River restoration project requires a model that incorporates the physics necessary to analyze water surface elevation, current velocities, salinity, sediment transport, and water quality. The model has to be dynamic, capable of handling bi-directional flow, high resolution to identify important processes, and flexible enough to link with other potential modeling tools (e.g., biological models) in an adaptive management setting. After evaluation of over 10 of the most capable hydrodynamic models in conjunction with the goals of the restoration project, the Environmental Fluid Dynamics Code (EFDC) model was selected to simulate the Herring River estuarine system. The model has been applied to studies of circulation, discharge dilution, water quality, Total Maximum Daily Load (TMDL), and sediment transport. EFDC is capable of predicting hydrodynamics and water quality in multiple dimensions and is a widely accepted Environmental Protection Agency (EPA) approved model.

ES.3 – MODEL APPROACH

The overall model approach that was applied to develop the hydrodynamic model for the Herring River system consisted of a phased approach that allowed for key stopping points to evaluate model performance and progress. This allowed for a flexible approach that included the incorporation of new data, and/or a re-direction of the effort based on the results of the current modeling phase. The primary steps in the modeling approach include:

1. Model Calibration - Model calibration is the process by which adjustments are made to the model parameters to ensure the model appropriately simulates measured water surface elevation, salinity, and other observed parameters.

2. Model Validation - Model validation is achieved by applying the calibrated model, with its fixed parameters, to one or more sets of observed data that are independent from the calibration data. Typically, sets of data for validation are collected at a different time and under conditions that differ from the calibration period.

3. Existing Conditions Simulations - Once the model has been calibrated and validated, additional simulations are conducted to provide a better understanding of the behavior of the system over a broader range of forcing conditions. These existing conditions simulations also provide a baseline for comparison to proposed restoration alternatives in order to gauge the potential benefits and/or risks associated with different restoration alternatives. Various conditions simulated include the spring/neap tidal conditions, storm scenarios, and sea level rise cases.

4. Chequessett Neck Road Dike Alternative Simulations – Several alternatives were simulated to evaluate the response of the Herring River system to modifications of the Chequessett Neck Road dike. These simulations included, but were not limited to, the removal of all anthropogenic structures (to provide an estimate of maximum restoration potential and assess historic conditions), optimization of a new dike opening width, and

various opening heights with flow control structures to provide potential adaptive management openings.

5. Upstream Feature Evaluations and Alternative Simulations - Alternative simulations focused on the culverts located in the upstream portions of the system. Specifically, this included evaluation of the crossing at High Toss Road, removal of the large flood tidal shoal existing just upstream of the dike, and assessment of the various road/culverts upstream throughout the system.

6. Mill Creek Sub-Basin Alternative Simulations - Alternative simulations were focused on evaluation of the Mill Creek sub-basin, including the potential implementation of a new dike restricting tidal exchange into this portion of the system. Evaluation of these simulations included construction of a Mill Creek Dike, optimization of a Mill Creek dike culvert (height and width), a re-graded Chequessett Yacht & Country Club (CYCC) golf course, and a preliminary assessment of potential groundwater impacts.

ES.4 – MODEL DEVELOPMENT

The development of the Herring River hydrodynamic model required configuration so the model would represent the form and function of the real system (i.e., the Herring River Estuary). Model configuration involves compiling observed data from the actual estuarine system into the format required for the execution of the model. The Herring River estuary model was developed using various data observed throughout the Herring River system. Data were provided by various agencies and were assumed to be correct and appropriate for model development of the Herring River system. Evaluation of the accuracy of the data observations was not a component of this modeling study.

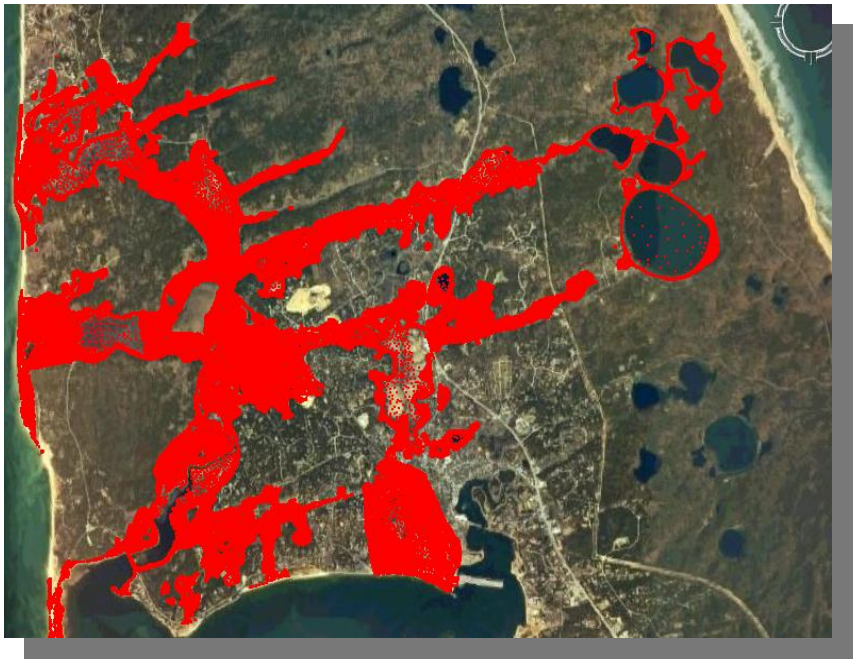

Figure ES-2. Elevation data from photogrammetric survey collected in 2007. Each red dot represents a data point.

ES.4.1 Existing Data

The data required for the development of a more robust and detailed hydrodynamic model, are of two distinct types, topographic and hydrographic. The topographic data are required to construct the model geometry, while the hydrologic data are required for model forcing and proper calibration and verification to ensure the model will provide accurate predictions. Additional data types are also required to further utilize the model to assess other

physical processes. For example, sediment information is required for sediment transport modeling, salinity observations to assess salt levels in the system, etc.

High-resolution photogrammetry data (approximately 200,000 points within the estuary above the mean low water elevation) collected in 2007 were used to accurately develop the model elevations throughout the marsh system (Figure ES-2). Bathymetric data (at elevations below the lower limit of the photogrammetry data) were used to provide depths within the creeks and streams of the Herring River estuary system, as well as for the area just downstream of the dike.

Water surface elevation data were collected by the National Park Service at various locations throughout the estuary. Data were collected in 2007 and 2010. Figure ES-3 shows the water surface elevation data collected in 2010 from locations just upstream and downstream of the dike. Salinity and temperature data were also collected at two (2) locations. Subsets of these data were used for both model calibration and verification. Other hydrologic data that was also used in model verification includes the data collected for the earlier modeling studies from 1999-2000. Water surface elevation, salinity, temperature, and other data records continue to be collected throughout the Herring River estuary system by National Park Service.

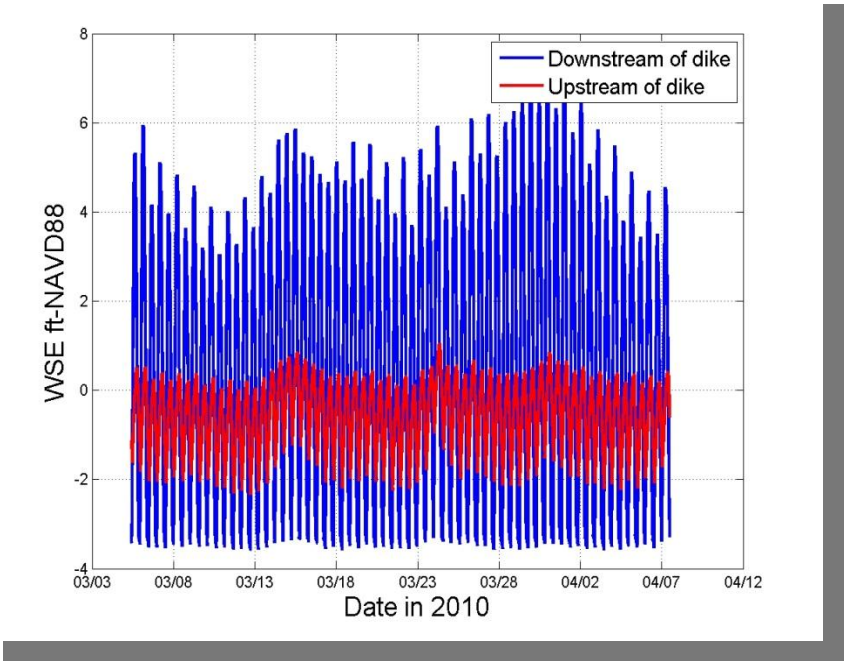

Figure ES-3. Water surface elevation data collected in 2010 from locations just upstream (red) and downstream (blue) of the dike.

Various types of sediment data were also used to analyze and model sediment mobilization and transport. These data included sediment samples and associated grain size analysis, sediment cores, synoptic measurements of total suspended solids, and continuous measurements of turbidity.

ES.4.2 Model Grid Generation

The development of a model grid defines the spatial domain on which the model performs its calculations. The model grid is a digital abstraction of the real life geometry of the Herring River system. The grid building process involves using geo-referenced digital maps or aerial photos to define the model domain, generating a grid within this domain providing the desired degree of spatial resolution, and assigning elevation values to the grid using the topographic and bathymetric data sets. The accuracy of the model is highly dependent on accurate representation

of the form of the real system expressed through the model grid. For this system, a curvilinear orthogonal grid was developed because of its increased flexibility, allowing grid boundaries to better follow natural irregular boundaries. The curvilinear orthogonal grid also allows gradual variation in horizontal resolutions, such that higher resolution areas can be defined in areas where greater detail is required. The resulting Herring River grid has over 85,000 cells with resolution of less than 10 feet in critical areas. The grid has satisfactory orthogonality and aspect ratio, as well as smooth boundary point distribution and resolution change. Figure ES-4 shows a portion of the modeling grid near the Chequessett Neck Road dike. The black boxes show the resolution of the grid, while the color scale shows the elevation of the topography in the model domain.

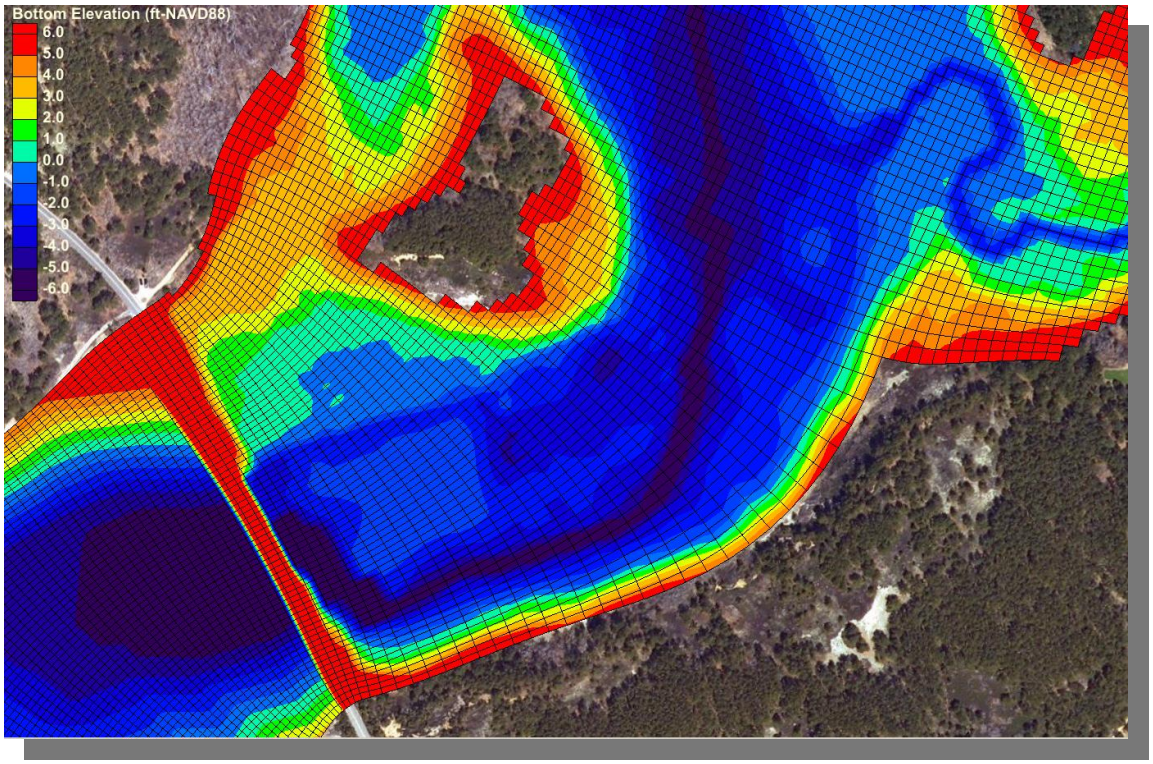

Figure ES-4. Detail of model grid showing bottom elevation contours and individual grid cells near the Chequessett Neck Road dike.

ES.4.3 Boundary Conditions and Model Parameters

In order for the Herring River model to compute a hydrodynamic solution it is necessary to specify the model variables on the domain boundaries. The Herring River model consisted of the following:

- Most of the model's boundary is considered to be a "land" boundary, which for the Herring River model was specified at an elevation of 12 feet NAVD88. This elevation provides the upper limit of expected water surface elevation during extreme storm events (100-year return period). At these land boundaries, water is constrained to flow only parallel to the boundary.

- The primary forcing for the model is provided by an open boundary at the southern end of the model domain in Wellfleet Harbor. At this location, time dependent water surface elevation and salt concentration is specified, as observed by gauge data from Wellfleet Harbor.

- Freshwater inflow volumetric flux is also specified in the model at three separate locations (Bound Brook, upper Herring River, and Pole Dike Creek) to simulate freshwater inflow into the estuary.

- Bihourly precipitation data collected at the National Atmospheric Deposition Program (NADP) station MA01 was used to provide rainfall input to the model.

- Bottom friction (or roughness length) throughout the model domain was assigned to individual cells to represent the characteristics of the flow through the system. Physically, bottom drag forces depend on a number of phenomena that are difficult to characterize. These include bottom material type, growth of biota, and the amount of channel meander, which all contribute to the overall energy loss that are accounted for by the bottom friction. Bottom friction parameters are typically used for "tuning" hydrodynamic model to reproduce the data observations. For the Herring River model, local adjustments were made to the roughness length values in order to improve the model results to match observed data. For example, observed data at the Pole Dike Creek gauge locations show the complete dampening of the tidal signal at this point in the estuary. This is likely due to the dense submerged aquatic vegetation (SAV) that exists in this creek and other vegetative influences in this relatively narrow channel. Observations conducted in 2008 indicated the creek to be almost impenetrable by canoe. Therefore, there are significant frictional and/or constriction influences in this portion of the estuarine system and a higher frictional parameter was assigned to replicate the real world conditions. All final assigned values are considered within the range of normal bottom friction values determined through empirical laboratory testing.

- Various types of flow control structures were also modeled throughout the systems. This included developing hydraulic routines embedded in the model to simulate culverts, slide (sluice) gates, and flap gates.

ES.4.4 Model Calibration and Validation

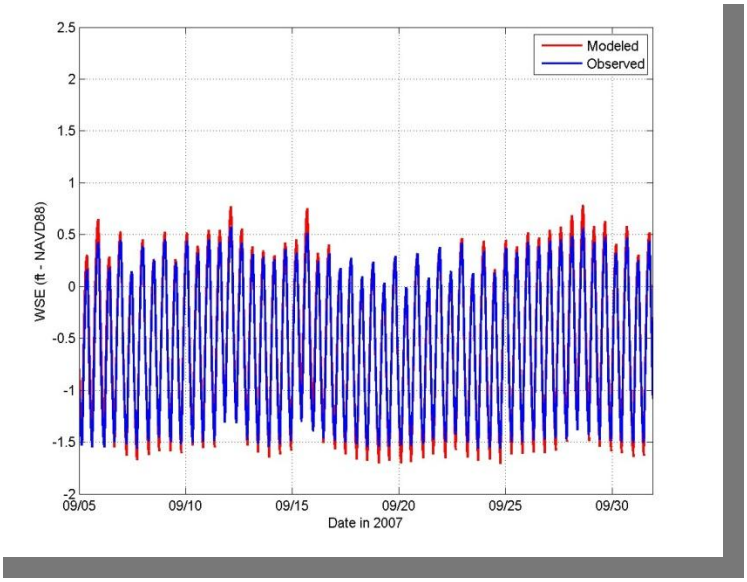

Figure ES-5. Water surface elevation data comparison for modeled (red) and measured (blue) time series just upstream of High Toss Road.

Model calibration is the process in which model parameters are systematically adjusted through a range of acceptable values and results are examined using standard measures of error. The Herring River model was calibrated to water surface elevation observations collected between September 5, 2007 and October 3, 2007 at seven locations throughout the estuary and calibrated to salinity at a station in the Lower Herring River. The model performance is evaluated by comparing time series output from the model to the observed time series at specific locations. The results are presented visually as time series plots and scatter plots, and absolute error of the model is quantified by calculating the bias and Root Mean Square Error (RMSE). For example, Figure ES-5 shows a visual comparison of the modeled (red) and measured (blue) water surface elevations at the tide station just upstream of High Toss Road for data collected in 2007. Figure ES-6 shows the associated scatter plot and calibration errors for the same location. Additionally, the five most dominant modeled and measured tidal constituents are compared using both amplitude and phase.

The magnitudes of the water surface elevation errors were well within bounds of standard calibration limits for hydrodynamic models. The model bias was less than 0.1 feet for all locations meaning that the calibration simulation reproduced average water levels that were within an inch or two of observed levels. The root mean square error was less than 0.4 feet for all locations indicating that on average the modeled water level is within a few inches of the observed level at any given time. Relative errors were approximately 1-2% at all locations.

Salt penetration in the Herring River in its current restricted state is not normally observed above High Toss Road. As such, verifying that the model could accurately simulate salinity throughout the entire system was not feasible since currently salt only penetrates into the lower portion

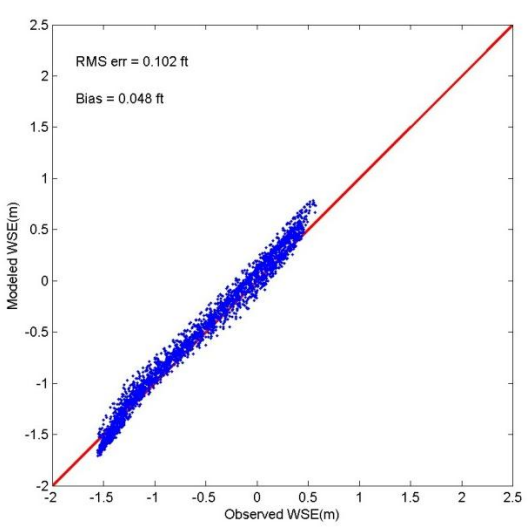

Figure ES-6. Scatter plot comparing modeled and measured water surface elevation just upstream of High Toss Road.

of the Herring River system. In the Lower Herring River where salinity data are available, the model is well calibrated with a relative error of 11%, which is well below the EPA recommended value.

Following calibration, the model was also validated to two additional data sets collected in 1999 and 2010. Validation involves applying the calibrated model to set of observed data that are independent from the calibration data set without changing the model configuration or parameterization. The water surface elevation relative errors were 1.7% and 2.8% for the 1999 and 2010 data sets, respectively.

ES.5 – EXISTING CONDITIONS

The calibrated and validated model was further applied to simulate a number of scenarios to aid in understanding the behavior of the Herring River estuary in its current restricted state. In addition to providing better understanding of the current system, these simulations also provided a baseline for comparison to alternative simulations. For example, the impact of opening the Chequessett Neck Road dike on the potential storm surge signal throughout the estuary system can be evaluated compared to existing conditions.

The existing conditions simulations consisted of normal tidal conditions, storm scenarios, and sea level rise cases. Normal tidal conditions were simulated by using the same water surface elevation data used during calibration and validation without the inclusion of temporally specific atmospheric forcing (wind, rainfall, etc.). Storm events and forecasted sea level rise (SLR) scenarios were simulated by modifying the water surface elevation boundary conditions to represent storm surge and/or long-term sea level rise increases.

The return-period tidal flood simulations demonstrate the effectiveness of the existing Chequessett Neck Dike in reducing storm surge. For example, during the 100-year flood event, the greatest increase in peak elevation is only 0.7 feet above the normal high water conditions in Lower Herring River, a 63% reduction in storm surge height between Wellfleet Harbor and High Toss Road. Sea level rise simulations were also conducted to provide an estimate of future projected water levels in the Herring River over the next half century. Three (3) projected rates of sea level rise (high, intermediate, and low) were used based on federal guidelines for incorporating sea level change considerations in civil works programs.

ES.6 – ALTERNATIVE EVALUATION AND SCREENING

A series of alternatives were simulated that were geared towards gaining a better understanding of system response to potential modifications, while determining potential adaptive management steps and restoration endpoints. The results of alternative evaluation and screening were used to assist in defining specific restoration alternatives that were further analyzed, detailed, and selected for design consideration.

First a simulation of the "natural" Herring River system through the removal of all anthropogenic features (e.g., culverts, dikes, railroad beds, etc.) was conducted. In this scenario, the system was allowed to be fully open to tidal flow and allow relatively uninhibited exchange throughout the entire estuarine system. This simulation could be considered a reasonable representation of the greatest restoration level that may be expected for a natural system (excluding natural and/or

anthropogenic changes to the bathymetry/topography) and a reasonable facsimile of the historic (a century ago) conditions of the system. Although the fully open alternative is not likely a reasonable final solution given the upland infrastructure that has been developed over the last century, this alternative does provide a reasonable estimate of the maximum restoration potential for the Herring River system and is used for comparison purposes. Figure ES-7 shows a comparison of the maximum water surface elevation for existing conditions (left panel) and for the simulation that removed all anthropogenic structures (right panel), under normal tidal conditions. Tidal water is shown in yellow in both the upper and lower panels.

Figure ES-7. Maximum water levels in the Herring River system for existing conditions (left panel) and for the no anthropogenic structures simulation (right panel).

Next, a range of potential opening widths at Chequessett Neck Road was simulated to determine the water surface elevations, tidal ranges, and salinity levels throughout the Herring River system. The results indicated that a 100 foot (30 meter) opening would optimize the water surface elevations and tidal range within the Herring River system, while a 165 foot (50 meter) opening would optimize the salinity penetration into the system.

Figure ES-8 shows water surface elevation time series results for opening sizes ranging between approximately 30 feet (10 meters) and 325 feet (100 meters), while Figure ES-9 shows the levels of Mean High Water (MHW) and Mean Low Water (MLW) in the lower Herring River sub-basin for increasing opening

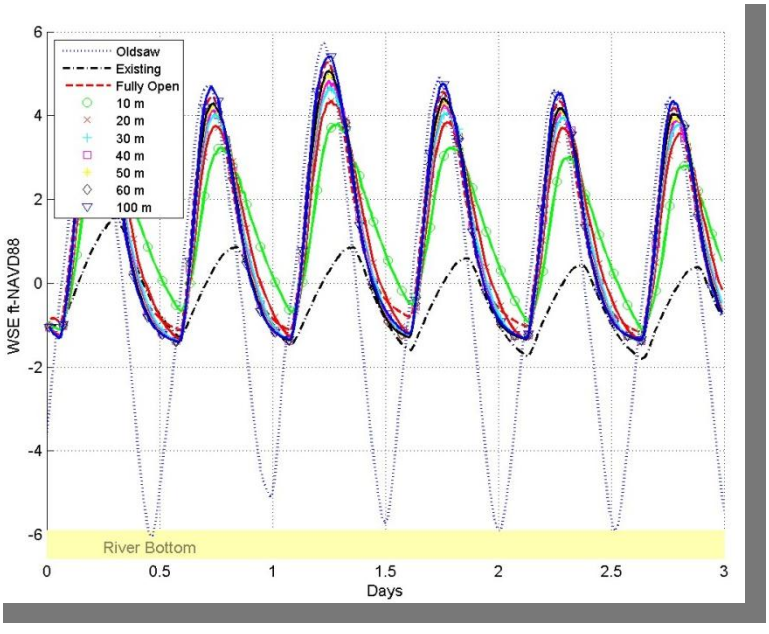

Figure ES-8. Water surface elevation (WSE) results in the lower Herring River sub-basin for a range of opening widths at Chequessett Neck Road.

widths at Chequessett Neck Road. While a 100 foot (30 meter) opening optimized the water surface elevation levels, salinity levels were optimized with a 165 foot (50 meter) opening. Figure ES-10 shows the increased salinity penetration resulting from a 165 foot (50 meter) opening (right panel) compared to a 100 foot (30 meter) opening (left panel). Although wider openings (greater than 165 feet) continued to let more tidal water and salt into the system, the changes were minimal and therefore produced diminishing restoration value. A 165 foot opening at Chequessett Neck Road was determined to be the largest width required to optimize restoration.

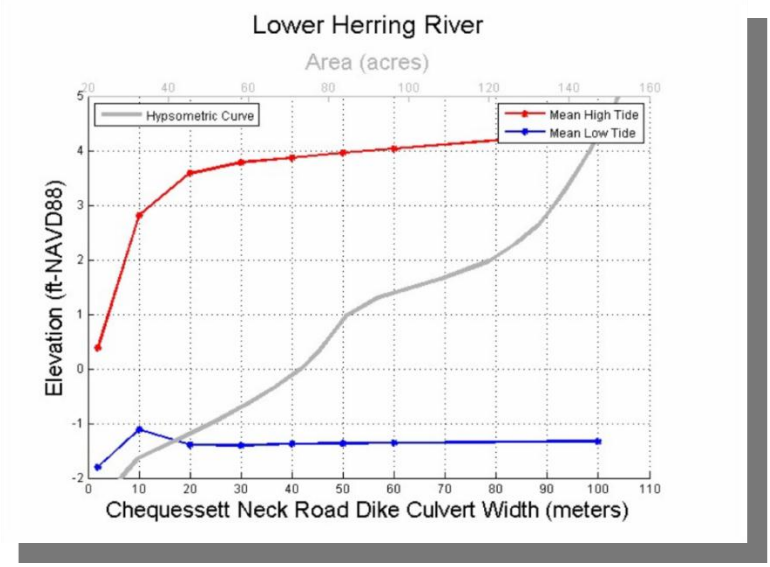

Figure ES-9. Mean High Water (red) and Mean Low Water (blue) levels in the lower Herring River sub-basin for a range of opening widths at Chequessett Neck Road.

Following the selection of the optimal Chequessett Neck Road dike opening width, simulations for various opening heights (assumed to be controlled by slide/sluice gate structures in the new dike opening) were conducted. These simulations evaluated targeted endpoints for restoration (based on limiting water surface elevations that could be accepted during storm conditions throughout the system) and provided opening sizes that could be used as initial set points in the adaptive management process. Results indicated that:

- A uniform 3' slide (sluice) gate opening across the entire 165' dike opening would limit the 100-year storm event water surface elevation to less than 6.0 feet NAVD88 throughout the system.

- A uniform 10' slide (sluice) gate opening, which is fully vertically open, limits the 100-year storm event water surface elevation to less than 7.5 feet NAVD88 throughout the system.

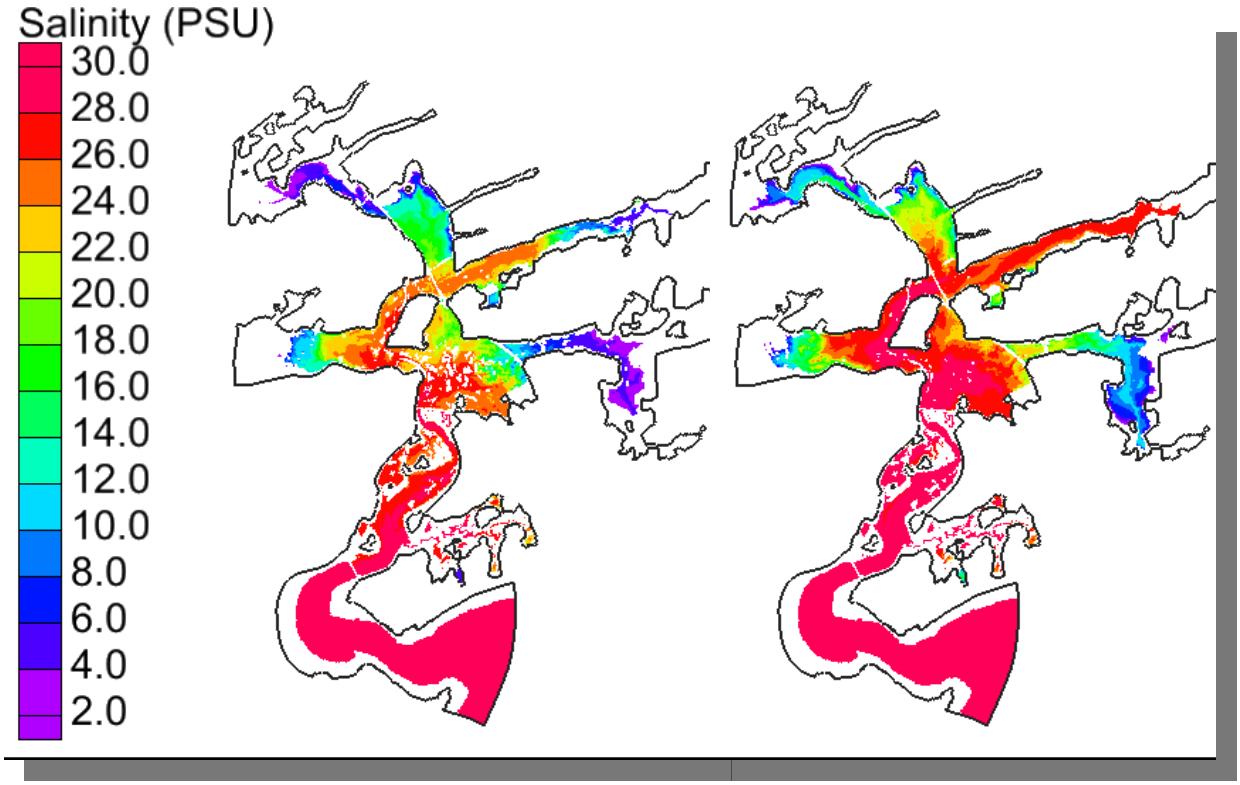

Figure ES-10. Salinity concentration throughout the Herring River system with an opening width at Chequessett Neck Road of 100 feet (30 meters) and 165 feet (50 meters). Color scale show salinity levels in practical salinity units (psu).

Based on the width and height variants simulated, recommended alternatives were selected for the new dike opening at Chequessett Neck Road that represented specific restoration endpoints. These restoration endpoints were intended to be eventually achieved through an adaptive management approach that would allow for controlled advancement towards the endpoints. Specifically, the following three alternatives were defined for the Chequessett Neck Road dike:

1. A new Chequessett Neck Road dike with a 165' wide opening and a future targeted maximum 100-year storm water surface elevation of 6.0 feet NAVD88 in the Lower Herring River (achieved with an approximate 3' slide [sluice] gate opening). Golf course re-grading and other flood proofing would be required in the Mill Creek sub-basin for this alternative. Several segments of low-lying roads would also require elevation increases and re-grading. Restoration would be significant through most of the system, but would not be maximized since the lower infrastructure elevations in the Mill Creek sub-basin would limit the maximum water surface elevation allowed in the system as a whole.

2. A new Chequessett Neck Road dike with a 165' wide opening and a future targeted maximum 100-year storm water surface elevation of 7.5 feet NAVD88 in the Lower Herring River (achieved with an approximate 10' slide [sluice] gate opening) with a new dike at Mill Creek to ***eliminate*** tidal exchange. A new proposed dike at the entrance to

Mill Creek with a one-way flap gate flow control structure would be installed to eliminate the tidal exchange into Mill Creek. This would allow freshwater flow out of the Mill Creek basin, but would not allow tidal water into the Mill Creek basin. As such, this alternative would maximize restoration throughout the Herring River system, but the Mill Creek sub-basin would remain a non-tidal system. No re-grading or flood proofing in the Mill Creek sub-basin would be proposed, but flood mitigation would be required in other sub-basins, including elevating and re-grading low lying roads.

3. A new Chequessett Neck Road dike with a 165' wide opening and a future targeted maximum 100-year storm water surface elevation of 7.5 feet NAVD88 in the Lower Herring River (achieved with an approximate 10' slide [sluice] gate opening) with a new dike at Mill Creek to ***limit*** tidal exchange. This alternative would maximize restoration throughout the entire system; however, the new dike at the entrance to Mill Creek with appropriate flow control structure(s) would limit the tidal exchange into Mill Creek. This new Mill Creek dike would produce similar water levels as the 3' slide/sluice gate opening alternative within the Mill Creek sub-basin. Flood proofing and mitigation would be needed in select locations within the Herring River flood plain.

Since the Mill Creek sub-basin was a critical element of each of these defined alternatives, these three (3) final alternatives were further detailed through detailed assessment of the Mill Creek sub-basin. Therefore, simulation of potential tidal control at the entrance to the Mill Creek sub-basin, which followed a similar approach to the modeling and assessment of an opening at the Chequessett Neck Road dike, were conducted. This includes (1) optimization of an opening width at a new Mill Creek dike; (2) potential opening heights of a flow control structure to allow limited water into Mill Creek sub-basin; (3) simulations of a re-graded golf course region; (4) evaluation of the Mill Creek sub-basin completely blocked from tidal exchange and the effect on freshwater outflow, and (5) a preliminary assessment of potential groundwater impacts in the Mill Creek sub-basin relative to both sea level rise and the restoration effort. These results indicated that:

- A 25 foot opening in a new dike at the entrance to Mill Creek would optimize restoration in the Mill Creek sub-basin with the optimized opening at the Chequessett Neck Road dike.

- Alternatives that could be considered for managing water levels within Mill Creek include a maximum 3 foot sluice opening at Chequessett Neck Road with no dike at Mill Creek, or a dike at Mill Creek that would allow for managed water levels when the sluice opening at the Chequessett Neck Road dike is increased to opening sizes greater than 3 feet. The Mill Creek sluice/slide gate could also be closed completely and only allow flow out of the system.

- A re-graded golf course would remove some flood storage capacity from the Mill Creek sub-basin. For example, under the alternative with a 10 foot sluice opening at Chequessett Neck Road and a 3 foot sluice opening at Mill Creek, a peak water surface elevation of approximately 6.4 feet would occur during a 100-year storm surge event in the re-graded Mill Creek sub-basin, while a peak water surface elevation of 6.0 feet

would occur with the existing topography. Therefore, for a re-graded golf course area, an adaptive management approach would need to be implemented that would be able to adequately anticipate and manage water surface elevations in the Mill Creek sub-basin.

- Simulations of freshwater storm events (heavy rainfall) in the Mill Creek sub-basin indicated that proposed alternatives would decrease the ability of the additional water to drain from the system, but would not increase the water surface elevation level above the normal mean high water level within Mill Creek. For the alternative that would completely eliminate tides from the Mill Creek sub-basin, the water surface elevation would not exceed 2 feet NAVD88 during any of the storm cases considered.

- Using the results of a preliminary evaluation, the impacts of sea level rise on the groundwater levels in the Mill Creek sub-basin indicate that under all three sea level rise scenarios (low, intermediate, high), the greatest increase in water table elevation would be 1.12 feet in 50 years in areas closest to Wellfleet Harbor. In general, a larger increase in water table elevation is expected at locations closer to Wellfleet Harbor, while a smaller increase is expected at locations near Mill Creek.

Additional findings and recommendations, corresponding to the overall restoration effort, include:

- Lowering the culvert inverts at the Chequessett Neck Road dike does allow a greater volume of flow (slightly higher tides); however, without a significant adjustment to the local bathymetry upstream and downstream of the dike, the low water level does not decrease. It may be feasible that a lower culvert invert, combined with the increased volumetric flow, would cause scour and an eventual lowering of the river bed and thereby a more significant change to the mean low water elevation. However, this lowering would have to occur over a significant distance both upstream and downstream of the dike and it is more likely that the actual scour would occur in a localized area at the dike only.

- Assessment of High Toss Road indicates that under restored conditions (Chequessett Neck Road dike openings of 65 feet or greater), the roadway will be overtopped. As such, the road would require mitigation to remain useable, or be abandoned. The existing High Toss Road and culvert also negatively impact restoration potential in the upper portions of the Herring River estuary. Specifically, the restrictive culvert and causeway impede the draining of the upper system during an ebbing tide, resulting in a reduced tidal range, excessive ponding, and higher MLW. The removal of the High Toss Road culvert and creation of an open channel at this location is recommended.

- As the restoration process advances, several upstream culverts, specifically the culverts at Pole Dike Road and Old County Road, may need to be replaced with larger culverts. However, since the effect on water surface elevation is relatively small, especially in the early stages of the restoration, these culverts do not need to be replaced during the initial restoration effort. Monitoring of water surface elevations and salinities during the

adaptive management process should be conducted to determine the potential influence of these anthropogenic structures.

ES.7 – FINAL ALTERNATIVE ASSESSMENT AND MODEL OUTPUT

Modeling results of the recommended alternatives were summarized to analyze potential changes to the Herring River system and to provide more easily digestible modeling output. The detailed results of the hydrodynamic model were also used to complete a preliminary sediment transport assessment. This assessment does not determine actual sediment movement but rather areas where there is potential for erosion or deposition. However, the analysis does provide reasonable results that can be utilized to help guide the adaptive management restoration approach.

ES.7.1 Tidal Benchmarks and Salinity

Water surface elevations and salinity throughout the Herring River system were evaluated using the results of the hydrodynamic model. Water surface elevation results from the alternative simulations were presented in three specific ways:

1. Tables that present relevant tidal benchmarks (Mean Low Water, Mean High Water, Mean High Water Spring, Annual High Water), the 100- year storm water level, and potential future sea level rise scenarios for restoration endpoint alternatives. These water surface elevation values were provided for each sub-basin.

2. Graphical aerial overviews and geo-rectified bounds of the water surface elevation level for each specific tidal benchmark. An example showing mean high water spring (MHWS) for existing conditions and for a 165 foot wide and 3 foot high opening at Chequessett Neck Road is presented in Figure ES-11. Graphical aerial overviews of salinity penetration are also provided.

3. Interactive Google© Earth files that provide both the tabular and spatial data files for each of the simulated water levels.

Results are provided within each sub-basin and include data for existing conditions, fully open, and a range of sluice/slide gate openings associated with the proposed opening sizes both at Chequessett Neck Road and Mill Creek. Water surface elevation results show the limited tidal range under existing conditions, as a vast majority of the system is non-tidal, and the overall intertidal area is minimal, even jsust upstream of the dike. From a salinity perspective, under existing conditions, the salt water does not propagate beyond High Toss Road, while for the proposed 3 foot sluice opening and greater, salt water advances into a significant portion of the upper sub-basins. Modeling results for all the various adaptive management cases can be used to determine changes to intertidal areas, expected high water locations, and assess potential marsh vegetation areas.

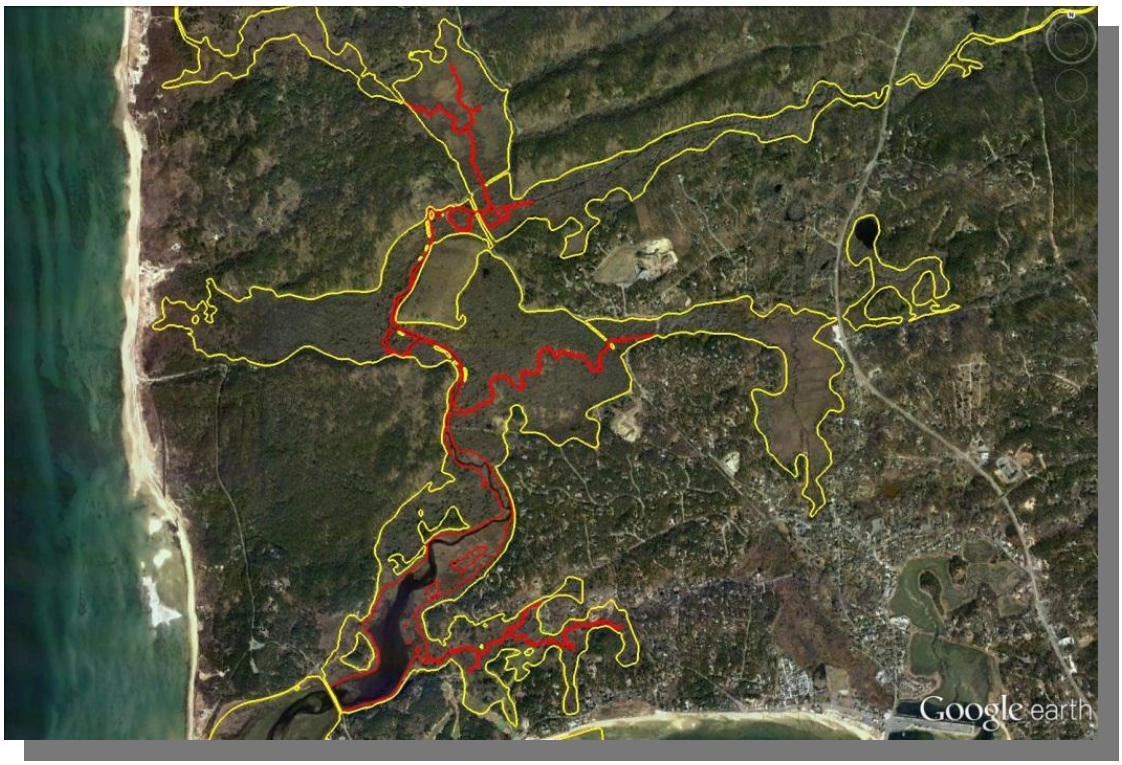

Figure ES-11. Mean High Water Spring for existing conditions (red) and 165 foot wide, 3 foot high opening at Chequessett Neck Road (yellow).

ES.7.2 Tidal Flushing

The proposed opening at Chequessett Neck Road would result in substantially improved flushing within the system. The improved opening size is particularly effective at flushing the extents of the system beyond High Toss Road. Under existing conditions, the sub-basins of the system do not exchange water efficiently with Wellfleet Harbor. For example, the Herring River System above High Toss Road takes approximately 200 days to fully flush with Wellfleet Harbor under existing conditions, while under the alternative opening scenarios the flushing time is reduced to 6-8 days.

ES.7.3 Sensitive Receptors

Sensitive receptors include specific low-lying infrastructure (e.g., roadways, etc.), as well as other critical locations (e.g., golf course areas), that may potentially be influenced by the restoration and changes to the water surface elevations. Model results were evaluated to determine the water surface elevation at critical locations. Water surface elevation results from the alternative simulations were presented at the sensitive receptor locations as:

1. Tables that present relevant tidal benchmarks (Mean Low Water, Mean High Water, Mean High Water Spring, Annual High Water), the 100- year storm water level, and potential future sea level rise scenarios for restoration endpoint alternatives. These water surface elevation values are provided for each sensitive receptor (e.g., roadway).

2. Interactive Google© Earth files that provide the tabular results at each sensitive receptor location.

ES.7.4 Marsh Receptors

Similar to the sensitive receptors, water surface elevations and salinity values were evaluated at specific locations throughout the marsh plain. Additional metrics, hydroperiod, percent of tides wetting, and a classification values were also determined at each marsh receptor location. These locations can be used to assess the relative changes, and potential ecological changes that may occur throughout the Herring River system. The model results for the marsh receptor locations are presented as:

1. Tables that present relevant tidal benchmarks (Mean High Water and Mean High Water Spring) critical for marsh vegetation delineation, mean and maximum salinity levels, hydroperiod (the length of time [in hours] a point stays wet once it has gotten wet), and percent wetting (the percentage of high tides that wet that point). The tables also provide classification values.

2. Interactive Google© Earth files that provide the tabular results at each marsh receptor location.

ES.7.5 Ponding

Simulations of the adaptive management steps and restoration endpoints revealed there were certain areas within the system that were prone to ponding of water with the introduction of the increased tidal exchange. These areas are generally due to subsidence that has occurred over the century of marsh degradation, or caused due to poor drainage pathways. Although these potential ponding areas appear in the hydrodynamic model for restoration endpoint simulations (3 foot and 10 foot height openings), this does not indicated that these will occur during the restoration process. The hydrodynamic model is using the existing bathymetry to simulate future restoration endpoints. However, due to the adaptive management approach that is intended to be applied to the system (smaller incremental openings over time); it is likely that this topography will change as the system responds to increased tidal exchange. For example, it is expected that additional sediment will be transported into the system and be deposited in the lower velocity zones of the subsided areas. Additionally, existing channels leading to limited drainage areas will be naturally widened and deepened due to the increased tidal flux during the restoration process. Therefore, widespread ponding during the restoration effort is not expected as long as monitoring is conducted and the appropriate adaptive management actions are applied.

ES.7.6 Sediment Mobilization and Transport

In order to assess the potential impact of the proposed dike openings, a preliminary sediment transport assessment was conducted using the results of the hydrodynamic model. The analytical sediment transport model employed was based on the established concept that sediments begin to move when sufficient stress is applied to the grains on the estuary seabed. The sediment transport potential was determined for normal tidal conditions and for a 100 year extreme storm surge event. Each scenario was simulated for existing conditions, and for the restoration alternative with a 165 feet wide span at Chequessett Neck Road with sluice openings of 3 feet.

- Under existing conditions with normal tides, increased tidal asymmetry imposed by Chequessett Neck Road dike reduces the total volume of water and suspended sediment that can physically be transported into the lower Herring River. Any suspended sediment that does pass through the sluice gate quickly settles out because flood tide currents in the lower Herring River are severely reduced by the dike (this is supported by existence of the flood tidal shoal in that is present in the existing system). The dike also causes a significant reduction in the flood tide current velocity in the area downstream of the dike. This reduction in current velocity likely deposits a portion of suspended sediment in the upper region of the area downstream of the dike during slack flood tide.

- When compared to existing conditions, the 3 foot opening shows similar pathways for sediment transport in the areas downstream of the dike. Generally, bed load is expected to move slightly seaward or remain in the same location, while a majority of the suspended sediment would ultimately be transported farther upstream into the estuary. For the 3 foot opening, this general process is expected to increase, with potential bed load transport extending from the lower Herring River to the area downstream of the dike, while an increased suspended load would be transported upstream of Chequessett Neck Road during flood tides. Over time, these processes would likely lead to a coarsening of the sediment, particularly in the area downstream of the Chequessett Neck Road dike. With the new dike opening, potential sediment transport in the lower Herring River during both the flood and ebb tides would begin to occur. Initially, this is likely to lead to some transport of fine-grained material out of the lower Herring River. This fine-grained material would not easily settle and would be transported into Cape Cod Bay and possibly dispersed within Wellfleet Harbor. In addition, a significant portion of this material would be transported into the subsided, upper portions of the estuary due to asymmetry in the tidal current and trapping by vegetation. The upper Herring River would remain primarily a depositional environment with the exception of the area near High Toss Road. Considering the greater volume of sediment that is able to enter the upper Herring River, it is likely that 3 foot opening will lead to significant deposition of suspended sediment and fines in the upper estuary, specifically in lower lying areas that have historically subsided.

- During the 100-year storm under existing conditions, there is a large area of potential transport just downstream of the dike and sediment would be mobilized and transported upstream towards and potentially beyond Chequessett Neck Road (if the material can make it past the existing dike). Overall, the storm surge is not expected to cause significant mobilization of sediment in the lower or upper Herring River, although more suspended sediment mobilized from downstream of the dike would be carried above Chequessett Neck Road than during normal tidal conditions. The model results show a larger area of potential mobilization during the rising surge suggesting a net upstream transport of bed load and coarser suspended sediment. Fines entrained during the surge would likely make their way out of the system and ultimately become dispersed in Cape Cod Bay.

- Qualitatively, sediment transport pathways in the area downstream of the dike are similar for both existing conditions and the restoration alternatives. However, because the

Chequessett Neck Road dike severely restricts flow in the upstream reaches under existing conditions, a significantly smaller volume of water enters the estuary during the 100-year storm surge when comparing current conditions to proposed conditions. For existing conditions, there is practically no sediment mobilization above Chequessett Neck Road even during the 100-year storm surge. However, there will be a moderate increase of suspended sediment entering the lower Herring River and being deposited during a storm event when compared to normal tidal conditions. For the 3 foot opening, storm surge simulations indicate a significant mobilization of sediment in both the lower Herring River, as well as in the lower portion of the upper Herring River near High Toss Road. Significantly greater mobilization and erosion exists at the area near High Toss Road as the storm surge floods into the upper estuary and transports sediment upstream into depositional areas (primarily subsided regions). Downstream of High Toss Road, it is likely that bed load will be moved in both directions resulting in little net movement. Some sediment suspended during the flooding storm tide will likely deposit in areas of the estuary that are not typically flooded during normal conditions. As the surge recedes fines that are not deposited in the upper estuary will proceed toward the dike. Some of this sediment may make it into Wellfleet Harbor and become dispersed before the following tide brings it back into the estuary or it is carried into Cape Cod Bay.

Sediment transport processes are expected to change when the Herring River system is restored. Since the restoration project will use an adaptive management approach, it is expected that the changes to the sediment transport regime will occur over smaller incremental steps (via incremental opening of the sluice gates). As such, the sediment transport changes and amount of sediment transported will be less than is indicated in the modeling, which represents a significant opening size immediately after construction of a new dike.

Significant and valuable shellfish aquaculture exist in Wellfleet Harbor and there are concerns that the proposed restoration may result in smothering of these resources areas with sediment discharged from the Herring River system due to the increased tidal exchange. It is expected that when the system is initially opened, some fine-grain material would be likely transported downstream into the Wellfleet Harbor area. Over the long-term however, sediment would be transported upstream into the Herring River system. Figure ES-12 shows an illustration of the net upstream sediment transport process by tracking a suspended sediment particle through a complete tidal cycle. The suspended particle was initially mobilized in the High Toss Road region. The color of each dot represents the age of the suspended particle, progressing from blue (start of tracking) to red (end of tracking and a complete tidal cycle). The suspended particle is transported downstream during the ebb tide, but then returns upstream during the flood tide and settles in a position further upstream than where it originally started. If mobilized on the subsequent tide, it would be transported further upstream over the next full tidal cycle until it deposits in a depositional area and can no longer be easily mobilized.

In addition, the amount of sediment deposited in the Wellfleet Harbor area is not expected to be significant. The adaptive management approach will limit the total amount of material mobilized and a significant portion of the fine grained material will stay in suspension to areas seaward of Wellfleet Harbor. Additionally, the total volume of sediment mobilized from within the Herring River system is small compared to the area of Wellfleet Harbor. For example, if it is assumed that (1) all sluices are immediately opened to 3 feet (e.g., no adaptive management), (2) all sediment mobilized is transported downstream and deposited in Wellfleet Harbor, and (3) the depth of erosion for all mobilized areas is 1 foot, then the total thickness of sediment deposited in Wellfleet Harbor would be less than 1 cm (approximately 0.76 cm). As such, even using conservative assumptions, the potential sediment deposition thickness is minimal.

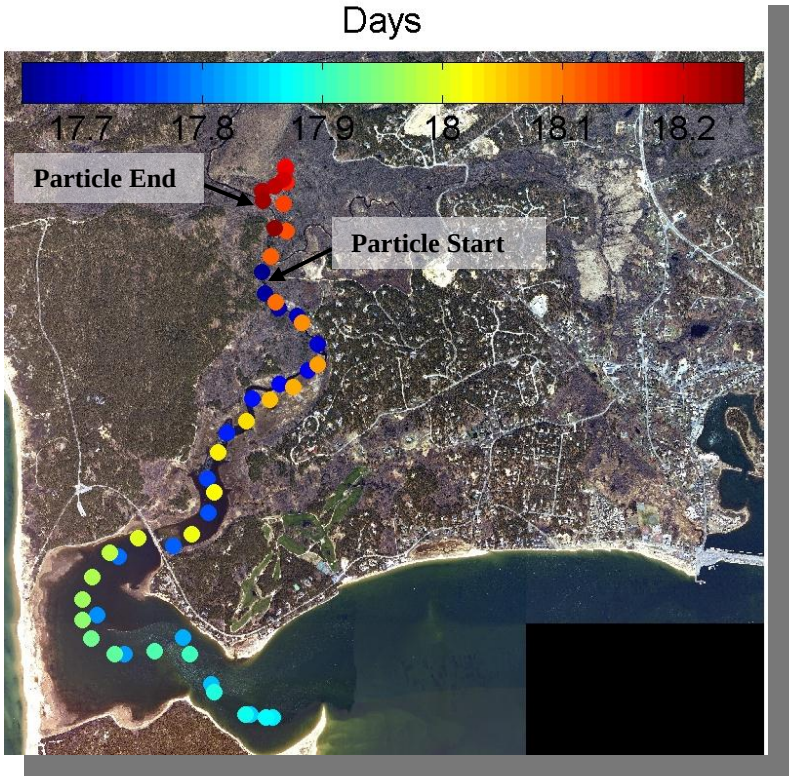

Figure ES-12. Suspended sediment particle tracking through a complete tidal cycle.

1.0 INTRODUCTION

The Herring River is the largest tidal river and estuary complex on Outer Cape Cod (Figure 1-1). It is a complex estuarine system that is forced by sea level fluctuations through a primary inlet connecting Herring River to Wellfleet Harbor. The inlet consists of a compound dike system at the Chequessett Neck Road crossing (Figure 1-2). The existing dike system consists of three 6-foot wide box culverts, each with an attached flow control structure. One culvert has an adjustable sluice gate, which is currently set to be partially open at 2 feet and allows bi-directional tidal flow. The remaining two culverts have tidal flap gates, which are designed to permit flow only during an ebbing (outgoing) tide. Therefore, limited seawater is allowed into the Herring River system. Subsequent constrictions (typically circular culverts) exist at upstream crossings (e.g., High Toss Road, Pole Dike Road, Pamet Point Road, Route 6, etc.) throughout the system. The system is further complicated by the extensive existing and potential marsh plains, tributaries, significant area, surrounding infrastructure, and varying and multiple natural and anthropogenic constrictions that make up the Herring River system. The natural marsh system, which has been restricted for a century, is now severely degraded, has subsided in certain areas, and offers little ecological benefit.

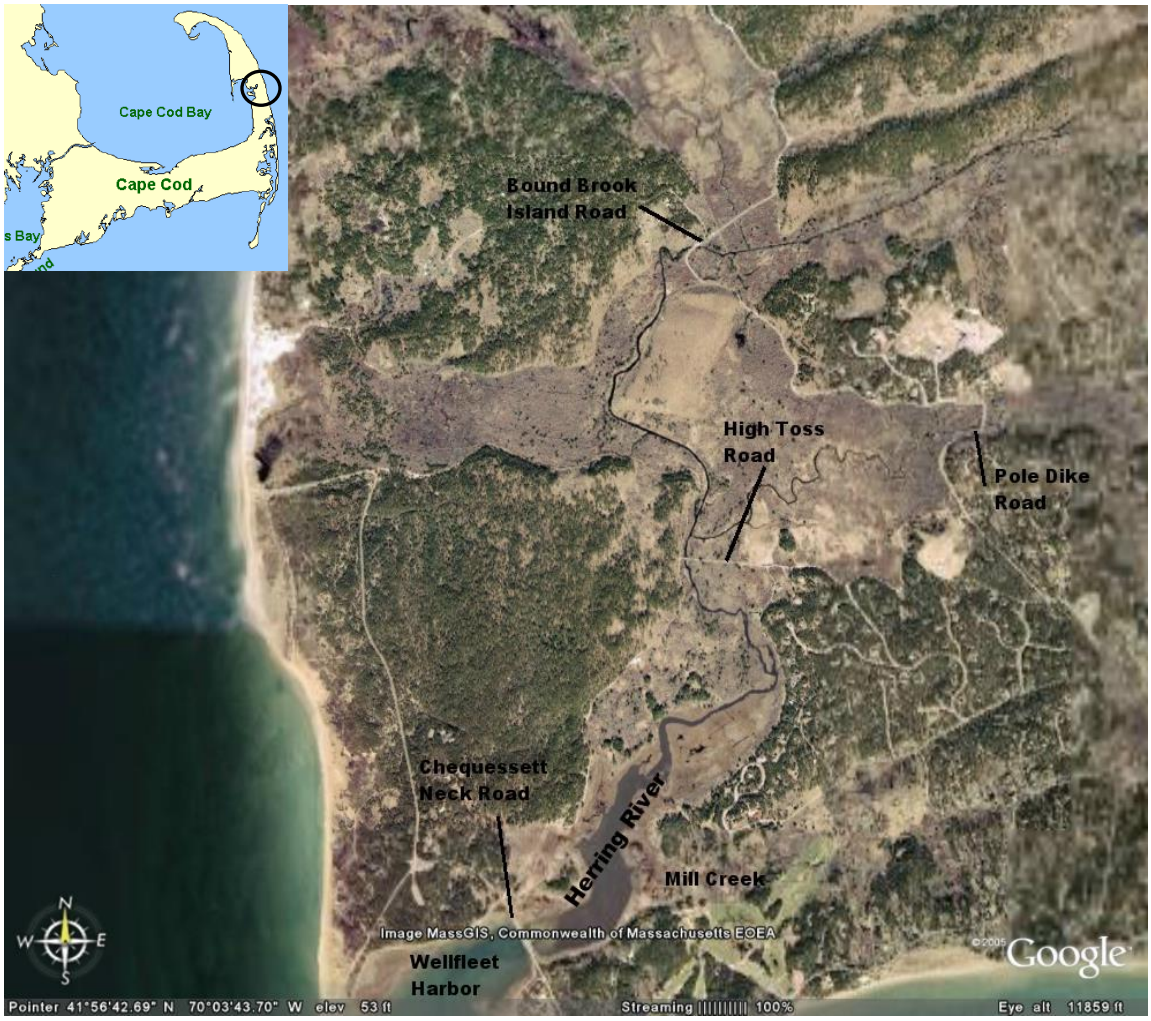

Figure 1-1. Herring River system (background image courtesy of Google Earth).

Figure 1-2. Dike structure at the Chequessett Neck Road crossing.

Prior to the dike construction in 1909, Herring River was connected to Wellfleet Harbor through a natural inlet at Chequessett Neck. The marsh system consisted of nearly 1,100 acres of thriving coastal wetlands, including a productive herring run, shellfishery, and tidal marsh habitats. The dike construction, intended to control mosquitoes and create additional developable land area, significantly degraded the natural marsh ecosystem. Today, after 100 years of tidal restriction, as well as numerous other anthropogenic impacts (e.g., upstream culverts, railroad crossings, ditch creation, etc.), hundreds of acres of intertidal tidal marsh have been degraded and are now dominated by freshwater and brackish wetland vegetation, non-native invasive plants, and, in some areas, opportunistic upland tree and shrub species that have colonized desiccated marsh areas. This transition has eliminated habitat for estuarine flora and fauna. The Herring River Restoration Committee (HRRC), a multi-agency group appointed by the Cape Cod National Seashore and the Towns of Wellfleet and Truro, (2008) indicates that:

> *"…non-native salt-intolerant grasses and woody vegetation have increased, even in the river channel, restricting boating and anadromous fish habitat. Surface waters have been acidified by wetland drainage and the oxidation of sulfur in the diked tidal marsh peat; high acidity leaches toxic metals from native clays to surface water; and in the summer, dissolved oxygen depletions are common due to reduced tidal flushing. All of this has caused fish kills in the river, while high acidity and periods of low oxygen have restricted fish access to mosquito breeding sites; thus, nuisance mosquitoes can still be abundant."*

The HRRC has recognized the environmental and socioeconomic benefits of restoring this tidally restricted and degraded wetland system, and is currently developing a comprehensive restoration

project/plan that is geared towards identification of restoration actions and adaptive management strategies that will improve the system through a monitored and adjustable approach.

As part of the restoration effort, the Town-appointed Herring River Technical Committee (HRTC), a predecessor of the HRRC, requested the development of a comprehensive hydrodynamic model that could be used to assess existing conditions within the estuarine system, as well as evaluate a range of alternatives and their potential impacts. The model was required to be sufficiently flexible to integrate with the adaptive management approach, capable of simulating the complexities of the Herring River system (e.g., marsh surface wetting and drying, salinity levels, a range of flow control structures, etc.), and be extendable to include potential additional technical items (e.g., sediment transport, water quality, etc.). Woods Hole Group, working with the Town of Wellfleet, Town of Truro and the HRRC, was contracted to identify and develop the hydrodynamic model for the Herring River system.

As discussed, the Herring River estuary system represents a significant floodplain (the largest estuary on outer Cape Cod), and through proper plan development has the potential to restore over 1,000 acres of estuarine wetland area. The hydrodynamic modeling effort is a major component of the restoration plan that addresses numerous concerns associated with re-establishing increased tidal exchange, as well as providing necessary information to design an appropriate system of dikes, culverts, and road crossings. Achieving these goals required the development of a high-quality, high-resolution hydrodynamic model that provided, to a reasonable extent, the technical information needed to evaluate potential restoration alternatives for Herring River. The modeling development and execution follows a phased-approach, centered on key stopping points that allow for progress assessment and refocusing based on lessons learned from each prior task or model simulation. Since the model was developed to be flexible, this allows for future inclusion of additional processes (e.g., water quality, etc.), adaptable alternative analysis, capacity to provide conceptual designs for the restoration plan, and incorporation of monitoring results to refine the model as the restoration progresses.

The purpose of this report is to provide details on the development and implementation of the hydrodynamic model for the Herring River System. It is expected that as the restoration plan continues to progress, the model could also be used to assess final design alternatives, refine the adaptive management approach, address additional physical mechanisms (e.g., water quality) as needed, provide visualizations of the proposed alternatives and their potential impacts, and provide an adaptive tool for integration of monitoring results. Therefore, the model presented herein may continue to be developed and refined in subsequent phases of the restoration project. This report summarizes the hydrodynamic model building process. Specifically, the report is divided into the following primary Chapters:

- Chapter 2.0 presents the model scoping portion of the modeling program. This includes the goals and objectives of the modeling program, and the relationship to the overall restoration project goals and objectives. This Chapter also presents a summary of all pertinent topographic, hydrographic, and hydrologic data that has been collected to date, including a brief summary of the existing literature related to Herring River. There are also numerous on-going data collection efforts (e.g., water quality, water level, marsh plain elevation data, sediment cores) being performed by various agencies (e.g., National Park Service) that can be used to continue to supplement the overall modeling effort.

This Chapter also presents some additional data collection efforts that may further support the modeling program as the model is potential refined during the adaptive management and restoration process.

- Chapter 3.0 presents the requirements of the model, based on the goals and objectives of the model program, and potential models that may be used to simulate the complex processes of the Herring River estuary. This Chapter also includes a "model matrix" that details a number of potential modeling candidates, with short descriptions of the limitations and capabilities. More detailed descriptions of the most suitable programs, addressing their particular abilities for simulating the unique combination of physical processes that occur within the Herring River Estuary, is also presented. Finally, Chapter 3.0 provides the final model selection, decided jointly by the HRTC and Woods Hole Group, as the most suitable modeling program or package for simulation of the complex physical processes of this estuarine system, with a key functionality that the model could be implemented as an adaptive management tool during the restoration process.

- Chapter 4.0 presents the proposed model approach, identifying the major tasks within the modeling scope and identifies key discussion points for evaluation of the modeling performance and progress. This allows for a flexible approach that can include the incorporation of new data, and/or a re-direction of the effort based on the results of the current modeling phase. The model approach also allows for model application into the future adaptive management stages of the restoration project.

- Chapter 5.0 presents the development of the hydrodynamic and salinity model of the Herring River system. The purpose of the model is to aid in planning for tidal restoration of the estuary by predicting time dependent water levels, velocities, and salinity levels for various restoration alternatives. This Chapter of the report describes how the model was calibrated and validated to existing conditions within the system, and then presents the use of the calibrated model to evaluate some various natural scenarios. As such, the report presents the results of a number of simulations with the estuary in its existing restricted state to aid in understanding of the current behavior of the system and to provide a baseline for comparison with future alternative simulations. These existing conditions simulations include: simulation of normal tidal conditions, simulation of 1 and 100 year return period tidal floods, and simulation of 50 years of sea level rise.

- Chapter 6.0 presents alternative simulations for evaluating changes within the system and evaluating the response of the system. The purpose of the various modeling alternatives, which are numerous, was to identify specific alternatives that would be considered restoration goals (endpoints) in the adaptive management process and would eventually be defined as alternatives considered in the Environmental Impact Statement. These include:

    - Simulation of the Herring River system with the removal of all anthropogenic features (culverts, railroad crossings) that represents potential maximum restoration levels and possible historical conditions of the system before the dike. This simulation is limited by use of existing topography and bathymetry to

represent the Herring River system as there is no reasonable way to know the historical topography of the system from over 100 years ago.

- Simulations for optimization of the dike opening width (ranging from a 30 foot opening to a 330 foot opening).

- After determination of the optimal dike opening width, simulations for various opening sizes (heights) that (1) evaluated target endpoints for restoration (based on limiting water surface elevations that could be accepted during storm conditions throughout the system) and (2) provided opening sizes that could be used as initial set points in the adaptive management process.

- Simulations of potential modification to the dike culvert inverts.

- Simulations assessing the potential removal of the flood tidal shoal.

- Simulations of potential modification to the opening at the High Toss Road crossing, including open channel and culvert options.

- Evaluations of the culverts in the upper portions of the system.

- Simulation of potential tidal control at the entrance to the Mill Creek sub-basin, which followed a similar approach to the modeling and assessment of an opening at the Chequessett Neck Road dike. This includes (1) optimization of an opening width at a new Mill Creek dike; (2) potential opening heights of a flow control structure to allow limited water into Mill Creek sub-basin; (3) simulations of a re-graded CYCC golf course; (4) evaluation of the Mill Creek sub-basin completely blocked from tidal exchange and the effect on freshwater outflow, and (5) a preliminary assessment of potential groundwater impacts in the Mill Creek sub-basin relative to both sea level rise and the restoration effort.

- Possible changes to the hydrodynamics of the system caused by expected vegetation changes.

- A summary of the alternatives and the restoration endpoints.

- Chapter 7.0 presents a summary of the expected changes to the physical processes within Herring River for the endpoint alternatives. Specifically, this includes evaluation of:

  - Water surface elevations and tidal benchmarks throughout the system

  - Tidal flushing and residence times of the system

  - Salinity levels throughout the system

  - Impacts on sensitive receptors (e.g., roadways, low-lying properties, etc.)

- Impacts to the marsh plains throughout the system
- Potential for ponding within the system
- Sediment mobilization and potential transport

This Chapter also includes the presentation of model output and format, including tables, graphics, and animations.

2.0 MODEL SCOPING

2.1 MODEL GOALS AND OBJECTIVES

The overall goal of the Herring River Restoration Project is to create a productive, natural environment that will sustain itself with improved water quality and a strengthened ecosystem by restoring tidal flow to the estuary. While it would be desirable to allow the Herring River estuary to simply resume its previous natural state of un-impeded tidal flow, human and environmental constraints pose limitations on the extent to which the natural tidal flow can be restored. The success of the project will largely depend on the successful implementation of a comprehensive restoration plan, which addresses all the important issues related to those limitations. Hydrodynamic modeling is a central piece in developing this plan as it allows for the evaluation of specific questions about potential changes to surface water flow, velocities, water surface elevation, and salinity levels within the estuary. Once properly constructed, developed, and calibrated, a hydrodynamic model can be applied to numerous alternative restoration scenarios with relative ease and expedience. Results from alternative simulations are then be used to assess the potential impacts expected on the system.

Restoring tidal flow to the Herring River is likely to increase both the tidal range and the salinity levels within the estuary. A hydrodynamic model can predict these increases and therefore help evaluate potential impacts to the habitat areas as well as property and low-lying structures. In addition, spatially-variable, time-dependent predictions of water surface elevation allow for assessment of flooding and drying, which determine the extent of the inter-tidal zone and aid in identifying potential restoration zones and ponding or stagnation areas. Expanding the openings in the Herring River dike control structure may also have effects on the current velocities within the system, which could impact fish passage or result in changes in sedimentation patterns and areas of erosion and deposition. With the increased tidal flow, saline water will also travel much further into the system than it has in the past century. Therefore, numerical modeling can also directly provide information on the extent and concentration of salt within the estuary. Salinity levels can then be used to deduce the potential effects on water chemistry, groundwater levels, and flora and fauna. Understanding these changes will be necessary for successful restoration planning. Specifically, the modeling program should meet a number of well-defined goals addressing all pertinent limits on the restoration of tidal flow to the estuary. For example, some of the potential goals initially developed include, but are not limited to:

- A restored water surface elevation not to exceed 6.0 feet NAVD 88 in the Mill Creek sub-basin, which has significant infrastructure (low-lying properties and portions of the Chequessett Yacht and Country Club golf course), during a 100-year storm surge event.

- If the Mill Creek sub-basin is diked, a maximum water surface elevation not to exceed 7.5 feet NAVD 88 during a 100-year storm surge event throughout the remainder of the system.

- Evaluate hydroperiod and percentage of time high tides wet the marsh in key areas

- Assess potential changes in the velocity regime and sedimentation patterns

- Assess potential impacts to low-lying roads and structures
- Assess potential impacts to property, including upland flooding
- At a preliminary level, assess vegetation changes and vegetation die off due to saltwater intrusion
- Assess potential water ponding and stagnation
- Identify extent of Mean High Water (MHW), Mean High Water Spring (MHWS), and Annual High Water Spring (AHWS) for each alternative

Although not all these objectives are directly accomplished by the hydrodynamic model, the results of the model provide information and input needed to address these, as well as a number of additional, objectives. The model also is flexible enough to allow for future integration of other modules (e.g., adaptive management uses, sediment transport modeling, water quality modeling, and biological modeling).

2.2 DATA AVAILABILITY

2.2.1 Previous Studies

Following an eel kill in the fall of 1980, which drew attention to the poor and declining water quality in the Herring River upstream of the newly (1974) re-built dike, a significant amount of literature has been generated documenting studies conducted within the area. Ecological and biogeochemical investigations have indicated the detrimental impact caused by diking and ditching of the river; and call for restoration of tides to the river in order to revitalize the ecosystem (Beskenis and Nuzzo, 1984; Portnoy, 1984; Portnoy et al., 1986; Portnoy and Giblin, 1997; Roman, 1987; Portnoy, 1999; Portnoy and Allen, 2006). However, the potential restoration also raised concerns that the re-introduction of tides may cause saltwater intrusion into nearby wells. This led to studies of groundwater in the area, which to some extent have quelled these concerns (Fitterman et al., 1989; Fitterman and Dennehy, 1991; Martin, 2004; Masterson and Portnoy, 2005; Martin, 2007). Additionally, due to concerns of groundwater impacts and flooding in the Mill Creek region, a study of stream flow in Mill Creek was undertaken to examine options for a potential dike that may be required as part of the restoration plan (Nuttle, 1990). Sedimentation concerns, particularly stability of areas downstream of the dike and potential effects on shellfish beds below the dike, have been addressed using historic evidence and existing hydrodynamic model results (Dougherty, 2004). Some of the above studies have used results provided by two previous hydrodynamic modeling efforts (Roman, 1987; Spaulding and Grilli, 2001). In the development of a more advanced model, as part of this scope of work, a brief summary of the two previous modeling efforts is presented below.

Twenty years ago, a group of researchers evaluated alternatives for restoration and management of the Herring River Ecosystem (Roman, 1987; Roman et al., 1995). They presented results of the first hydrodynamic modeling effort for the estuary. This model used stage data collected both above and below the dike over a single semi-diurnal tidal cycle on three occasions (August 21, 1984; December 4, 1984; May 17, 1985) with three different sluice gate openings (1.67 ft,

4.27 ft, 2.0 ft) to calibrate a "tide-height" model for the estuary. The model was formulated using the principles of conservation of momentum and conservation of volume considering the area upstream of the dike as a reservoir with an instantaneously horizontal water surface. Momentum is conserved by balancing the horizontal pressure gradient across the dike with friction losses using Manning's formulation, while volume is conserved assuming that surface area of the reservoir (which in turn determines the volume) can be represented by a piecewise linear function of the water surface elevation. Bottom profiles of the river channel in combination with marsh surface elevations were used to determine the required surface area function while Manning's n was determined by calibration to the three data sets. Once calibrated, the model was applied to nine different cases over a semi-diurnal tide period with a typical mean tide range and different configurations of sluice gate and tide gate openings. In addition, simulations were conducted for four cases using conditions from the February 1978 storm representing a 100-year storm event.

The Roman (1987) model results present high and low water elevation and tide range in the reservoir, and flood and ebb volumes. They also developed a one-dimensional salinity model for the Herring River in order to predict flushing time and tidally averaged salinity distribution within the estuary. This model was based on balancing the downstream advection of freshwater with the upstream turbulent diffusion of salt caused by tidal mixing and requires input of a diffusion coefficient and freshwater inflow. A freshwater inflow rate of 9.89 ft^3/s was used based on data collected between April and August 1985, and salinity data collected on August 23, 1984 was used to determine the diffusion coefficient. Once the diffusion coefficient was determined, the model was applied to the nine restoration alternatives modeled with the tide-height model.

More recently, an "inlet-basin" model similar to the previous tide-height model was developed (Spaulding and Grilli, 2001). Like the tide-height model (Roman, 1987; Roman et al., 1995), this model applies the principles of conservation of momentum and conservation of volume while considering the "basin" upstream of the dike as a simple reservoir. However, it is more elaborate in its formulation of bottom friction allowing for the inclusion of multiple inlet channels with variable cross-section, and allowing for the use of empirical coefficients to account for friction losses associated with jet formation within the dike inlets. A significant improvement over the previous model comes from the use of a more accurate surface area versus elevation curve that was determined from topographic data collected by the NPS in 1999 combined with USGS provided 0, 3, and 6 meter contours. This model was calibrated using time series data from a December 4, 1984 data set collected by Roman (1987), then validated using data collected from May to November of 2000 at two stations (upstream and downstream of the dike). Additional intensive data collections were conducted over the period of a single semi-diurnal tidal cycle on July 25, 2000 and September 27, 2000. These included measurements of depth and current velocities within the culverts under the dike and the culvert under High Toss Road, while salinity and temperature data were collected throughout the water column at twelve stations along the river (all downstream of High Toss Road).

A salinity model was also developed, which is based on a steady-state salt balance similar to the Roman (1987) model. This salinity model was calibrated and validated with the salinity measurements made on July 25, 2000 and September 27, 2000. These salinity data were collected at twelve locations (all downstream of High Toss Road) and consisted of salinity

measurements at 0.5 m (1.64 ft) intervals. The water depths varied considerably and most were shallow limiting the number of samples actually taken. For water depths of less than 1 meter, samples were taken at the surface and bottom. For water depths of less than 0.5 meters, samples were only taken at mid-water depth. The twelve stations were sampled approximately once every hour over the tidal cycle. No data were collected upstream of High Toss Road. The salinity data were limited to these two daily surveys, and as such, limited salinity data were available.

These models were applied to the same restoration alternatives used by the previous model (Roman, 1987; Roman et al., 1995) with inclusion of additional simulations that progressively increased the width of the inlet at the river mouth. This model was later adapted and applied to additional alternatives that included a series of sluice gates at the Herring River dike (Spaulding and Grilli 2005). A more detailed review of the Spaulding and Grilli modeling effort can be found in the peer review conducted by Woods Hole Group (WHG, 2006). These modeling efforts provide a good initial evaluation of potential restoration options for Herring River. The model developed as part of this scope of work further advances the hydrodynamic understanding throughout the entire Herring River estuarine system.

Overall and not surprisingly, the previous modeling efforts demonstrated that larger openings in the dike would cause increases in the mean tidal elevation and the tidal range. Increasing the opening will also increase the saltwater penetration distance. Using their model, Spaulding and Grilli found that increasing the opening in the dike to 30 meters (98 feet) will allow fully unrestricted flow and that larger opening(s) would not substantially increase the tidal range within Herring River. While these models provide reasonable results for water surface elevation just above the dike, the results are less certain further upstream. The reservoir representation of the river neglects frictional effects upstream of the dike that will likely cause phase shift and attenuation of the tidal signal in the real system. Additionally, Spaulding and Grilli (2001) point out the difficulty in modeling systems with large flat marsh areas. In flat marsh plains, a small change in water surface elevation can result in a large change in the volume of water in the estuary. In order to accurately model this situation, it is imperative to have highly precise topographic data coupled with detailed modeling, especially within the range of the marsh surface elevation. For the tide-height and inlet-basin models, this constitutes creating a more accurate surface area versus elevation curve. However, it is not enough to consider only the flooded area of the estuary, its shape also has significant impact on the resulting water elevation and currents. Because it takes time to flood the marsh, a long narrow estuary will behave differently than a short wide one. Similarly, the one-dimensional salinity models give reasonable results for the steady-state conditions to which they are applied, but they should not be applied to conditions that are significantly different from those to which they were calibrated. In their formulation, they use a constant empirically determined longitudinal dispersion coefficient to account for mixing of the salt and fresh water. Actual dispersion, however, is highly dependent on velocity gradients and therefore, in a dynamic tidal system, its magnitude is both temporally and spatially variable. Variations in the volume of fresh water inflow, residual tidal currents, stagnation, and other factors all contribute to mixing within the estuary and can have significant effects on the resulting saltwater penetration. Considering the limitations of the earlier models, a more complex model was developed herein to provide improved accuracy in water surface elevation, tidal circulation, and salt concentration throughout the estuary. The model identified and developed in this report more precisely represents the geometry of the estuary (including its

plan form); considers variable frictional effects throughout the estuary; allows for flooding, drying, and ponding of water; produces accurate current velocities and water surface elevations throughout the estuary; and properly represents the physics of mixing for a wide range of forcing conditions.

2.2.2 Existing Data

The data required for the development of a robust and detailed hydrodynamic model are primarily of two distinct types, topographic and hydrographic data. The topographic data were required to construct the model geometry, while the hydrologic data were required for model forcing and proper calibration and verification to ensure the model provided accurate predictions. Additional data types were also required to further utilize the model to assess other physical processes. For example, sediment information was required for sediment transport modeling, salinity observations to assess salt levels in the system, etc. Massachusetts Coastal Zone Management (MCZM) provided recent photogrammetric data (2007) for the Herring River area. These data provide high-resolution land surface elevation, including approximately 200,000 points within the estuary above the mean low water elevation. The photogrammetry provided the necessary high resolution and precision required to accurately model the flooding and drying of the marsh surface. For the river and stream bottoms (below the lower limit of the photogrammetry data), two sources of data were available. Hydrographic data collected by the National Park Service (NPS) in 1999 and used by Spaulding and Grilli (2001) in their model, as well as supplementary data collected by NPS in 2008. These data were used to provide the depths within the creeks and streams of the Herring River estuary system. Figures 2-1 and 2-2 show the distribution and density of the existing topographic and hydrographic data sets, respectively. The blue dots in Figure 2-2 show the location of the 1999 creek elevation data, while the green dots show the location of the 2007 elevation data. These data sets were also supplemented with some supplemental topography and observation collected as a part of this study, as discussed in Chapter 5.

Once the model geometry was in place using the existing topographic data, the model was calibrated and verified with hydrologic data. The details of this process are described in Chapter 4. In terms of hydrologic data, recent water surface elevation data at six (6) key locations were collected at 15-minute resolution from August 30 to October 4, 2007 by NPS (Figure 2-3). Additional water surface, salinity, and temperature data were also collected at 15-minute resolution at two (2) more locations (Dog Leg-River and Old Saw Harbor) between June 1 and October 26, 2007 (Figure 2-3). Subsets of these data can be used for both model calibration and verification. Other hydrologic data that was also used in model verification includes the data collected for the earlier modeling studies (Roman 1987, Spaulding and Grilli 2001). Table 2-1 shows a summary of all the hydrologic data observed within the Herring River System at the initialization of the hydrodynamic modeling effort. Water surface elevation, salinity, temperature, and other data records continue to be collected throughout the Herring River estuary system by the National Park Service. The more recent data collected by the NPS always included at least the observation of a full neap to spring tidal cycle. The August to October 2007 data also included the observation of an annual high water spring tide.

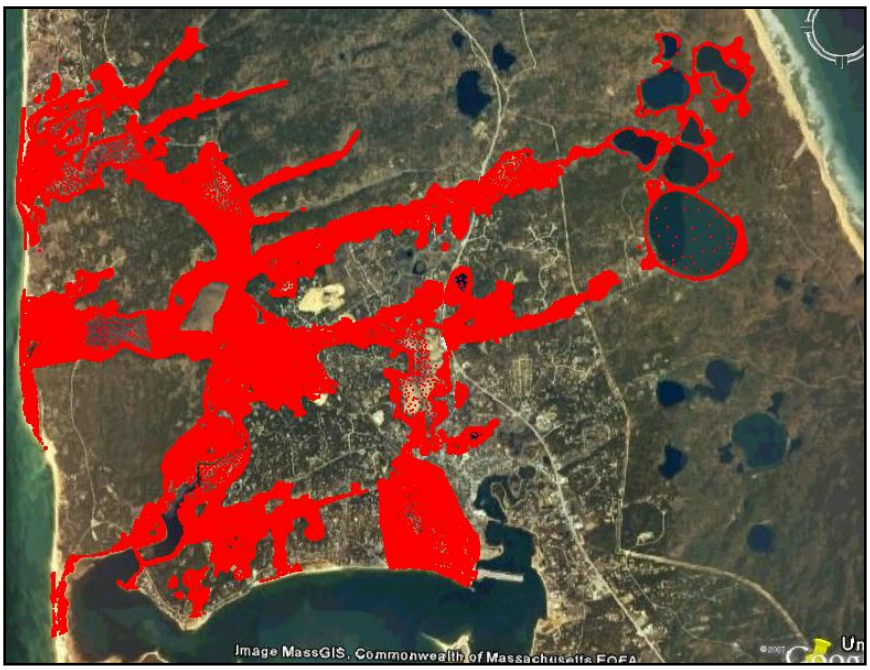

Figure 2-1. Land elevation data from MCZM photogrammetric survey collected in 2007 (background image courtesy of Google Earth).

Figure 2-2. Bathymetric data from 1998-1999 NPS total station surveys (blue dots) and 2008 NPS RTK Surveys (green dots) - (background image courtesy of Google Earth).

Figure 2-3. Hydrologic data gage locations (background image courtesy of Google Earth).

2.3 DATA LIMITATIONS

A model, at best, is nothing more than a good approximation of its prototype. The better the data used to build it, the more potential it has to give accurate predictions. The elevation data available to construct this model comes from the combination of two different data sets. Where the photogrammetry data are comprehensive (Figure 2-1), the bathymetric data (Figure 2-2) are not nearly as dense. As such, the model domain required some interpolation for certain bathymetric areas in the river, especially some of the upper reaches of the estuary. However, the amount of bathymetric data is sufficient based the consistent channel cross-sections observed in the upper portion of the system to provide a reasonable model of the system, especially in the areas where the most significant changes are expected (e.g., Lower Herring River, Mill Creek, etc.). Therefore, the topographic and bathymetric data applied in the current model are adequate to provide the required level of detail.

Water surface elevation data are available at eight (8) locations throughout the system and over various time frames, which allowed for comprehensive calibration and verification of the model with respect to this variable throughout the system. However, a significant portion of the system (upstream of High Toss Road) is no longer tidal because of the restriction caused by the existing dike. In these areas, there are limited tidal fluctuations, and the water resides only in the channels and creeks. As such, the upstream water surface elevation observations had to be positioned within the channels and creeks and the wetting and drying processes could not be directly calibrated. The wetting and drying scheme applied in the Herring River model has been applied, tested, and verified in other modeled estuarine systems. Ultimately, the water surface elevation in the channels throughout the system were accurately calibrated and standard values were assigned to represent the frictional effects associated with the marsh plains and vegetated areas.

Table 2-1. Hydrologic data availability (black areas indicate no data available).

	Roman	Spaulding & Grilli				NPS			
Locations	**12/4/84**	**8/12/99-8/27/99**	**9/17/99-9/24/99**	**9/29/99 - 10/13/99**	**5/23/00 - 11/02/00**	**6/1/07 - 8/30/07**	**8/30/07 - 10/04/07**	**10/04/07--10/26/07**	**2/2010 – 3/2010**
Just Below Dike	wse*								wse*
Just Above Dike									
1km Above Dike									
Above Dike		wse*, temp*, salinity, pH							
Below Dike			wse*, temp*, salinity, pH						
Bound Brook, Up							wse*		
Pole Dike, Down									
Rt6, Down									
Old County, Down									
Pole Dike, Up									
High Toss, Up									
Dog Leg-River						wse*, temp*, salinity, pH			wse*
Old Saw Harbor									

* wse = water surface elevation, temp = temperature

In addition, there are limited time series salinity data; primarily because there is limited salinity within the existing system. The existing dike structure limits salinity penetration to areas downstream of High Toss Road under normal conditions and historical observations have shown no salinity upstream of High Toss Road (National Park Service, 2008). Therefore, the model could only be calibrated to salinity downstream of High Toss Road, where salinity current exists. Additional salinity observations upstream of High Toss Road would not provide any additional data to calibrate the salinity model.

Finally, although some limited vertical salinity data has been collected (over a single day), it is unclear the level of stratification that may exist within the system. Spalding and Grilli (2001) indicate the possible presence of a salt wedge, but the magnitude, distance, and persistence of the feature cannot be adequately determined from their limited data set. Additionally, under the

current restricted conditions, salinity does not penetrate upstream of High Toss Road. Therefore, as discussed, salinity observations for existing conditions would provide limited value for model calibration purposes since a vast majority of the system currently remains fresh. Any stratification that does exist under existing conditions would likely be ephemeral in nature and only exist in the lower portion of Herring River. In much of the upper portions of the system, the water depth is too shallow to support stratified conditions. As such, a 2-dimensional model was determined to be adequate to accurately simulate the processes within the Herring River, as well as being able to adequately address the questions associated with the proposed restoration project.

Salinity observations under potentially restored conditions, and during the adaptive management processes, could be important for continued model refinement. Under restored conditions, the level of stratification may become a more important feature of the system that could influence circulation and mixing dynamics, and as such, vertical salinity data observations (during periods of low and high outflow) should be considered at specific steps during the adaptive management process. If significant stratification is identified in the restored system, the model developed and presented herein can be modified to three-dimensions. The model developed for Herring River is flexible enough such that transitioning from a 2-D model to a 3-D model would be relatively seamless, if needed.

Overall, there is sufficient data to develop a reasonable two-dimensional hydrodynamic model of the system, as well as assess potential impacts and answer key questions associated with the proposed restoration approach. Of course, model improvements can always be made with collection of additional data, model refinements, and expanded calibration, verification, and validation procedures; however, the data currently available does not limit the model's ability to function at the conceptual design level, for which it was intended. The model can also be applied as an adaptive management tool in the future and continue to be refined and extended through additional data collection and integration efforts.

3.0 MODEL SELECTION

3.1 MODEL REQUIREMENTS

A successful model aids in restoration planning by providing information needed to meet the overall defined goals of the restoration project. These goals required a model that incorporates the physics necessary to solve for water surface elevation, current velocities, and salinity, as well as potential future expansion into water quality and sediment transport. The model also needs to be flexible enough to link with other potential modeling tools (e.g., biological models) in an adaptive management setting. The model needs to be dynamic, capable of handling bi-directional flow, high resolution to identify circulation dynamics and detailed tidal areas (e.g., near the dike structure, the narrow tidal creeks, and in areas of critical upland infrastructure such as road crossings), and capable of being forced at its downstream boundary with an elevation time series, and at upstream boundaries with a freshwater inflow. Additionally, the Herring River estuary has a number of site-specific features that required specialized model abilities, including:

- The complex shape of the estuary, which requires, at minimum, a two dimensional (depth-integrated) model. The model selected also needs to have the ability to quickly adapt to three dimensions, if required by the physical processes being simulated in the adaptive management portion of the project.

- The large, relatively flat, flood plain that used to be tidal marsh prior to construction of the dike in 1908. With tidal restoration, the intent is to restore this to an active tidal marsh and therefore the areas must be included within the model domain. Portions of this flood plain have undergone substantial subsidence caused by the past century's dewatering of the marsh soils. This has created a unique topography that will be intermittently flooded and drained. Additionally, as the tide falls, depressions in the flood plain may also trap water in a network of ponds that could have a significant impact on the overall circulation patterns throughout the estuary. To effectively model this situation, the selected model must be able to efficiently handle wetting and drying of the flood plain, while having sufficient detail to resolve any type of ponding network.

- Variable vegetation and soil types throughout the estuary cause variable bottom friction. The successful model needs to be able to handle this by allowing for specification of variable bottom friction coefficients. For the current approach, existing vegetation maps were used to determine bottom friction coefficients. Additionally, soil types, depth levels, and grain size information are used to simulate sediment transport throughout the system.

- Another important feature that must be considered when choosing a model for the Herring River is the flow control structures in the dike. The selected model must be able to simulate the control that these structures (flap gates, culverts, and sluice gates) have on flow within the estuary; and do so with consideration of the proper hydraulics involved, for example super-critical versus sub-critical flow through the sluice gate. The model must also be capable of handling potential flow control structures that may be designed or implemented in a future improved dike.

Therefore, in selecting the model best suited for the Herring River estuary, some of the key required features that were considered include:

- At minimum, a 2-D depth integrated model
- At minimum, solves for water surface elevation, velocity, salinity
- Sufficient grid resolution and flexibility to represent important details (e.g., local circulation patterns, intertidal areas, flooding areas, road crossing, flow control structure dimensions, etc.)
- Wetting and drying, and ponding
- Control structures (flap gates, culverts, sluice gates)
- Variable bottom friction
- Elevation and inflow specified boundary conditions
- The ability to simulate hydrodynamic processes over a minimum of a month and up to a year
- Flexible time stepping in the solution schemes
- Ability to expand to 3-D
- Sediment transport capabilities
- Water quality capabilities

3.2 MODEL MATRIX

There are numerous numerical, hydrodynamic models available, both commercial and non-commercial. A smaller subset of these meets the requirements for Herring River. Hydrodynamic models differ in many ways, all having their unique strengths and weaknesses. In order to help select the most suitable model for the Herring River application, Table 3-1 presents a model matrix summarizing a number of model features. Each of the models listed in Table 3-1 were considered as candidates for use in developing the Herring River model. There are a number of additional hydrodynamic models that were considered (e.g., Finite Volume Coastal Ocean Model [FVCOM]); however, these had significant limitations in respect to the requirements of the Herring River estuary system, or were in development stages at the time of the assessment.

From this matrix of twelve (12) candidate models, Woods Hole Group has identified a short list of three (3) models (Resource Management Associates [RMA/TABS], Advanced Circulation Model [ADCIRC], and Environmental Fluid Dynamics Code [EFDC]) that had the greatest potential for developing an accurate model of the Herring River estuary. A brief description of these models is provided below.

RMA (Resource Management Associates) represents a suite of models. The models needed for the Herring River application include: (1) RMA2 for simulating 2-D water surface elevation and horizontal velocity and, (2) RMA4 for simulating 2-D transport of conservative and/or non-conservative substances (i.e., salt). RMA2 computes a finite element solution of the depth-integrated, 2-D shallow water equations using a combination of triangular and quadrilateral finite elements. The solution uses linear basis functions for water surface elevation and quadratic basis functions for velocity requiring elements with mid-side nodes. The solution is implicit in time

allowing for relatively large time steps in the solution. Subsequently, RMA4 uses the hydrodynamic solution provided by RMA2 to calculate a finite element solution of the 2-D advection-diffusion equation for the vertically well-mixed concentration of up to six (6) constituents. Unstructured finite element grids have the advantage of easily representing complex coastlines and allowing high grid resolution in areas where it is needed with easy transitions to lower grid resolution where it is not.

The ADvanced CIRCulation model (ADCIRC) solves the shallow water equations for water surface elevation and velocity using a modified form of the continuity equation called the Generalized Wave Continuity Equation (GWCE). It employs the finite element method using grid linear triangles and is explicit in time. ADCIRC can be run in either a 2-D depth integrated mode or 3-D mode. When run in the 3-D mode, an equation of state is simultaneously solved including salinity and temperature. ADCIRC's wetting and drying is accomplished by elemental elimination in which an element is considered dry and removed from computations when one of its nodes becomes dry. This method of wetting and drying can create unwanted channelization and blocking of flow and can be disadvantageous when applied to broad flat shallow areas. However, ADCIRC is also a modern code with an efficient matrix solver and an available multiple processor parallel version allowing for efficient simulations even with very large grids. Thus, an ADCIRC model with a large number of nodes and higher resolution may be able to explicitly resolve the micro-topographic features.

The Environmental Fluid Dynamics Code (EFDC) solves the shallow water equations for water surface elevation and velocity simultaneously with dynamically coupled transport of salt and temperature. The EFDC model is a two and three-dimensional model capable of simulating a diverse range of environment flow and transport problems. The model has been applied to studies of circulation, discharge dilution, water quality, TMDL (Total Maximum Daily Load), and sediment transport. EFDC is capable of predicting hydrodynamics and water quality in multiple dimensions and is a widely accepted EPA approved model. EFDC is also capable of simulating 21 water column state variables (e.g., nitrogen, algae, DO, phosphorus, carbon, etc.).

The EFDC model solves the three-dimensional, vertically hydrostatic, free surface, turbulent-averaged equations of motions for a variable-density fluid. In two-dimensions, the results of these equations are depth-averaged. The model includes dynamically coupled transport equations for turbulent kinetic energy, turbulent length scale, salinity and temperature. In addition, the EFDC model simulates cohesive and non-cohesive sediment transport, eutrophication processes, both near field and far field dilution of discharges, and the transport and fate of toxic contaminants. The model is capable of simulating multiple size classes of cohesive and non-cohesive sediments along with the associated deposition and resuspension processes and bed geomechanics. The transport of toxics in both the water and sediment phases is simulated.

The model allows for the wetting and drying of shallow areas using a mass conservation scheme. EFDC uses a staggered computational grid on which water levels are computed at cell centers and current velocity and scalar variable fluxes (e.g. salt, temperature, suspended sediment concentration) at cell interfaces. Mass conservation is guaranteed because the change of mass within each cell is always precisely equal to the net flux into or out of the cell. When wetting and drying is enabled in EFDC the user specifies a minimum depth (typically a few centimeters)

below which a computational cell is flagged as dry. WHG made modifications to the wetting and drying logic in EFDC to handle this particular situation better and allow for smooth wetting and drying of tidal marsh plains. These modifications do not affect the guarantee of mass conservation which is inherent in EFDC. Once a cell is flagged as dry, flux out of the cell is disallowed until the net flux into the cell increases the water level above the minimum depth. EFDC also includes measures for simulating flow control structures and highly vegetated areas. An embedded single and multi-port buoyant jet module is also included for coupled near and far field mixing analyses.

The model matrix, presented in Table 3-1 provides a comparative tool for evaluating the various hydrodynamic models available to simulate the Herring River estuary. Key abilities and other factors that may be critical to success of the modeling effort, or are important from the HRRC's perspective, were evaluated through using this matrix. The matrix was ultimately used by Woods Hole Group and the HRRC to help guide the selection of the most appropriate model.

Table 3-1. Model selection matrix.

	RMA/TABS	EFDC	ADCIRC	ELCIRC	SELFE	MIKE	DELFT3D	ROMS/TOMS	ADH	TELEMAC	TRIM/unTRIM
2-D Hydrodynamics	yes (RMA2)	Yes	Yes	Yes	Yes	Yes (Mike 21)	Yes	Yes	Yes	TELEMAC-2D	Yes
3-D Hydrodynamics	yes (RMA10)	Yes	Yes	Yes	Yes	Yes (Mike 3)	Yes	Yes	Yes	TELEMAC-3D	Yes
Grid Type	Unstructured Triangles and Quadrilaterals	Curvilinear Orthogonal	Unstructured Triangles	Unstructured Orthogonal Triangles and Quadrilaterals	Unstructured Triangles and Quadrilaterals	Many different options	curvilinear, sigma-verticle	curvilinear Orthogonal, terrain folowing	Unstructured	Unstructured Triangles	Curvilinear Orthogonal / Unstructured Orthogonal
Equations/Numerics	SWE, Primative Continuity, Finite Element(quadratic for velocity, linear for WSE), Implicit	SWE, finite volume or finite difference	SWE, GWCE, Finite Element(linear), Explicit, CFL limited	SWE, finite-volume/finite-difference Eulerian-Lagrangian algorithm, based on UNTRIM	SWE, finite-volume/finite-element Eulerian-Lagrangian algorithm, based on UNTRIM	Equations/Numerics are unclear, Finite Difference, Finite Volume, many different programs for different applications	SWE	primative equations,	SWE or NS, Finite Elements with Adaptive Mesh Refinement	SWE(2D), N-S(3D), Finite Element Method	RANS, finite-volume/finite-difference Eulerian-Lagrangian algorithm
Wetting/Drying	Marsh Porosity or Elemental Elimination	Yes	Yes, Wet or Dry Elemental Elimination	Yes	Yes	Yes	Yes	Yes	Yes	Yes	Yes
Salinity	Yes, RMA4,RMA11	Yes	yes, in 3-D mode	Yes	Yes	Yes	Yes	Yes	Yes	Yes	Yes
Temperature	Yes, RMA4,RMA11	Yes	yes, in 3-D mode	Yes	Yes	Yes	Yes	Yes	Yes	Yes	Yes
Water Quality	Yes, RMA4,RMA11	Yes	No	No	No	Yes	Yes	No	Yes	Yes	No
Sediment Transport	Yes, SED2D	Yes	Not readily available	No	No	Yes	Yes	Yes	Yes	Yes	No
Contaminant Transport	Yes, RMA4,RMA11	Yes	No	No	No	Yes	Yes	No	Yes	Yes	No
Particle Tracking	Yes, RMATRK	Yes	WHG developed	Yes	Yes	Yes	Yes	Yes	Yes	Yes	No
Boundary Conditions	Inflow, Elevation, Wind, Rainfall,Control Structures	Inflow, Elevation, Wind, Rainfall,Control Structures	Inflow, Elevation, Wind,Control Structures, Radiation Stress	Flux,Elevation,Wind,radiation,etc…	Flux,Elevation,Wind,radiation,etc…	Many	Many	atomospheric, tidal, river	Many	Many	Many
Data Assimilation	No	Yes	No	Yes	Yes	No	No	yes	Yes	N/A	N/A
Parallel	No	No	MPI	MPI	No	Coming in 2008	No	openMP, MPI	Yes	Yes	no
Pre-/Post-Processor	SMS	WHG developed	SMS, ADMAT	WHG developed	WHG developed	Has its own	Has its own	Yes	SMS, GMS	Has its own	has its own
Open Source	No	Yes	Yes	Yes	Yes	No	Not for Commercial	Yes	Yes	no	No
Language	Fortran	Fortran	Fortran	Fortran	Fortran	Not released	Not released	Fortran	Fortran and C	Not released	Not Released
Operating System	Windows	Windows/linux	Windows/linux	Linux	Linux	Windows	Windows/linux	linux	linux	linux,windows	N/A
Support	USACE-ERDC	TetraTech	email User Group	email user group	email user group	DHI	Delft Hydraulics	large usergroup	For USACE only	EDF, Sogreah	N/A
Peer Reviewed	Yes	Yes	Yes	some	Some	Yes	Yes	Yes	Yes	Yes	Yes
Documentation	Yes	Yes	Yes	Yes	Yes	Yes	Yes	Yes	Yes	Yes, for users	Yes
Commercial Use	Yes	Yes	Yes	Yes	Yes	Yes	Yes	N/A	Yes	Yes	Yes
Upgradeable	Yes	Yes	Yes, frequent new versions	Yes	Yes	Yes	Yes	Yes	Yes	N/A	N/A
Training	Yes	No	Yes	No	No	Yes	Yes	N/A	No	N/A	N/A
Cost	$3800 for SMS TABS Module	Free	$ 5300 for SMS Module	Free	Free	$30 to $100k	$100k	free	Free	~$40k depends on modules	$10 to $20k
Comments	Marsh porosity is an advantage for wetting/drying where microtoporgaphy cannot be resolved	EPA supported model. Does everything including a number of control structures	mainly used for large region tidal circulation and hurricane storm surge, but has also been applied to rivers and estuaries with some success	seems like it has good poteitial, local mass conservation, relatively new code, requires "close to orthogonal" grid for accuracy, has not yet been used extensively	compared to ELCIRC: orthogonality not necessary, but local mass conservation not ensured by FE, minimum linear shape functions(compared to constant), has sigma-Z coordinates not just Z	has modular structure and can do many things, has good support, Closed Source, Unsure of solution methods	has modular structure and can do many things, many options for water quality and sediment,unfortunately commercial dedicated applications have fixed grid geometry, has good support, but must work closely with Delft Hydraulics	well developed large scale ocean circulation model with steep learning curve	Being developed at ERDC, works for supercritical, subcritical, and nonhydrostatic flow,good for modeling hydraulic structures, I.e. lock intake, still under development	there is a suite of programs associated with TELEMAC for doing just about anything for free surface flows, used exensively in France where it is developed	ELCIRC is based on this code, but free

3.3 FINAL MODEL SELECTION

The final model selection was made through a joint selection process with Woods Hole Group and the HRRC. The model selection focused on:

- the technical abilities of the model
- the ability of the model to meet the specific needs of the Herring River estuary system
- the ability of the model to provide visualizations and results to foster public understanding
- the flexible nature of the model to expand and adapt to future technical requirements

Based on the information presented herein, a discussion between stakeholders was conducted focusing on the pros and cons of the models on the "short list" (ADCIRC, RMA/TABS, EFDC). The discussion also raised specific technical questions related to the ability of these models, in addition to the numerous requirements defined above, including:

- The models ability to provide velocity data at various structure types, including sluices, weirs, and for a variety of flow types (sub and super critical, transition flow, etc.)
- The accuracy of the model at predicting water surface elevation, velocities, and salinity
- Ability to simulate additional physical processes, including wind, freshwater inflow, sea level rise, etc.
- The reliability and methodology for simulation of sediment transport, including rates of erosion and deposition
- The ability to spatially adjust bottom drag values for different bottom conditions (higher drag for marsh grasses lower drag for sandy bottom).

After a detailed discussion, the Environmental Fluid Dynamics Code (EFDC) was selected because of its ability to meet all necessary requirements for the Herring River Estuary model, specifically the flexible nature of the model to handle future technical requirements and data integration as it is developed. A detailed explanation of the EFDC model is presented in Chapter 4.

4.0 MODEL APPROACH

This Chapter presents the overall model approach that was applied to develop the hydrodynamic model for the Herring River system. The approach presented herein identifies the major tasks within the model development, and provides key points for evaluation of the modeling performance and progress throughout the study. This allowed for a flexible approach that included the incorporation of new data, and/or a re-direction of the effort based on the results of the current modeling phase. Therefore, the modeling approach is presented in phases.

4.1 PHASE I – MODEL CALIBRATION

Model calibration is the process by which adjustments are made to the model parameters to ensure the model appropriately simulates measured water surface elevation, salinity, and other observed parameters. This requires conducting a series of iterative model simulations to ensure the model is stable, and results compare favorably with measured data. Calibration can be a lengthy process involving hundreds of model simulations. Specifically, the model coefficients are adjusted (within acceptable ranges) until the modeled water surface elevation, salinity, and temperature closely approximates the measured field observations.

In practice, hydrodynamic models require input of some physical parameters that are unknown or only known within a reasonable range. For example, bottom friction parameters, because their formulations often account for a combination of frictional effects, leave some freedom in choosing an appropriate value. The calibration process involves "tuning" the model by systematically adjusting some unknown parameters, such as bottom friction, so that its results match reasonably well to a set of observed data. Horizontal eddy viscosity is another parameter that can reasonably fall within a significant range, however for different models its effect on results is considerably different due to the use of different numerical methods. In addition, different models have numerous different parameters that can be tuned to achieve better model results. To accomplish this, the observed data set must provide both the necessary information outside the model domain to drive the boundaries, while also providing information within the model domain for comparison to model output. Once a set of parameters has been found that produces the best possible fit to the data (and the selected parameters are reasonable compared to empirically defined values), the parameters are fixed for subsequent model simulations. The more extensive the calibration data set in terms of duration, spatial extent, and observed quantities, the better chance the model has at matching other independent sets of data and producing accurate predictions.

4.2 PHASE II – MODEL VALIDATION

Model validation is achieved by applying the calibrated model, with its fixed parameters, to one or more sets of observed data that are independent from the calibration data. Typically, sets of data for validation are collected at a different time and under conditions that differ from the calibration period. Results from validation simulations are quantitatively compared to the observed data in the same way as in the calibration process. However, during validations there is no freedom to tune parameters. This demonstrates that the model performs reasonably under a different set of conditions. As such, validation simulations act as a check to see how well the model is capable of predicting accurate results under conditions that differ from calibration. A

model must be satisfactorily verified before it can be used for forecasting (e.g., alternative simulations or different forcing conditions).

4.3 PHASE III – EXISTING CONDITIONS SIMULATIONS

Once the model has been calibrated and validated, further simulations using the unmodified model provide a better understanding of the behavior of the system over a broader range of forcing conditions. In addition to elucidating the present state of the Herring River estuary, these existing conditions simulations also provide a baseline for comparison to proposed restoration alternatives in order to provide a gauge of the potential benefits and/or risks associated with different components of the restoration design.

4.3.1 Normal Tidal Conditions

While the calibration and validation results ensure the accuracy of the model, they represent the behavior of the system during specific time periods and may not be fully representative of the normal function of the estuary. Harmonic analysis of historically observed water surface elevation data from nearby NOAA tidal stations provides forcing conditions that include average spring and neap tide events. Evaluating the existing Herring River system under normal conditions will allow for assessment of the flushing characteristics, the overall hydrodynamics, and the regular volume flux that occurs between Wellfleet Harbor and the Herring River upstream of the Chequessett Neck Road Dike. These normal tidal conditions also provide elevational tidal benchmarks (e.g., Mean High Water, Mean High Water Spring, Annual High Water) that can be used to compare and contrast various restoration alternatives to existing conditions.

4.3.2 Storm Scenarios

Perhaps one of the biggest risks involved in restoring tidal flow the Herring River is the increased potential for flooding associated with storm events. Therefore, simulation of storm events is important. At a minimum, water levels representing storms with 1-year and 100-year return periods will be simulated for the system. Storm surge elevations were developed from historical records in the U.S. Army Corps of Engineers (USACE) New England Coastline Tidal Flood Survey of 1988, as well as the Federal Emergency Management Agency (FEMA) Flood Information Study for Wellfleet, MA (1992). In addition, winds associated with large storms can have a significant impact on water levels, therefore wind forcing is included in these model scenarios. Understanding how the existing system responds to storm forcing, is critical in assessing the potential impacts/risks that may be involved with each potential restoration scenario.

4.3.3 Sea Level Rise

The current degraded state of the Herring River estuary is the result of a century of anthropogenic modifications. With restoration, in another century, the state of the estuary may be significantly improved. However, into the 21st century and beyond, it is feasible that other long-term processes may have a significant effect on the state of the system. The topic of accelerated sea level rise in the 21st century and beyond has been the subject of much discussion. The Intergovernmental Panel on Climate Change (IPCC) has spent considerable time and energy reviewing and analyzing the current state of knowledge of past and future changes in sea level in

relation to climate change. Taking this information, the United States Army Corps of Engineers (USACE) has developed guidance for incorporating sea-level change considerations in civil works programs (USACE, 2009, 2011). Values for low, intermediate, and high sea level rise based on USACE guidance are incorporated into the Herring River modeling approach. The projected sea level rise values are added to the normal tides to produce boundary conditions for the sea level rise scenarios. However, due to the inherent uncertainty in sea level rise predictions, there is also a significant amount of uncertainty in the results of sea level rise simulations. Ultimately, the model is used to simulate these high, intermediate, and low sea level rise predictions for the preferred alternative(s), using estimates to help determine potential impacts of rising sea levels on future conditions within the Herring River system. These sea level rise simulations were also conducted for existing conditions in order to evaluate potential changes that may occur to the system without any restoration effort. The assumptions in the sea level rise simulations also include:

- Freshwater discharge into the Herring River system remains similar under future conditions
- Rainfall conditions remain similar under future conditions
- Changes in the rate of subsidence is not included in projections of sea level rise
- There is no change in the intensity or frequency of storm surge events (e.g., a 100-year return period storm today is the same magnitude as in the future)

4.4 PHASE IV –CHEQUESSETT NECK ROAD DIKE ALTERNATIVE SIMULATIONS

The focus on the initial set of alternatives was to evaluate the response to the Herring River system expected with modifications to the Chequessett Neck Road dike. The alternatives simulated are presented in detail in Chapter 6.0. Each alternative is evaluated for at least three (3) tidal forcing events (average tidal conditions [neap/spring], 1-year tide forcing, and 100-year tide forcing). Sea level rise scenarios are also assessed for specific alternatives (e.g., endpoint restoration alternatives). The evaluation of the Chequessett Neck Road Dike Alternatives (Sections 6.1 and 6.2) included the following specific simulation groups:

- Evaluation of the Herring River system with the removal of all anthropogenic structures. This simulation was completed to provide an estimate of maximum restoration potential, as well as provide a demonstration of the potential historic conditions within the Herring River system. This alternative removed the dike, all culverts, all restrictive road crossings, and railroad embankments. However, the physical topography of the system was not changed. For example, subsidence that occurred over the past century, or berms that may have been created in the system due to mosquito trenching were not modified, primarily since the historic conditions are unknown.
- A range of simulations conducted to optimize the opening width of the Chequessett Neck Road dike. These alternatives were geared towards identifying the optimal opening width (no height impediment) that would maximize restoration in the system. The simulations evaluated both the water surface elevation and the salinity levels throughout

the system and used the results from the various opening sizes to determine the maximized restoration ability for the system.

- Following the determination of the optimal opening width, various opening heights (assumed to be controlled through tidal control structures such as slide gates) were simulated to provide results for potential adaptive management openings and to target the desired endpoints for restoration levels. Specifically, the incremental opening height simulations were used to identify the preliminary alternatives for impact evaluation. These endpoint restoration alternatives were selected based on limitations of maximum water surface elevation that would be allowed within the system.
- Model simulations that assessed the current invert levels of the Herring River dike culverts. These simulations were aimed at determining the potential impacts associated with modification of the existing invert elevations.

4.5 PHASE V – UPSTREAM FEATURE EVALUATIONS AND ALTERNATIVE SIMULATIONS

The next set of alternative simulations focused on the culverts located in the upstream portions of the system. Specifically, this included evaluation of the crossing at High Toss Road, removal of the large flood tidal shoal existing just upstream of the dike, and assessment of the various road/culverts upstream throughout the system. These simulations and evaluations are presented in Sections 6.3, 6.4, and 6.5.

4.6 PHASE VI – MILL CREEK SUB-BASIN ALTERNATIVE SIMULATIONS

The final alternative simulations were focused on evaluation of the Mill Creek sub-basin (Figure 1-1) and are presented in Section 6.6, including the potential implementation of a new dike restricting tidal exchange into this portion of the system. The simulations for a potential new dike at the Mill Creek followed the same approach as used for the Chequessett Neck Road dike. Specifically, this included:

- A range of simulations conducted to optimize the opening width of the Mill Creek dike to limit the water surface elevation to a specific elevation (no higher than 6 feet NAVD88 under 100-year storm conditions. These alternatives were geared towards identifying the opening width (no height impediment) that would maximize restoration while still providing flood damage protection in the system.

- Following the determination of the optimal opening width, various opening heights (assumed to be controlled through tidal control structures such as slide gates) were simulated to provide results for potential adaptive management openings and to target the desired endpoints for restoration levels solely within Mill Creek.

- Evaluation and model simulations assuming complete blockage of tidal exchange from Mill Creek were also completed. This assumed the use of a one-way flap gate(s) at a newly constructed Mill Creek dike. This would allow water to flow out of the system (e.g., during freshwater discharge events during significant rainfall), but not allow saline water from Herring River into Mill Creek. Simulations were conducted to assess if rainfall storm events would adequately drain from the Mill Creek sub-basin with a new Mill Creek dike and one-way flap gate installed.

- Model simulations were conducted with and without a re-graded Chequessett Yacht & Country Club (CYCC) golf course. The CYCC re-grading consisted of raising specific golf holes and areas within the CYCC property to create both natural restoration areas and higher ground for golf course utilization. The HRRC provided the re-graded layout for modification of the model in the Mill Creek sub-basin. Re-graded topography was simulated for conditions with and without a new Mill Creek dike.

- Finally, a preliminary estimate of potential groundwater impacts in the Mill Creek sub-basin was evaluated. Specifically, the expected change in groundwater levels that may occur for the restored Herring River system, with and without sea level rise were examined. This analysis also consisted of an assessment of the groundwater levels that may occur for the existing system relative to sea level rise projections.

4.7 FUTURE ALTERNATIVE SIMULATIONS

The alternatives simulated and presented in this report provide details on a number of potential design components and restoration alternatives. These alternatives provide both adaptive management options, as well as restoration endpoints for environmental impact evaluation. However, the model has also been developed to be flexible and can be applied as an adaptive management tool throughout the restoration process. The model may also be applied in the future to evaluate other size openings, tidal control methods, or assess other system parameters (e.g., water quality constituents, dynamic sediment transport, etc.).

5.0 MODEL DEVELOPMENT

This chapter describes the development of the hydrodynamic model for the Herring River estuary. In addition to describing the configuration, calibration, and validation of the model, this chapter also presents the results of a number of simulations for the existing estuary conditions. These simulations, with the estuary in its existing restricted state, aid in developing an understanding of the current behavior of the system, and provide a baseline for comparison with alternative simulations. All data observations presented in this report were provided to Woods Hole Group by the HRRC. Therefore, the accuracy of the observations, corrections to the proper datum, instrument models, setups, and calibration, were not a component of this modeling study. Data provided were assumed to be correct and appropriate for model development of the Herring River system.

5.1 THE ENVIRONMENTAL FLUID DYNAMICS CODE

After careful consideration of a number of hydrodynamic, numerical models (Chapter 3), the Environmental Fluid Dynamics Code (EFDC) (Hamrick, 1996), originally developed at the Virginia Institute of Marine Science (Hamrick, 1992), was selected as the most appropriate tool for modeling the Herring River estuary. EFDC has been applied to numerous aquatic systems including Chesapeake Bay (Hamrick, 1994), Mobile Bay in Alabama, Cape Fear River in North Carolina, and the Suwannee River in Florida. Woods Hole Group has applied EFDC for numerous estuarine, harbor, and wetland restoration systems in the northeast, including, Stony Brook (Brewster, MA), Broad Cove (Hingham, MA), Goose Cove (Brooksville, ME), Eau Gallie River (Melbourne, FL), and Brides Brook (East Lyme, CT). The model has been applied to studies of circulation, discharge dilution, water quality, TMDL, and sediment transport. EFDC is capable of predicting hydrodynamics and water quality in multiple dimensions and is a widely accepted EPA approved model. EFDC was chosen because of its ability to meet all necessary requirements for the Herring River Estuary model including the ability to simulate in two (and potentially three) dimensional time dependent water levels, current velocities, salinity, wetting and drying, and hydraulic control structures; and because it can be easily extended to simulate sediment transport and water quality parameters if needed in the future.

It is not important for the reader to understand the details and formulations presented in this section to be able to understand the results of the modeling. The EFDC model solves the three-dimensional, vertically hydrostatic, free surface, turbulent-averaged equations of motions for a variable-density fluid. The model includes dynamically coupled transport equations for turbulent kinetic energy, turbulent length scale, salinity and temperature. In addition, the EFDC model can simulate cohesive and non-cohesive sediment transport, eutrophication processes, both near field and far field dilution of discharges, and the transport and fate of toxic contaminants. The model is capable of simulating multiple size classes of cohesive and non-cohesive sediments along with the associated deposition and resuspension processes and bed geomechanics. The model allows for the wetting and drying of shallow areas using a mass conservative scheme. EFDC also includes measures for simulating flow control structures and highly vegetated areas.

To represent the geometry of a water body, the EFDC model uses Cartesian or curvilinear-orthogonal horizontal coordinates and, when applied in three dimensions, terrain-following vertical coordinates. A finite difference numerical scheme is employed within EFDC with two time levels and a procedure that splits the internal-external modes. The free-surface gravity

wave or barotropic external mode is solved explicitly along with the simultaneous computation of a two-dimensional surface elevation field using an iterative conjugate gradient solver. Calculating the depth-integrated barotropic velocities using the newly computed surface elevation completes the external solution. Horizontal boundary condition options for the external mode solution include specifying the water surface elevation, the characteristic of an incoming wave, free radiation of an outgoing wave, or the normal volumetric flux on arbitrary portions of the boundary. For the Herring River model, a water surface elevation and salinity time series was specified at the boundary of the model in Wellfleet Harbor.

The EFDC model implements a mass conservation solution scheme for the Eulerian transport equations, which is at the same time step or twice the time step of the momentum equation solution. The advective step of the transport solution uses either a central difference scheme (used for the Herring River model) or a hierarchy of positive definite upwind difference schemes. The horizontal diffusion step is explicit in time, while the vertical diffusion step is implicit. Horizontal boundary conditions include material or constituent inflow concentrations, which can be specified as being depth-dependant and both constant and time-variable. The EFDC model can be used to drive a number of external water quality models using internal linkage processing procedures described in Hamrick (1994).

5.2 MODEL CONFIGURATION

The development of the Herring River hydrodynamic model required configuration so that this particular application of EFDC would best approximate the form and function of the real system (i.e., the Herring River Estuary). Model configuration involves compiling observed data from the actual estuarine system into the format required for the execution of EFDC. This can be broken down into three major steps that are described below.

- First, topographic and bathymetric data are used to generate the computational grid on which EFDC's finite difference calculations are performed.

- Second, observed water levels, salinity, and atmospheric conditions are used to define boundary conditions for driving the model. The development of boundary conditions also includes the assignment of bottom friction for the various types of marsh substrate throughout the estuary system.

- Third, for this application, additional subroutines were applied within the EFDC code to dynamically compute discharge through different types of hydraulic control structures that are present in the estuary and have a significant effect on the hydraulics. Thus, the methods used to compute discharge through slide (sluice) gates, flapper gates, circular pipe culverts, and box culverts, and their parameterization in the Herring River hydrodynamic model are also described. Additional control structure routines, for structures not currently installed in the Herring River system, were also developed for future alternative cases that may include other control structure designs (e.g., combination gates, weir structures, etc.).

Again, it is not critical that the reader be familiar with the concepts and/or equations presented in this section in order to understand the results of the Herring River model. This model

configuration section presents details on the setup of the model, including the explicit steps followed to generate the grid, input boundary conditions, and determine flow dynamics at control structures. Following model setup, the governing equations are solved at each grid point through an iterative method. The model is then able to calculate the water surface elevation, velocity, and salinity at each time step. Once a certain level of accuracy is attained, the model advances to the next time step in the simulation and repeats the calculations. This methodology is continued until the model has simulated the entire time period of interest.

5.2.1 Grid Generation

After choosing the appropriate model, the first step in building the model is constructing the model grid. The grid is a digital abstraction of the prototype's geometry that provides the spatial discretization on which the model equations are solved. Different numerical methods require different types of grids, each having unique geometrical requirements. The grid building process involves using geo-referenced digital maps or aerial photos to define the model domain, then the grid is generated within this domain providing the desired degree of spatial resolution, and topographic data is incorporated by interpolation of elevation values to grid nodes or cells within the domain.

For EFDC, the computational grid defines the spatial domain on which EFDC performs its finite difference calculations. EFDC requires a structured grid, either Cartesian or curvilinear orthogonal, comprised of a number of grid cells on which model the variables are computed. The accuracy of the model is highly dependent on accurate representation of the form of the real system expressed through the model grid. While a curvilinear orthogonal grid is more difficult to implement than a strict Cartesian grid, the curvilinear option was chosen because of its increased flexibility, allowing grid boundaries to better follow natural irregular boundaries. The curvilinear orthogonal grid also allows gradual variation in horizontal resolutions, such that higher resolution areas can be defined in areas where greater detail is required. The model grid developed for the Herring River model is complex, and the generation of a satisfactory grid required modification of the typical methods used to generate computational grids for EFDC. To create the Herring River grid system, a method for 'nearly-orthogonal' grid generation (Akcelik et al., 2001) was implemented and is described in detail within this section.

Topographic data from a number of sources were provided to Woods Hole Group for use in constructing the Herring River model grid. These data include: (1) a collection of RTK-GPS data, total station data, and map estimates collected in 1998-1999 used in the previous modeling study conducted by the University of Rhode Island for the National Park Service (Spaulding and Grilli, 2001) shown in Figure 5-1; (2) recent photogrammetric survey data provided by Massachusetts Coastal Zone Management shown in Figure 5-2; (3) additional RTK-GPS river cross section data collected by the National Park Service in March 2008 in order to better define the bathymetry in the lower portion of the Herring River shown in Figure 5-3; and (4) a bathymetric survey of the area downstream of the dike conducted by Woods Hole Group on February 26, 2009 (shown in Figure 5-4). Furthermore, the low-lying road survey conducted in December 2006 by Slade and Associates, Inc. was used to ensure that all roadways were accurately represented in the model grid and additional RTK-GPS "observation points" collected by the National Park Service in August 2008 were compared to the grid to verify its accuracy.

Figure 5-1. Bathymetric and topographic data collected in 1998-1999.

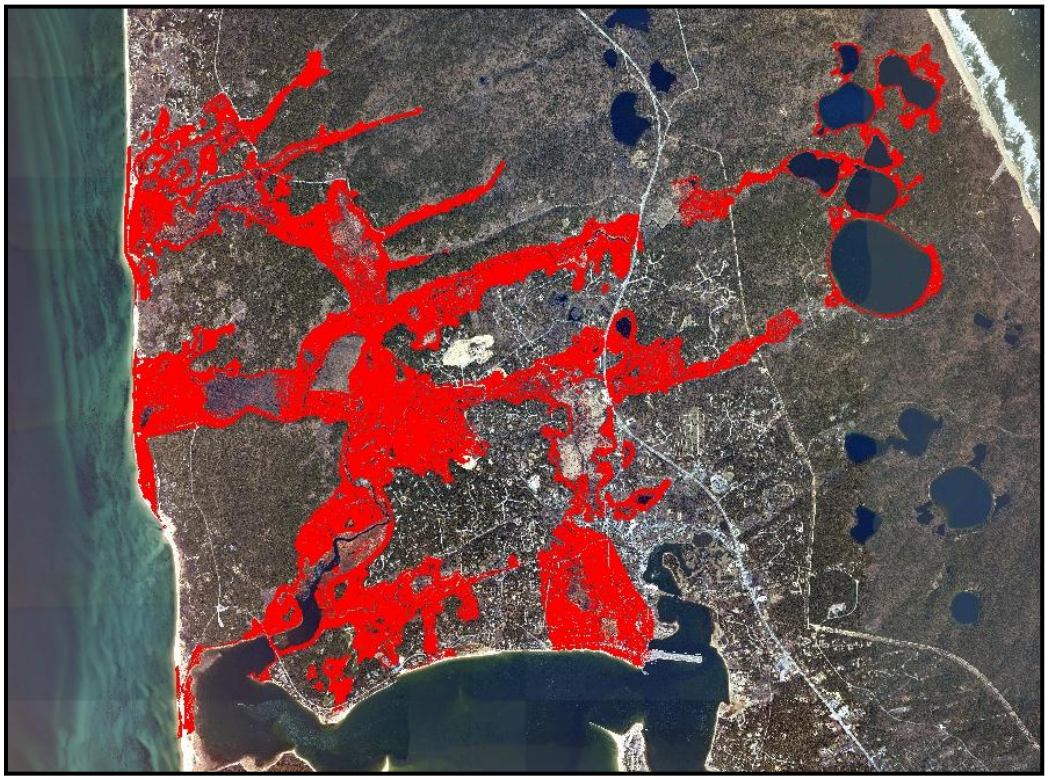

Figure 5-2. Photogrammetric data collected in 2007 and provided by Massachusetts Coastal Zone Management.

Figure 5-3. Additional RTK-GPS bathymetric cross sections collected by National Park Service in 2008.

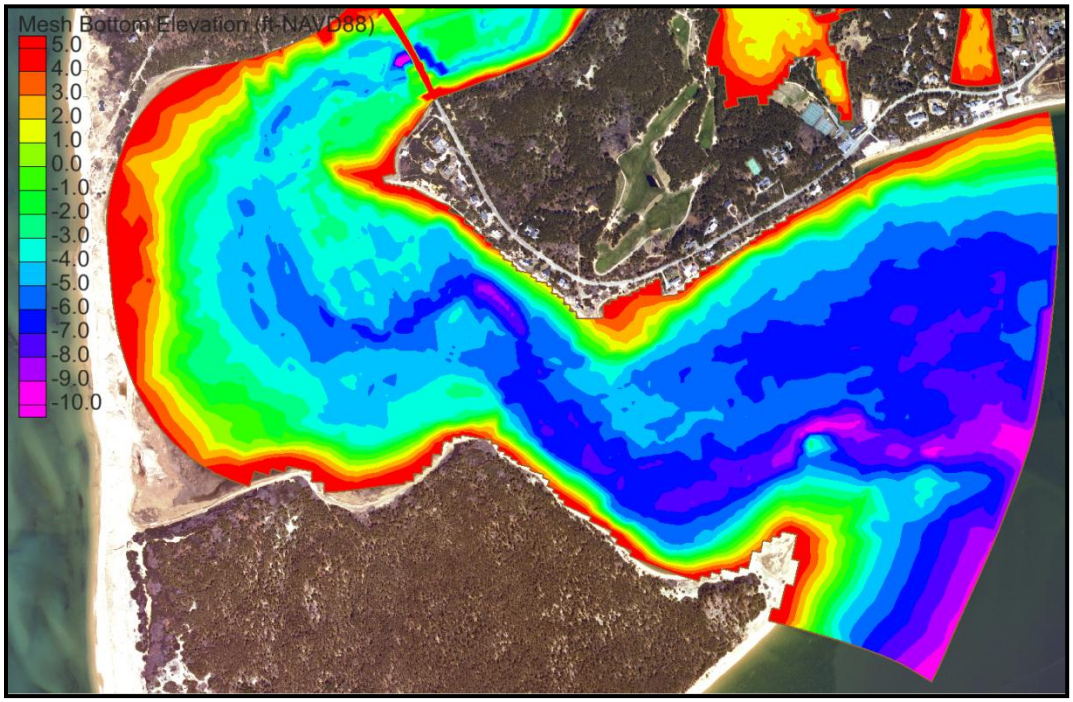

Figure 5-4. EFDC model showing actual bottom elevation contours from 2009 Woods Hole Group bathymetric survey and used in the Herring River model.

All topographic and bathymetric data were checked for consistency, and when necessary converted to the Massachusetts Mainland State Plane NAD83 horizontal datum and NAVD88 vertical datum, then merged into a single data set. The 12 foot NAVD88 contour line from the merged data set was then used to roughly define the domain's boundaries in block rectangular fashion. This elevation was selected as the upper boundary limit since the 100-year storm surge elevation in Wellfleet Harbor (approximately 10 feet NAVD88) is below this elevation. Figure 5-5 shows the 12 foot NAVD88 contour in green and the rough block rectangular boundary used for initial grid generation in red.

The block rectangular boundary definition is required input for the EFDC companion grid generation code, GEFDC. Definition of the grid boundary as a block rectangular boundary is the first step in grid generation and is constrained such the number of "east" facing sides is equal to the number of "west" facing sides and the number of "north" facing sides is equal to the number of "south" facing sides. Figure 5-6 shows how the block rectangular boundary is represented in the logical domain where the orientation of the block rectangular boundary segments is more evident. Once the boundary of the domain has been approximated in this way grid points are distributed along the boundary with spacing that ultimately determines the resolution of the final grid. Although Figure 5-6 doesn't look anything like the actual Herring River estuary at this point in the modeling process, this is only the preliminary step in the grid generation process for the Herring River model.

Figure 5-5. 12 foot contour from merged elevation data (green) and block rectangular boundary definition in the physical domain (red).

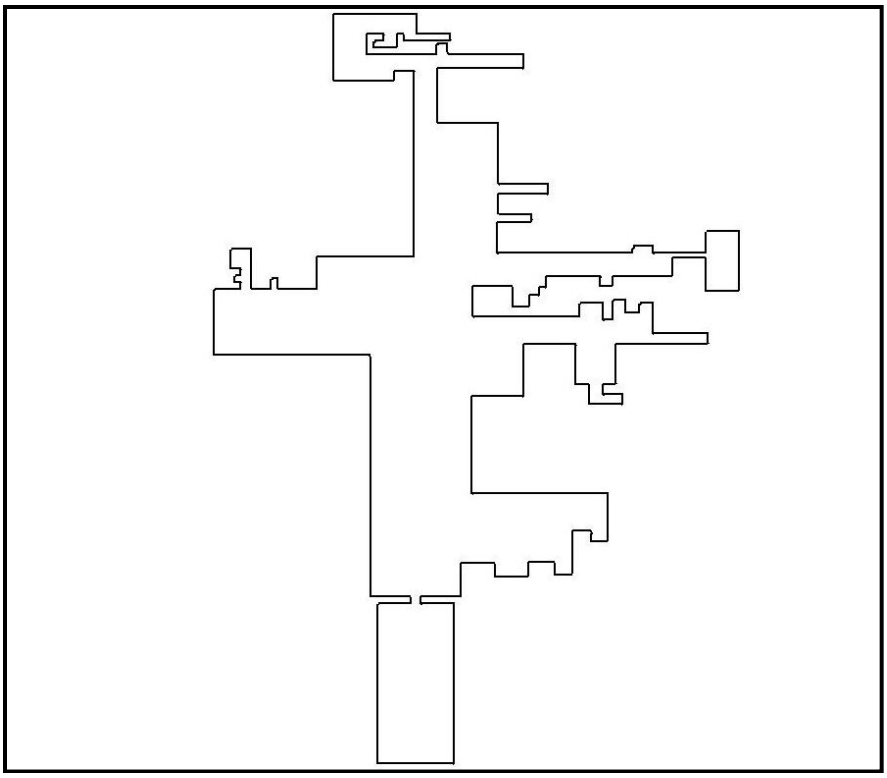

Figure 5-6. Block rectangular boundary definition in the logical domain.

Curvilinear-orthogonal grids are created by determining the computational domain coordinates (ξ,η) in the interior of the domain that correspond to the physical domain coordinates (x,y). Given that physical Cartesian coordinates (x,y) are linear in nature, Equation 1 can be used to determine grid vertex points in the interior of the domain.

$$\frac{\partial}{\partial \xi}\left(f \frac{\partial x}{\partial \xi} \right) + \frac{\partial}{\partial \eta}\left(\frac{1}{f} \frac{\partial x}{\partial \eta} \right) = 0 \tag{1a}$$

$$\frac{\partial}{\partial \xi}\left(f \frac{\partial y}{\partial \xi} \right) + \frac{\partial}{\partial \eta}\left(\frac{1}{f} \frac{\partial y}{\partial \eta} \right) = 0 \tag{1b}$$

where

$$f = \frac{h_\eta}{h_\xi} \tag{2}$$

is the scale factor ratio, and the scale factors are described by

$$h_\xi = \sqrt{\left(\frac{\partial x}{\partial \xi} \right)^2 + \left(\frac{\partial y}{\partial \xi} \right)^2} \tag{3a}$$

$$h_\eta = \sqrt{\left(\frac{\partial x}{\partial \mu}\right)^2 + \left(\frac{\partial y}{\partial \eta}\right)^2} \tag{3b}$$

GEFDC uses the method of Ryskin and Leal (1983) to generate the horizontal model grid. In this method, *f* is allowed to vary throughout the domain as it is first calculated on the boundary then interpolated into the domain in an iterative fashion until a sufficiently converged solution for the grid is found. In areas where the scale factors iterate towards zero, the GEFDC code was modified to incorporate the method of (Akcelik et. al., 2001) for nearly orthogonal two-dimensional grid generation with aspect ratio control. Using this method, additional terms are added to Equation (1) which makes the local scale factors approximately the mean scale factor across each grid line. Equation (4) shows the additional inhomogeneous source terms that are added to Equation (1).

$$\frac{\partial}{\partial \xi}\left(f\frac{\partial x}{\partial \xi}\right) + \frac{\partial}{\partial \eta}\left(\frac{1}{f}\frac{\partial x}{\partial \eta}\right) + P_X(h_\xi) + Q_x(h_\eta) = 0 \tag{4a}$$

$$\frac{\partial}{\partial \xi}\left(f\frac{\partial y}{\partial \xi}\right) + \frac{\partial}{\partial \eta}\left(\frac{1}{f}\frac{\partial y}{\partial \eta}\right) + P_y(h_\xi) + Q_y(h_\eta) = 0 \tag{4b}$$

where

$$P(h_\xi) = c\left(h_\xi - \frac{\overline{h}_\xi^2}{h_\xi}\right) \tag{5a}$$

$$Q(h_\eta) = c\left(h_\eta - \frac{\overline{h}_\eta^2}{h_\eta}\right) \tag{5b}$$

$P(h_\xi)$ and $Q(h_\eta)$ favorably control the value of the scale factors and thus improve the aspect ratio of the resulting grid. They act as distributed forces repelling or attracting neighboring grid points, preventing grid lines from collapsing, when the local scale factor deviates from the mean scale factors $\overline{h_\xi}$ and $\overline{h_\eta}$ (computed on grid lines of constant η and constant ξ, respectively). The aspect ratio forcing constant, c, controls the strength of the forcing functions and can be varied throughout the domain. Also to improve grid quality, GEFDC was modified to allow the grid boundary points to "slide" along the boundary from their initial evenly distributed positions during the iterative grid generation process resulting in boundary point distribution that allows for better orthogonality of the generated grid.

After the grid was generated by this method, grid cells that lay outside the 12 foot contour were removed from the grid resulting in a better approximation of the upper bounds of the marsh surface. The resulting grid has 85,157 cells ranging in size from less than 10 ft wide near the Chequessett Road Dike to more than 100 ft wide in the kettle ponds. The grid has satisfactory orthogonality and aspect ratio, as well as smooth boundary point distribution and smooth resolution change. A histogram showing the deviation from orthogonality for the Herring River model grid is presented in Figure 5-7 and a color contour plot in Figure 5-8 shows how this deviation is distributed throughout the model domain. More than half of the grid cells have less than 1 degree deviation from orthogonality while more than 90% of the cells have less than 6

degrees deviation. Essentially, this means the Herring River grid is of sufficient quality and has more than adequate resolution. The resolution of the model was determined to be adequate when the orthogonality deviation was small, but also such that critical components of the system were resolved in the model domain. For example, the dimensions of the existing, and potentially proposed, culverts could be defined in the model and the model could adequately define all road crossings, upland properties, etc. In general, the resolution of the model was 3 meters or less in most areas, which was adequate to define all the critical features within the system.

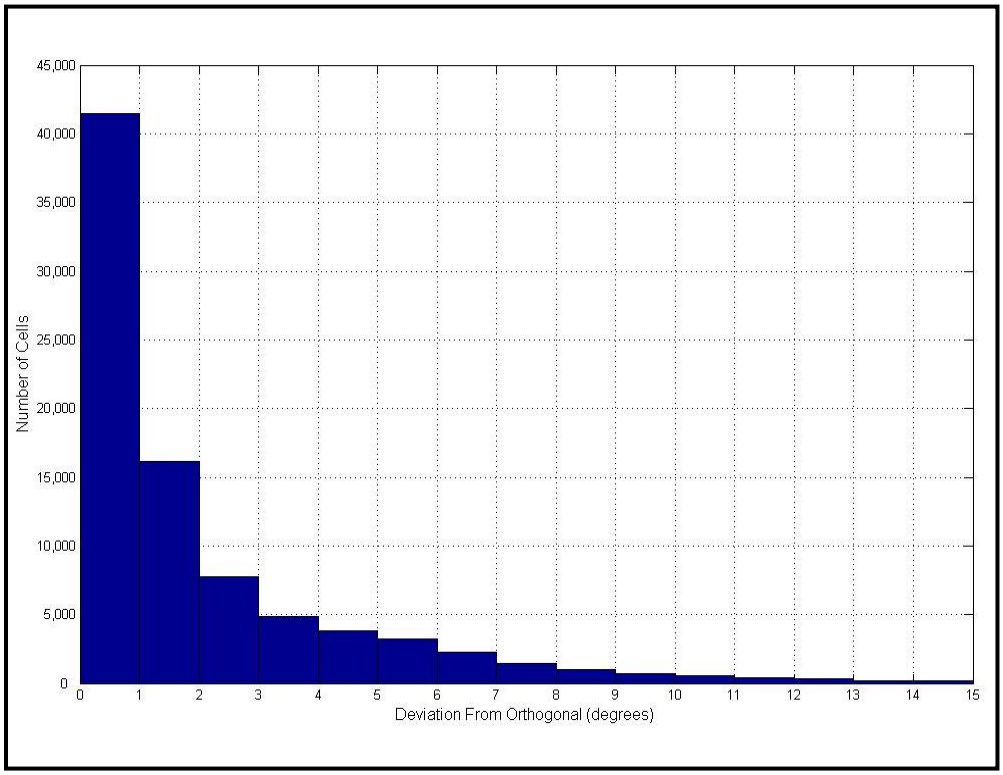

Figure 5-7. Histogram of grid cell deviation from orthgonality.

After the horizontal definition (2-D) of the grid was defined, the merged elevation data set was linearly interpolated to the model grid and the grid was carefully checked to ensure accurate elevation information. As discussed, bathymetric data were limited for most of the estuary's upper reaches including Mill Creek, Bound Brook and the upper parts of Pole Dike Creek and the Herring River. In all these areas, cell elevations were interpolated between measured data points to best represent the channel and marsh plain. The final model domain with colored elevation contours is presented in Figure 5-9, and a closer viewpoint of the Chequessett Road dike region is shown in Figure 5-10, to illustrate the detailed resolution in this region.

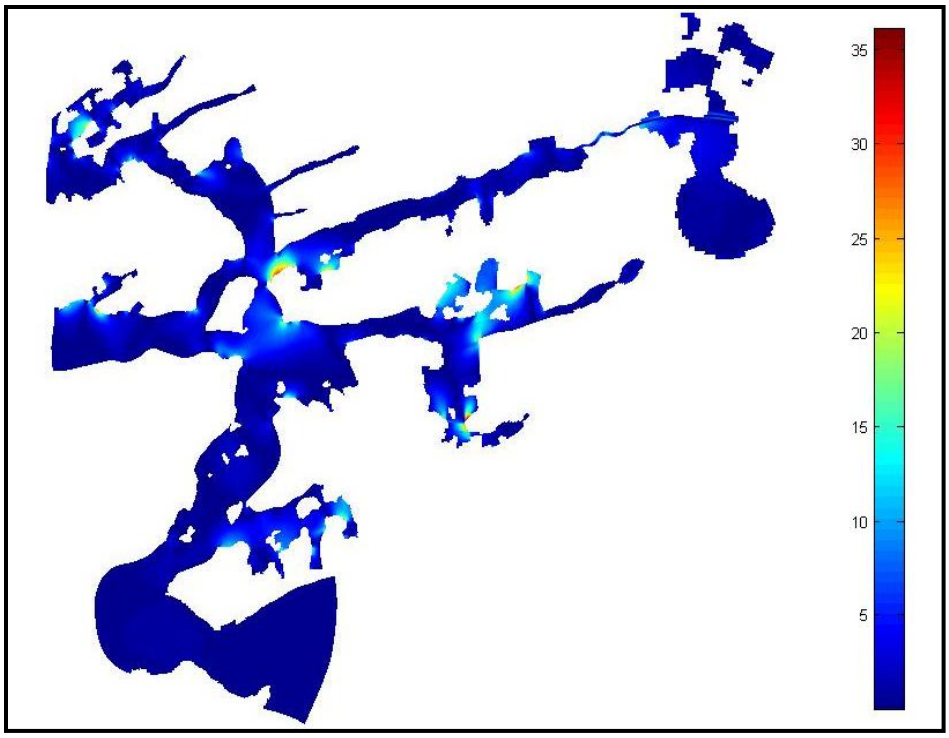

Figure 5-8. Color Contours showing deviation from orthogonality.

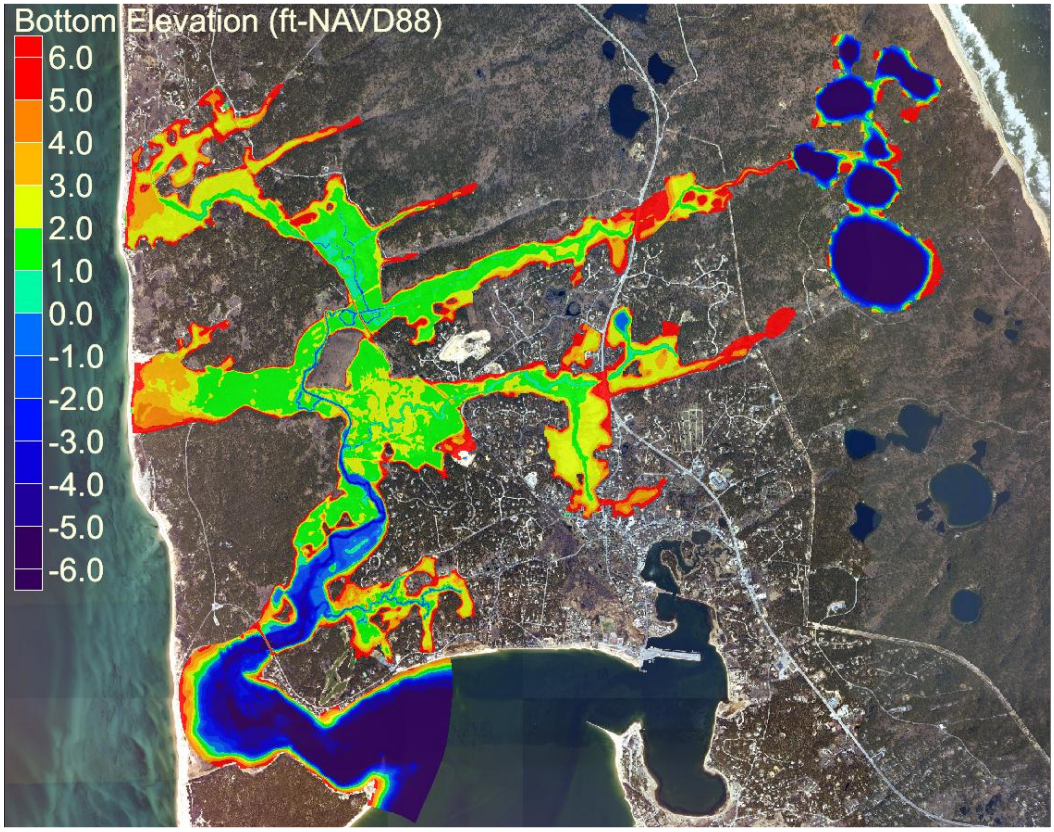

Figure 5-9. Herring River model grid bottom elevation contours.

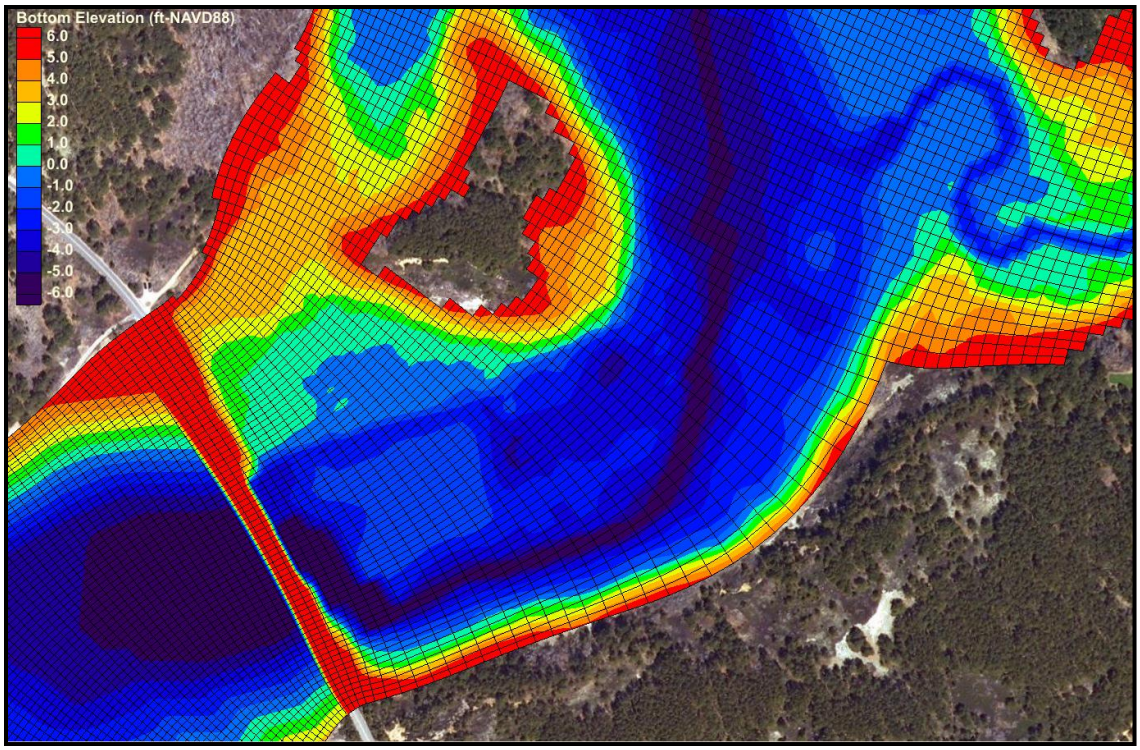

Figure 5-10. Detail of model grid showing bottom elevation contours and individual grid cells near the Chequessett Neck Road Dike.

5.2.2 Boundary Conditions

In order for the Herring River model to compute a hydrodynamic solution it is necessary to specify the model variables on the domain boundaries. Most of the model's boundary is considered to be a "land" boundary, which for the Herring River model was specified at an elevation of 12 feet NAVD88. This elevation provides the upper limit of expected water surface elevation during extreme storm events (100-year return period). At these land boundaries, water is constrained to flow only parallel to the boundary. The primary forcing for the model is provided by an open boundary at the southern end of the model domain in Wellfleet Harbor. At this location, time dependent water surface elevation and salt concentration is specified, as observed by gauge data from Wellfleet Harbor. Freshwater inflow volumetric flux is also specified in the model at three separate locations (Bound Brook, upper Herring River, and Pole Dike Creek) to simulate freshwater inflow into the estuary. The approximate location of these freshwater boundary conditions is shown in Figure 5-11. The red arrows show the freshwater influx locations, while the blue line shows the primary forcing boundary condition for water surface elevation and salinity. Figure 5-11 also shows the location of observation gauge stations in green. These stations are referenced throughout the report. All hydrologic data collected for this project was provided by various agencies (members of the HRRC) and provided to Woods Hole Group referenced to a vertical datum and corrected for atmospheric pressure.

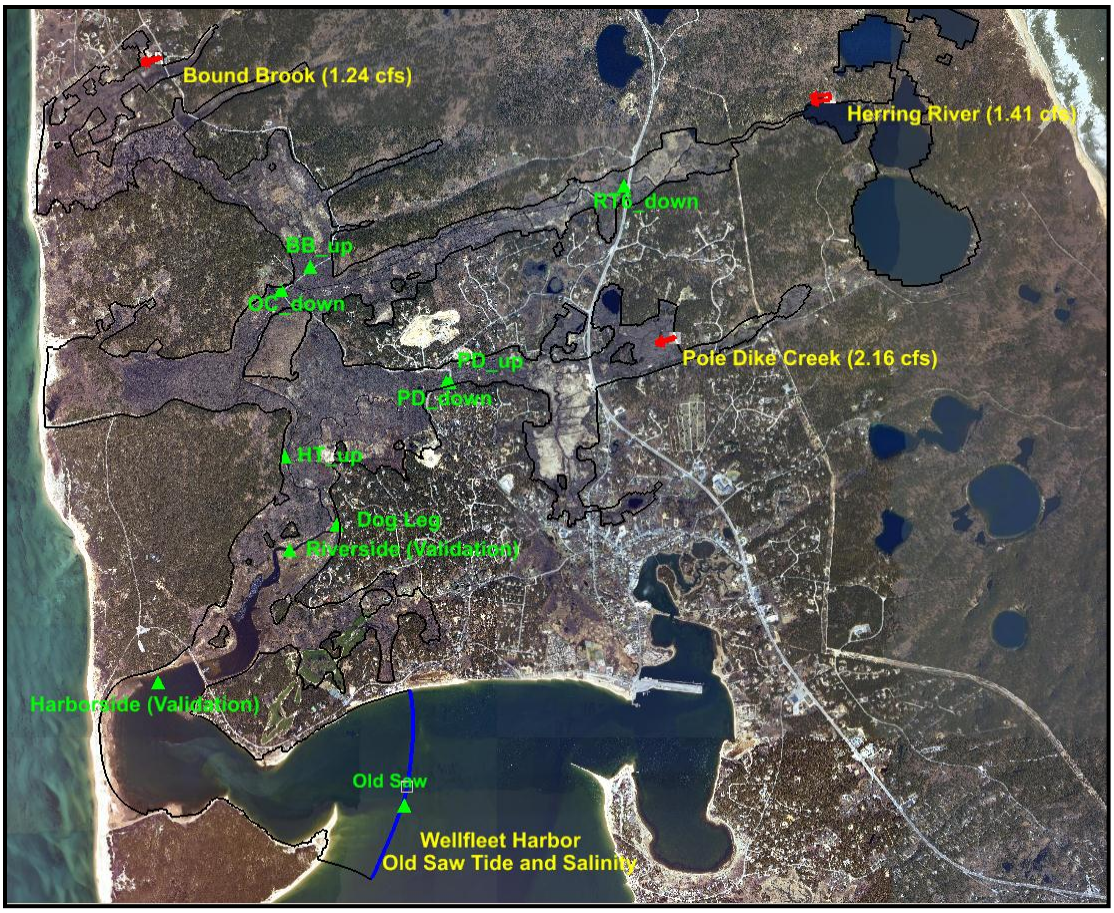

Figure 5-11. Locations of boundary conditions and observation gage locations.

Additional boundary conditions are applied over the entire model domain. These include atmospheric forcing and bottom frictional coefficients. For the Herring River model rainfall is input over the entire domain when appropriate and spatially variable bottom roughness length is specified and was varied to help achieve model calibration.

5.2.2.1 Tidal and Salinity Forcing Data

Tidal data observed at the Old Saw location, including water surface elevation and salinity measurements for the time period between September 4, 2007 and October 4, 2007 are shown in Figure 5-12. These data were used to provide the tidal boundary conditions for the model calibration period. During this time period, the tide progress through an entire spring-neap-spring cycle representing a good range of conditions for model calibration. Figure 5-12 represents one specific example of the tide data specified at the Wellfleet Harbor boundary condition. Additional tidal boundary conditions were used for model validation and simulation of various conditions and return period storm events, as described in greater detail later in this Chapter. For example, projected storm surge time series were developed for specification at the boundary for simulation of storm surge conditions.

The salinity data presented in Figure 5-12 was also used for calibration of the Herring River model to salinity values. Although Woods Hole Group did not collect the salinity data, there appears to be an error in the portion of the salinity time series presented in Figure 5-12 from approximately September 4 to September 8, 2007. Weather records during this time indicate no precipitation, no change in pressure, or any other weather condition that would have resulted in a natural depression in the salinity observations. In addition, the significant discontinuity that exists in the between the observed data (i.e., a change in salinity of approximately 7 part per thousand) in one sample step indicated there was likely a problem in the observations. If this occurrence was a natural phenomenon, the salinity levels would be expected to return to a more average level over a more gradual time frame. Therefore, these data (from September 4 to 8) were not used in the salinity calibration effort (section 5.3.3), while the remaining portion of the time series was used in the salinity calibration. For other scenarios (e.g., typical normal tidal conditions for tidal benchmarking, storm conditions) and alternatives (e.g., various dike openings), a constant salinity value of 30 practical salinity units (psu) was specified at the boundary condition in order to assess salinity penetration and compare alternatives more effectively. This constant value was derived from an average of the salinity observations from the Old Saw (Wellfleet Harbor) location.

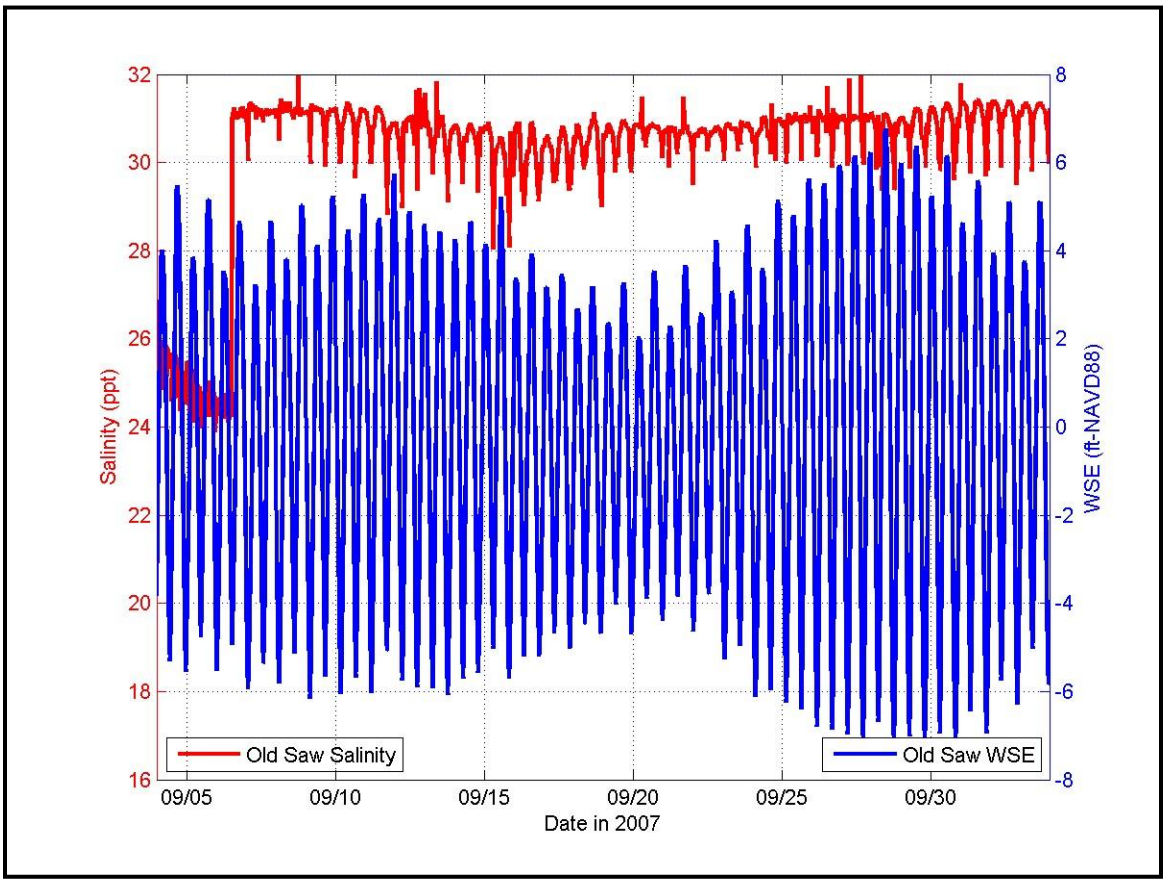

Figure 5-12. Water surface elevation and salinity at the Old Saw location during September 2007 (collected by NPS).

5.2.2.2 Freshwater Input

Freshwater input into the Herring River comes from a combination of rainfall, direct runoff, and groundwater flow. While the volume rate of freshwater input is known to be quite low, less than 11 cubic feet per second (Spaulding and Grilli, 2001; Roman 1987), actual fresh water input rates vary in time and spatial distribution, and are difficult to measure. Directly measured stream flow discharge data are not available for the river during the time periods used for model calibration and validation, which is a limitation of the model for the upper portions of the system. However, estimates of freshwater inflow by sub-basin produced by a USGS groundwater model (Masterson, 2004) were used as a starting point for providing freshwater inflow to the model domain at the Bound Brook, Upper Herring River, and Pole Dike Creek locations shown in Figure 5-11. The USGS groundwater model data are presented in Figure 5-13.

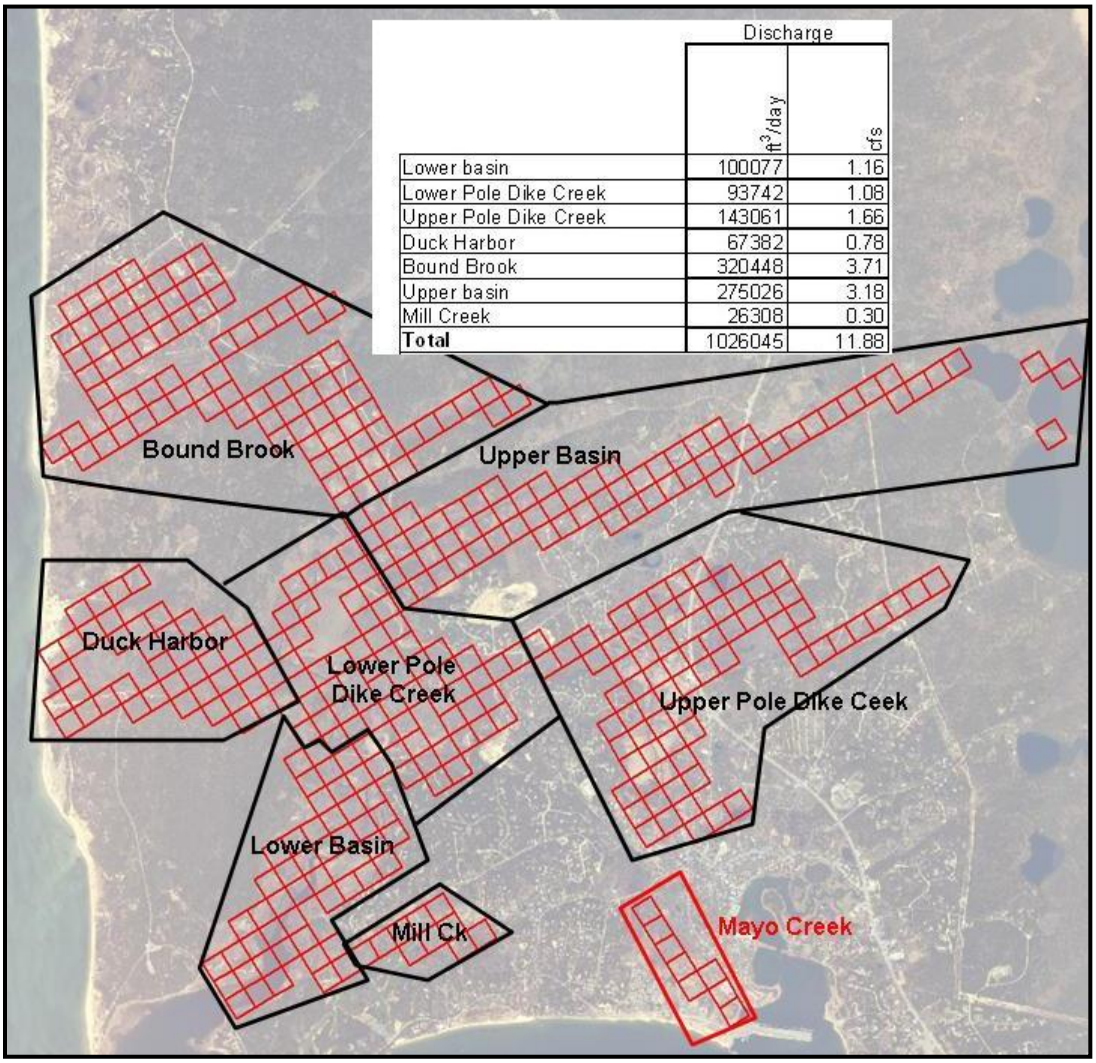

Figure 5-13. USGS groundwater model sub-basins and freshwater discharge by sub-basin.

Under existing conditions, the model results in the upper brooks and creeks was sensitive to the volumetric flux of freshwater inflow. This was particularly true in the upper reaches of the estuary where the tidal influence is minimal. In these areas, the brooks and creeks were primarily riverine in character, and therefore were more sensitive to the freshwater inflow under existing conditions. Since no freshwater flow observations were made during the calibration time period, the freshwater inflow was varied within reasonable ranges at the three input locations. Ultimately, constant freshwater inflow was specified for model calibration and validation at the constant flow rates shown in Figure 5-11 (1.24 cfs for Bound Brook, 1.41 cfs for upper Herring River, and 2.16 cfs Pole Dike creek). These flow rates are reasonable compared to output from the USGS groundwater model and information from the previous two modeling studies (Roman 1987, Spaulding and Grilli 2001). They also provide good agreement for observed water surface elevations for calibration of the Herring River model. These rates will ultimately vary given different environmental conditions; however, they are reasonable approximations of the freshwater inflow during the typical time periods associated with the calibration and validation. As tides are restored to the estuary system, the relative contribution of freshwater input will become less important when compared to tidal influences, and therefore the Herring River system becomes far less sensitive to freshwater inflow variations for the restoration alternatives.

5.2.2.3 Atmospheric Data

Bihourly precipitation data collected at the National Atmospheric Deposition Program (NADP) station MA01, as shown in Figure 5-14, was used to provide rainfall input to the model. Figure 5-15 shows the bihourly rainfall totals collected during September of 2007. Rainfall from this single location is assumed to fall uniformly over the entire model domain when applicable, which may not be an accurate assumption considering the significant land area that comprises the Herring River estuarine system.

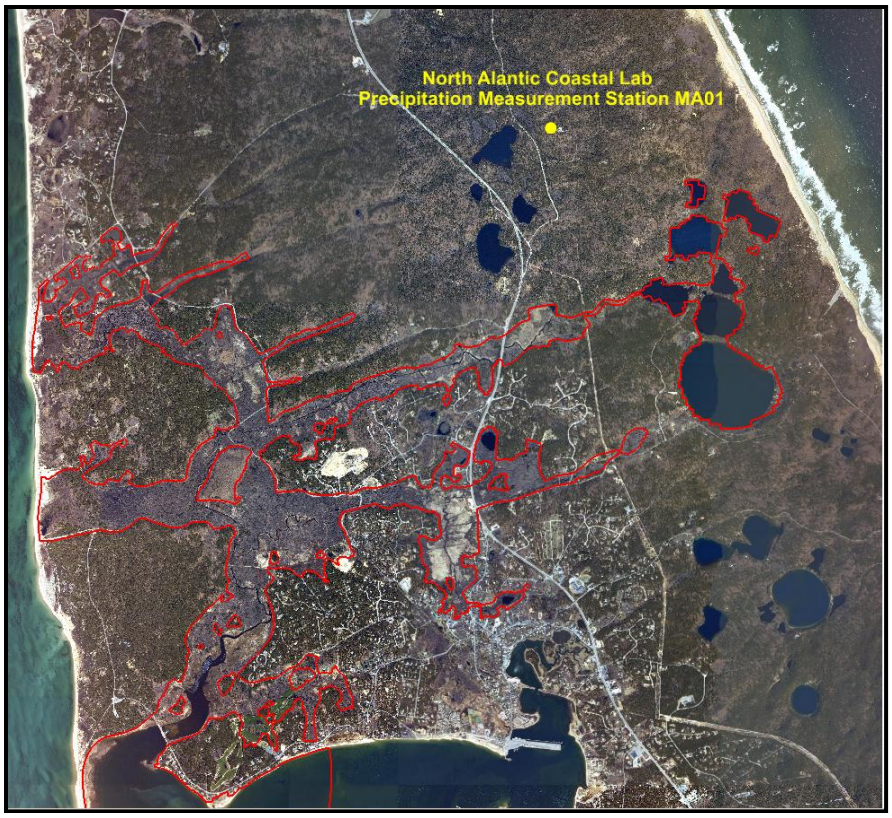

Figure 5-14. Location of rainfall observations used to specify rainfall levels within the model during calibration and validation time periods.

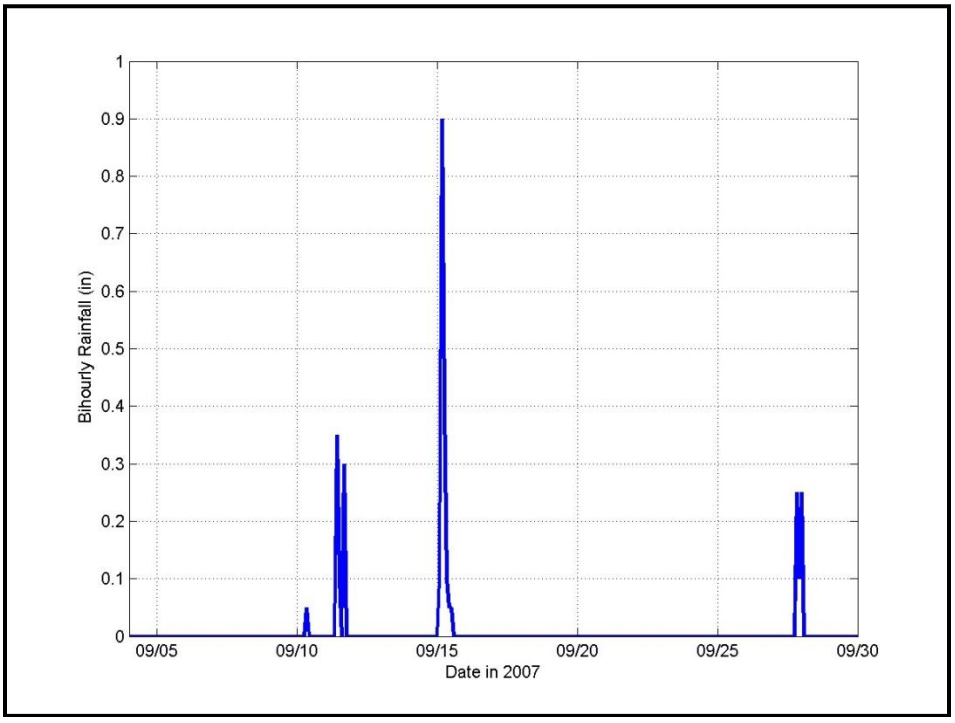

Figure 5-15. Bihourly rainfall collected at NADP station MA01 during September 2007.

5.2.2.4 Bottom Friction

EFDC uses the log law roughness length to parameterize bottom drag forces. Roughness length is a composite resistance including both form-drag and skin friction of the sediment and is a dynamic length rather than a mere geometric scale. EFDC utilizes a quadratic friction relationship to relate the bottom stress to the velocity in the bottom cell layer. The bottom stress ($\vec{\tau}$) is calculated as:

$$\frac{\vec{\tau}}{\rho} = C_d\sqrt{u^2 + v^2}(\vec{u} + \vec{v}) \tag{6}$$

Where C_d is a quadratic drag coefficient, $\vec{u}$ and $\vec{v}$ are the *x* and *y* components of the velocity, and ρ is the water density. Assuming that the bottom boundary layer exhibits a logarithmic velocity profile, the drag coefficient can be related to the dimensional roughness length (Z_0) by:

$$C_d = \left(k\frac{1}{\ln\left(\frac{H}{Z_0}\right)} \right)^2 \tag{7}$$

where *k* is the Von Karman constant and H is the depth of the flow. In EFDC, values of Z_0 are specified by cell to control the bottom drag forces. Physically, Z_0 represents the distance from bottom within the bottom boundary layer at which the velocity appears to go to zero based on the logarithmic velocity profile.

Each grid cell may have a different value for roughness length. Physically, bottom drag forces depend on a number of phenomena that are difficult to characterize. These include bottom material type, growth of biota, and the amount of channel meander, which all contribute to the overall energy loss that are accounted for by the roughness length. Because the bottom friction parameterization in the model accounts for the effect of a number of different factors, it is difficult to determine a priori what values will provide the best results and thus it is typically used as the primary parameter for "tuning" the model. For the Herring River model, a value of 0.033 meters was initially used throughout the model domain. Then local adjustments were made to the roughness length values in order to improve the model results to match observed data. Table 5-1 summarizes the roughness length values used for the final calibration of the Herring River model. These values are considered within the range of normal bottom friction values determined through empirical laboratory testing. However, the value used in the lower portion of Pole Dike Creek is relatively high. Observed data at the Pole Dike Creek gauge locations show the complete dampening of the tidal signal at this point in the estuary. This is likely due to the dense submerged aquatic vegetation (SAV) that exists in this creek and other vegetative influences in this relatively narrow channel. Observations conducted in 2008 indicated the creek to be almost impenetrable by canoe. Therefore, there are significant frictional and/or constriction influences in this portion of the estuarine system. In order to match

the observed water surface elevations in this portion of the estuary, a higher roughness length value was specified for the Pole Dike Creek portion of the estuary.

Table 5-1. Bottom roughness length for the Herring River model.

Location Description	Roughness length (meters)
Herring River between Chequessett Neck Rd dike and High Toss Rd	0.025
Herring River between High Toss Rd. and Bound Brook Is. Rd.	0.05
Herring River between Bound Brook Is. Rd. and Route 6	0.06
Lower Pole Dike Creek	0.20
Remaining Model Domain	0.033

5.2.3 Control Structures

In addition to the culverts and gates at the Chequessett Neck Road dike, there are sixteen additional hydraulic control structures found within the Herring River estuary. Therefore, due to the high number, as well as varying type of anthropogenic influences, EFDC was upgraded to specifically model these types of control structures, as well as a number of other future potential control structures that may be implemented in the adaptive restoration process. Additional subroutines were applied within the EFDC code, using well established methods to dynamically compute discharge though the control structures. Flow charts showing the decision tree and equations used by these subroutines for calculating flow through circular pipe culverts, slide (sluice) gates, and flapper gates are described in more detail throughout this section. The locations of the control structures within the Herring River estuary are shown in Figure 5-16, with the control structures that are directly modeled labeled in blue. Control structures that were of less importance, specifically those located in the far upper reaches of the system, are shown in red and were not directly included in the model simulations. Circular pipe culverts that were installed throughout the system are of various lengths, pipe diameters, and construction materials.

5.2.3.1 Culverts

The characteristics of flow through culverts are complicated by many variables including the geometry, slope, size, roughness, approach, and headwater and tailwater conditions. Chow (1959) classified flow through a culvert into six flow types based on culvert slope, culvert height, headwater depth and tailwater depth and presents a method for approximating the flow. This method was simplified by assuming only hydraulically long culverts (limiting the number of flow types to four) and implemented in a subroutine within EFDC to dynamically calculate the flow though the culverts. Figure 5-17 presents a flowchart, which describes how the flow is determined within this subroutine. At each model time step, the discharge through each culvert is calculated and the appropriate volume is transferred from the upstream culvert cell to the downstream culvert cell. The tailwater and headwater depths are also determined dynamically in the model, since the tidal fluctuations result in bidirectional flow through each of the culverts.

For the Herring River model, culvert invert elevations and construction material detailed in the 2006 Slade and Associates Inc. low-lying road survey were used to provide input for the culverts. Some culvert lengths had to be estimated from aerial photographs and historic survey

records since limited information was available for some upstream culverts. These estimates were likely within feet of the actual culvert lengths, did not inhibit the ability to calibrate, or impact the accuracy of the model. An initial value of 0.035 was used for the friction coefficient for each culvert, a typical value for culvert friction. During model calibration, some culvert roughness values were adjusted to provide better agreement between model results and observations. The final culvert parameters used in the calibrated model are summarized in Table 5-2.

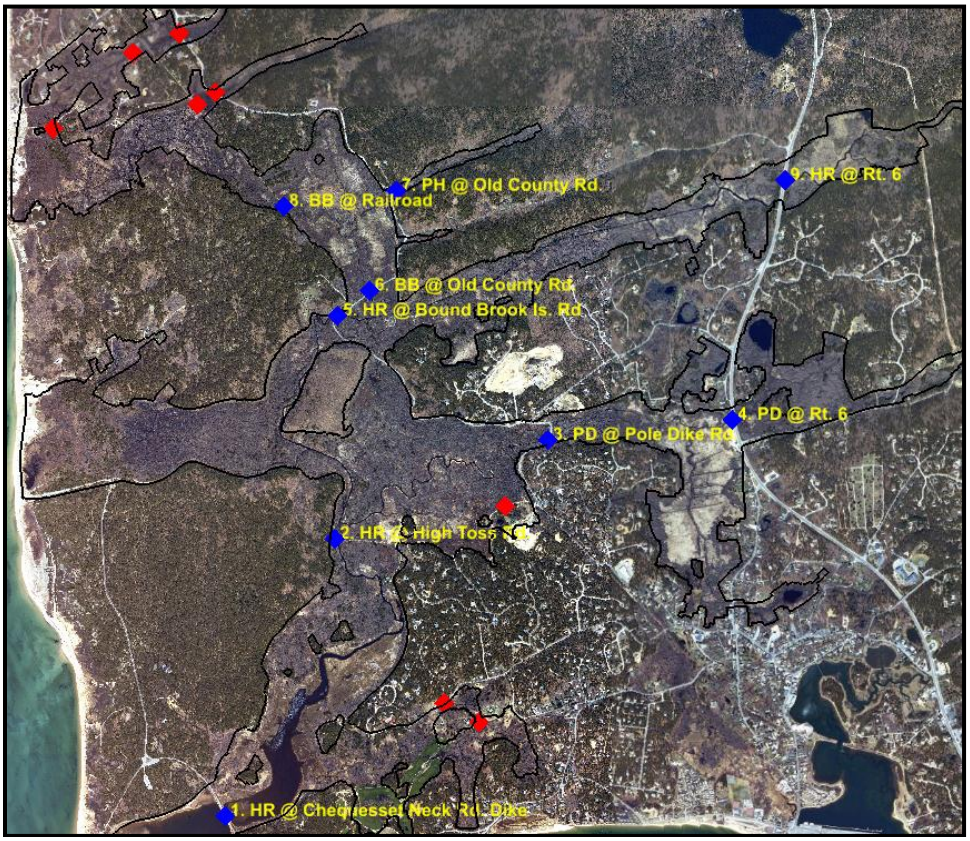

Figure 5-16. Location of culverts in the Herring River estuary. Locations presented in blue were dynamically simulated within the model, while those in red were treated as simple hydraulic connections.

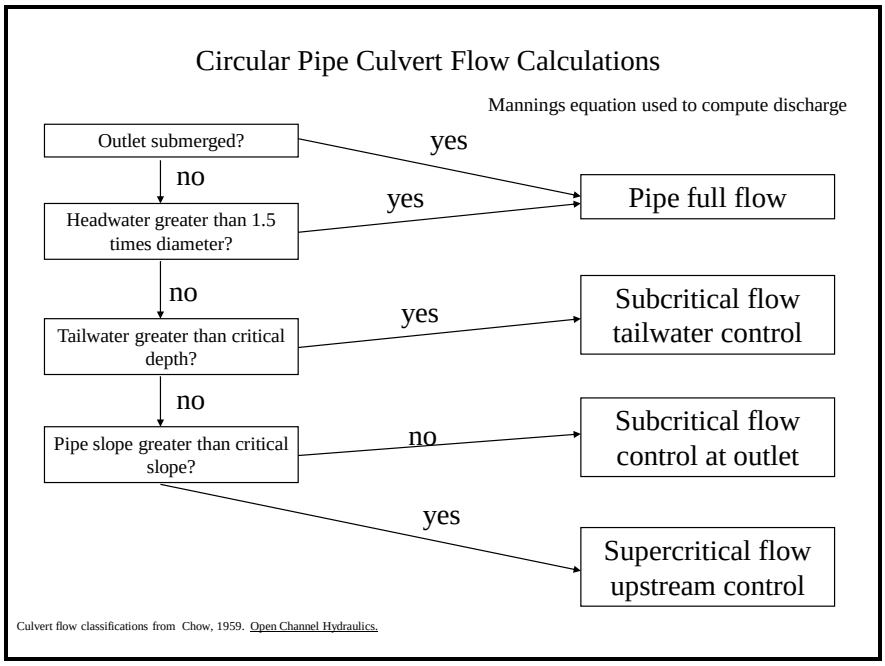

Figure 5-17. Flow chart for culvert flow type determination in the Herring River model.

Table 5-2. Herring River model circular pipe culvert details.

Location	Material	Length (ft.)	Dia. (ft)	Upstream Invert (ft - NAVD88)	Downstream Invert (ft - NAVD88)	Manning's n
Herring River @ High Toss Rd.	Concrete	39	5	-3.8	-4.3	0.035
Pole Dike Creek @ Pole Dike Rd.	Ceramic	46	3	-1	-1.3	0.035
Pole Dike Creek @ Rt. 6	Concrete	86	3	-0.44	-0.64	0.035
Herring River @ Bound Brook Is. Rd.	Concrete	46	5	-3.3	-3.5	0.04
Bound Brook @ Old County Rd.	Ceramic	36	2	-2.1	-2.3	0.08
Paradise Hollow @ Old County Rd.	Ceramic	49	0.5	-0.1	-0.75	0.035
Bound Brook @ Railroad	Corrug. Metal	82	2	-2.6	-2.6	0.035
Herring River @ Rt. 6	Concrete	82	7	-2.2	-2.2	0.035

5.2.3.2 Slide (Sluice) Gates

Tidal flow from Wellfleet Harbor into the Herring River estuary is currently controlled by a single sluice gate in the Chequessett Neck Road dike. An accurate model of the entire estuarine system in its existing state depends greatly on accurate representation of this single control

structure. Therefore, a subroutine designed specifically for dynamically calculating the discharge through a slide (sluice) gate(s) was incorporated into the EFDC code. Flow through a slide (sluice) gate can be characterized by two basic parameters: the nature of the flow (subcritical or supercritical flow) and the water depth (gate submerged or not). Figure 5-18 shows how the sluice gate flow is characterized in the model based on these parameters. When the water surface is effectively determined to be below the top of the gate, the gate is modeled as a broad crested weir. When the gate is submerged, the appropriate equation for either free sluice flow (super-critical) or submerged orifice flow (sub-critical) is applied. To determine the flow through the sluice gate at a given model time step the depth of water on the upstream side of the gate is compared to the depth on the downstream side of the gate. If the depth on the downstream side is less than 0.64 times the depth on the upstream side, the red colored path in Figure 5-18 is applied and the appropriate super-critical flow equations are used. If the ratio of downstream head to upstream head is greater than 0.68, the purple colored path is applied and the appropriate formula for subcritical flow (sub-critical weir or submerged orifice) is applied. Otherwise both discharges are computed and a weighted average of the two is used (the yellow path). The equations for calculating broad-crested weir flow are the same as those applied to barrier flow in SIMSYS2D (Leendertse, 1987). For super-critical weir flow,

$$Q = C1 \times W \times \frac{2}{3} \times \sqrt{\frac{2}{3} G} \times H_{up}{}^{\frac{2}{3}} \tag{8}$$

for sub-critical weir flow,

$$Q = C2 \times W \times H_{dw} \times \sqrt{2G(H_{up} - H_{dw})} \tag{9}$$

where $C1$ and $C2$ are the super-critical and sub-critical discharge coefficients respectively, W is the width of the gate, G is acceleration due to gravity, and H_{up} and H_{dw} are the upstream and downstream depths above the gate bottom. The equations used to compute free sluice flow and submerged orifice flow are the same as those applied in the Brunner (2002). For free sluice flow,

$$Q = C3 \times W \times B \times \sqrt{2GH_{up}} \tag{10}$$

and for submerged orifice flow,

$$Q = C4 \times W \times B \times \sqrt{2G(H_{up} - H_{dw})} \tag{11}$$

where $C3$ and $C4$ are discharge coefficients for free sluice flow and submerged orifice flow respectively and B is the height of the gate opening. The invert elevation, gate opening, and discharge coefficients applied in the calibrated Herring River model are shown below in Table 5-3. The opening height refers to the distance between the bottom of the culvert and the bottom of the sluice, or in other words, the vertical distance of the opening.

Different values of the discharge coefficients were used during an ebb and flood flow to achieve the best agreement between model results and observations. A similar approach was taken by

Spaulding and Grilli (2001) in their inlet-basin model, where less frictional loss was applied during a flooding tide. Considering that the modeled sluice gate must reproduce the observed flow in the real system (a sluice gate that is asymmetrically placed in the downstream end of a box culvert) and that flows observed during flood and ebb tides exhibit different set-down characteristics, the use of variable discharge coefficients should be acceptable and provides the best agreement between modeled results and observations.

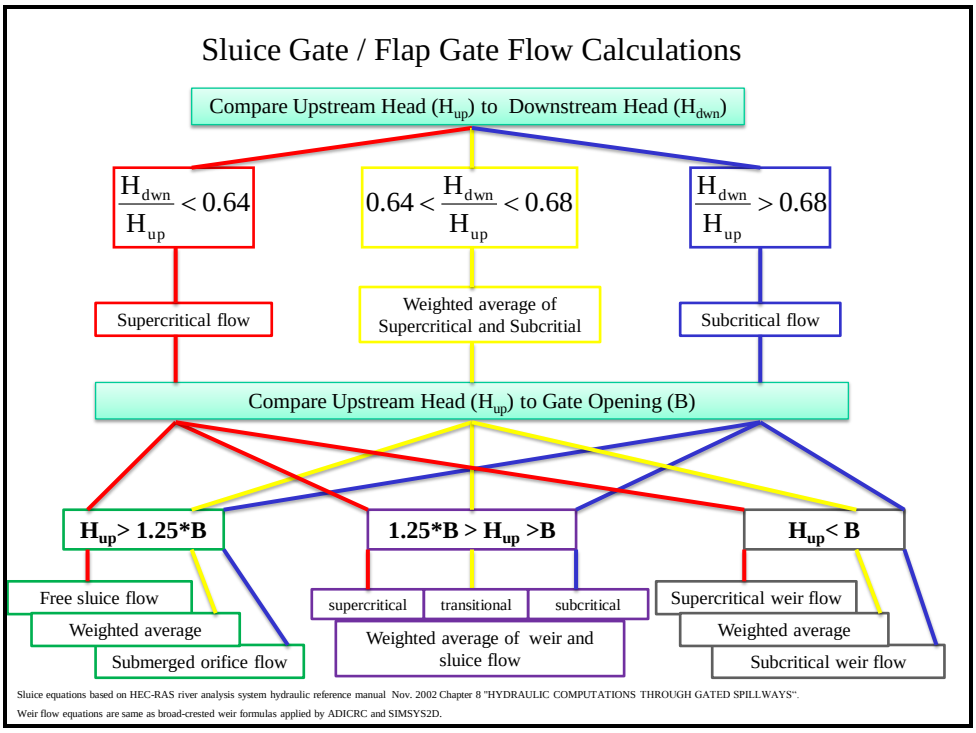

Figure 5-18. Flow chart for sluice and flap gate flow type determination for the Herring River model.

Table 5-3. Sluice gate invert elevation, opening height, and discharge coefficients.

Gate	Invert Elevation (ft-NAVD88)	Opening Height (ft)	C1	C2	C3	C4
Sluice Upstream	-3.38	1.67	1.375	1.375	1.4	1.35
Sluice Downstream	-3.38	1.67	1	1	0.6	0.8

5.2.3.3 Flap Gates

While a flooding tide is severely limited by the existing slide (sluice) gate, ebbing tide has significantly greater conveyance since the flap gates on the two neighboring box culverts open

during an ebb flow under existing conditions. The flap gates are modeled like the sluice gate with a few modifications. The flap gates are modeled at all times as broad crested weirs with an additional head loss, *HL,* which reduces the depth, H_{up}. The additional head loss is varied depending on the how much the flap is open. It is assumed, in order to open the flap some additional energy is required. As the flap opens, the energy required to hold it open decreases, as the water level increases. The additional head loss is calculated by:

$$HL = HL_{\max} \times \left(1 - \frac{\frac{1}{2}\left(H_{up} + H_{dw}\right)}{D_{HL}} \right) \tag{12}$$

The values used in the calibrated Herring River model are presented below in Table 5-4.

Table 5-4. Flap gate discharge coefficients and additional head loss parameters.

Gate	HL_{max} (ft)	D_{HL} (ft)	$C1$	$C2$
Flapper gates	1.97	2.9	1.375	1.375

5.3 MODEL CALIBRATION

Model calibration is the process in which model parameters are systematically adjusted through a range of acceptable values and results are examined using standard measures of error. Through a number of iterative simulations the configuration of model parameters (e.g., roughness lengths, culvert friction factors, diffusivity parameters, etc.) that provided the best agreement between modeled variables and observed measurements is determined. Parameters adjusted during calibration of the Herring River model include: bottom roughness lengths, pipe culvert roughness coefficients (Manning's n), and sluice gate and flap gate discharge coefficients. The values presented in Tables 5-1 thru 5-4 are those used in the calibrated model. The Herring River model was calibrated to observations collected between September 5, 2007 and October 3, 2007 at seven locations throughout the estuary. These locations are shown in Figure 5-11 and descriptions of their locations are given in Table 5-5.

The model performance is evaluated by comparing time series output from the model to observed time series for both water surface elevation and salinity at specific locations throughout the modeling domain. The results are presented visually as time series plots and scatter plots, and absolute error of the model is quantified by calculating the bias and Root Mean Square Error (RMSE). Additionally, the most dominant tidal constituents (both amplitude and phase) as determined from tidal constituent analysis are compared.

Table 5-5. Description of observation station locations.

Gauge Name	Location/Description
Dogleg	Approximately 5000 ft upstream of the Chequessett Neck Road Dike
HT_up	Immediately upstream of the culvert at High Toss Road
PD_down	Immediately downstream of the Pole Dike Creek culvert under Pole Dike road
PD_up	Immediately upstream of the Pole Dike Creek culvert under Pole Dike road
OC_down	Immediately downstream of the culvert on the main stem of the Herring River under Old County road
BB_up	Immediately upstream of the culvert on Bound Brook under Old County Road
Rt6_down	Immediately downstream of the culvert on the main stem of the Herring River under Route 6

The time series plots allow for a direct visual comparison of how the observed and modeled variables evolve through time and provide a "first glance" at the performance of the model. On the scatter plots, a point is plotted showing the modeled value for each discrete observed value. When the model has perfect agreement with the observed data, the points lie on a line with a slope of unity (45 degrees) passing through the origin. The vertical distance between a point on the scatter plot and the line of perfect agreement represents the model error for that particular measurement. The overall error for a given observation time series is quantified in two ways:

$$Bias = \frac{\sum_{1}^{n}\left(p_{\mathrm{mod}} - P_{obs}\right)}{n} \tag{13}$$

$$RMSE = \sqrt{\frac{\sum_{1}^{n}\left(p_{\mathrm{mod}} - p_{obs}\right)^{2}}{n}} \tag{14}$$

Where P_{mod} and P_{obs} are the modeled and observed values respectively and n is the number of discrete measurements in the time series. The bias provides a measure of how close on average the modeled results are to the observed data. A positive value indicates that the model is over-predicting the observation while a negative value indicates that the model is under-predicting the observations; a bias of zero indicates that on average over the time series the model reproduces the observations. The RMSE is an average of the magnitude of the error of each measurement in the time series. RMSE is always positive with smaller values indicating better model

performance. Both the bias and RMSE are measures of absolute error having the same units of the measured quantity from which they are computed.

The U.S. EPA provides technical guidance on error statistic criteria for estuarine water quality models recommending that hydrodynamic variables (i.e. water surface elevation) have relative error less than 30% and transport variables (i.e. salinity) have relative error less than 25% (EPA, 1990). For example, to compute relative error for water surface elevation the RMSE is normalized by the mean tidal range for Wellfleet Harbor of 9.74 feet.

5.3.1 Water Surface Elevation Calibration

This section presents the results of the calibrated Herring River model for water surface elevation. Visual comparison for the Dogleg and just upstream of the High Toss Road locations are shown in Figures 5-19 and 5-20, respectively. Figures 5-21 through 5-27 show scatter plots for all observation gauge locations, and include the Bias and RMSE error on each plot. Error measures for all observation gauge locations are summarized in Table 5-6. At the Dogleg gauge, results have a relative error less than 1% of the Wellfleet Harbor tidal range. Upstream of High Toss Road (HT_up), the error is nearly as small with a slight over-prediction of the peak water levels corresponding to rainfall events and a slight over-prediction of the overall tidal range. Downstream of Old County Road (OC_down) and upstream of Bound Brook (BB_up), the discrepancy in rainfall induced peaks and tidal range becomes more apparent, however, the error is still small and well within recommended limits. For example, the peak that occurs after the September 15, 2007 rain event at the BB_up location that is over predicted by nearly one foot may be accounted for by the potentially oversimplified assumption of equally distributed rainfall amounts. Additionally, actual runoff rates into the main channels are potentially slowed by the resistance of the multitude of small streams and ditches which feed the larger channels, infiltration into the soil, resistance to flow from vegetation, and evapotranspiration. The lack of actual runoff rates and freshwater inflow data (a constant within a reasonable range was assumed is discussed in Section 5.2.2.2) also is a source of the potential error. These freshwater inflow rates would be expected to increase in observed data, but could not be included in the model. However, since the main goal of the model is accurate prediction of tidal propagation, and not rainfall runoff directly, this is not a significant concern. As shown in the next section (tidal constituent calibration), when calibrating the model just to tidal processes, the error is less than an inch at all locations.

Overall the agreement is reasonable. The magnitude of the bias is less than 0.11 feet for all locations meaning that the calibration simulation reproduced average water levels that are within an inch or two of observed levels. RMSE is less than 0.4 feet for all locations indicating that on average the modeled water level is within a few inches of the observed level at any given time.

Generally, in the locations where tidal influence is apparent, the modeled water surface is characterized by a slight over prediction of the tidal range, which increases with distance upstream of the dike. In other words, the tidal range predicted by the model is slightly larger than the observed tidal range. This result can somewhat be expected when considering that the streams above High Toss road are quite narrow, in some places only a few meters wide. While the model grid resolution is quite high, it is not able to fully resolve the narrower streams and their meanders in the upper reaches of the estuary. Because of this and other less understood factors (e.g. resistance due to algal growth, micro-topography, storage in the marsh soils, SAV

growth, anthropogenic flow blockages) in the upper reaches and marsh plains of the actual estuary, there is likely slightly greater tidal attenuation in reality than what is shown in the model. However, even considering these factors, the results are still well within recommended error levels, with average water levels within 0.1 feet of those observed. As such, the calibrated model reproduces the observed water levels within inches at all locations. The RMSE relative to the Wellfleet Harbor tidal range is less than 3.7% for all gages and is well below the 30% limit recommended by the EPA for model calibration.

Table 5-6. Calibration water surface elevation error measures.

Gauge Location	Bias (ft)	RMSE (ft)	Relative Error (%)
Dogleg	-0.01	0.097	1.00
HT_up	0.05	0.102	1.05
PD_down	-0.11	0.150	1.54
PD_up	-0.06	0.133	1.37
OC_down	0.06	0.166	1.70
BB_up	0.08	0.357	3.67
Rt6_down	-0.10	0.179	1.84

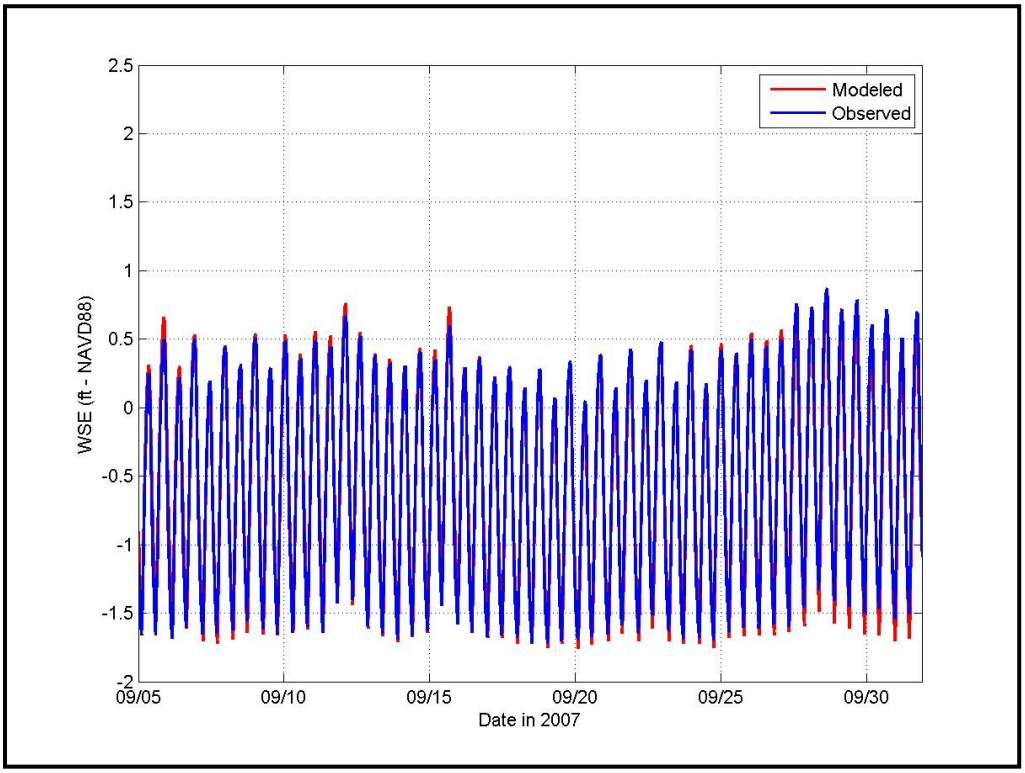

Figure 5-19. Dogleg water surface elevation comparison for modeled (red) and measured (blue) time series.

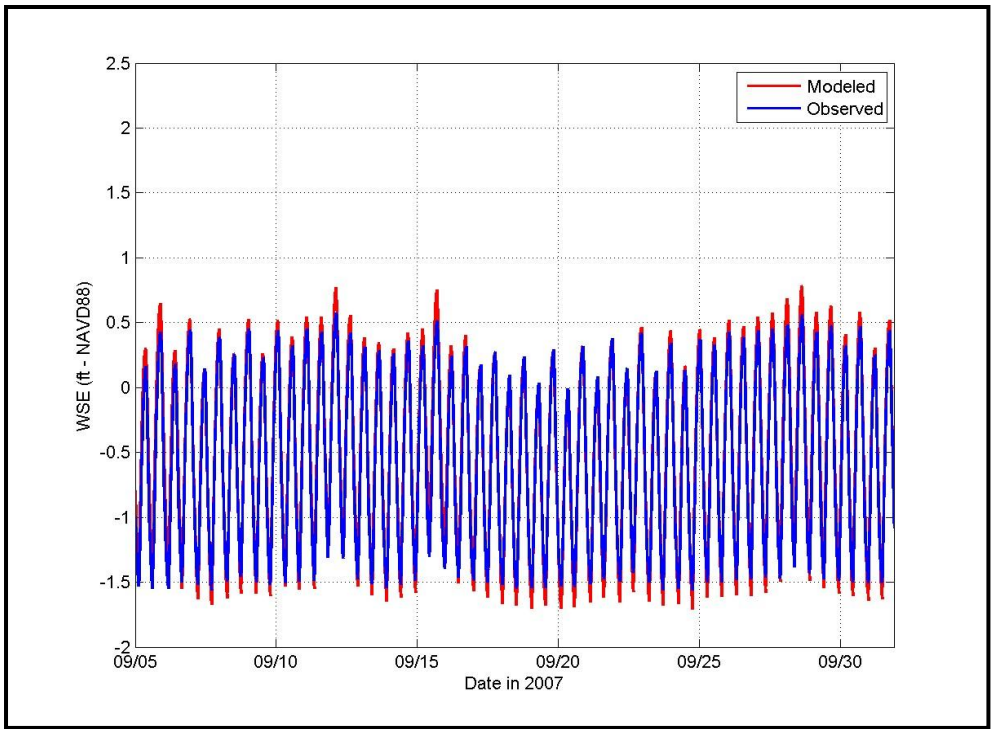

Figure 5-20. Upstream of High Toss Road (HT_up) water surface elevation comparison for modeled (red) and measured (blue) time series.

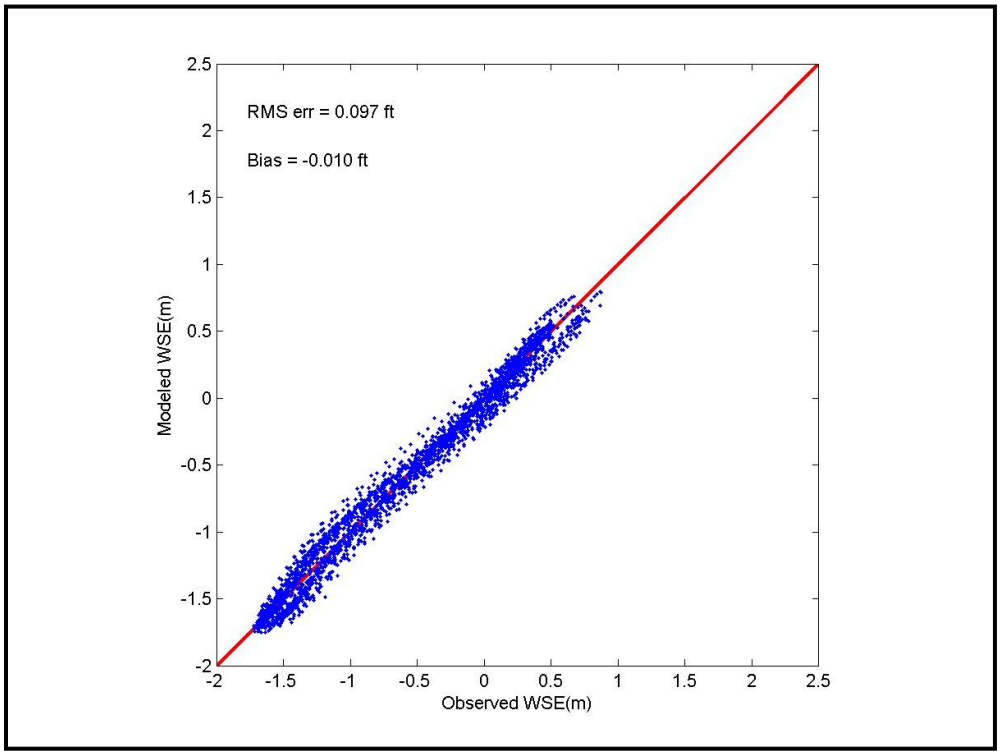

Figure 5-21. Dogleg water surface elevation scatter plot comparing modeled and measured water surface elevations.

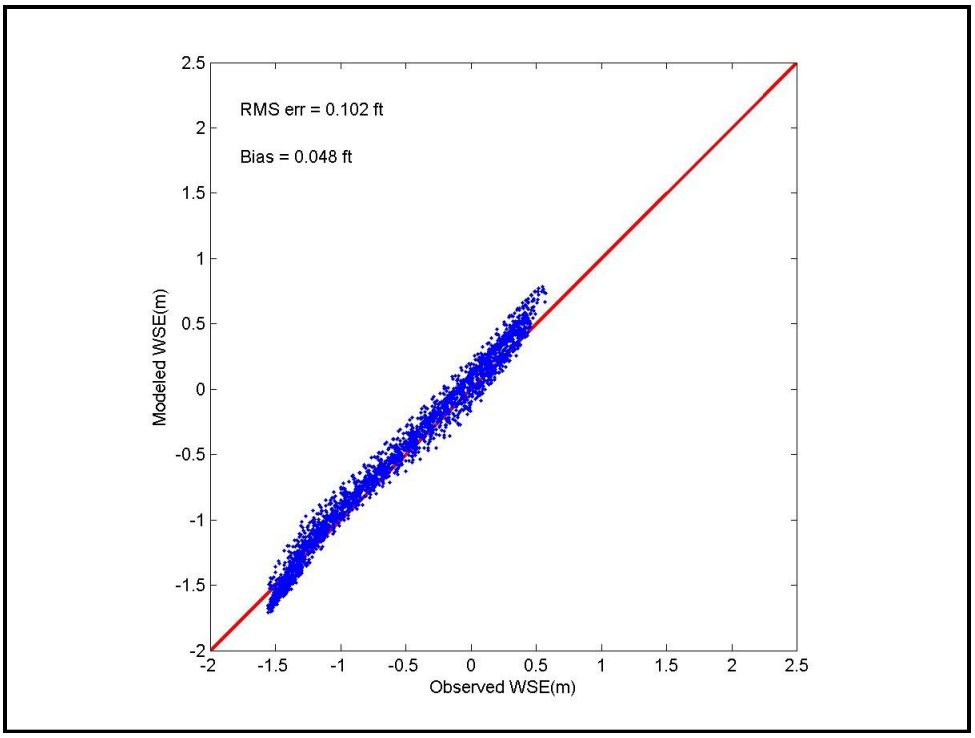

Figure 5-22. HT_up water surface elevation scatter plot comparing modeled and measured water surface elevations.

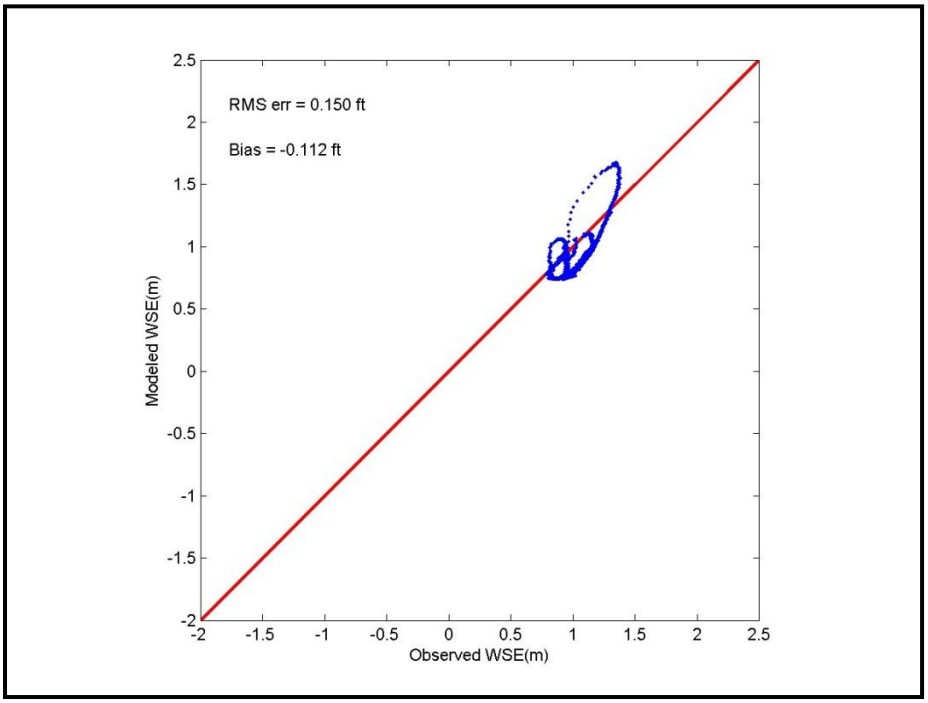

Figure 5-23. PD_down water surface elevation scatter plot comparing modeled and measured water surface elevations.

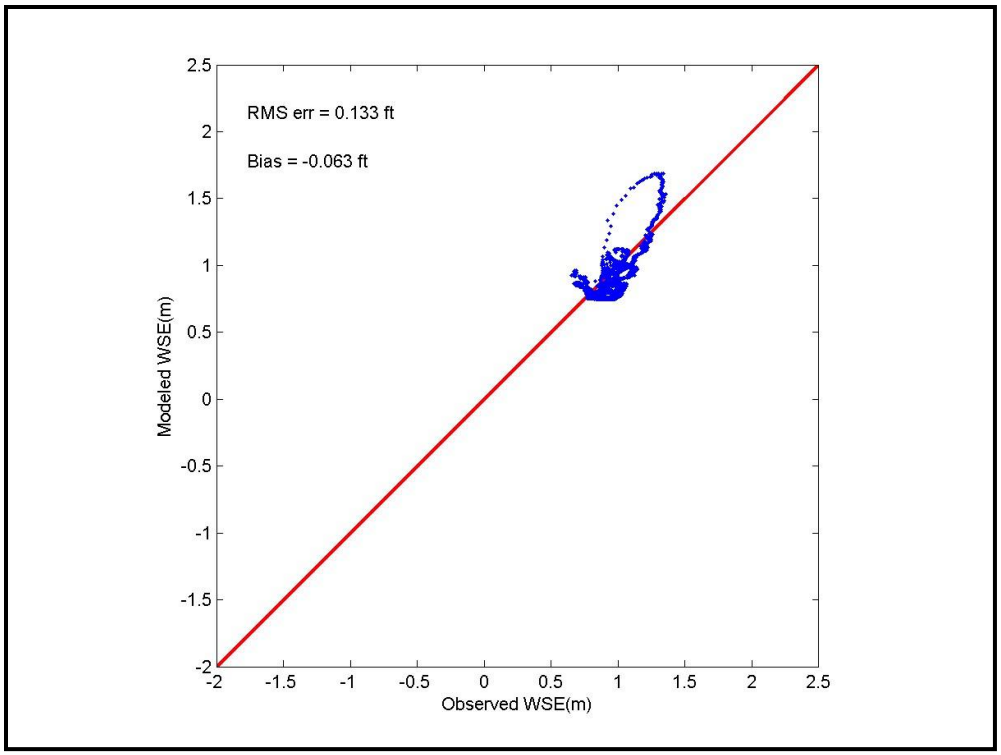

Figure 5-24. PD_up water surface elevation scatter plot comparing modeled and measured water surface elevations.

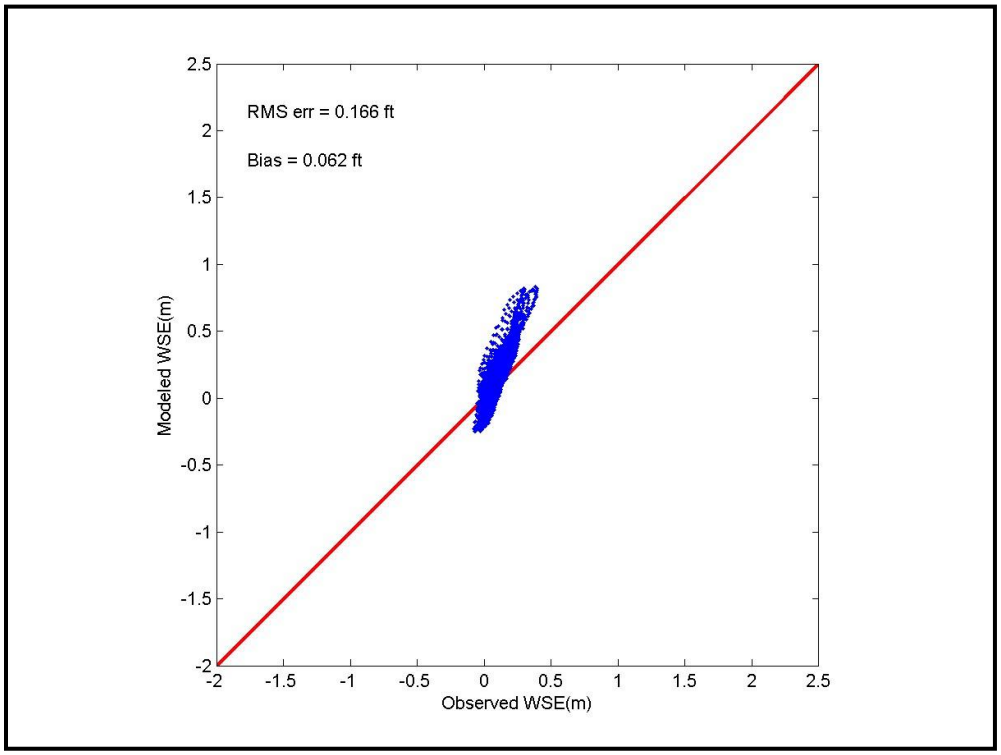

Figure 5-25. OC_down water surface elevation scatter plot comparing modeled and measured water surface elevations.

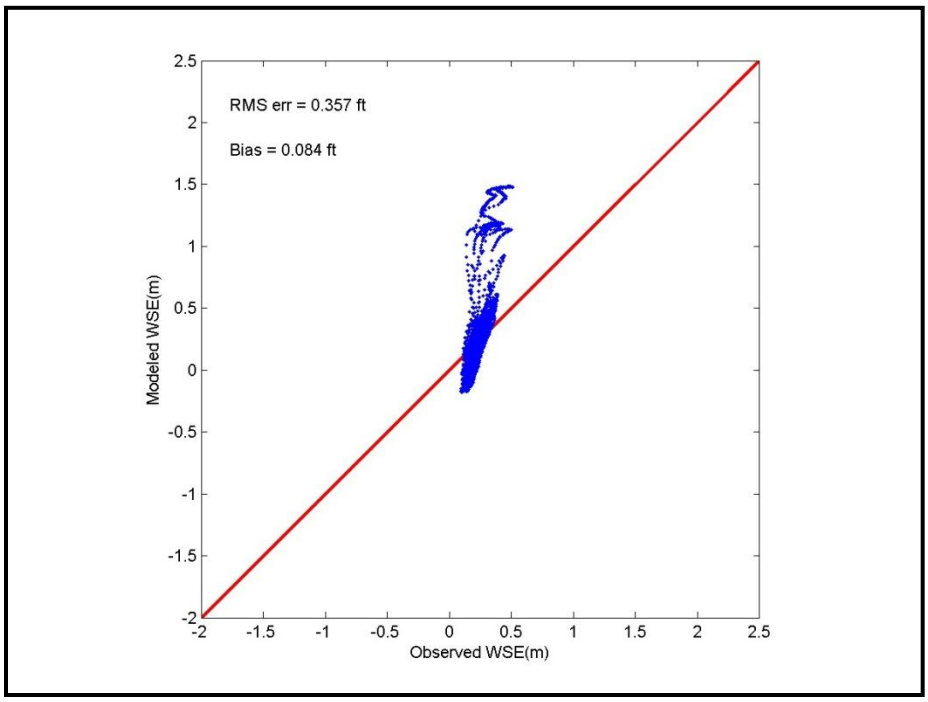

Figure 5-26. BB_up water surface elevation scatter plot comparing modeled and measured water surface elevations.

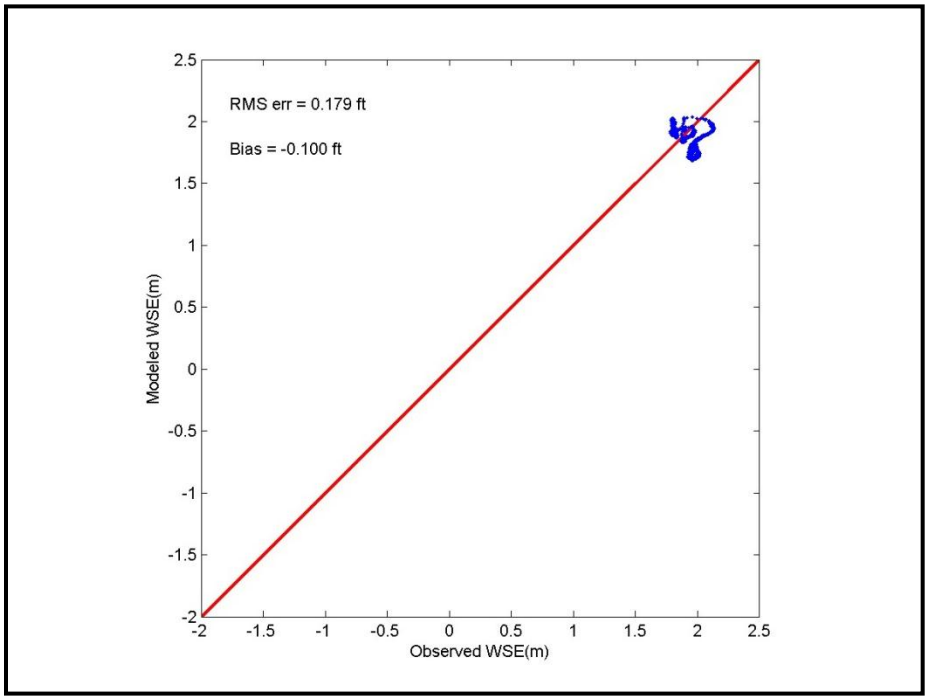

Figure 5-27. Rt6_down water surface elevation scatter plot comparing modeled and measured water surface elevations.

5.3.2 Tidal Constituent Calibration

To further verify the calibration of the Herring River model, data and model result comparisons are made for five dominant tidal constituents within the system. Table 5-7 presents the tidal constituent amplitude and relative phase for modeled and measured tides at the four locations that were primarily tidal under existing conditions. The constituent calibration resulted in satisfactory agreement between modeled and measured tides. Standard errors between the modeled and observed tides were less than 0.1 feet in all cases, and a majority of the time less than 0.03 feet. Tidal phase errors were also reasonable (less than 15-20 minutes in most cases) and were typically equal or less than the time step of the data observations (15 minutes). Ultimately simulating tidal components accurately is important for proper simulation of restoration alternatives since the restoration parameters are based on the tidal fluctuations and not episodic events (precipitation, wind, etc.).

Table 5-7. Tidal constituents for measure water surface elevation data and calibrated model output, with modeled error amplitudes and phases during the modeled calibration time period.

Measured Data										
	Constituent Amplitude (ft)					Phase (degrees)				
Location	M_2	S_2	N_2	K_1	O_1	ΦM_2	ΦS_2	ΦN_2	ΦK_1	ΦO_1
Dog Leg	0.96	0.12	0.16	0.08	0.09	39.60	88.78	36.00	198.44	173.16
HT_up	0.87	0.11	0.14	0.08	0.09	76.79	122.26	71.06	224.46	192.13
OC_down	0.09	0.02	0.02	0.02	0.03	162.23	181.96	137.20	296.19	248.38
BB_up	0.07	0.01	0.02	0.02	0.02	174.82	192.83	148.83	297.61	254.27
Modeled Calibration Data										
	Constituent Amplitude (ft)					Phase (degrees)				
Location	M_2	S_2	N_2	K_1	O_1	ΦM_2	ΦS_2	ΦN_2	ΦK_1	ΦO_1
Dog Leg	0.93	0.12	0.16	0.09	0.11	43.15	80.84	41.66	203.55	180.90
HT_up	0.89	0.11	0.15	0.09	0.11	46.43	85.00	45.65	207.98	184.38
OC_down	0.19	0.08	0.04	0.05	0.05	116.26	134.01	105.31	273.49	227.74
BB_up	0.17	0.02	0.04	0.05	0.05	129.10	123.62	113.88	285.33	222.07
Error										
	Constituent Amplitude (ft)					Phase Error (minutes)				
Location	M_2	S_2	N_2	K_1	O_1	ΦM_2	ΦS_2	ΦN_2	ΦK_1	ΦO_1
Dog Leg	0.02	0.00	0.01	-0.01	-0.01	-1.42	3.18	-2.26	-2.04	-3.10
HT_up	-0.02	-0.01	-0.01	-0.02	-0.02	12.14	14.90	10.16	6.59	3.10
OC_down	-0.10	-0.07	-0.02	-0.03	-0.03	18.39	19.18	12.76	9.08	8.26
BB_up	-0.10	-0.01	-0.02	-0.03	-0.03	18.29	27.68	13.98	4.91	12.88

5.3.3 Salinity Calibration

Lateral and longitudinal dispersion is computed within the numerical scheme of EFDC based on the physical processes that are simulated in the estuary system (as determined by the hydrodynamic model). The coefficients for dispersion are based on the work of Smagorinsky (1963). This eliminates the need for selection of dispersion coefficients for model simulation

and more accurately represents dispersion since it is based solely on the physical processes that are being represented in the model.

In its currently restricted state, salt is not normally observed upstream of High Toss Road in the Herring River; therefore, data were only collected at the Dogleg station by the NPS. The salinity calculated from the model represents a depth-averaged salinity since the Herring River model is a two-dimensional depth integrated model. Based on limited vertical observation data, Spaulding and Grilli (2001) also used depth-averaged salinity values to calibrate their hydrodynamic model and indicate that the water column was vertically well-mixed during their observation time period.

The Spaulding and Grilli (2001) salinity data were collected at twelve locations (all downstream of High Toss Road, with 10 being located upstream of the dike) and consisted of salinity measurements at 0.5 m (1.64 ft) intervals. The water depths varied considerably and most were shallow limiting the number of samples actually taken. For water depths of less than 1 meter, samples were taken at the surface and bottom. For water depths of less than 0.5 meters, samples were only taken at mid-water depth. The twelve stations were sampled approximately once every hour over the tidal cycle. For observations that included multiple samples in the water column, approximately 40-45% of the samples indicated any level of stratification, with denser salt-laden water on the bottom and fresher water on the surface, in the Lower Herring River. Approximately 20% of the samples showed significant stratification (greater than 3 parts per thousand between the surface and bottom). Overall, the salinity samples varied significantly (e.g., in some cases samples higher salinity was observed on the surface than at depth), such that any clearly identifiable stratification could not be determined. These data represent only two tidal cycles with discrete samples taken over a 12 hour tidal cycle. Therefore, it may be feasible that an enhanced data collection effort may reveal more pronounced stratification exists in the Lower Herring River under certain conditions. On one hand, the lack of available salinity data is a limitation of the modeling effort. On the other hand, the fact that salt does not penetrate further upstream than High Toss Road indicates that more data collection (at least spatially) would not be useful. Both of these factors make calibration of the Herring River model to salinity difficult.

Figure 5-28 and Figure 5-29 show the time series comparison (between modeled and measured data) and scatter plot for salinity at the Dogleg location, respectively. The model under-predicts the time-averaged salinity over the duration of the calibration period as indicated by the bias of -0.85 ppt. The RMSE of indicates that for discrete measurements, on average, the model computed salinity at the Dogleg location is within 3.3 ppt of observed salinity. Overall the model is reasonably calibrated for salinity with a relative error of 11%, which is well below the EPA recommended value. Although relatively small, the 11% error is likely related to potential depth variations that may exist in the system during the calibration time frame, as the model tends to under predict the high tide (peak) salinity at times.. For example, the NPS salinity observations were collected at a single depth level in the water column (near the bottom), while the model assumes a depth-averaged result. Although limited historical data (Spaulding and Grilli, 2001) seem to indicate the Herring River system is fairly well mixed, this may not have been the case during the calibration time period. Therefore, while the data were collected near the bottom, the model is computing a depth-averaged salinity. Therefore, if there was stratification that existed during the calibration period (which would have occurred near high tide due to the relatively shallow depths in the system), the data would have observed saltier water

than the depth-averaged model would have been able to predict. In other words, the data are observing the salt-laden water that existed at the bottom of the water column, while the model averages the salinity through the entire water column including the fresher surface layer. Therefore, in that case, the model under predicts the salinity, especially near periods of high tide in the Lower Herring River.

Due to the flexible nature of the model selected, the model can be extended to 3-D if additional data collected in the future (e.g., during the adaptive management restoration process) reveals seasonal or temporary stratification, or if increased resolution and processes handling is desired.

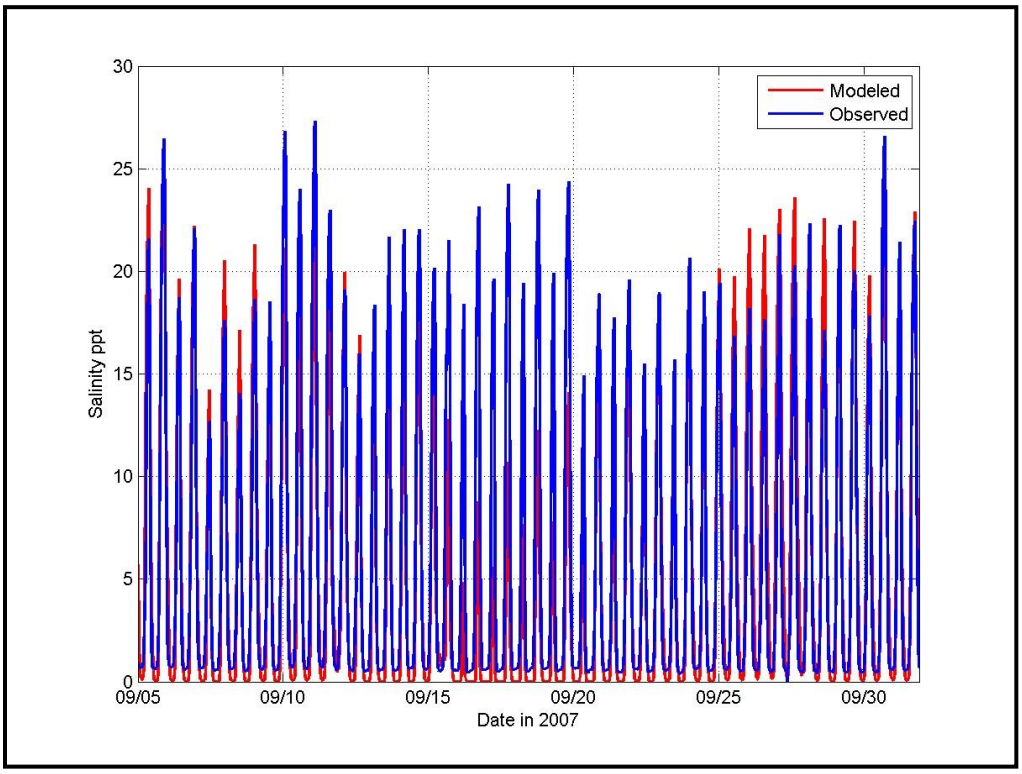

Figure 5-28. Dogleg salinity time series comparison between modeled (red) and measured (blue) salinity data.

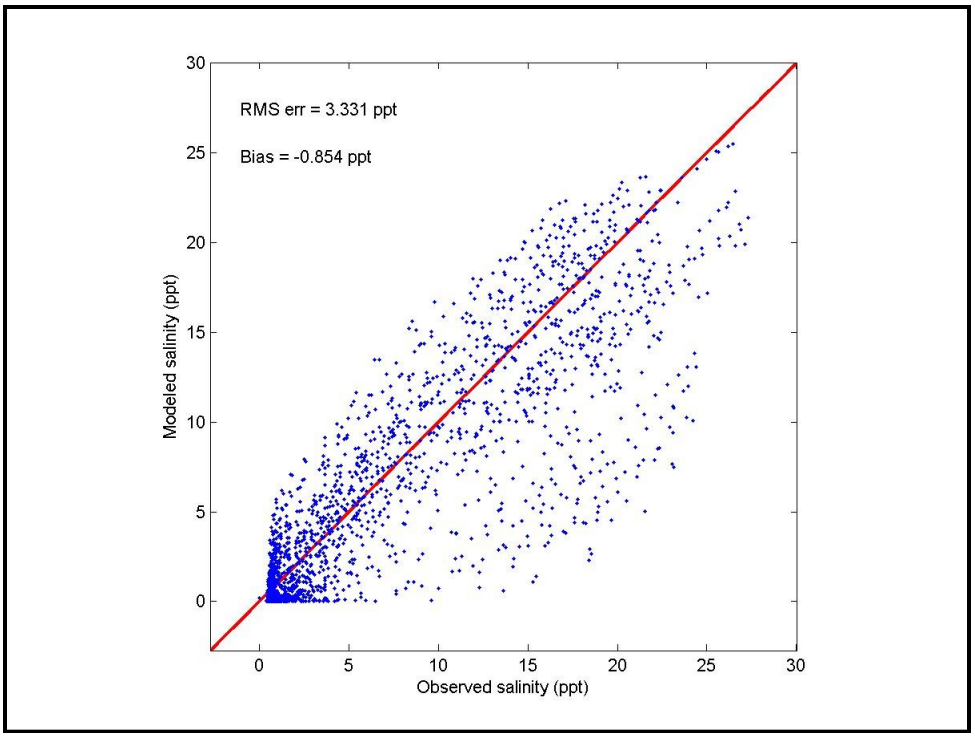

Figure 5-29. Dogleg salinity scatter plot comparing modeled and measured salinities.

5.4 MODEL VALIDATION

Prior to using a hydrodynamic model as a predictive tool it is common practice to validate a calibrated model to confirm the model's applicability to a reasonable range of conditions. Validation involves applying the calibrated model to set of observed data that are independent from the calibration data set by modifying the boundary conditions without changing the model configuration or parameterization. Error statistics for model validation should meet the same guidelines as those applied to model calibration.

Observations of salinity and water levels collected from September 29, 1999 to October 13, 1999 for a previous modeling study (Spaulding and Grilli, 2001) were used to validate the Herring River model. Figure 5-30 shows a subset of these data, which were collected at two locations, "Riverside" and "Harborside", shown in Figure 5-11. Data collected at the Harborside location were used to provide boundary conditions for the validation simulations. The impact of shoals and mudflats in the area downstream of the dike is apparent when comparing the water surface elevation data collected at Old Saw (Figure 5-12) and the water surface elevation time series at the Harborside location (Figure 5-30). The shape of the tidal observations, particularly at low tide, shows the effect on water levels as the lower portion of the tidal signal is limited by the bathymetry and shoals in this region. Therefore, it would be inappropriate to apply the Harborside boundary condition at the same open boundary used for model calibration, and for the validation simulation the grid was modified slightly to move the open boundary closer to the Harborside location. Beyond this necessary modification the model configuration and parameterization remains unchanged for everything upstream of the Chequessett Neck Road dike.

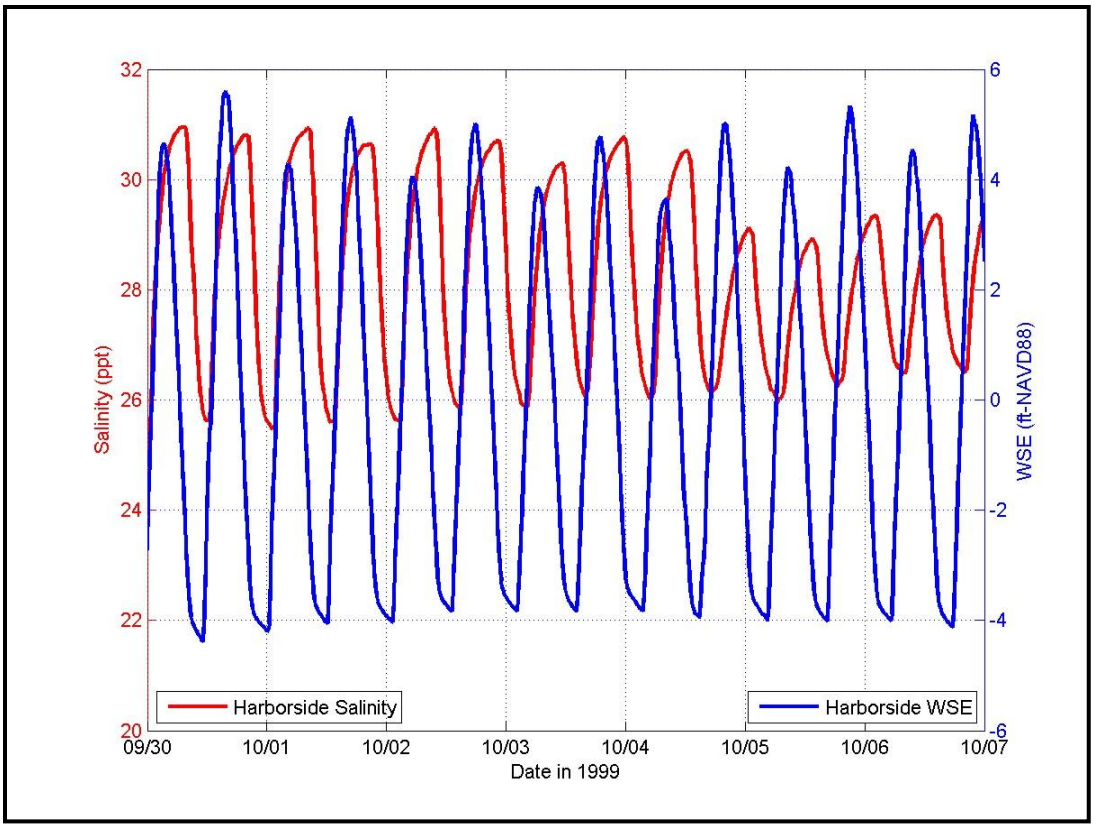

Figure 5-30. Water surface elevation and salinity boundary conditions used for model validation.

5.4.1 Water Surface Elevation Validation

Results for water surface elevation at the Riverside location are presented in Figure 5-31 and Figure 5-32. The agreement is reasonable with a slight (0.068 ft) under-prediction of the average water surface elevation and a RMSE of 0.136 ft. The relative error is 1.7% which is well below the recommend value.

5.4.2 Salinity Validation

Results for salinity at the Riverside location for the validation simulation are presented in Figure 5-33. The results are again reasonable, with a model over prediction of the average salinity at the Riverside location by about 3.6 ppt. Overall, the relative error of 20% is within the acceptable limits; however, the salinity peaks are not consistently identified. The model generally under predicts the higher of the daily high tides, while over predicting the lower of the daily high tides. Although individual modeled high tide salinity does not replicate the observed salinity peaks, with errors up to approximately 3-4 ppt, the average peak salinity over all high tides is approximately the same in the model and in the observations. From a restoration perspective, the difference in salinity levels between observations and modeled results is not significant enough to result in different conclusions regarding the projected vegetation types or change the average salinity within a sub-basin. The error associated with the salinity may be due to (1) the slight offset in phasing between the modeled and measured salinities, (2) the potential inconsistencies when comparing depth-averaged model results to observations collected at a

single depth level (at the bottom), and (3) the potential limitation associated with assuming a well-mixed estuary at this location due to limited data. Due to the flexible nature of the model selected, the model can be extended to 3-D if additional data reveals seasonal or temporary stratification, or if increased resolution and processes handling is desired.

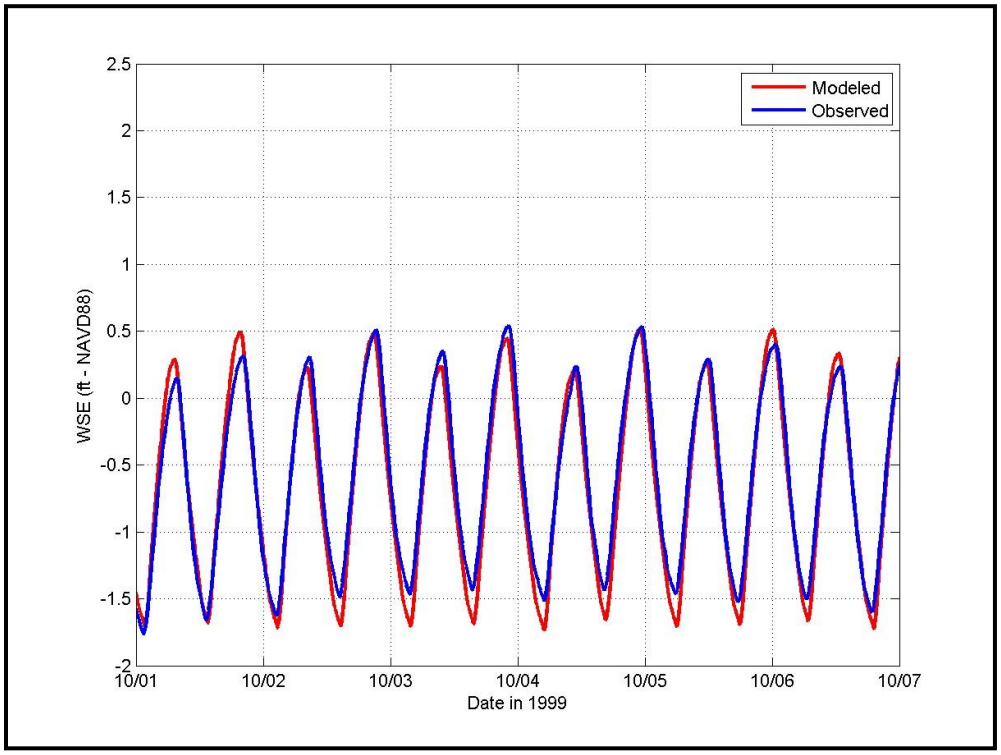

Figure 5-31. Riverside water surface elevation comparison for modeled (red) and measured (blue) time series.

5.4.3 Additional Water Surface Elevation Validation

A secondary water surface elevation validation assessment was also made using data collected in February to March, 2010. Figure 5-34 shows the water surface elevation data collection locations, and Figure 5-35 presents a scatter plot of the model results compared to the data observations at the restricted side location. The agreement is reasonable with a small (0.228 ft) over-prediction of the average water surface elevation and a RMSE of 0.276 ft. The relative error is 2.8%, which is well below the recommend value.

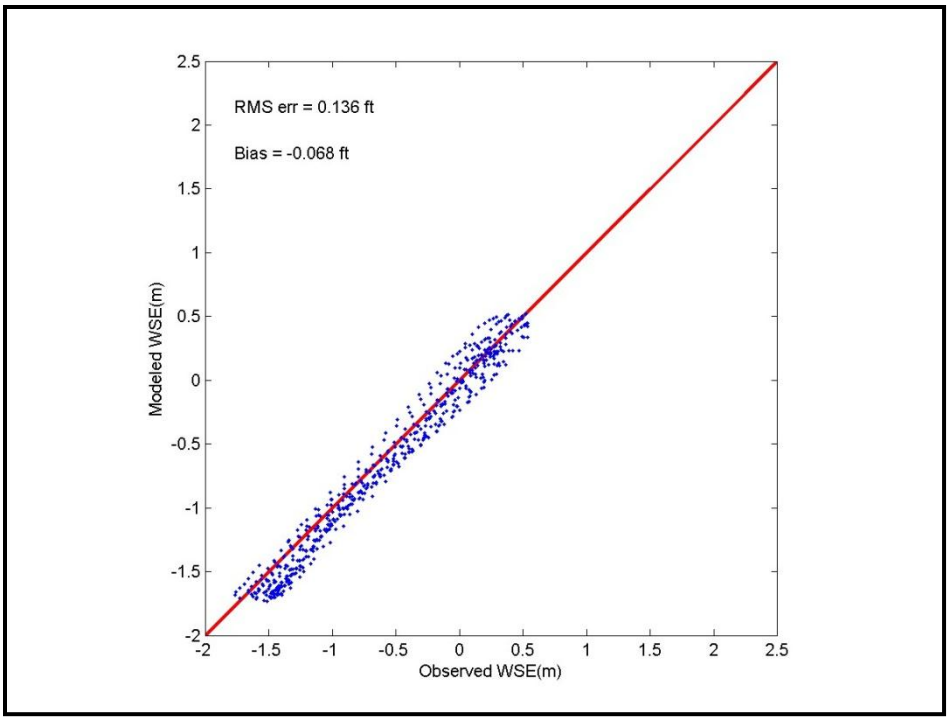

Figure 5-32. Riverside water surface elevation scatter plot comparing modeled and measured water surface elevations.

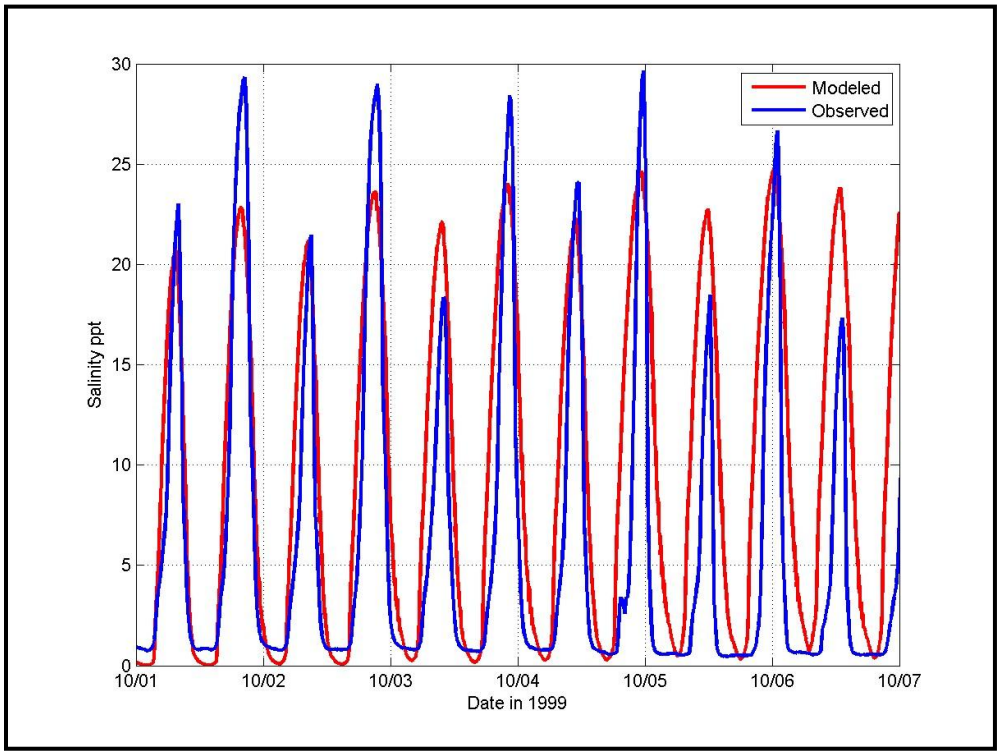

Figure 5-33. Riverside salinity time series comparison between modeled (red) and measured (blue) salinity data.

Figure 5-34. Location of water surface elevation observation in 2010.

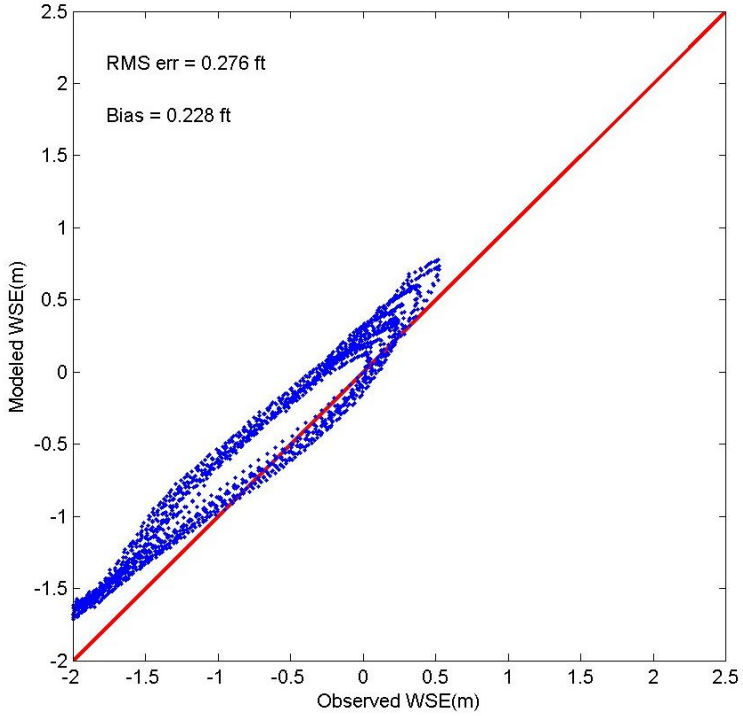

Figure 5-35. Restricted side (2010) water surface elevation scatter plot comparing modeled and measured water surface elevations.

5.5 EXISTING CONDITIONS

The calibrated and validated model was further applied to simulate a number of scenarios to aid in understanding the behavior of the Herring River estuary in its current restricted state. In addition to providing better understanding of the current system, these simulations are also useful by providing a baseline for comparison to alternative simulations. For example, the impact of opening the Chequessett Neck Road dike on the potential storm surge signal throughout the estuary system can be evaluated. Storm events and forecasted sea level rise (SLR) scenarios are simulated, and the results presented in this section. Boundary conditions for these simulations were created by modifying the water levels observed at the Old Saw boundary conditions station to represent storm surge and/or long-term sea level rise increases. All other parameters were kept the same, including the freshwater input boundary condition. The baseline results used for comparison to the tidal flood and sea level rise simulations were taken from a simulations of normal tidal conditions, which are identical to the calibration case without the inclusion of atmospheric forcing (wind, rainfall, etc.). Therefore, the calibration and validation simulations presented above included simulation of normal tidal conditions (including spring and neap tides). For example, the calibration simulation included 30 days of model simulation incorporating a full spring and neap tidal cycle. Results of all existing conditions scenarios (normal tidal conditions, storm surge conditions, sea level rise scenarios) and comparisons to alternative results are presented in greater detail in Chapter 7.0.

5.5.1 Tidal Flood Events

Tidal flood elevations (1-year and 100-year return periods) acquired from The New England Tidal Flood Profiles published by the U.S. Army Corp of Engineers (1988) were used to create a representative water surface elevation boundary condition for simulation of the tidal flood events. To create the boundary conditions, the water surface elevation data used for model calibration was modified by adding the surge (a sinusoidal peak with a 24 hour period) to the spring high tide that occurred on September 28, 2007. This produces three high tides that are higher than the normal conditions and represent the tidal flood conditions that might occur with the passing of slow moving Nor'easter, somewhat like the conditions that occurred during the Northeast Blizzard of February 1978. The 1 year return period storm peaks at 6.9 feet NAVD88, while the 100-year return period storm peaks at 9.3 feet NAVD88, slightly less than the maximum high water level of 9.7 feet observed during the 1978 blizzard (Roman, 1987). As such, the blizzard of 1978 was approximately a 100-year event for this location. The water surface elevation boundary conditions used for these simulations are shown in Figure 5-36.

A summary of the peak water surface elevations at the gauge locations shown in Figure 5-10 is provided in Table 5-8, while time series plots showing the water surface elevation at the various locations are given in Figure 5-37 through Figure 5-43. After day 2.5 in the simulation, the storm has passed, and the time series for the return period storm (tidal flood) conditions matches the normal conditions (or baseline). The 1-year flood case is not clearly distinguishable from normal conditions since the spring high tide on September 28, 2007 was a significant hig tide and only slightly less than the 1-year flood event. In fact, at the locations further up in the estuary (the Pole Dike gauges and the Rt6_up gauge) the tidal attenuation caused by the system produces results that are similar to spring tide conditions. The Rt6_up location is not affected by the storm surge for any of the flood scenarios since the current restrictions throughout the system render this location completely non-tidal. The return-period tidal flood simulations demonstrate

the effectiveness of the Chequessett Neck Road Dike, assuming it is structurally sound, in reducing storm surge. For example, during the 100-year flood event, the greatest increase in peak elevation over the base line is 0.7 feet at the Dogleg location. This increase is only 27% of the increase that occurs due the return period storm at the boundary in Wellfleet Harbor. In other words, these results show a 63% reduction in storm surge height between Wellfleet Harbor and High Toss Road caused by the existing dike.

Table 5-8. Peak water surface elevation for return period tidal flood simulations (ft-NAVD88).

Location	September 28, 2007	1-Year Flood	100-Year Flood
Wellfleet Harbor	6.7	6.9	9.3
Dogleg	0.75	0.80	1.44
HT_up	0.72	0.77	1.37
PD_down	0.79	0.79	0.95
PD_up	0.79	0.79	0.95
OC_down	0.65	0.71	1.33
BB_up	0.71	0.73	1.1
Rt6_down	Non-tidal	Non-tidal	Non-tidal

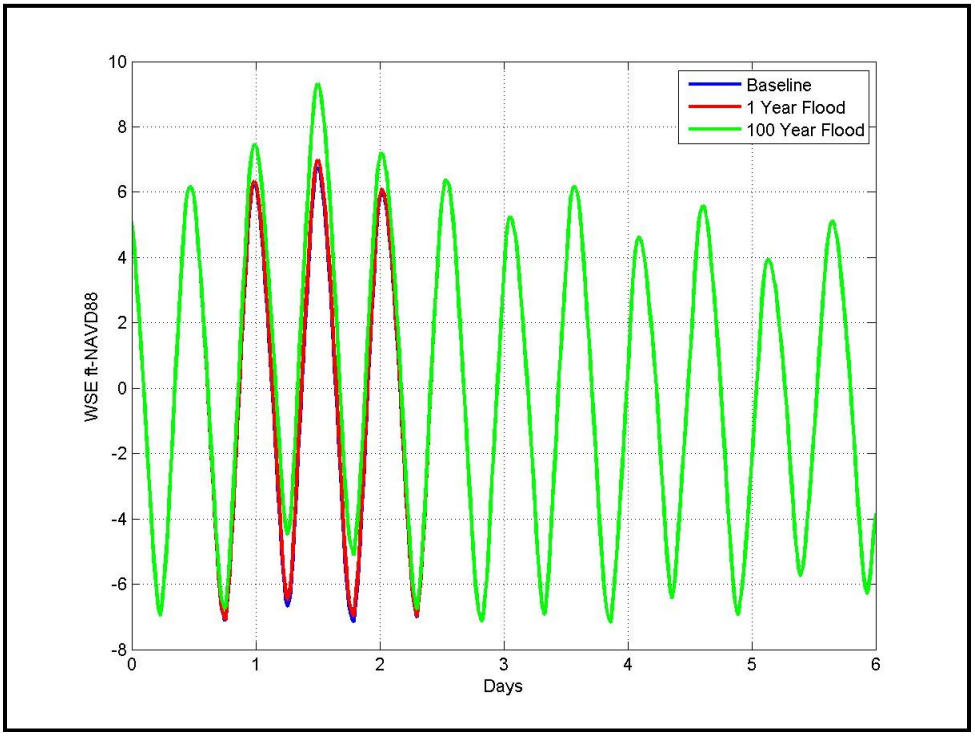

Figure 5-36. Open boundary water surface elevation boundary condition for return period storm simulations.

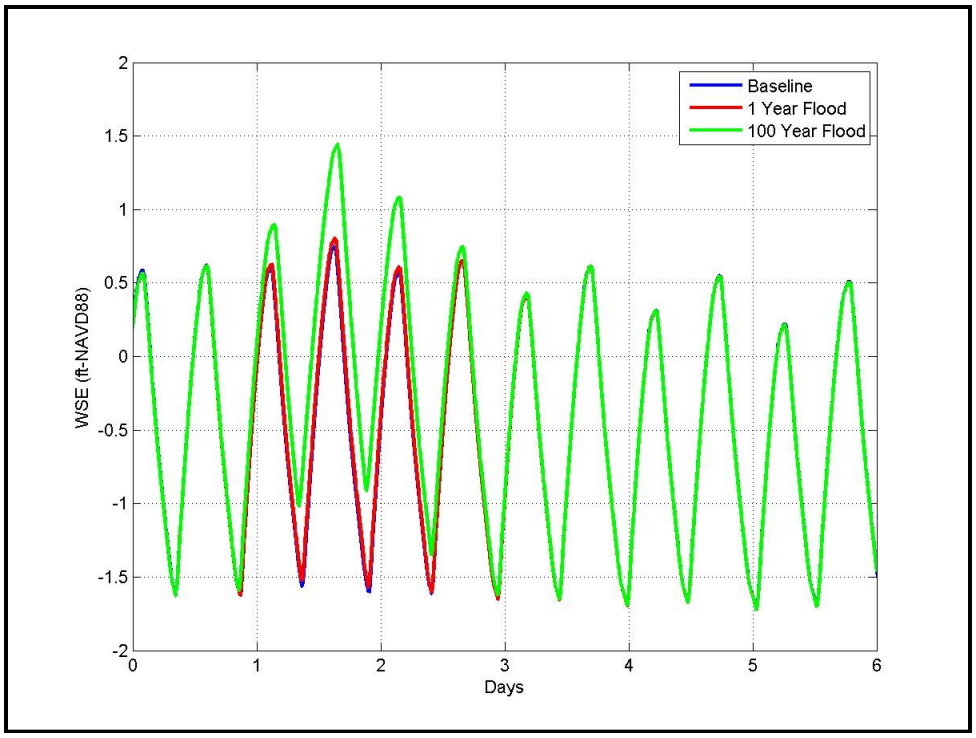

Figure 5-37. Tidal flood water surface elevation time series at Dogleg location.

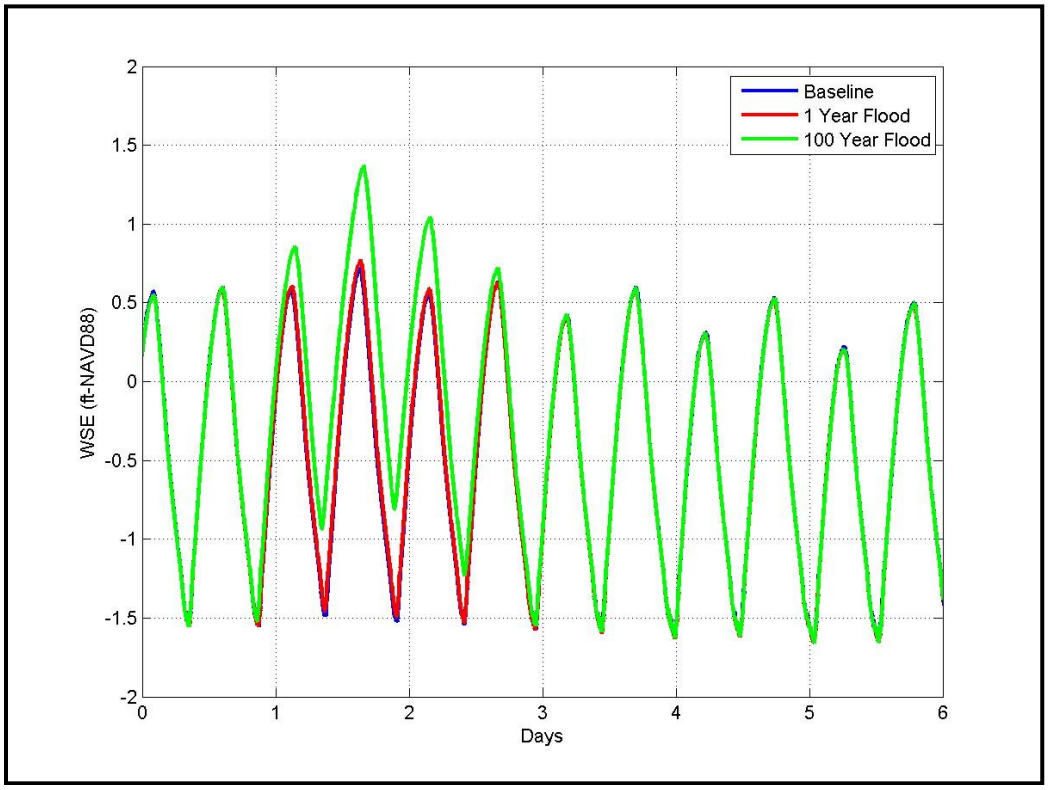

Figure 5-38. Tidal flood water surface elevation time series at HT_up location.

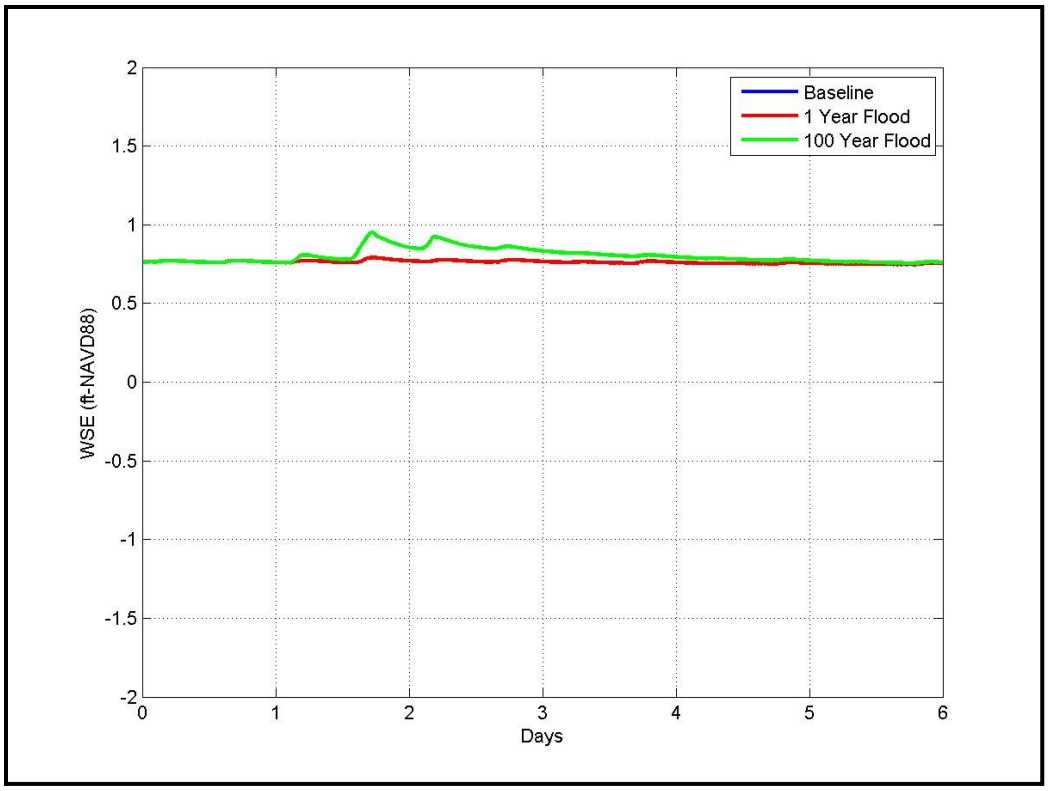

Figure 5-39. Tidal flood water surface elevation time series at PD_down location.

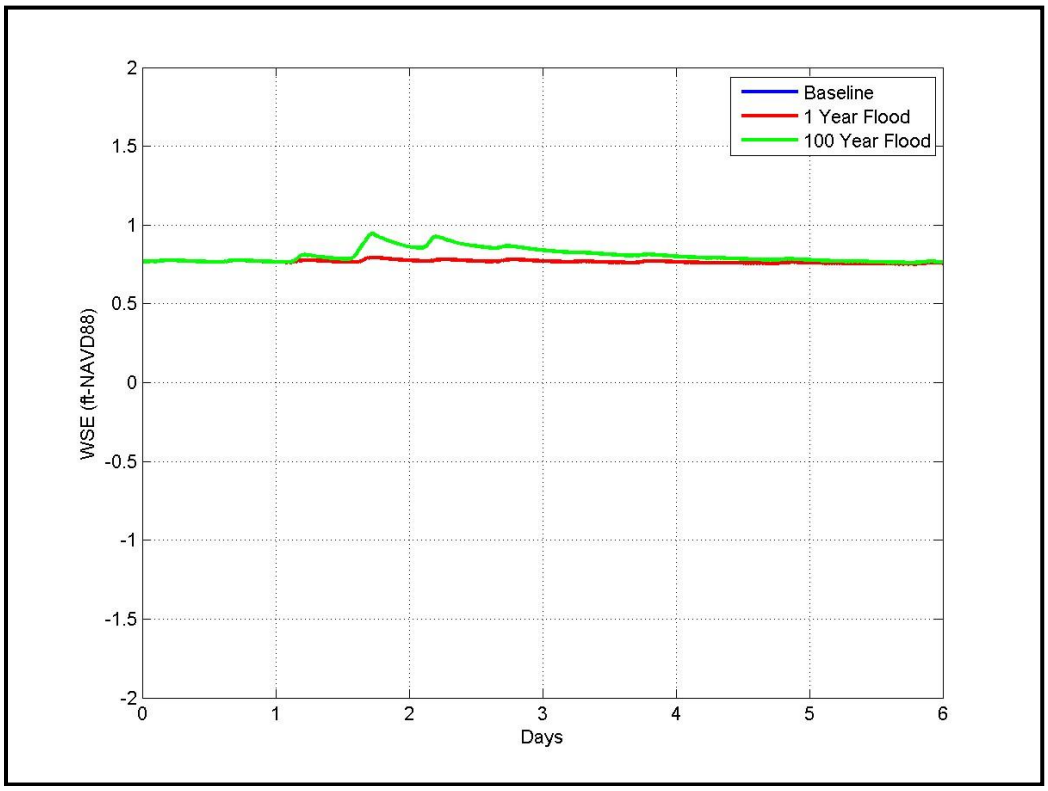

Figure 5-40. Tidal flood water surface elevation time series at PD_up location.

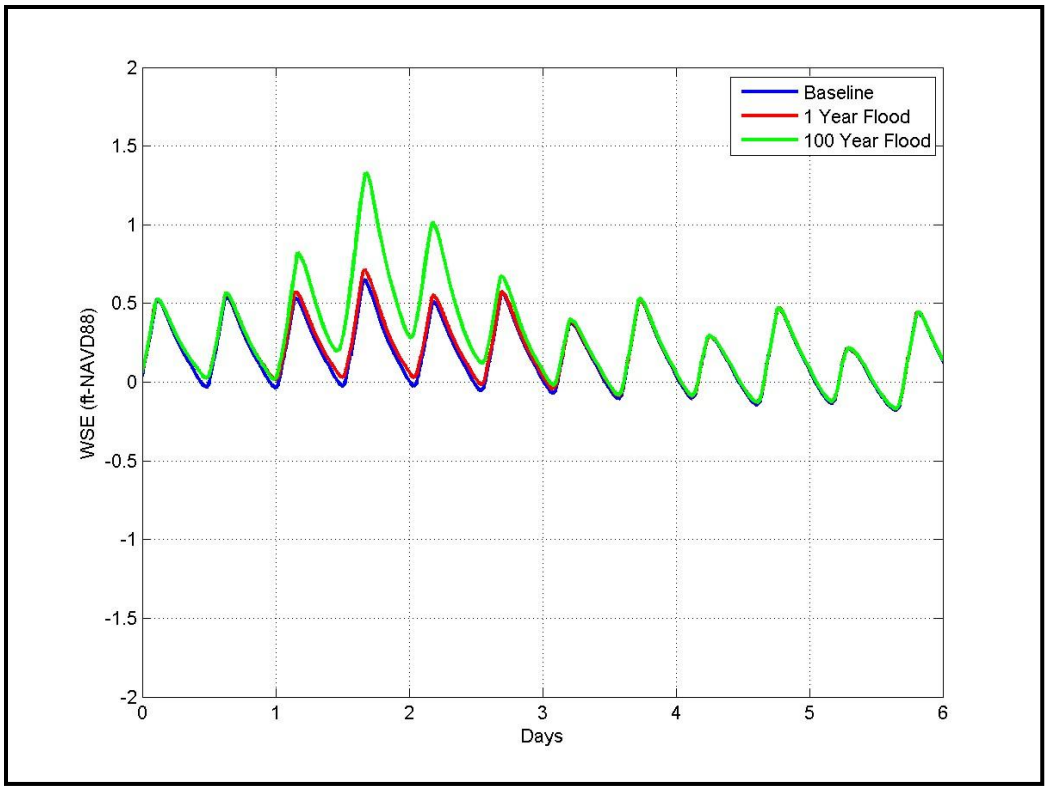

Figure 5-41. Tidal flood water surface elevation time series at OC_down location.

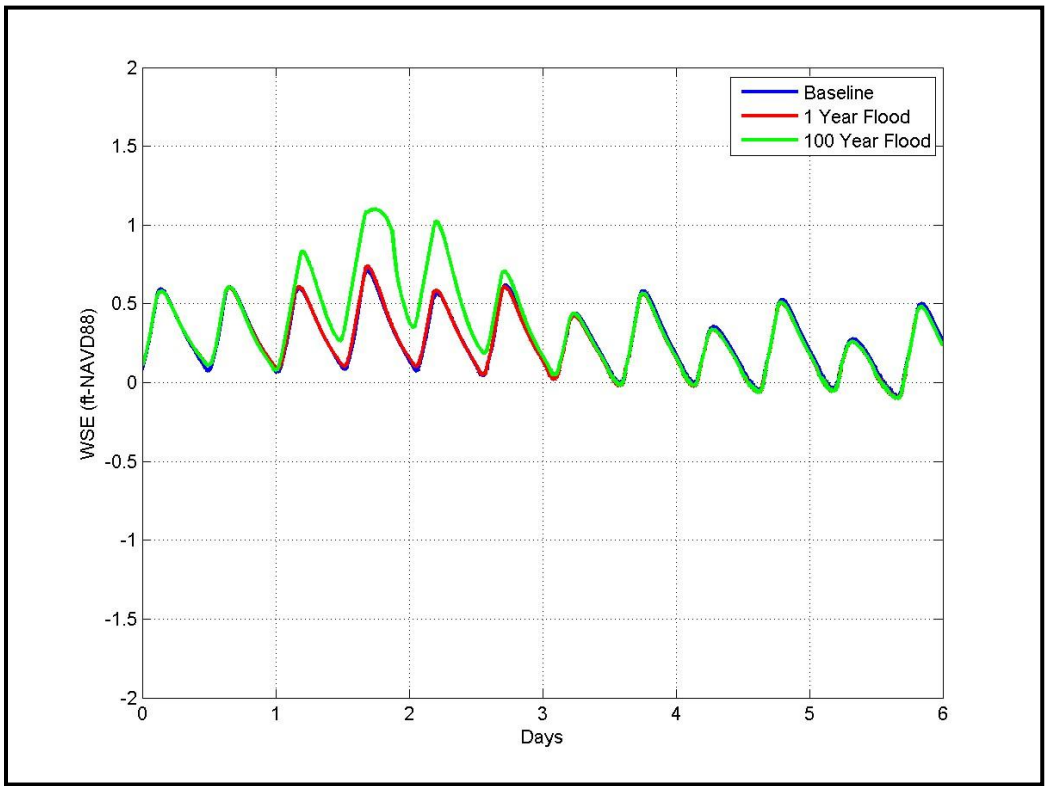

Figure 5-42. Tidal flood water surface elevation time series at BB_up location.

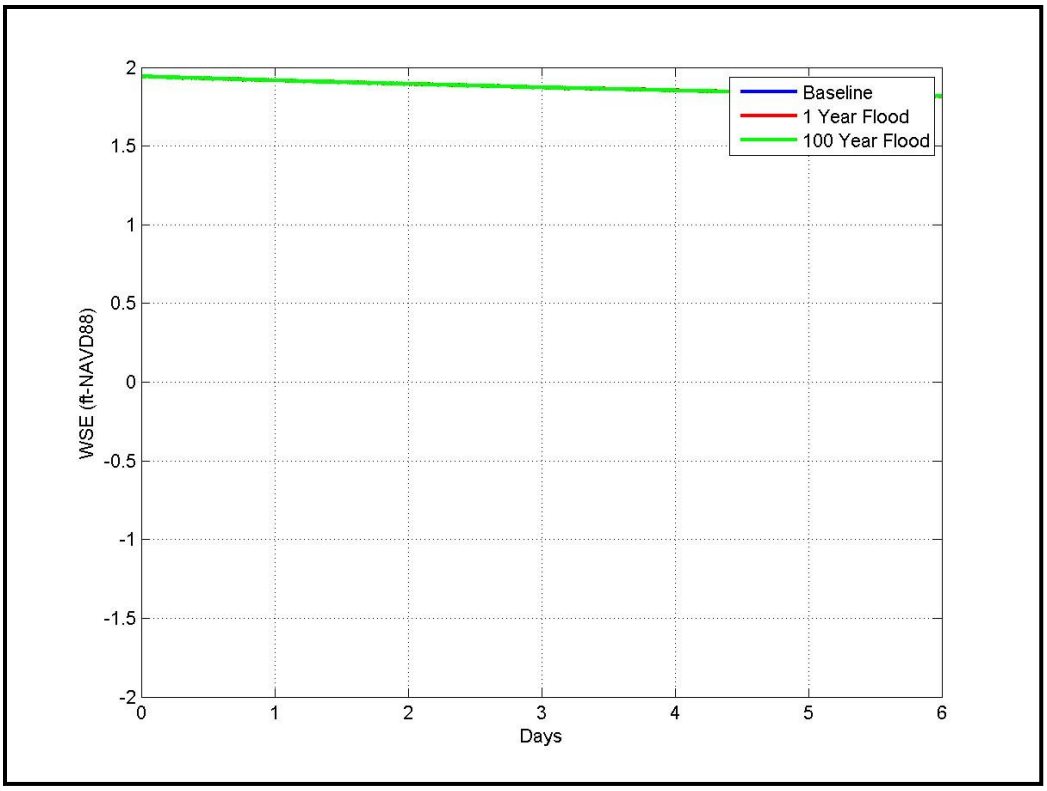

Figure 5-43. Tidal flood water surface elevation time series at Rt6_down location.

Salinity results for the tidal flood simulations are summarized in Table 5-9 and time series plots for salinity at Dogleg and HT_up are shown in Figure 5-44 and Figure 5-45, respectively. The results for the 1-year return period flood show minimal difference from normal conditions (again due to the restrictive nature of the dike and the high spring tide of September 28, 2007), while the 100-year return period flood indicates an increase at both locations. As for the water surface elevation, the dike significantly reduces salt water intrusion even during significant storm events. Results from the 100-year return period storm simulations shows minimal salt penetration north of High Toss Road. A constant of 30 ppt was used at the boundary conditions for the storm events (since the value is unknown) and set for normal conditions to allow for comparison.

Table 5-9. Peak salinity for tidal flood simulations (in ppt).

Location	Normal Conditions	1 Year Flood	100 Year Flood
Wellfleet Harbor	30	30	30
Dogleg	24.0	24.4	27.35
HT_up	5.1	6.6	16.4

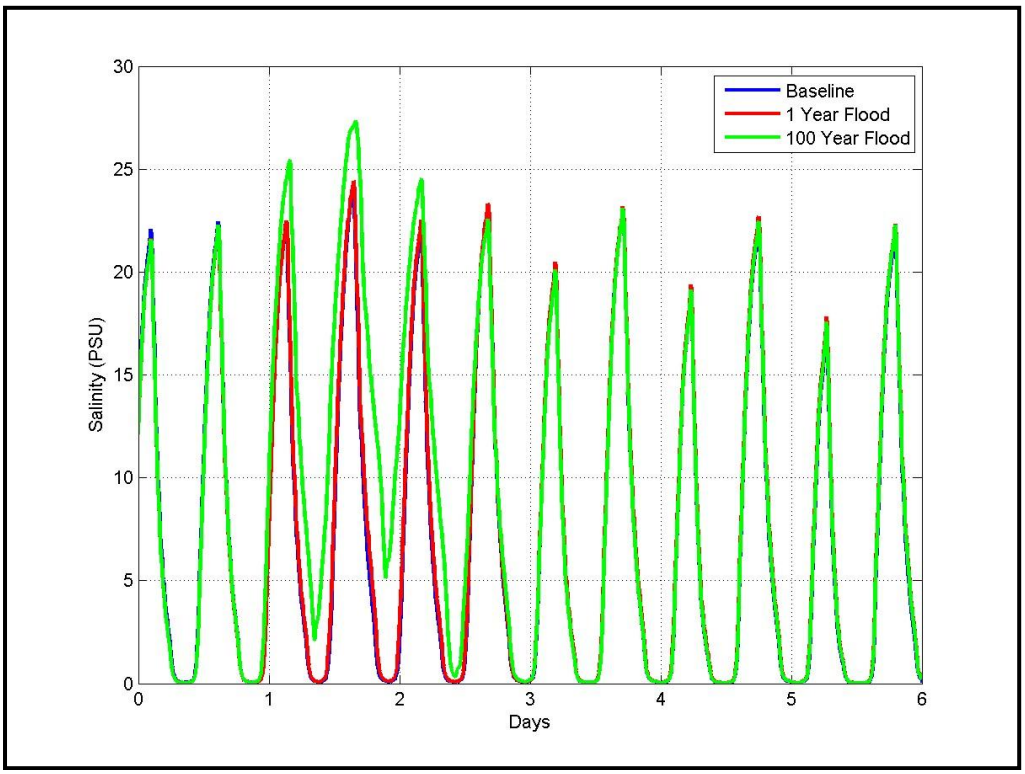

Figure 5-44. Tidal flood salinity time series at Dogleg location.

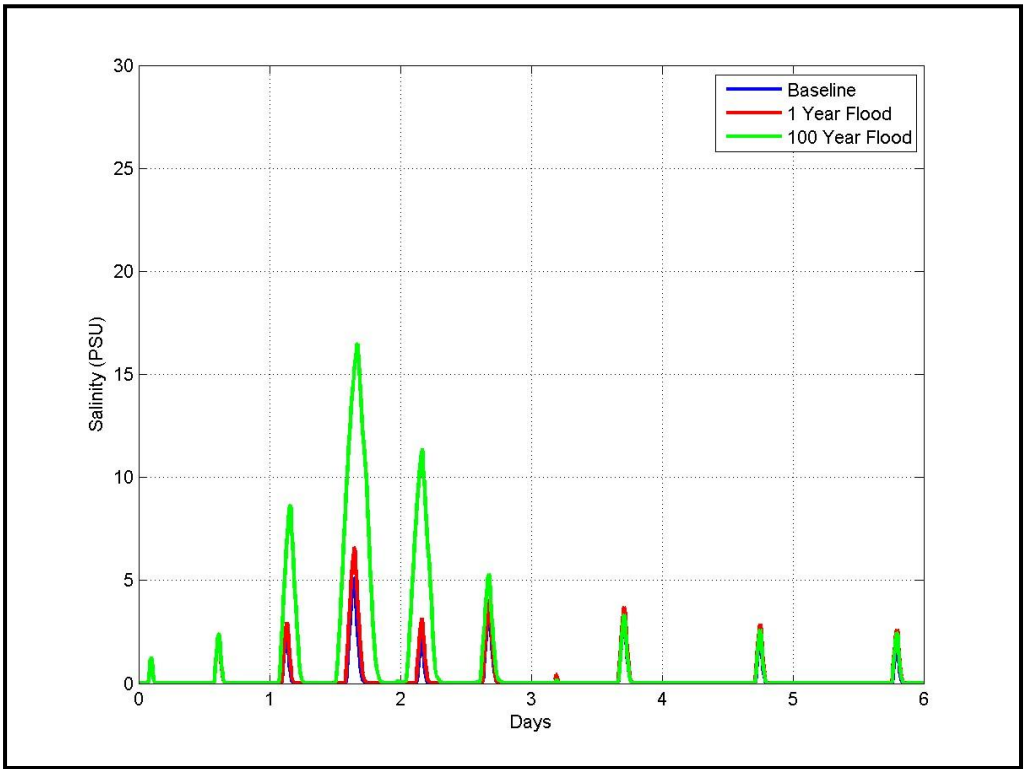

Figure 5-45. Tidal flood salinity time series at HT_up location.

5.5.2 Sea Level Rise

Further simulations were conducted to provide an estimate of future projected water levels in the Herring River over the next half century as relative sea level increases. Specifically, simulations for 50 years of sea level rise were conducted using the USACE guidance for incorporating sea-level change considerations in civil works programs (USACE, 2009, 2011). Under this design guidance, the USACE provides three (3) projected rates of sea level rise (high, intermediate, and low) to use in the design of civil works projects. The Corps guidance uses current local sea level rise rates based on historic water surface elevation data to form projections for the "low" scenario, and a combination of these local rates with IPCC (2007) scenarios and the National Research Council's (1987) equations for the "intermediate" and "high" scenarios for accelerated sea level rise. This method derives locally specific estimates for sea level rise that span a broader range of scenarios than the IPCC estimates alone. Figure 5-46 provides the projected sea level rise curves calculated specifically for the Wellfleet Harbor area based on the USACE guidance. The figure shows the expected increase in sea level for the low (blue line), intermediate (green line), and high (red line) rates as a function of time (starting in the year of 2010). Table 5-10 provides the values for the low, intermediate, and high rates of sea level rise over a 50 year time horizon (between 2010 to 2060). These values would be expected to increase the mean water surface elevation within the Herring River system. This increase in mean water surface elevation would also then increase the high and low elevation of all tides. These values were utilized in the hydrodynamic modeling of Herring River to estimate the potential impact of sea level rise on the system.

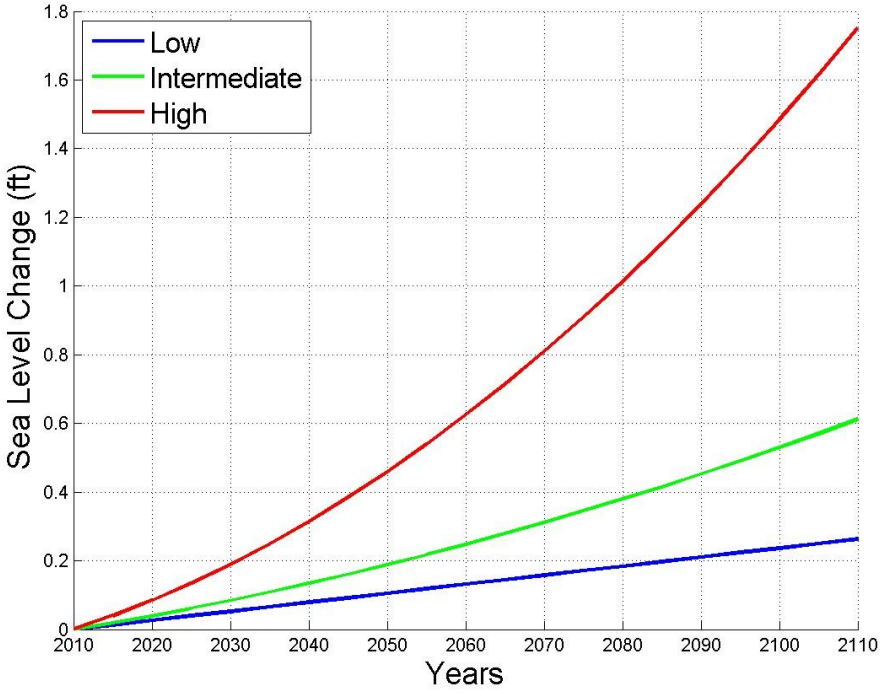

Figure 5-46. Projected sea level rise for the Wellfleet Harbor area using USACE (2009, 2011) guidance for low, intermediate, and high expected sea level rise.

Table 5-10. Projected sea level rise for the Wellfleet Harbor area over a 50 year time horizon between 2010 and 2060.

Sea Level Rise Rate	Sea Level Increase (feet)
Low	0.44
Intermediate	0.81
High	2.05

Since there continues to be additional studies on sea level rise, and the range of projected sea level rise rates is highly variable, additional sea-level rise scenarios could be conducted as the adaptive restoration project is underway.

To quantify the effect of the sea level rise on water levels in the existing estuary, projected increases in Mean High Water (MHW) and Mean Low Water (MLW) were determined from the sea level rise simulations. The increases in these tidal benchmarks were determined in sub-basins that indicated an increase in water levels. The upstream sub-basins (e.g., Pole Dike Creek, Bound Brook, Duck Harbor, Upper Herring River) that are currently non-tidal, remain relatively unaffected by the sea level rise increase. The projected sea level rise increases in MHW and MLW and are presented in Table 5-11 and Table 5-12, respectively. Although over the long-term it may be theorized that the mean water surface elevation would increase uniformly throughout the system (e.g., a 0.44 foot increase in Wellfleet Harbor would translate to a 0.44 increase in Herring River), the broad, flat marsh plains of the Herring River system create a hypsometry that does not produce uniform water level increases in the system.

Table 5-11. Increase in mean high water above normal conditions due to sea level rise (feet).

Sea Level Rise Rate	Wellfleet Harbor	Lower Herring River	Mill Creek	Mid Herring River
Low	0.44	0.05	0.06	0.05
Intermediate	0.81	0.10	0.13	0.09
High	2.05	0.25	0.33	0.22

Table 5-12. Increase in mean low water above normal conditions due to sea level rise (feet).

Sea Level Rise Rate	Wellfleet Harbor	Lower Herring River	Mill Creek	Mid Herring River
Low	0.44	0.07	0.04	0.04
Intermediate	0.81	0.12	0.07	0.07
High	2.05	0.35	0.17	0.18

This approach to predicting the effect of sea level rise is simplistic and does not consider a number of other factors that may also cause significant changes to tidal flows in the Herring River over the next century. For example, sea level rise may not cause a uniform increase in water levels over the entire tidal range, (i.e. the tidal range might change as the mean level increases). The projected sea level rise considered is only eustatic sea level rise and does not include land/marsh based elevation changes (e.g., subsidence). For example, as water levels increase, vegetation will likely grow and cause marsh surfaces to accrete. It is also impossible to predict future anthropogenic activities or adaptive management activities. Additional assumptions in the sea level rise simulations also include:

- Freshwater discharge into the Herring River system remains similar under future conditions
- Rainfall conditions remain similar under future conditions
- There is no change in the intensity or frequency of storm surge events (e.g., a 100-year return period storm today is the same magnitude as in the future)

However, these sea level rise simulations are useful in increasing our understanding of the behavior of the Herring River estuary system in its current restricted state, albeit not necessarily a perfect prediction for the future.

Figures 5-47 and 5-48 present the sea level rise simulation results for the Lower and Mid Herring River basins under existing dike conditions, respectively. The figures provide a short sample of a water surface elevation time series for existing conditions in 2010 (black broken line), 2060 low sea level rise projection (blue line), 2060 intermediate sea level rise projection (red line), and 2060 high sea level rise projection (green line). In general, the increases in water levels induced by the increase at the boundary are uniform throughout the time series, shown in Figure 5-47 and 5-48. At the current observed rate of sea level rise (low rate), there is minimal change to water levels upstream of the dike under existing conditions in 50 years. For all cases, at the locations that currently do not experience significant tidal fluctuations under normal conditions (e.g., Pole Dike Creek and Route 6), the effect of projected sea level rise is insignificant.

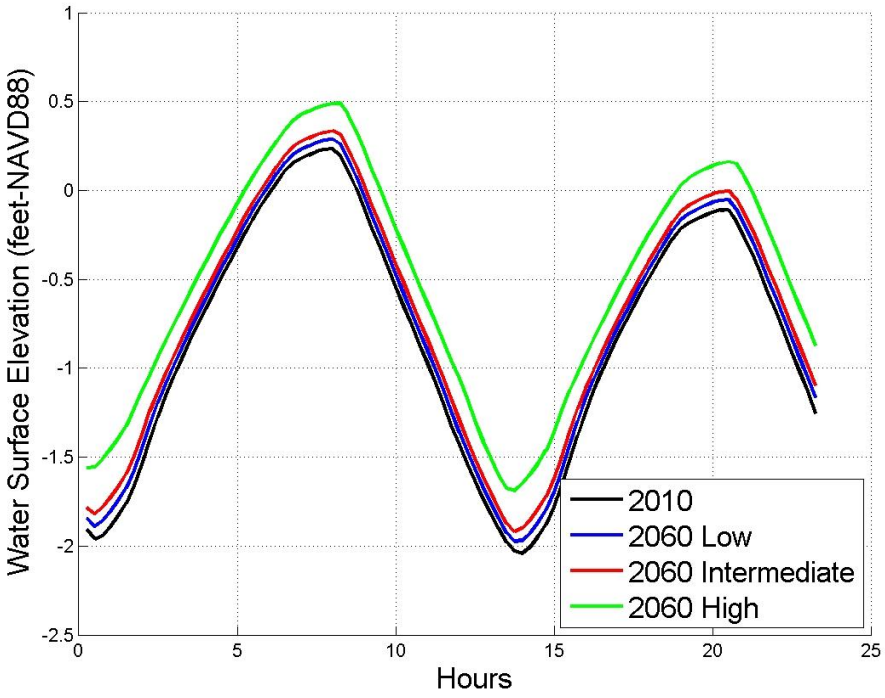

Figure 5-47. Projected sea level rise results in Lower Herring River sub-basin.

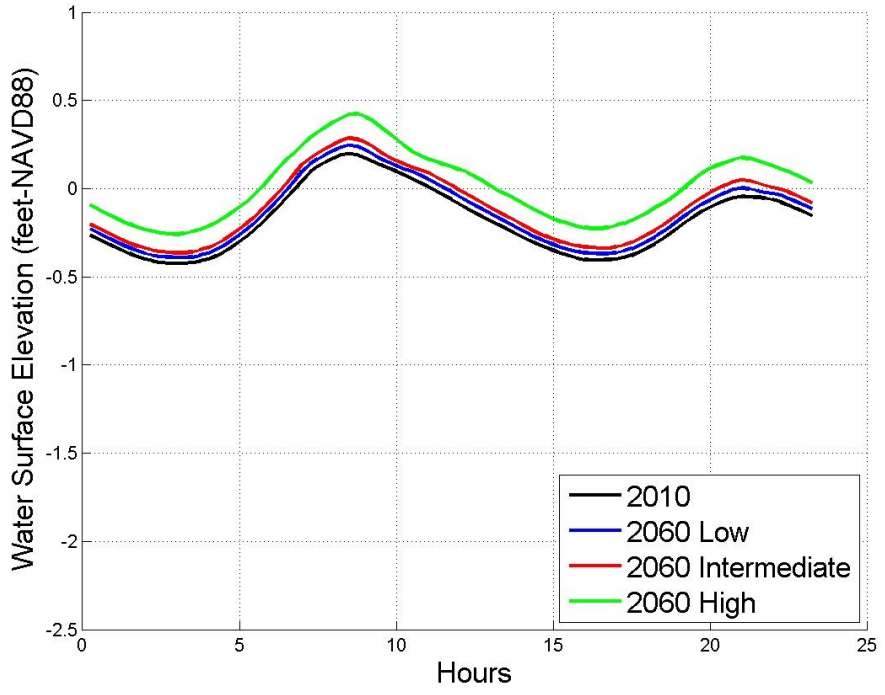

Figure 5-48. Projected sea level rise results in Mid Herring River sub-basin.

6.0 ALTERNATIVE SIMULATIONS

This chapter provides results and discussion from a series of alternative simulations using the calibrated and validated hydrodynamic model of the Herring River System. The focus of these alternatives include, 1) evaluation of the opening at the Chequessett Neck Road dike, which is the primary restriction for the Herring River system (sections 6.1 and 6.2); 2) evaluation of the upstream infrastructure and features in the system (section 6.3, 6.4, and 6.5); and 3) evaluation of the Mill Creek sub-basin (section 6.6). The development and simulation of these alternatives was geared towards identifying preferred restoration alternatives that function appropriately for the Herring River system. The alternatives developed and presented throughout this chapter are used to gain a better understanding of the system and refine potential restoration options. As such, the alternative analysis process was a comprehensive phased evaluation of the various anthropogenic and critical natural components of the system that identified the optimal state of each component. The results provided potential adaptive management steps and were used to develop and assess the final restoration alternatives presented in the Environmental Impact Statement and more comprehensively analyzed in Chapter 7. Specifically, the alternatives presented in this chapter were the first phase in developing the final alternatives for consideration. The alternatives simulated include:

- Simulation of a representative "natural" Herring River system through the removal of all anthropogenic features (e.g., culverts, dikes, railroad beds, etc.). As such, system was allowed to be fully open to tidal flow and allow relatively uninhibited exchange throughout the entire estuarine system. This alternative simulation could be considered a reasonable representation of the greatest restoration level that may be expected for a natural system (excluding natural and/or anthropogenic changes to the bathymetry/topography) and a reasonable facsimile of the historic (a century ago) conditions of the system. This simulation is discussed in section 6.1.

- Simulation of a range of opening sizes replacing the existing dike at the Chequessett Neck Road crossing. These alternative simulations removed the existing dike and replaced them with box culverts of varying sizes, ranging from the current 30 foot opening to a 330 foot opening. These alternatives initially eliminated all flap gates and/or manual control from the culvert opening(s). Therefore, full flow was allowed in both the flood and ebb direction through the dike. Ultimately, the results of these alternative simulations were used to determine the opening size that maximized the tidal range and salinity penetration in the Herring River estuary system. The model results indicate that increasing the opening beyond an optimal size does produce diminishing returns in terms of tidal exchange, salinity penetration, and restoration potential. This set of alternatives is presented in section 6.2.1.

- After determination of the optimal dike opening width, simulations for various opening heights that (1) evaluated target endpoints for restoration (based on limiting water surface elevations that could be accepted during storm conditions throughout the system) and (2) provided opening sizes that could be used as initial set points in the adaptive management process were simulated. This set of alternatives is presented in section 6.2.2.

- An assessment of lowering the culvert inverts at the Chequessett Neck Road dike. These alternatives briefly examined if lowering the culvert inverts would significantly reduce tidal attenuation, improve tidal flux, or significantly impact water surface elevations or salinity levels. This alternative was also geared to determine if the local bathymetry was more of a limiting factor in the tidal attenuation. These alternatives are discussed in section 6.2.3.

- Removal of the significant flood tidal shoal that has formed just upstream of the Chequessett Neck Road dike in response to the restriction imposed by the existing culverts in the dike. Proposed restoration alternatives with larger openings in the dike have raised concerns that this shoal may begin to impose a restriction, influencing tidal propagation farther up into the estuary as the current limiting restriction imposed by the dike's culverts is removed. However, the increased tidal exchange may also relocate the flood tidal shoal farther upstream in the system throughout the restoration process. In order to assess any potential restriction the shoal may cause in the restored Herring River, a simulation was conducted with the flood tidal shoal removed, and is discussed in section 6.3.

- A series of alternative simulations of the Herring River hydrodynamic model designed to assess the impact of the High Toss road causeway and High Toss road culvert on the tidal water levels and salinity in the Herring River estuary. These alternatives evaluated potential modifications to the High Toss road crossing, including open channel and larger culvert options. These alternatives are discussed in section 6.4.

- Assessment of some of the culverts in the upper portions of the system to determine if potential replacement of theses culverts may be required. Results from these alternatives are presented in section 6.5.

- Simulation of potential tidal control at the entrance to the Mill Creek sub-basin, which followed a similar approach to the modeling and assessment of an opening at the Chequessett Neck Road dike. This includes (1) optimization of an opening width at a new Mill Creek dike; (2) potential opening heights of a flow control structure to allow limited water into Mill Creek sub-basin; (3) simulations of a re-graded CYCC golf course; (4) evaluation of the Mill Creek sub-basin completely blocked from tidal exchange and the effect on freshwater outflow, and (5) a preliminary assessment of potential groundwater impacts in the Mill Creek sub-basin relative to both sea level rise and the restoration effort. The Mill Creek sub-basin alternatives are discussed in section 6.6.

- A brief assessment of possible changes to the hydrodynamics of the system caused by expected vegetation succession that may occur during the restoration process. This alternative is presented in section 6.7.

6.1 REMOVAL OF ALL ANTHROPOGENIC STRUCTURES

Figure 6-1 presents the locations where anthropogenic features were removed from the model domain. This included the removal of all culverts, dikes, bridge crossings, and other anthropogenic structures that were directly restricting the tidal propagation in the system. The modification did not include changes that may have been made to the bathymetry/topography of the system through direct or indirect anthropogenic influences, or natural changes that may have occurred since the dike was constructed in the early 1900s. As such, this alternative represents the maximum restoration that could be expected with the current topographic and bathymetric conditions. This alternative also represents a reasonable facsimile of the conditions of the Herring River system (a century ago) that may have existed prior to the construction of the dike, with the exception that the bathymetric/topographic conditions may have been different 100 years ago.

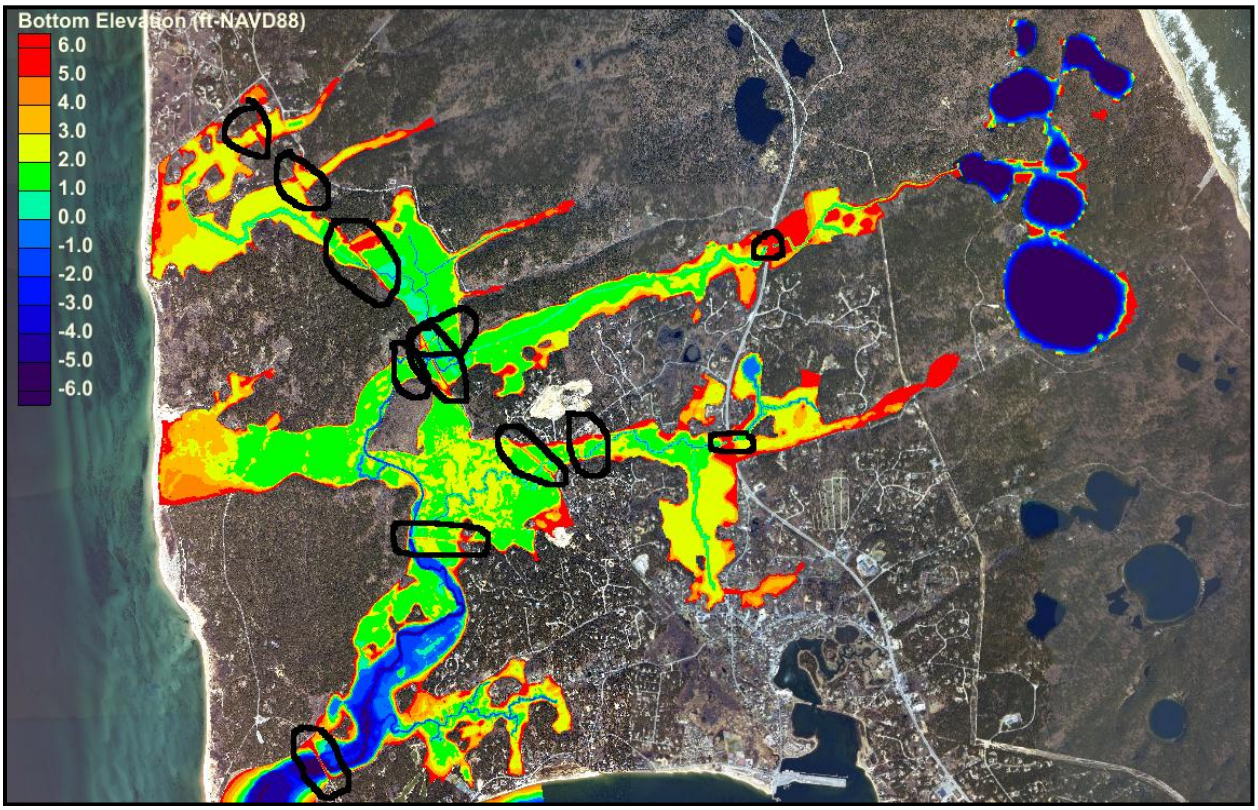

Figure 6-1. Locations within the model domain that were modified (represented by the black circles) to represent removal of anthropogenic features.

As an initial measure of the impact caused by the anthropogenic structures, the Mean High Water Spring (MHWS) water surface level reached under existing conditions was compared to the maximum MHWS water surface level reached for the simulation with anthropogenic structures removed. Figure 6-2 presents a comparison of the maximum water surface elevation for existing conditions (upper panel) and for the simulation that removed all anthropogenic structures (bottom panel), under normal tidal conditions. Tidal water is shown in yellow in both the upper and lower panels.

Figure 6-2. Mean High Water Spring location for existing conditions (upper panel) and for the no anthropogenic structures alternative (bottom panel).

Figure 6-3 presents a comparison of the maximum salinity levels for existing conditions (upper panel) and the no anthropogenic structure alternative (lower panel). Color contours range from freshwater (blue) to salinity levels approximately equal to the average Wellfleet Harbor salinity (30 ppt shown in red). Significant increases in water level and salinity are clearly shown in Figure 6-2 and Figure 6-3 when comparing existing conditions to the fully open alternative. Maximum water levels increase by over 3.5 feet, while maximum salinities increase from freshwater to approximately 30 ppt in numerous places. The spatial extent of the increases also illustrates the amount of historic marsh area that may have existed centuries ago.

Although the fully open alternative is not likely a reasonable final solution given the upland infrastructure that has been developed over the last century, this alternative does provide a reasonable estimate of the maximum restoration potential for the Herring River system and is used for comparison purposes throughout the report, specifically in Chapter 7. Additionally, specific tidal water elevations benchmarks (e.g., MHW, MLW, Annual High Water, storm surge levels, tidal range, etc.), time series comparison plots, salinity levels, and other critical parameters were determined for many of the restoration alternatives evaluated, including the fully open scenarios presented herein. This information is discussed further in Chapter 7.0.

6.2 CHEQUESSETT NECK ROAD OPENING

6.2.1 Optimization of the Opening Width

A critical part of the restoration success for Herring River will be based on the selection and optimization of the Chequessett Neck Road opening. As such, a wide range of potential openings from 30 feet to 330 feet was simulated in order to identify the optimal opening that will maximize restoration potential. These simulations were used as preliminary assessment tools to assist in identifying the target opening size at Chequesset Neck. These simulations do not represent final or recommended alternatives. Model results were evaluated in terms of both modeled water surface elevation and salinity levels. In these scenarios, no additional upstream changes were made to the Herring River estuary. So unlike the fully open scenario, which included the removal of all upstream anthropogenic features, these alternatives focus solely on the dike opening.

Figure 6-4 shows a 3-day subset (from the full 30 day simulation) of the water surface elevation (WSE) results in the Lower Herring River sub-basin (just upstream of the dike) for all opening width alternative cases. The 3 day subset is presented such that the time series of water surface elevation changes can be easily seen. The vertical axis presents the water surface elevation (in feet NAVD88), while the horizontal axis presents time. The yellow bar at the bottom of the figure represents the bottom of the River just upstream of the dike and the broken blue line indicates the tide in Wellfleet Harbor. The broken black line shows the current tidal signal just upstream of the dike, and simulation results are presented for opening width of 10 meters (30 feet) through 100 meters (330 feet). From a water surface elevation perspective, the tidal attenuation between Wellfleet Harbor and Herring River is reduced the most when the dike opening is increased from existing conditions to 100 feet (30 meters). Larger openings have a reduced impact on the amount of water exchanged and the amount of area inundated with tides.

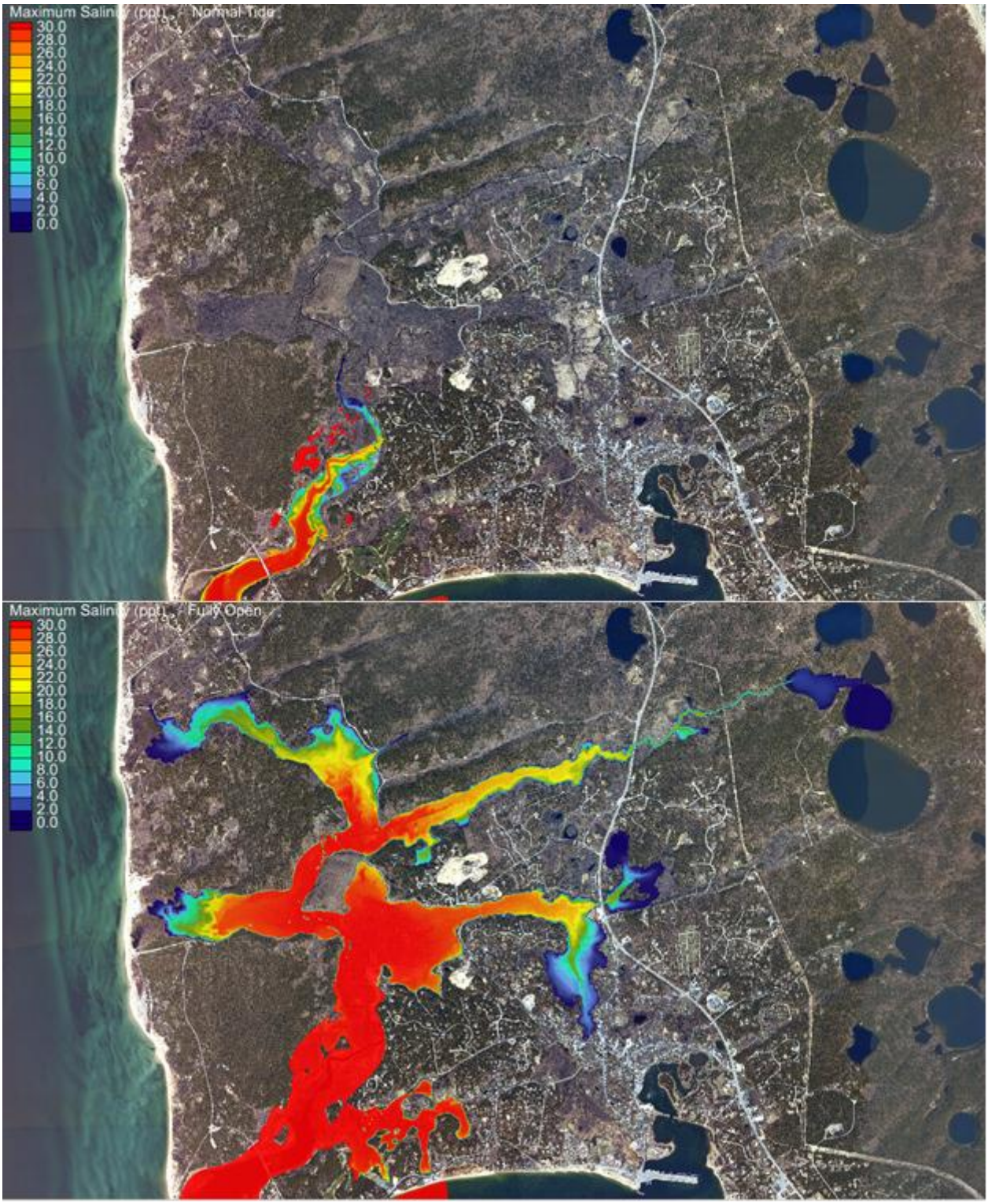

Figure 6-3. Maximum salinity levels for existing conditions simulation (upper panel) and for the no anthropogenic structures alternative (bottom panel). Color contours present the salinity level with blue being freshwater.

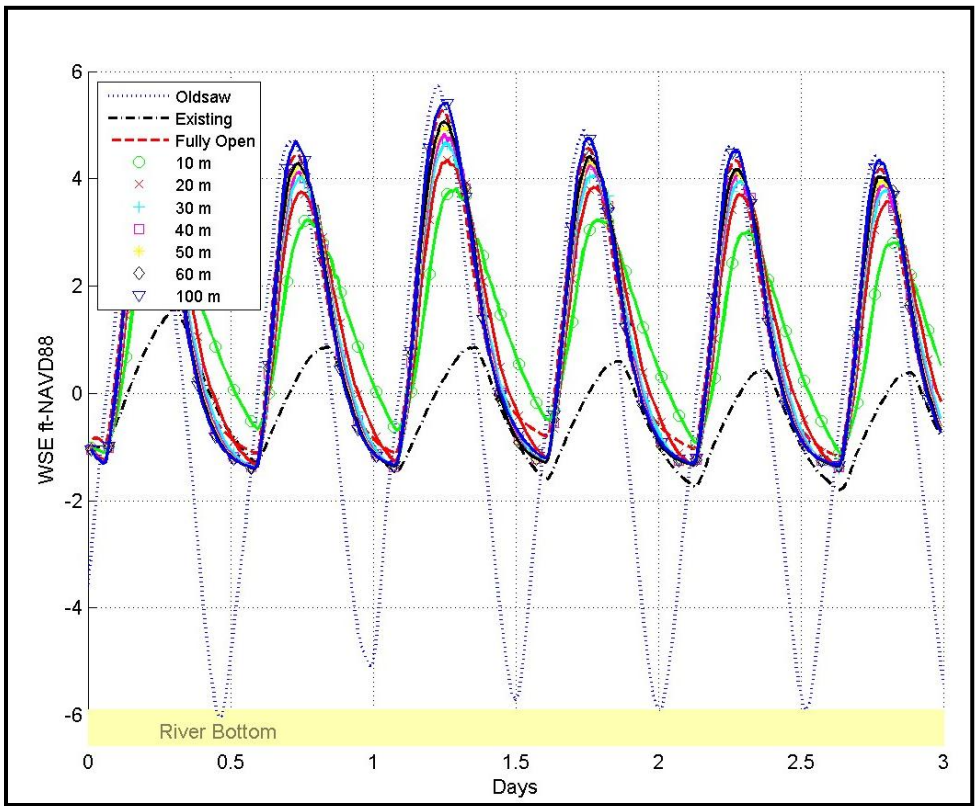

Figure 6-4. Water surface elevation (WSE) results in the Lower Herring River location for all alternative cases of dike opening width.

Figure 6-5 graphically shows the change in Mean High Water (red line) and Mean Low Water (blue line) in the Lower Herring River sub-basin as a function of opening width. The initial marker on both lines represents existing conditions Mean High Water (MHW) and Mean Low Water (MLW) in the Lower Herring River. The gray line in the figure represents the hypsometry of the Lower Herring River sub-basin in acres (shown along the top horizontal axis). A hypsometric curve is a simple histogram of a landscape or watershed (or cumulative frequency distribution of elevation points on marsh surface).

The tidal range (the elevation difference between MHW and MLW) increases significantly as the dike is opened to a greater extent. Under existing conditions, the tidal range (as shown in Figure 6-5) is approximately 2 feet. Increasing the opening width of the dike to 30 meters (approximately 100 feet) increase the tidal range to over 5 feet. In addition, the MHW elevation increases drastically under even relatively minor openings and continues to increase with wider opening sizes. The elevation of MLW also initially increases, as there is significantly more water flooding into the system than under existing conditions (only one culvert bay open 2 feet under existing conditions) and the existing asymmetry of tidal exchange (3 culvert bays allow ebb flows, while 1 culvert bay allows flood flow) is eliminated under the alternative openings. However, MLW eventually remains relatively consistent as the opening size increases further as the combined effect of the culvert inverts and bathymetric features in the vicinity of the dike control the MLW elevation.

From a water surface elevation perspective, a 100 foot (30 meter) opening at the dike optimizes tidal exchange. Larger opening at the dike continue to increase the MHW level, tidal range, and tidal exchange; however, these increases result in less significant gains with diminishing returns, as shown by the smaller gains in tidal range and MHW elevation. In addition, the marsh hypsometry can be used to assess the inundated and intertidal area that would be created from the wider opening. This can be done by evaluating the hypsometric curve in relation to MHW and MLW. For example, a significant majority of the sub-basin (approximately 145 acres inundated) is inundated under MHW with a 100 foot opening. The intertidal area (the area between approximately 58 and 145 acres) is approximately 90 acres, compared to an existing intertidal area of only approximately 45 acres in the Lower Herring River sub-basin. Larger opening widths do not add much additional intertidal area to the restoration. Similar figures were evaluated for each individual sub-basin to ensure that the dike opening optimized tidal exchange, as well as to check the hypsometric curve relative to the new expected water levels and determine new intertidal areas. In all sub-basins, openings beyond a 100 foot (30 meter) width indicated diminishing returns in terms of intertidal area.

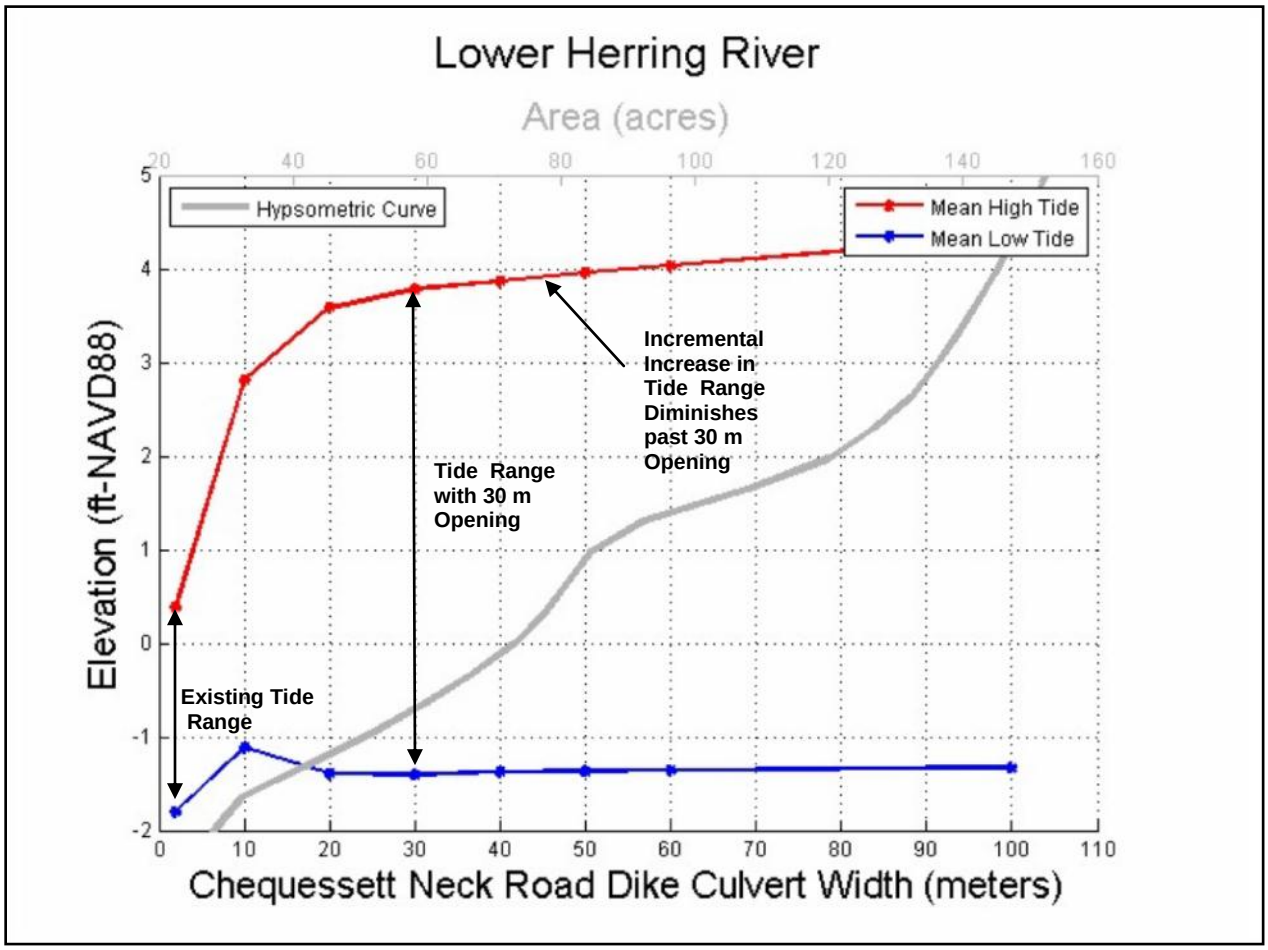

Figure 6-5. Water surface elevation (WSE) results in the Lower Herring River location for all alternative cases of dike opening width.

The potential optimal opening at Chequessett Neck Road dike was also evaluated from a salinity level perspective. While 100 feet (30 meters) appears to maximize the restoration potential from a water surface elevation perspective, larger openings continue to maximize the restoration potential from a salinity perspective (i.e., increased salinity penetration occurs). Figures 6-6 through 6-10 show the peak salinity concentrations during normal tidal conditions throughout the Herring River system for dike opening sizes of 20 meters, 30 meters, 40 meters, 50 meters, and 60 meters, respectively. Based on visual observations of the results, as well as time series of salinity levels extracted from the model within each sub-basin, a 165 foot (50 meter) opening best maximizes the salinity levels throughout the system. Increasing from a 165 foot (50 meter) opening to a 197 foot (60 meter) opening indicates minimal improvement in salinity levels (comparison of Figure 6-9 and 6-10). Therefore, openings beyond 165 feet (50 meters) indicate diminishing returns in terms of salinity penetration, and possible restoration potential.

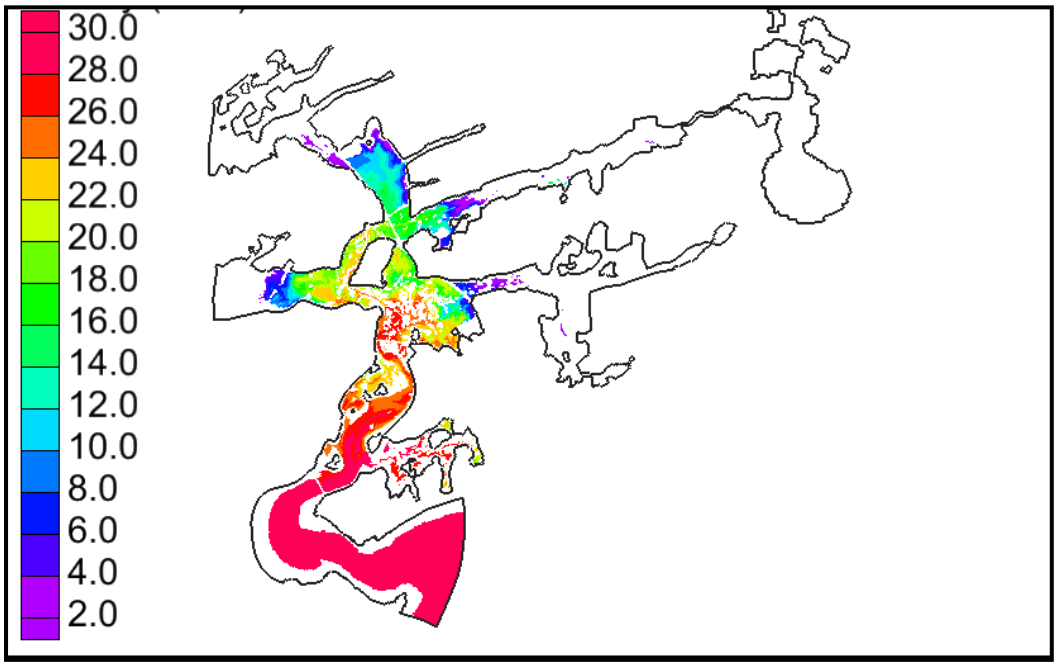

Figure 6-6. Salinity concentration throughout the Herring River system with an opening of 20 meters at the Chequessett Neck Road. Salinity contours are presented in ppt.

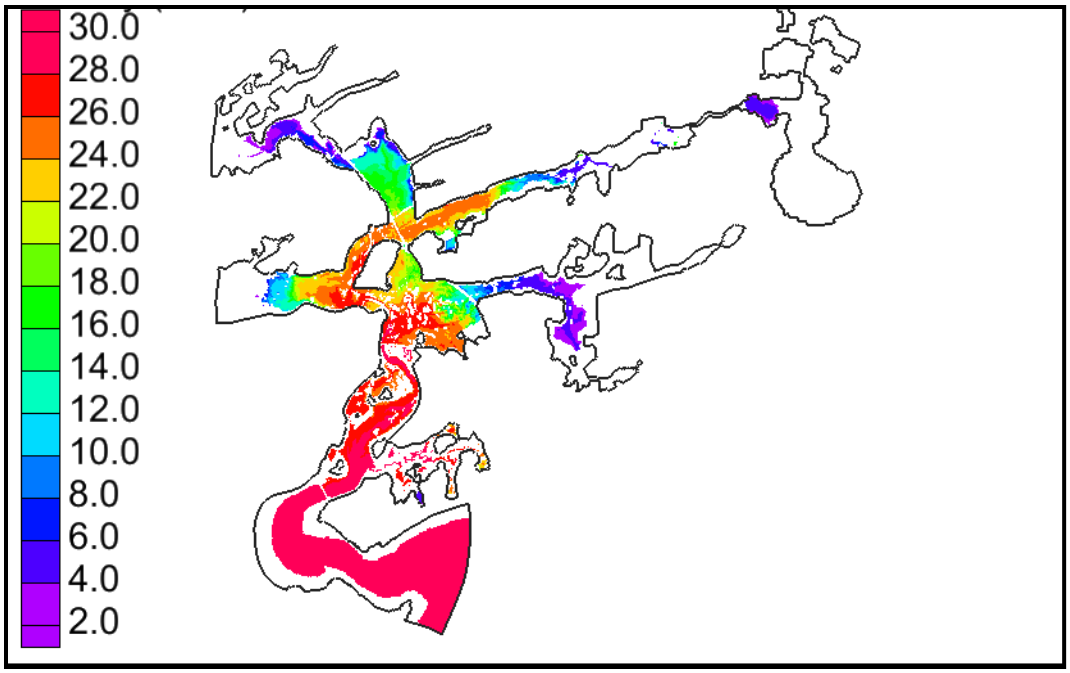

Figure 6-7. Salinity concentration throughout the Herring River system with an opening of 30 meters at the Chequessett Neck Road. Salinity contours are presented in ppt.

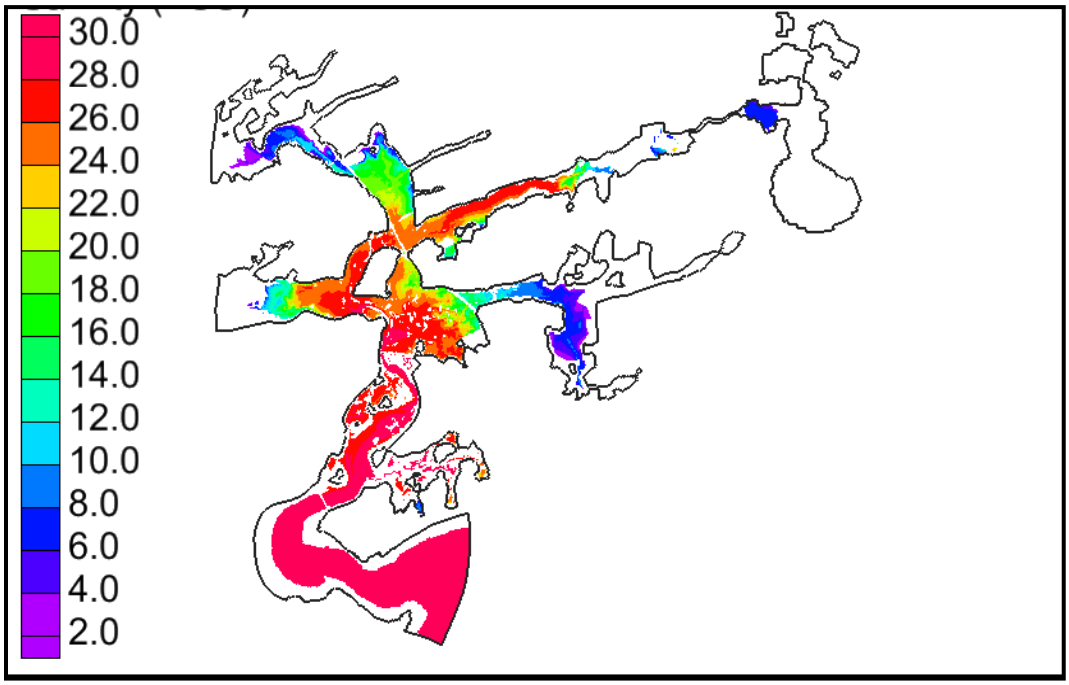

Figure 6-8. Salinity concentration throughout the Herring River system with an opening of 40 meters at the Chequessett Neck Road. Salinity contours are presented in ppt.

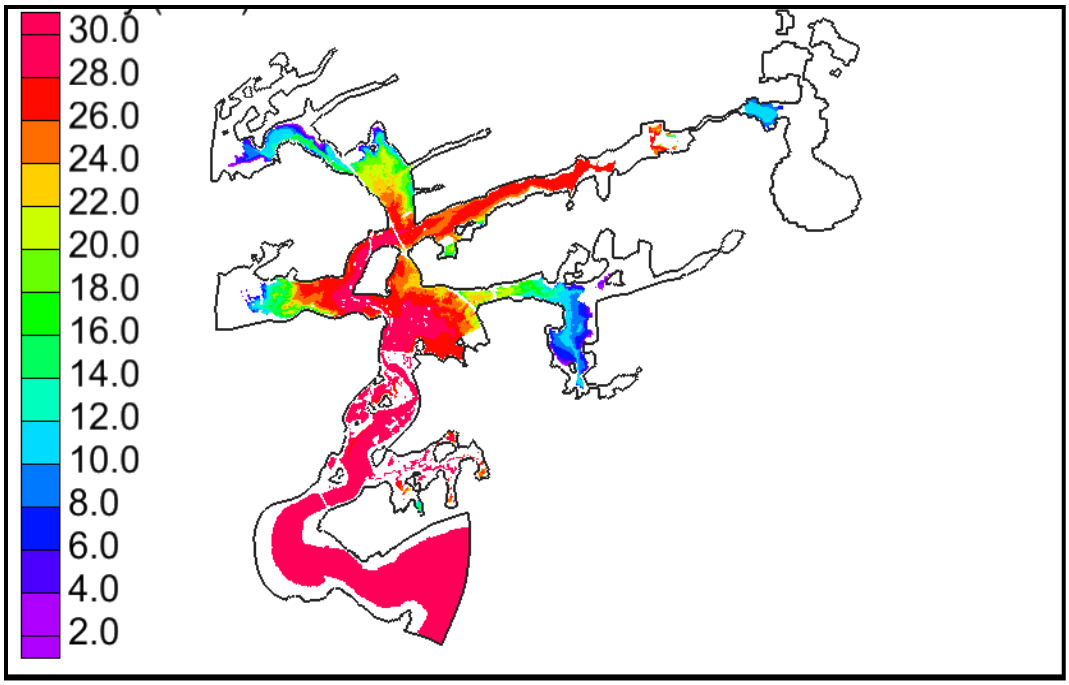

Figure 6-9. Salinity concentration throughout the Herring River system with an opening of 50 meters at the Chequessett Neck Road. Salinity contours are presented in ppt.

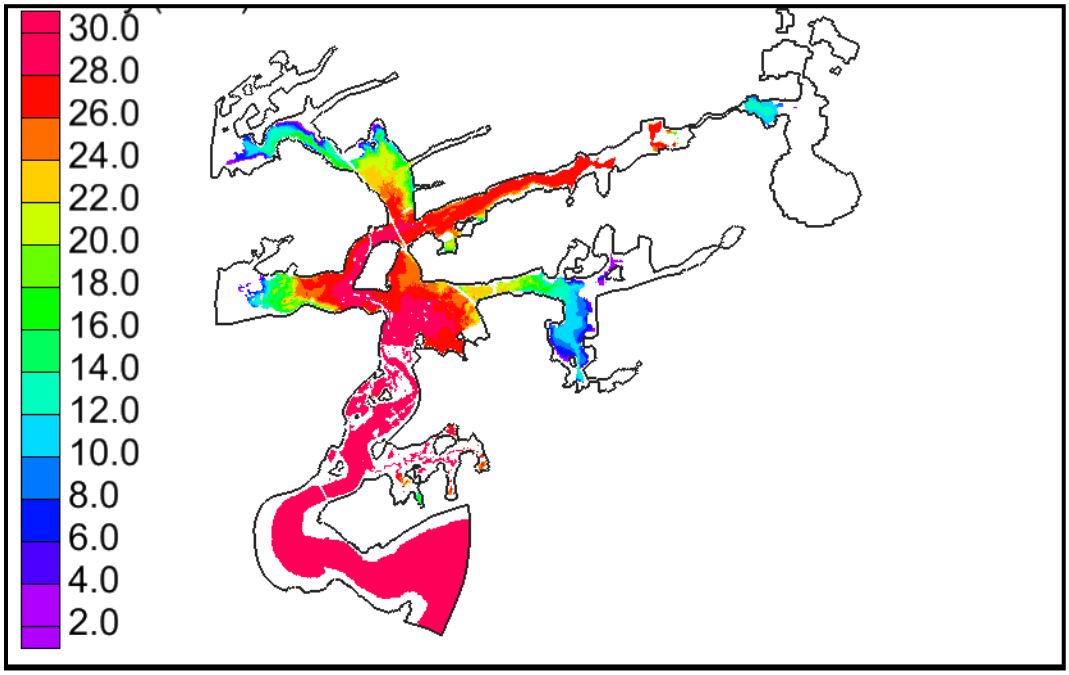

Figure 6-10. Salinity concentration throughout the Herring River system with an opening of 60 meters at the Chequessett Neck Road. Salinity contours are presented in ppt.

Based on the results of these alternatives, which evaluated the opening size at the Chequessett Neck Road dike, a 165-foot opening width was selected as the optimal opening size for a new dike. This was based on three main factors: (1) the increase in tidal range, (2) the intertidal area that would be created, and (3) the salinity penetration into the upper part of the system. These three factors were evaluated for all sub-basins and it was determined that a width of 165 feet was the optimal opening width in a new dike. This does not mean that the opening size would be 165 feet initially, or potential at any point in the future (depending on the adaptive management process). This opening size provides the ability to potential allow for maximum restoration of the system. Ultimately, the functional opening size could always be made smaller through implementation of tidal control structures, but would be difficult to make larger after the dike reconstruction.

6.2.2 Adaptive Management Slide (Sluice) Openings

Once the optimal opening width was determined, various height openings across the 165 foot width were simulated (assumed to be controlled through the utilization of slide gates). As such, these results provide incremental restoration levels and can be used to target adaptive management phases, identify openings that result in expected critical water levels (e.g., potential flooding of infrastructure in Mill Creek), and define restoration endpoints. Under the adaptive management approach, the proposed new dike could replicate the performance of the current system and then be slowly opened in a phased manner while changes throughout the system could be monitored. These simulations replicate this approach and provide various effective openings that could be applied to restore the Herring River system. For example, simulations were conducted with only 1/3 of the total width open 1 foot, 2/3 of the width open 1 foot, the entire width open 2 feet, etc. (Chapter 7).

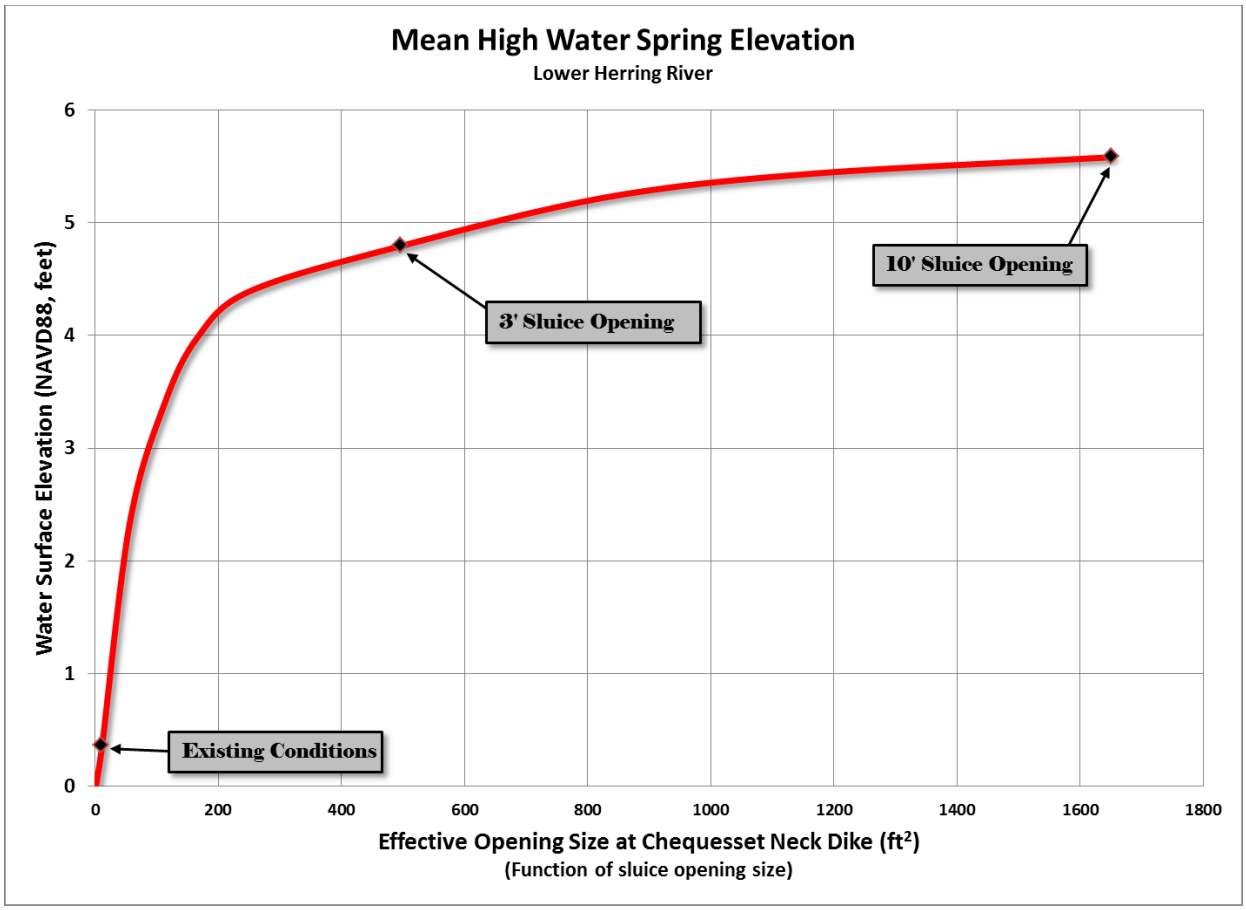

Figure 6-11. Mean High Water Spring water surface elevation in Lower Herring River as a function of effective opening size at Chequessett Neck Dike.

Figure 6-11 presents an example of some of the results that were developed for these simulations. The figure shows the water surface elevation of Mean High Water Spring (MHWS) in the Lower Herring River Basin (red line) as a function of effective opening size at Chequesett Neck Dike (horizontal axis). The effective opening size was adjusted based on various size slide (sluice) gate openings and a 165' width dike. The three black diamonds on the curve show the MHWS water elevation for existing conditions, and two of the endpoint restoration alternatives (3' and 10'sluice openings across the 165' dike). During the evaluation of various slide (sluice) gate openings, specific restoration endpoints were defined that met the water surface elevation objectives of the restoration project (Chapter 2). These restoration endpoints were subsequently used to define evaluated alternatives and impact assessment (Chapter 7). Specifically, the variable slide (sluice) gate simulations indicated that:

- A uniform 3' slide (sluice) gate opening across the entire 165' dike opening would limit the 100-year storm event water surface elevation to less than 6.0 feet NAVD88 throughout the system. Although this water surface elevation does not result in any flooding of concern throughout most of the system, the Mill Creek sub-basin, with lower upland infrastructure, would be at risk with water surface elevations over 6.0 feet NAVD88.

- A uniform 10' slide (sluice) gate opening, which is fully vertically open, limits the 100-year storm event water surface elevation to less than 7.5 feet NAVD88 throughout the system. This would results in significant flooding in several sub-basins, and as such would require targeted actions to mitigate flooding potential.

Therefore, based on these results at Chequessett Neck Road dike, the following three endpoint alternatives for the Chequessett Neck Road dike were developed. These endpoint restoration alternatives would advance using an adaptive management approach that would allow for controlled progress towards the endpoints.

1. A new Chequessett Neck Road dike with a 165' wide opening and a future targeted maximum 100-year tide elevation of 6 feet NAVD88 in the Lower Herring River (achieved with a 3' slide [sluice] gate opening). This would allow restoration with minimal changes to the upland infrastructure throughout most of the system; however, flood proofing would be required in the Mill Creek sub-basin for this alternative. Restoration would be significant through most of the system, but would not be maximized since the lower infrastructure elevations in the Mill Creek sub-basin would limit the maximum water surface elevation allowed in the system as a whole.

2. A new Chequessett Neck Road dike with a 165' wide opening and a future targeted maximum 100-yr tide elevation of 7.5 feet NAVD88 in the Lower Herring River (achieved with a 10' slide [sluice] gate opening) with elimination of tidal exchange within Mill Creek. A new proposed dike at the entrance to Mill Creek (section 6.6) with a one-way flap gate flow control structure would be installed to eliminate tidal exchange into Mill Creek. This would allow freshwater flow out of the Mill Creek basin, but no tidal water into the Mill Creek basin. This alternative would maximize restoration throughout the Herring River system, while the Mill Creek sub-basin would remain a non-tidal system. No flood proofing in the Mill Creek sub-basin would be necessary, although site-specific measures would be needed to protect low structures and roadways in other areas of the flood plain.

3. A new Chequessett Neck Road dike with a 165' wide opening and a future targeted maximum 100-yr tide elevation of 7.5 feet in the Lower Herring River (achieved with an approximate 10' slide [sluice] gate opening) with a limited tidal exchange in Mill Creek. This alternative would maximize restoration throughout the entire system, while limiting the maximum high tide within Mill Creek to less than 6 feet NAVD88. A new proposed dike at the entrance to Mill Creek (section 6.6) with appropriate flow control structure(s) would be installed to limit the tidal exchange into the Mill Creek producing similar water levels as the 3' sluice opening alternative. Flood proofing would be required throughout the flood plain, including in the Mill Creek sub-basin for this alternative.

Additional results of these various opening heights are further detailed in Chapter 7.

6.2.3 Assessment of Culvert Inverts

As an initial test to evaluate the potential influence of modifying the culvert inverts (specifically, lowering the inverts) at the Chequessett Neck Road dike, two simulations were performed. These simulations were geared towards determining if the culvert invert alone (without natural or dredging adjustment to the bathymetry) would influence the water surface elevation. A 65 foot (20 meter) wide culvert opening was used for both simulations; however, in one simulation the existing culvert invert elevation of -3.4 feet NAVD88 was used while in the other the invert was lowered 1.5 feet to -4.9 feet NAVD88. The tops of the culverts were set sufficiently high in both simulations to prevent them from flowing completely full. The results for water surface elevation from these simulations in the lower Herring River sub-basin are compared in Figure 6-12. These results show that the existing culvert invert elevation is sufficiently low as to not pose a restriction to low tide in the river. This also likely indicates that the bathymetry surrounding the dike tends to be the limiting factor for low tide levels in the river. Lowering the culvert does allow a greater volume of flow (slightly higher tides); however, without a significant adjustment to the local bathymetry upstream and downstream of the dike, the low water level does not decrease. It may be feasible that a lower culvert invert, combined with the increased volumetric flow, would cause scour and an eventual lowering of the river bed and thereby a more significant change to the mean low water elevation than indicated here. However, this lowering would have to occur over a significant distance both upstream and downstream of the dike and it is likely that the scour may occur in a localized area at the dike only. As such, based on the results of these simulations, the water surface elevation results are relatively independent of culvert invert, as long as the invert stays at the same or a lower elevation.

6.3 REMOVAL OF THE FLOOD TIDAL SHOAL

A significant flood tidal shoal has formed just upstream of the Chequessett Neck Road dike in response to the restriction imposed by the existing culverts in the dike. Proposed restoration alternatives with larger openings in the dike have raised concerns that this shoal may begin to impose a restriction, influencing tidal propagation farther up into the estuary as the current limiting restriction imposed by the dike's culverts is removed. However, the increased tidal exchange may also relocate the flood tidal shoal farther upstream in the system throughout the restoration process. In order to assess any potential restriction the shoal may cause in the restored Herring River, a simulation was conducted with the flood tidal shoal removed. This section describes the changes made to the model grid, and the effect of the removal of the shoal on water levels and depth-averaged current velocities.

6.3.1 Grid Modification

Figure 6-13 shows the bathymetry of the Herring River model grid in its current unaltered state. The figure clearly shows the flood tidal shoal which has formed just upstream of the Chequessett Neck Road dike. There is a significant portion of this shoal that lies between -1.5 and -1.0 feet-NAVD88 and, during typical low tides, becomes exposed. The Herring River model grid was modified to remove this shoal by reducing the elevation of grid cells to an elevation of -3.4 feet-NAVD88. This elevation is the same as the elevation of the culvert inverts in the dike and is roughly the same as the surrounding river bottom. The resulting model grid bathymetry is shown in Figure 6-14. Removing the flood tidal shoal to this elevation in the actual river would require extraction or natural transport of approximately 6,000 cubic yards of sediment. The channel

thalweg, which is located to the south of the flood tidal shoal and is approximately -6.0 feet NAVD88, may, like the shoal, be a response to the restriction imposed by the current configuration of the dike and shoal combination. Simulations were conducted using a 100 foot (30 meter) opening at the dike.

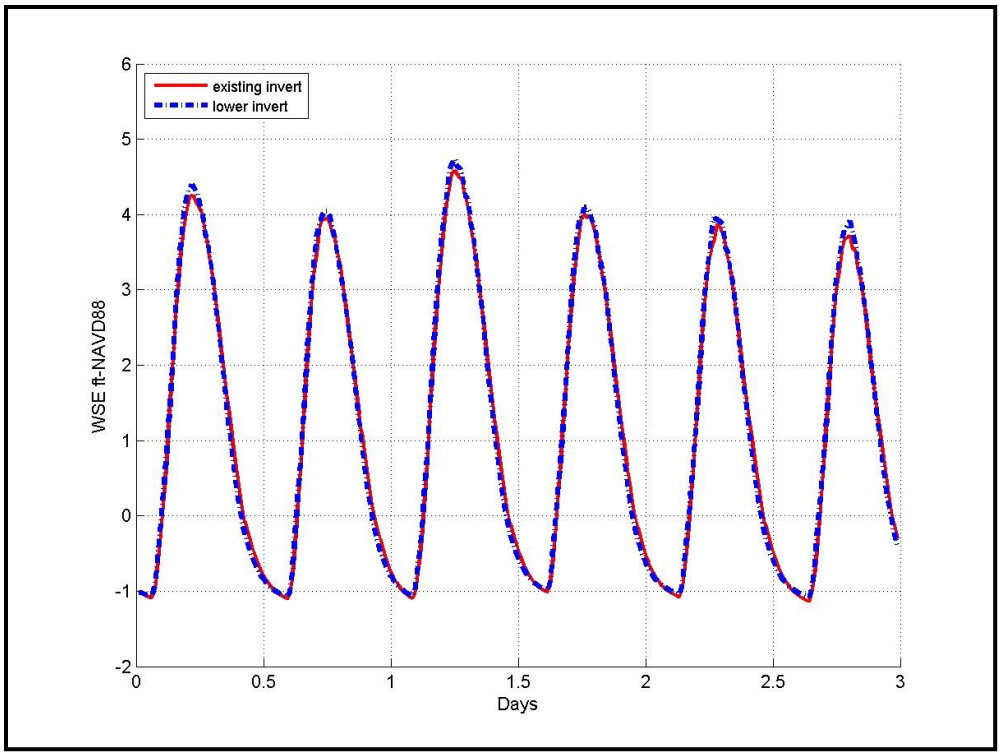

Figure 6-12. Time series of modeled water surface elevation (WSE) with existing Chequessett Neck Road dike culvert invert (red line) and with the invert lowered 1.5 ft (broken blue line).

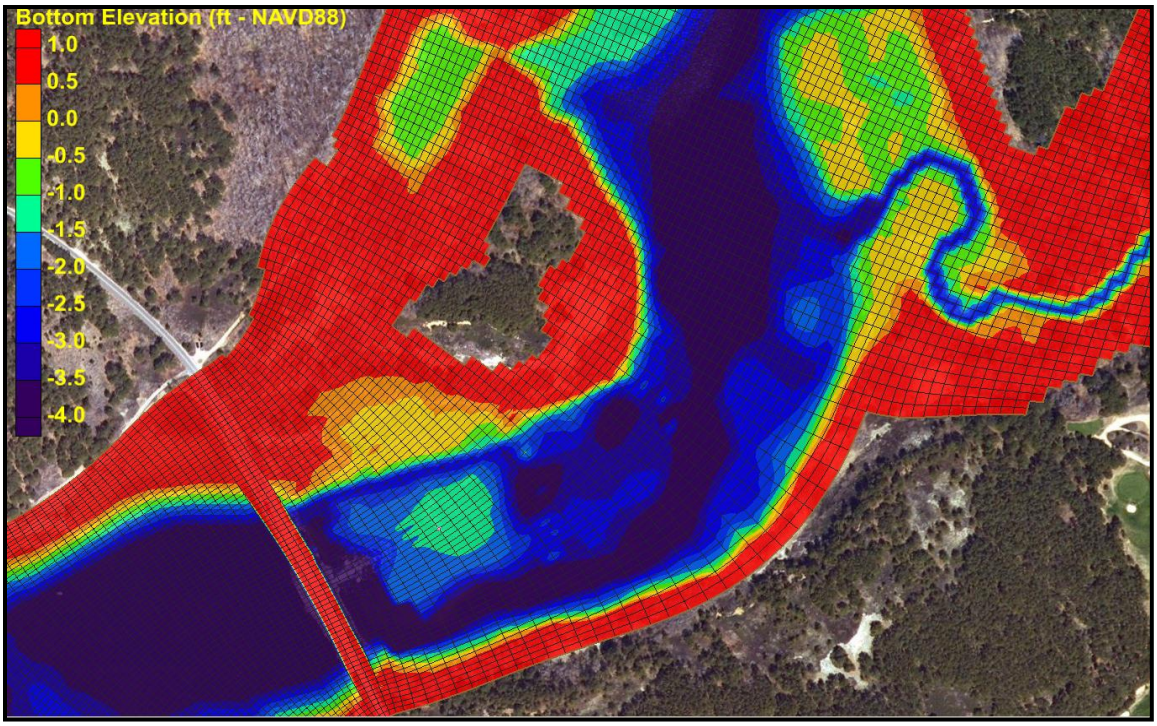

Figure 6-13. Current bathymetry of the Herring River model showing the flood tidal shoal.

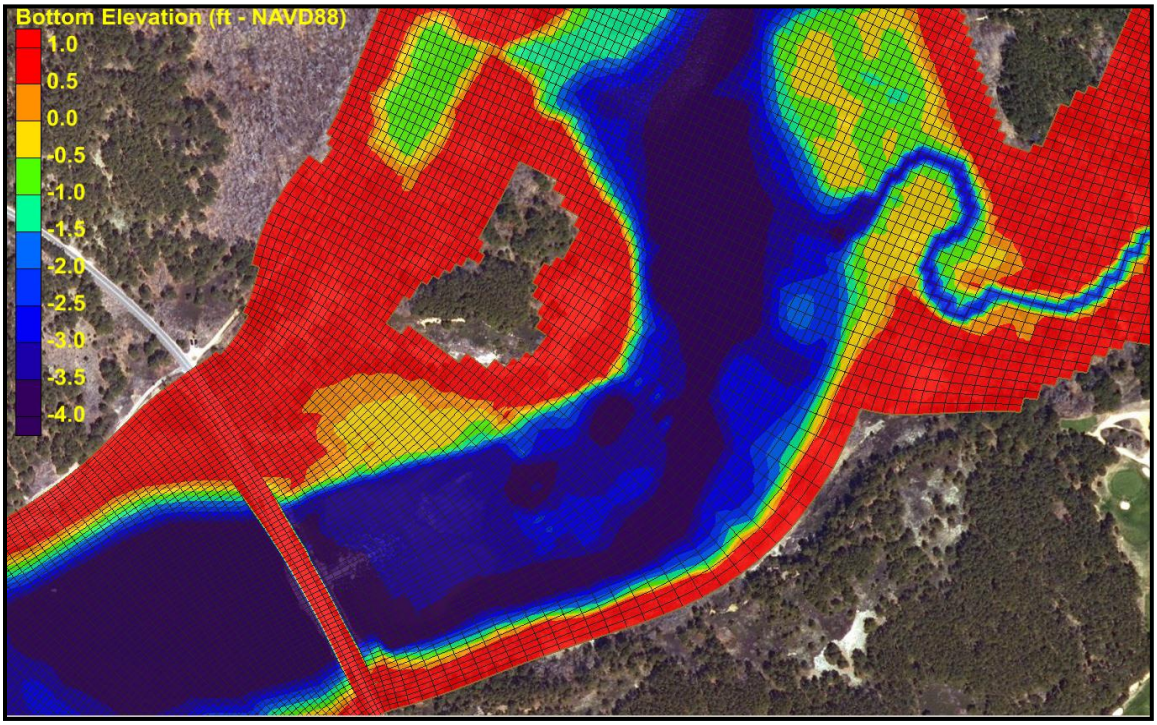

Figure 6-14. Bathymetry of the Herring River model with the flood tidal shoal removed.

6.3.2 Water Surface Elevation Results

Figure 6-15 presents water surface elevations within the lower Herring River sub-basin (from a location centrally located within the lower Herring River sub-basin and provides a representative sample of the water levels throughout lower sub-basin). Figure 6-15 shows the impact of the shoal removal on water surface elevations is relatively minor. The low tide elevations are slightly lower (approximately 1 inch) with the shoal removed. This is evidence, that the shoal does provide some minimal restriction to the ebbing tide, particularly when the tide is low and the shoal becomes exposed.

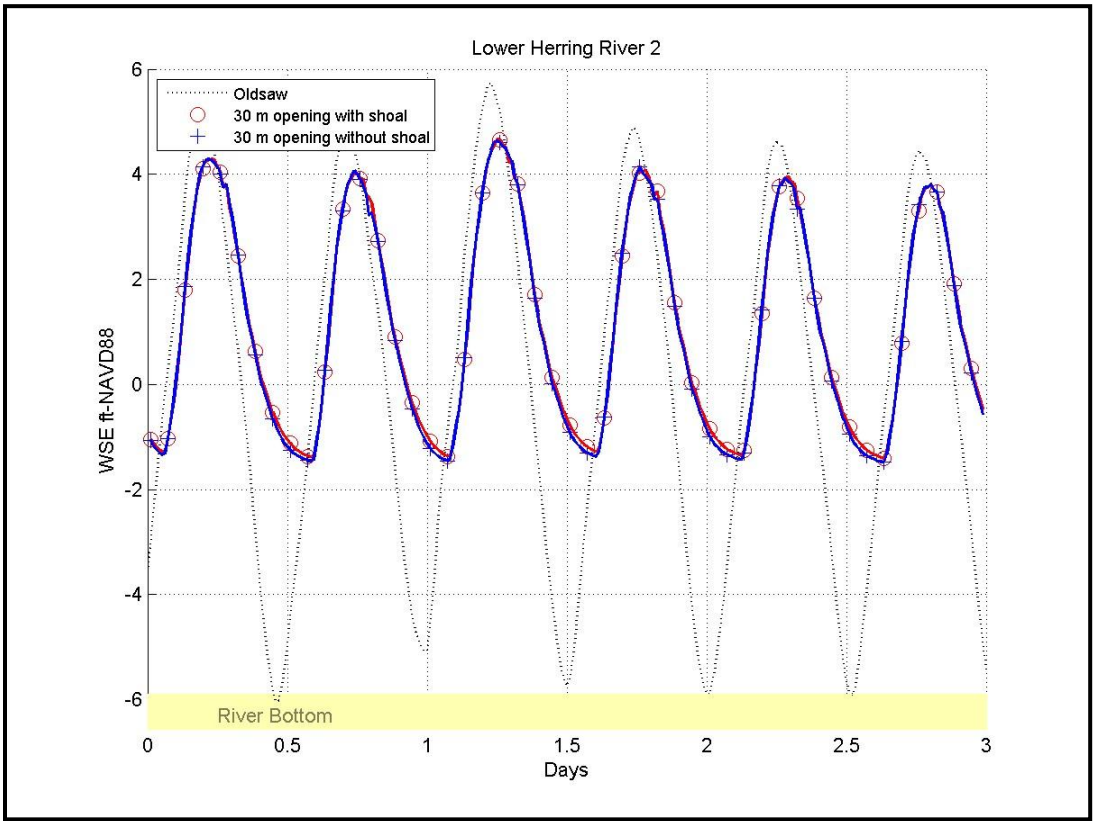

Figure 6-15. Water surface elevation time series within lower Herring River with a 100 foot dike opening with (red line) and without (blue line) the flood tidal shoal.

6.3.3 Depth Averaged Velocity Results

While the effect on water levels caused by the shoal removal is minor, there is a more pronounced effect on current velocities in the area just upstream of Chequessett Neck Road. The greatest velocities in the region around the flood tidal shoal occur during ebbing flows. Figure 6-16 shows the depth-averaged current velocity during ebb tide when the current speeds are greatest for the 100 foot dike opening with the flood tidal shoal present, while Figure 6-17 shows a similar snapshot from the same time in the simulation with the shoal removed. Comparison of these two figures illustrates that the shoal causes the ebb current to be concentrated to the south of the shoal with current speeds over 3 feet per second. With the shoal removed however, the

maximum current speeds are reduced by approximately half. While the maximum speed is greatly reduced by the removal of the shoal, the area with current speeds over 0.5 feet per second is greatly increased resulting in an overall greater total volume flux. This increased volume flux allows for the slightly greater tidal range shown in the lower sub-basin with the shoal removed.

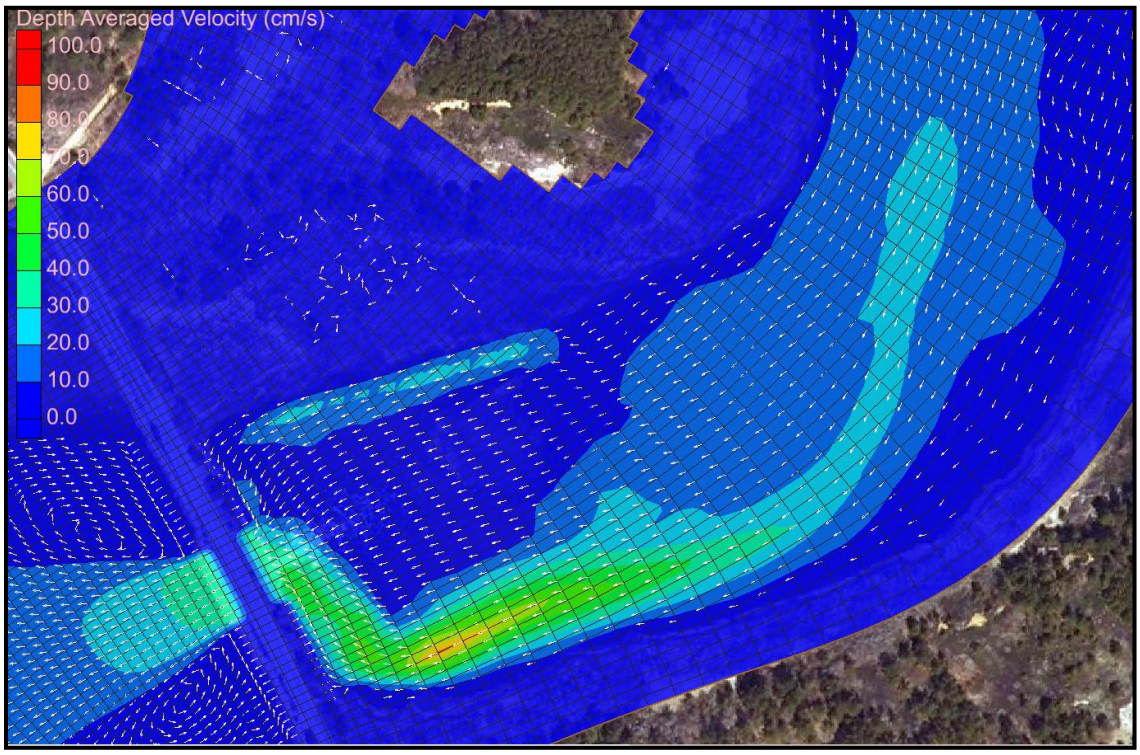

Figure 6-16. Depth averaged velocity color contours and vectors during ebbing flow for a 100 foot dike opening width and flood tidal shoal as existing.

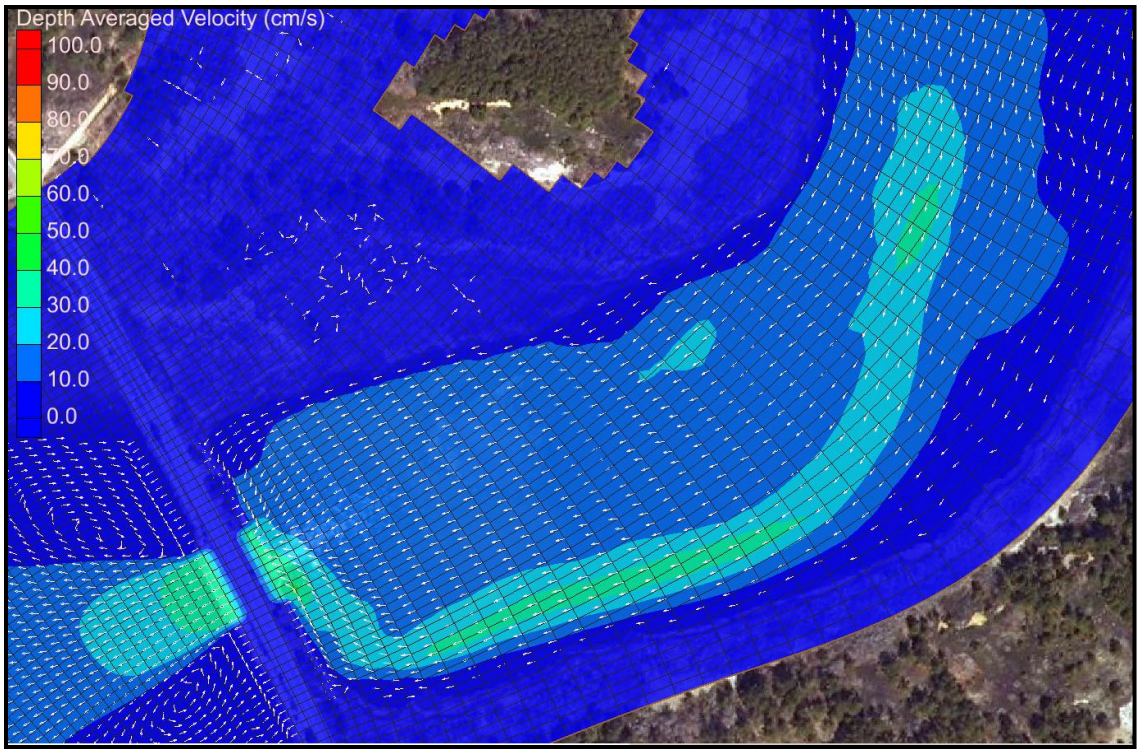

Figure 6-17. Depth averaged velocity color contours and vectors during ebbing flow for a 100 foot dike opening width and flood tidal shoal removed.

6.4 HIGH TOSS ROAD OPENING

This section describes the configuration and results of a series of alternative simulations of the Herring River hydrodynamic model designed to assess the impact of the High Toss Road causeway and High Toss Road culvert on the tidal water surface elevations and salinity in the Herring River estuary. Changes were made to the model grid to represent two different proposals for physical modification of High Toss Road. The first configuration considers the removal of the existing 5 foot diameter circular pipe culvert under High Toss Road and replaces the culvert with an open channel allowing the river channel to be restored to an unrestricted state. The second configuration considers the removal of the entire High Toss Road causeway, in addition to removal of the culvert. Figures 6-18 through 6-20 show the elevations of the Herring River hydrodynamic model grid near High Toss road for the existing conditions (Figure 6-18), the open channel alternative (Figure 6-19), and the causeway removed alternative (Figure 6-20). All figures present elevations in NAVD88 feet. To assess the potential impact of these different scenarios for various levels of restoration, all three High Toss Road alternatives were simulated with opening widths of 20, 30, 40, and 50 meters (65 feet – 165 feet) at Chequessett Neck Road. All simulations used normal tidal conditions.

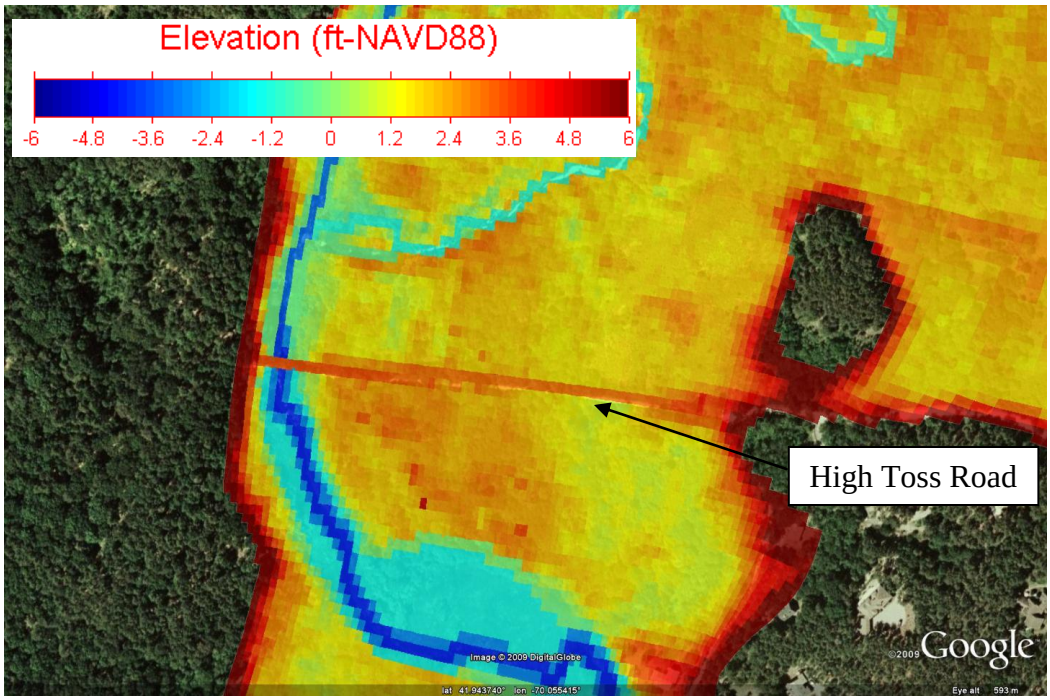

Figure 6-18. Existing elevations in the hydrodynamic model near High Toss Road.

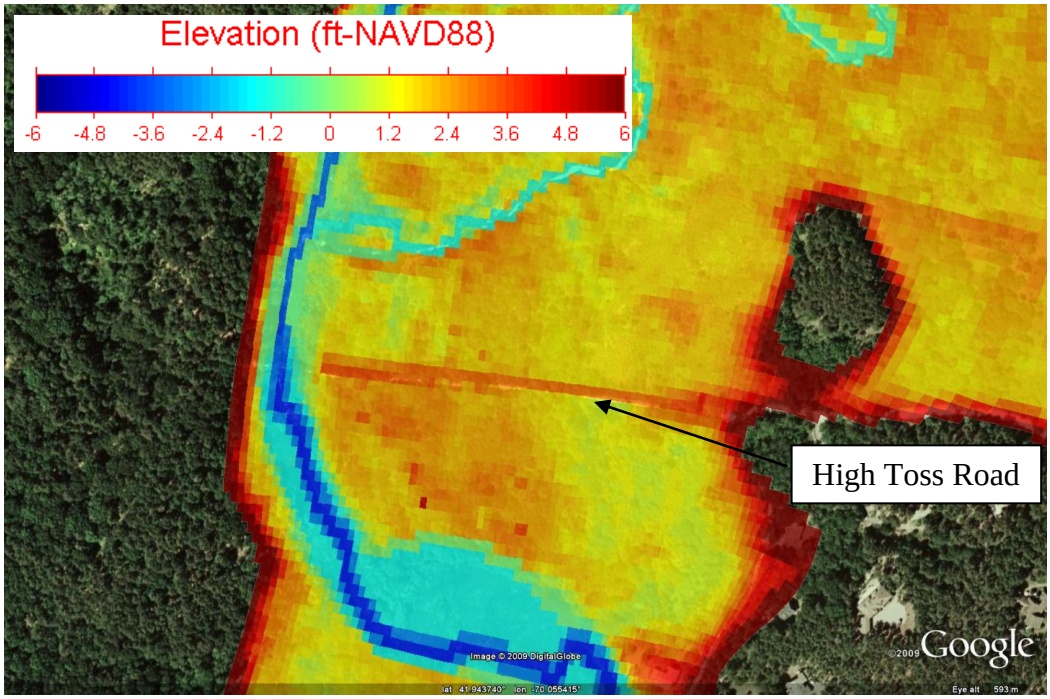

Figure 6-19. Proposed open channel alternative for High Toss Road.

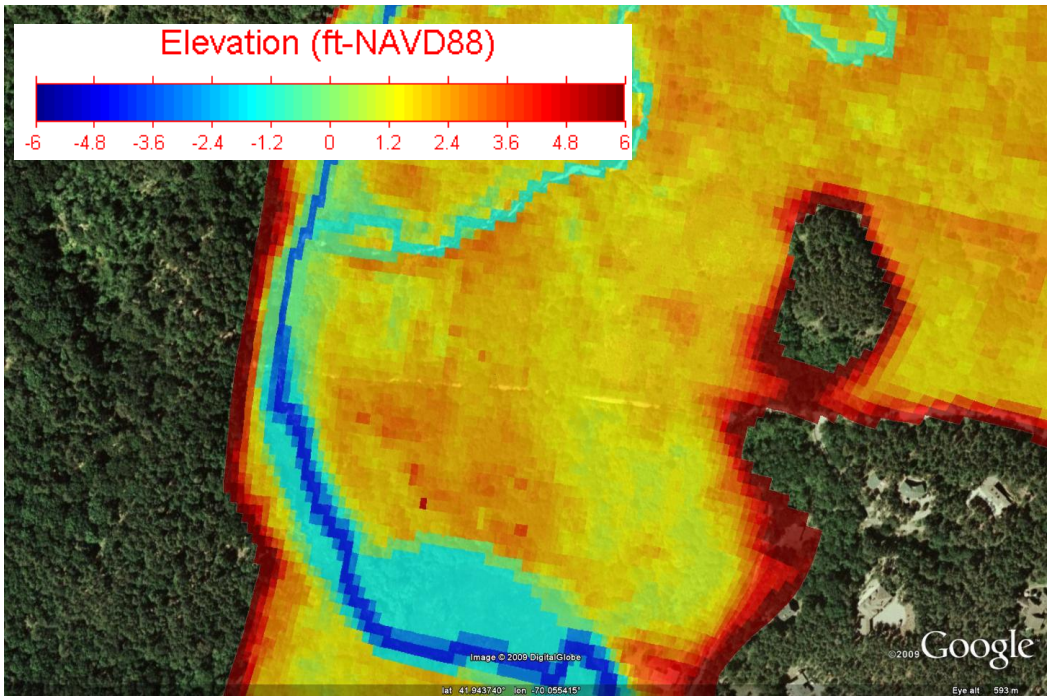

Figure 6-20. Proposed open channel and causeway removal alternative for High Toss Road.

Results from the High Toss Road alternative simulations were examined with regard to both water surface elevation and salinity throughout the estuary. To facilitate comparisons between these simulations, and previous simulations without alterations to High Toss Road, model output was extracted from each of the estuaries sub-basins (as detailed in Chapter 7). Focus was placed on the Mid Herring River sub-basin located just upstream of High Toss Road. In general, effects of the High Toss Road alternatives throughout the system can be determined through assessment of the response in the Mid Herring River sub-basin, since it provides downstream control for four other sub-basins in the system (Duck Harbor, Bound Brook , Upper Herring River, and Pole Dike Creek). Figure 6-21 shows a water surface elevation time series from the Mid Herring River basin for the High Toss Road alternatives with a 100 foot wide opening at the Chequessett Neck Road Dike. The red line shows the water surface elevation with High Toss Road in its existing configuration, while the blue and green lines show the water surface elevation for the open channel and causeway removed alternatives, respectively. In its existing state, High Toss Road will be overtopped by a typical high tide when the Chequessett Neck Dike is opened greater than 65 feet wide. Therefore, under restored conditions this road would require a raised elevation and mitigation if it is intended to remain in place.

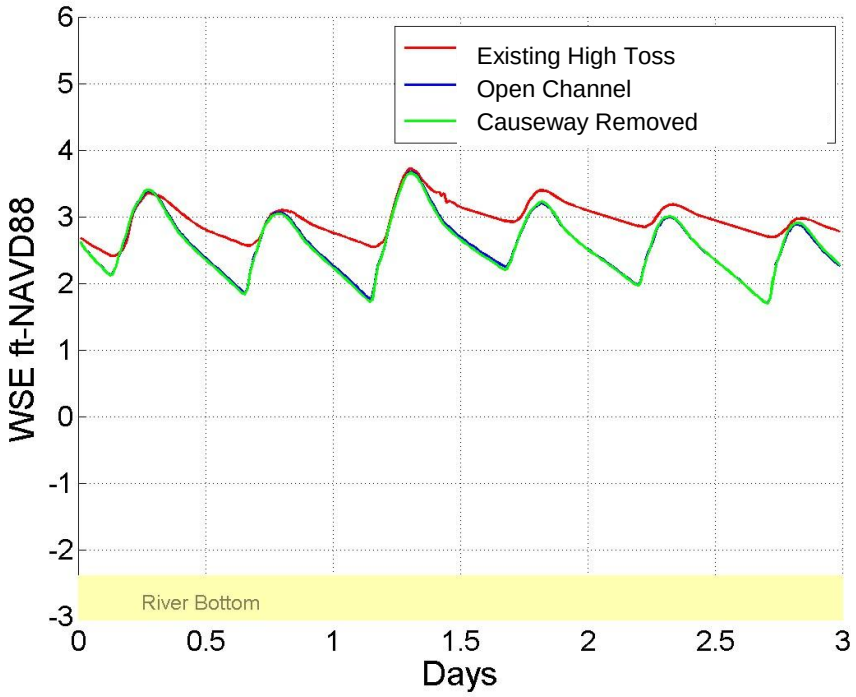

Figure 6-21. Water surface elevation time series at Mid Herring River for High Toss Road Alternatives with 100 foot (30 meter) total opening width at the Chequessett Neck Road Dike.

However, once overtopped, the causeway also acts like a low-lying weir and inhibits flow out of the system, and when the tide falls below the elevation of the causeway the ebbing flow is forced to go through the relatively restrictive existing culvert. This results in an increased mean water level and smaller tidal range upstream of High Toss Road. As such, modification to High Toss Road is an important component of the overall restoration. The High Toss Road alternatives (open channel and removing the causeway) remove the culvert restriction and allow water to better drain from the upper portions of the system in the restored conditions (i.e., with a new Chequessett Neck dike opening). This results in an improved MLW level and significantly greater tidal range. The difference between impacts on water surface elevation between an open channel scenario and full removal of the causeway is minimal. Therefore, although the existing High Toss Road configuration does not significantly impede flood tides into the upper portion of the system, it does have a significant impact on the ebb tides and drainage ability of the upper portion of the estuary.

Figure 6-22 shows water levels for the High Toss Road open channel configuration with various size openings at the Chequessett Neck Road dike. With Chequessett Neck Road dike openings greater than 100 feet, there are relatively small changes in the tidal levels in the Mid Herring River sub-basin. This is similar to the results for Chequessett Neck Road dike opening greater than 100 feet, which indicated that larger opening show minimal increases in restoration potential from a water surface elevation perspective.

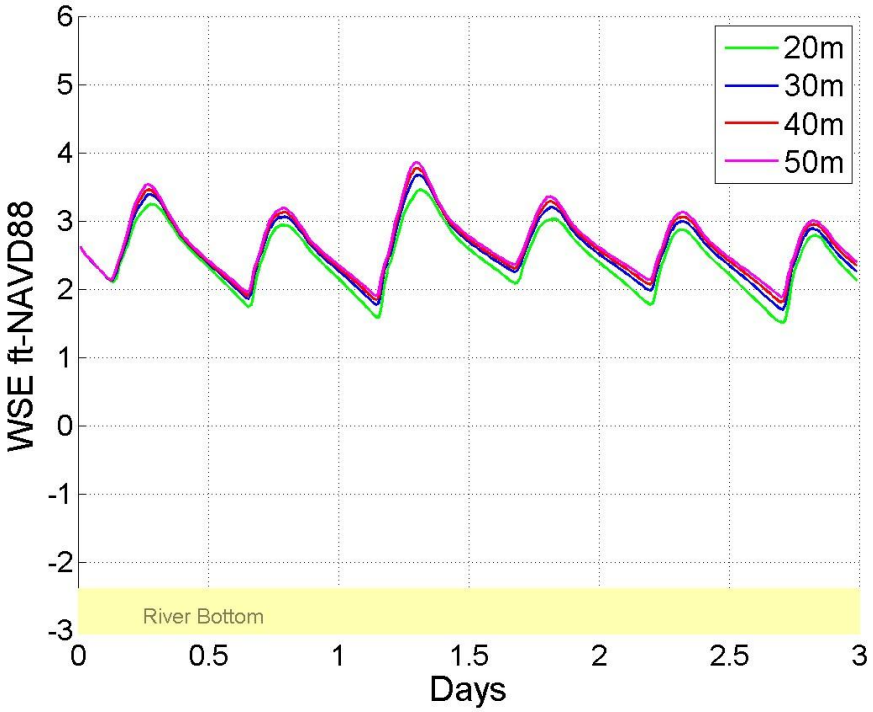

Figure 6-22. Water surface elevation time series at Mid Herring River for High Toss Road open channel with various Chequessett Neck Road Dike opening widths.

To evaluate the influence of the High Toss Road alternatives on salinity levels, maximum salinity throughout the estuary during the typical tidal conditions was assessed. Figures 6-23 and 6-24 show color contours of the maximum salinity for the High Toss Road open channel and causeway removed. The difference in maximum salinity for the High Toss Road alternatives is minimal, indicating that either alternative will function adequately for salinity penetration.

Overall, the assessment of High Toss Road indicates that under restored conditions (Chequessett Neck Road dike openings of 65 feet or greater), the roadway will be overtopped. As such, the road would require mitigation to remain useable, or be abandoned. The existing High Toss Road and culvert also negatively impact restoration potential in the upper portions of the Herring River estuary. Specifically, the restrictive culvert and causeway impede the draining of the upper system during an ebbing tide, resulting in a reduced tidal range, excessive ponding, and higher MLW. The removal of the High Toss Road culvert and creation of an open channel at this location is recommended.

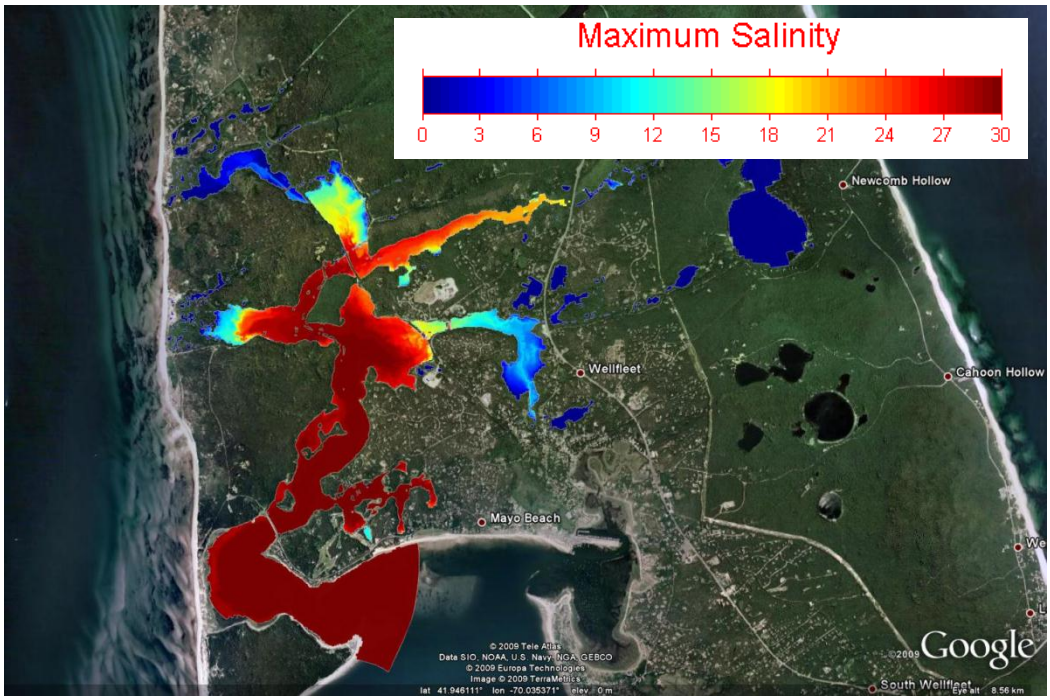

Figure 6-23. Maximum salinity for High Toss Road open channel alternative with 165 foot (50 meter) Chequessett Neck Road Dike opening.

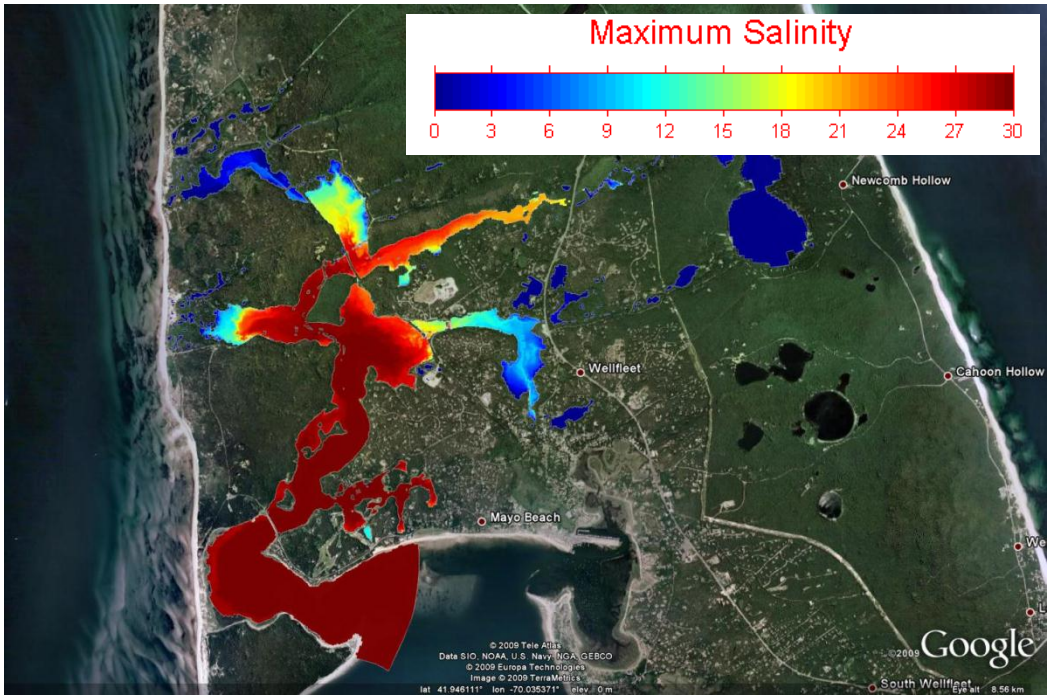

Figure 6-24. Maximum salinity for High Toss Road causeway removed alternative with 165 foot (50 meter) Chequessett Neck Road Dike opening.

6.5 CULVERTS IN THE UPPER PORTIONS OF THE SYSTEM

There are eight upstream culverts that exist within the upper portions of the Herring River estuary (Table 5-2). The potential influence of these culverts on the expected restored tidal exchange in the system was assessed using the Herring River model. To assess these culverts, the restored system (with Chequessett Neck Road dike open and High Toss Road made into an open channel) was simulated with and without all the upstream culverts in place. These alternatives were aimed at evaluating the upstream sub-basins to determine if the culverts in the upstream portions of the system had a significant impact on the water surface elevations in the system. Figure 6-25 shows the results from the model for the Duck Harbor region. The horizontal bottom axis presents the opening width at the Chequessett Neck Road dike, while the vertical axis presents the water surface elevation (or land elevation for the hypsometric curve) in feet NAVD88. The red and blue line present the Mean High Water and Mean Low Water tidal benchmarks with that specific sub-basin (in this case Duck Harbor). The gray line (and corresponding top horizontal axis) presents the hypsometric curve for this particular sub-basin. The two star markers on the figure show the results for MHW and MLW with a 130 foot (40 meter) dike opening with all the upstream culverts removed. If the stars lie on the blue and red lines, then the removal of upstream infrastructure has minimal impact on the water surface elevations in that particular sub-basin. As shown in Figure 6-25, the removal of upstream infrastructure had little impact on the restored water surface elevations in Duck Harbor.

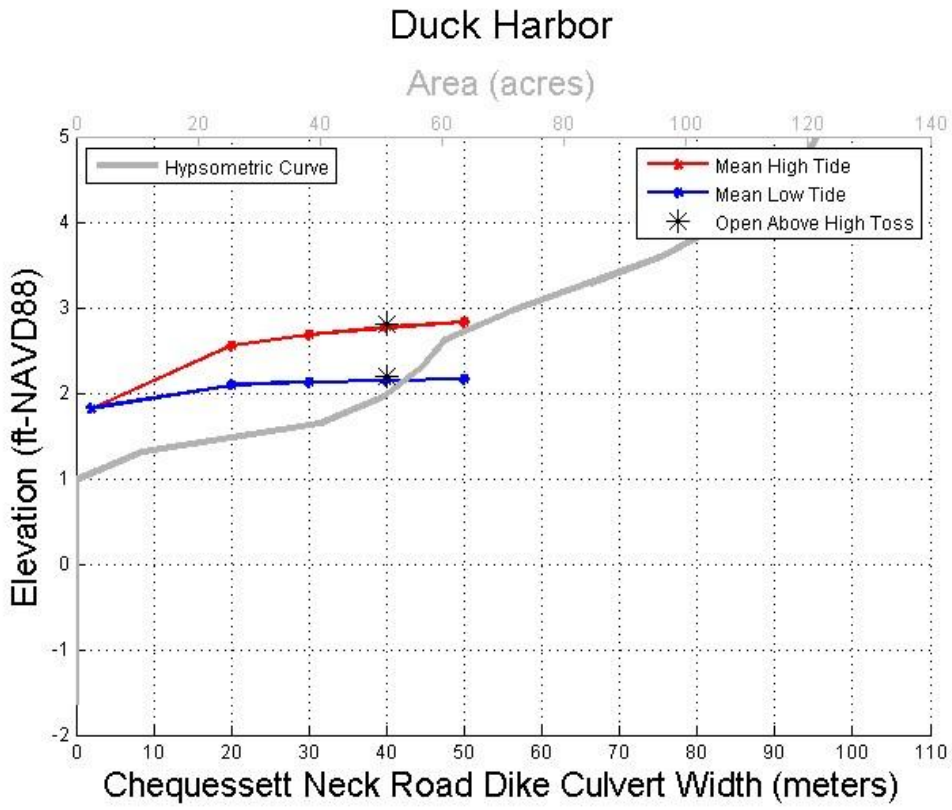

Figure 6-25. Water surface elevation results in the Duck Harbor sub-basin showing a comparison of upstream culverts in place and removed.

This analysis was completed for all sub-basins (including those downstream of High Toss Road), and the only sub-basins that showed an impact from the removal of the upstream culverts were Upper Pole Dike Creek (Figure 6-26) and Bound Brook (Figure 6-27). These changes were limited to relatively small modifications to the elevation of MLW, as shown by the star marker that is located below the blue line in both figures. The results indicate that the culverts in these sub-basins inhibit drainage ability of, and limit tidal range within, these sub-basins. It is expected that enlargement of the culverts at Pole Dike Road and Old County Road (Table 5-2) would reduce this restriction for these two particular sub-basins.

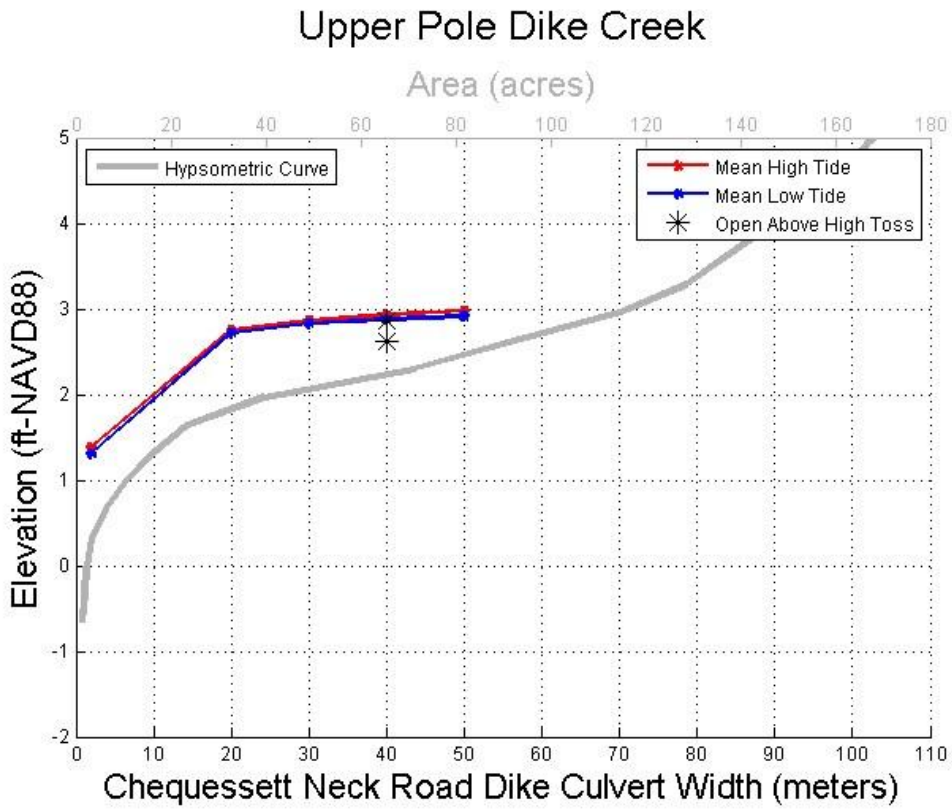

Figure 6-26. Water surface elevation results in the Upper Pole Dike Creek sub-basin showing a comparison of upstream culverts in place and removed.

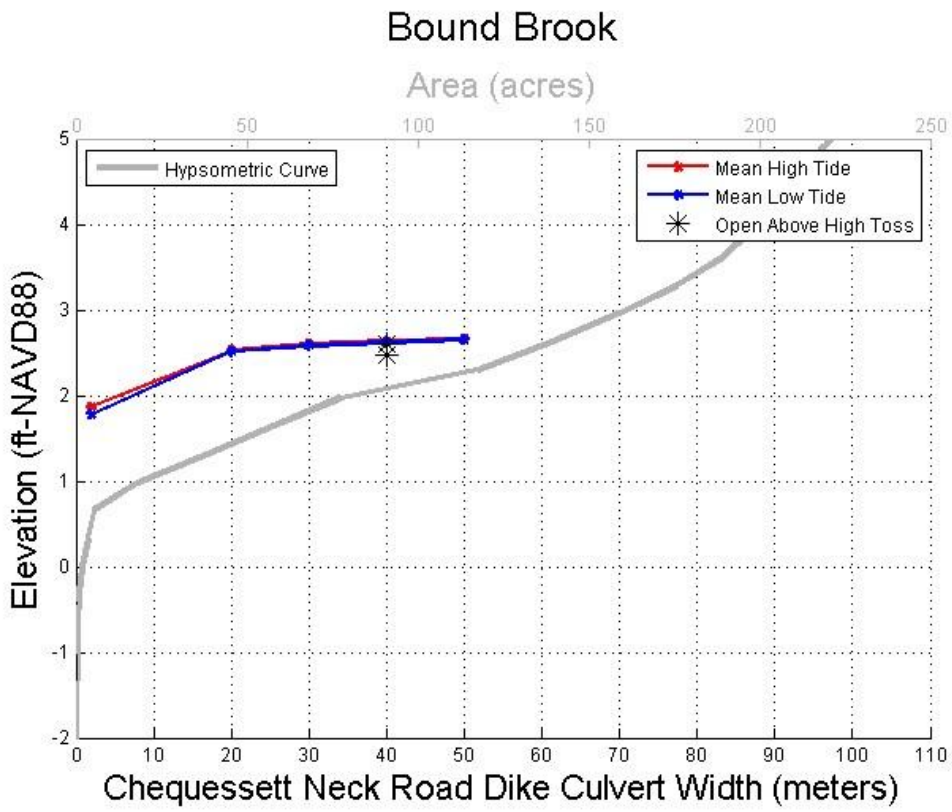

Figure 6-27. Water surface elevation results in the Bound Brook sub-basin showing a comparison of upstream culverts in place and removed.

6.6 MILL CREEK SUB-BASIN

The Mill Creek sub-basin is an extension of the Herring River estuary, just upstream and to the southeast of the main Herring River channel (see section 7.1). The Mill Creek sub-basin is one of the most developed sub-basins within the Herring River estuary. The Chequessett Yacht and Country Club's (CYCC) golf course, as well as several private homes, lie around the edge of the basin and within the historic flood plain (pre-dike construction). Due to the relatively developed nature of this particular sub-basin, alternatives to potentially segregate it from the remaining Herring River Restoration effort are being considered to provide more targeted restoration, while also limiting the potential impact on the developed areas (see section 6.2.2). Specifically, the construction of a new dike, separating the Mill Creek sub-basin from the greater Herring River, was evaluated in concert with the overall restoration project and used to assess alternatives that segregate the Mill Creek tidal regime.

Therefore, to assess the potential influence of a new Mill Creek dike, a detailed Mill Creek sub-basin model was developed that could be integrated with the larger Herring River model, but at the same time could be used independently to simulate specific cases within the Mill Creek sub-basin alone. The Mill Creek grid domain extends from the main body of the Herring River, along the course of Mill Creek. The model domain is approximately bounded by Old Chequessett Neck Road on the north, Chequessett Neck Road on the south, Hamblen Farm Road on the west, and the Herring River on the east. The Mill Creek domain can be simulated using

tidal signals produced by full domain runs, applying the driving signal from a cell in the Herring River. Therefore, simulated changes in the overall restoration project (e.g., various slide gate openings at Chequessett Neck dike) can be translated accurately to the Mill Creek sub model. The new, smaller domain is shown in Figure 6-28.

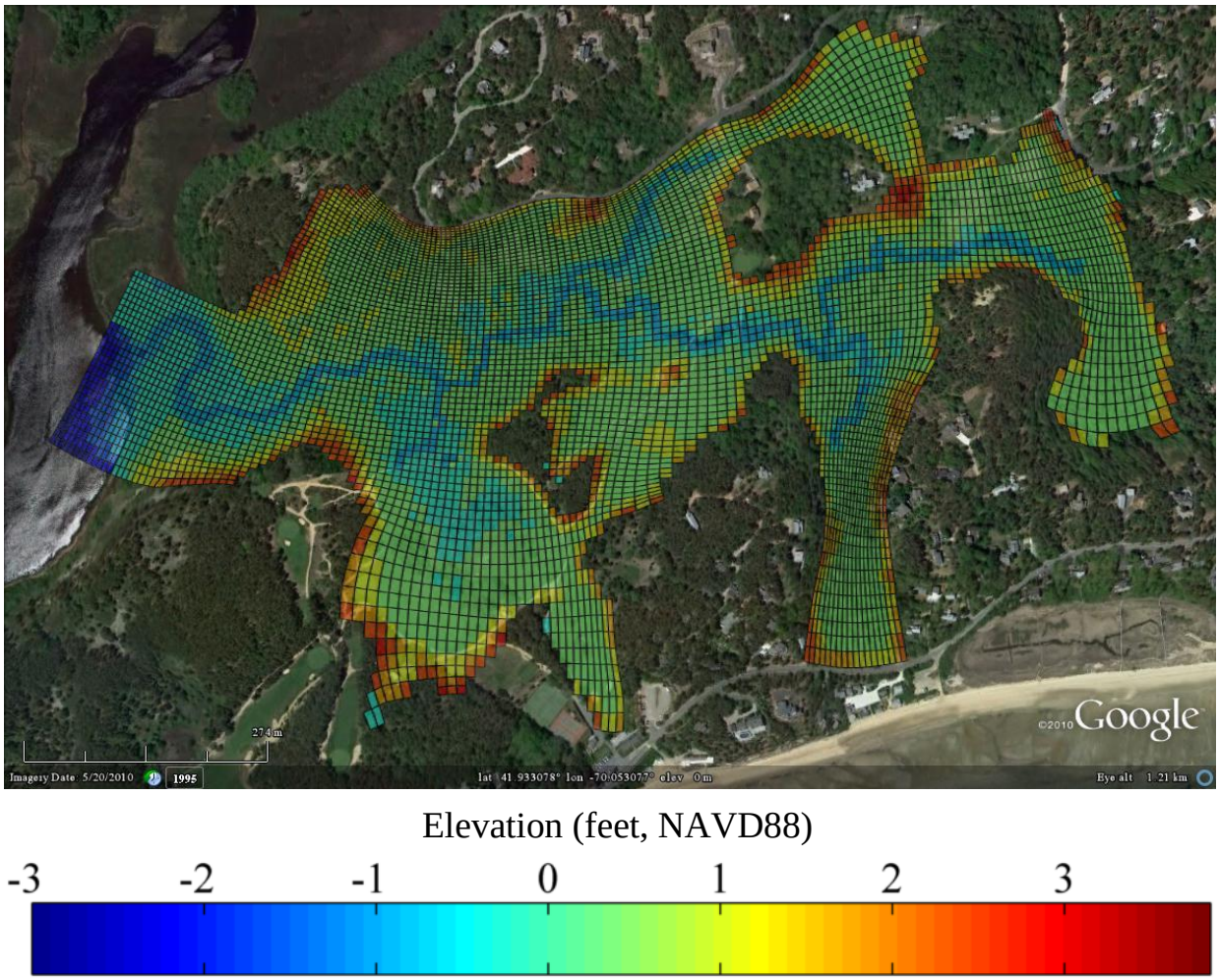

Figure 6-28. Mill Creek sub model domain with elevations in feet NAVD88 (as shown in colorbar).

In order to ensure that the Mill Creek sub-basin model was accurately replicating the results of the larger Herring River model (that included Mill Creek), results from the sub-basin model were compared to the results of the larger model for the same simulation conditions. This comparison revealed that the Mill Creek sub-basin model produced the exact same results that the larger model produced within Mill Creek. Therefore, the Mill Creek sub-basin model could be applied to assess hydrodynamics within Mill Creek without having to simulate the entire Herring River system.

To simulate the proposed dike separating Mill Creek from Herring River, a second version of the sub model domain was also created with a modified grid (Figure 6-29). The simulated dike includes a combination sluice/flap gate at the location where the main Mill Creek channel flows through the proposed dike.

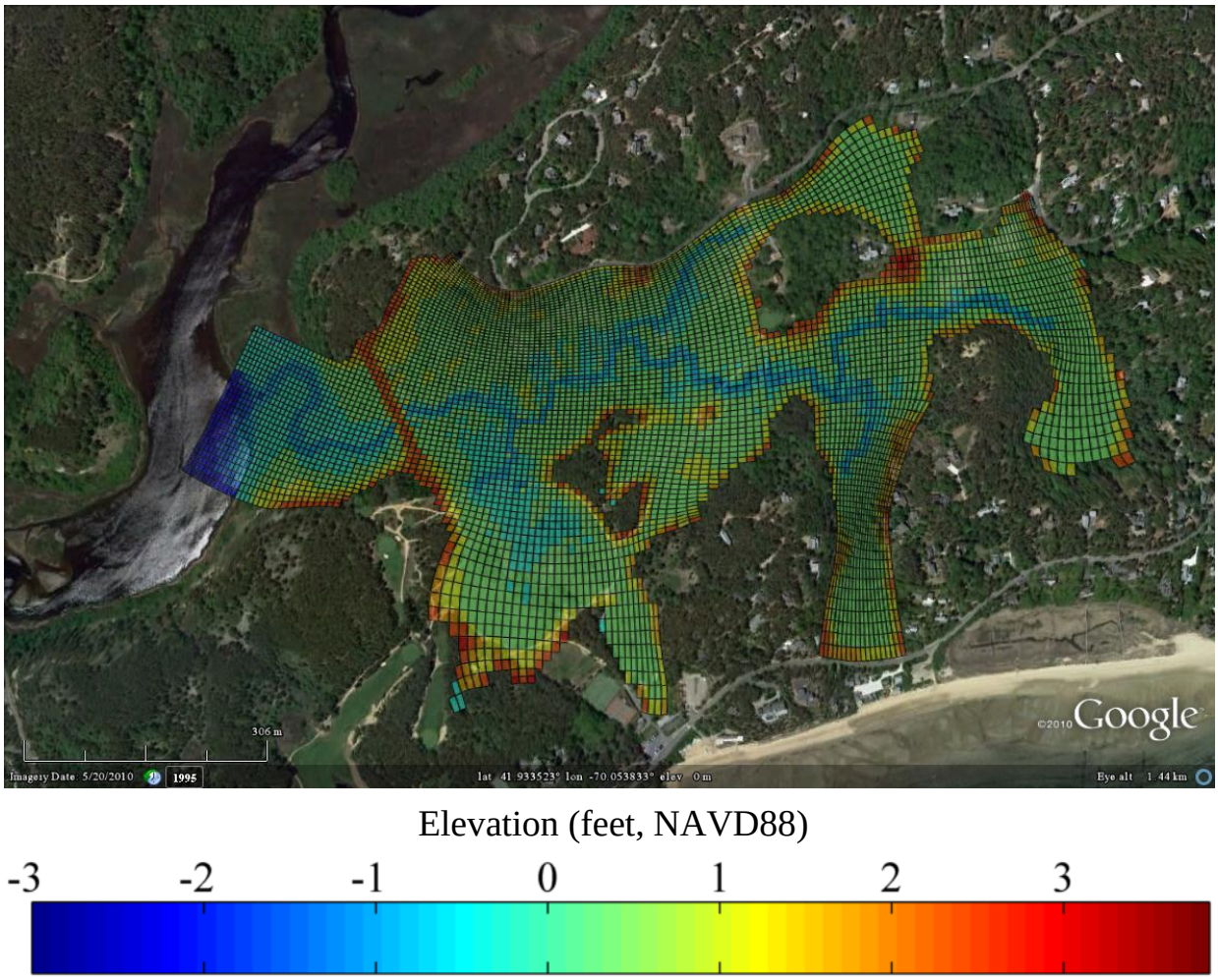

Figure 6-29. Mill Creek sub model domain with simulated dike added. Elevations in feet NAVD88 shown in color.

6.6.1 Optimization of Opening Width

Similar to the optimization of the opening at the Chequessett Neck Road dike, a number of Mill Creek sub model simulations were conducted to determine the opening size sufficient to allow full tidal exchange upstream of the proposed Mill Creek dike. Under normal conditions, the model was simulated using culvert widths ranging from 3 feet wide to 50 feet wide. The culvert height was set to be fully open (i.e. any slide/sluice gate structures fully raised). The assessment of the Mill Creek dike opening width assumed that the Chequessett Neck Road dike sluices (165 foot width opening) were opened 10 feet. Simulations were then conducted for various width openings at the proposed Mill Creek dike with Herring River modeling results from the 10' sluice opening at Chequessett Neck Road. Figure 6-30 shows the MHW and MLW water

surface elevations within Mill Creek (just upstream of the Mill Creek dike) for the various opening widths. The horizontal axis shows the sluice width opening, while the vertical axis shows the water surface elevation level (feet, NAVD88). The two blue lines and associated markers show the mean high water and mean low water tidal elevations as a function of opening width at the proposed Mill Creek dike. As expected, the results show that increasing the total culvert width causes a corresponding increase in the tidal range upstream of the dike. However, total culvert widths greater than 25 feet result in limited increases in tidal range. As such, a 25 foot width opening at the proposed Mill Creek dike was selected as the optimized opening size to allow for maximum restoration under an adaptive management approach. This opening size allows for future planning of the system and provides the ability to allow for full tidal exchange in the future, if so desired.

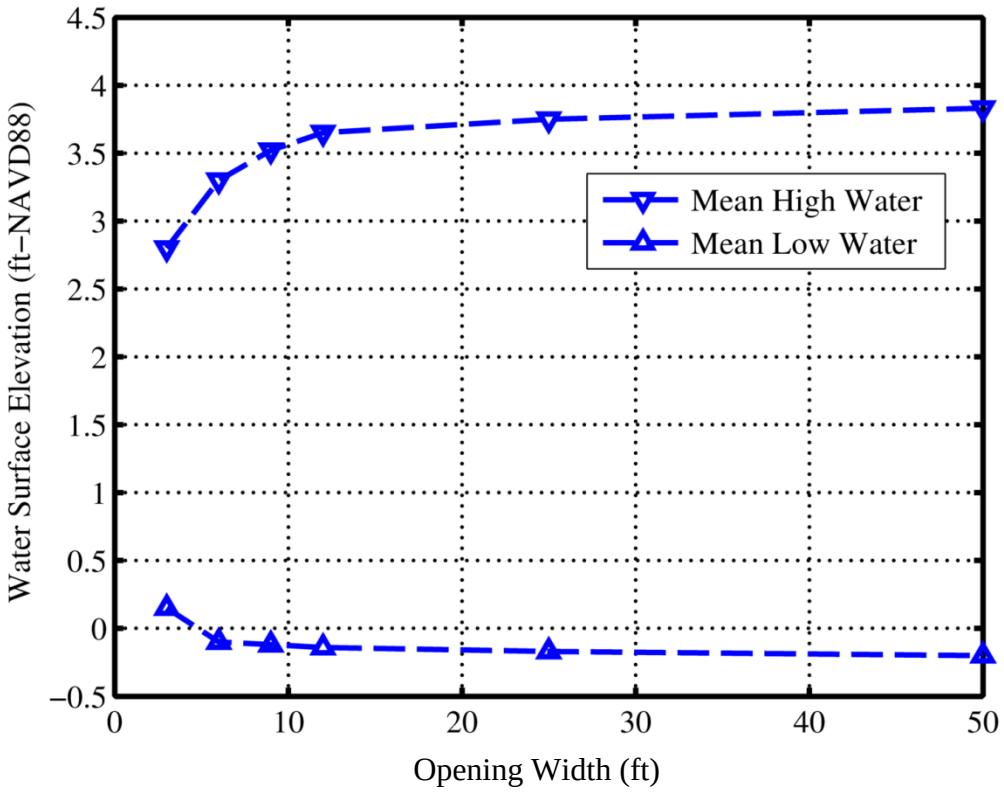

Figure 6-30. Proposed Mill Creek dike Mean High and Mean Low Water levels as a function of dike opening width.

6.6.2 Adaptive Management Sluice Gate Openings

Proposed plans for a potential Mill Creek dike would include fitting culvert(s) with adjustable sluice gates to allow for adaptive management of the system. The sluice gates would also be utilized to limit water levels in the Mill Creek basin to acceptable levels during tidal flood events, protect upland infrastructure, and control discharge from the system. To determine the variations in water surface elevation from sluice opening heights at the potential Mill Creek dike, an array of model runs were conducted with varying sluice heights from 1 foot to 6 feet and various boundary conditions (normal conditions, storm conditions, etc.) extracted from

simulations of the full Herring River model. These boundary conditions represent normal tides and tidal flood event scenarios with a net culvert width of 165 feet at the Chequessett Neck Road dike and Chequessett Neck Road sluice heights of 3 feet and 10 feet (as determined in section 6.2.2). Water surface elevation results from the model simulations are summarized in Table 6-1. The values in Table 6-1 show the water surface elevations in feet NAVD88 within the Mill Creek Basin for the various simulations.

The ideal slide/sluice gate opening height at the Mill Creek dike would allow for maximum amount of tidal exchange, while also limiting the maximum water surface elevation in Mill Creek to less than 6 feet NAVD88 under 100-year storm conditions (Chapter 3 and HRRC, 2011). From the results presented in Table 6-1, with a three foot sluice opening at the Chequessett Neck Road dike, the water surface elevation does not exceed 6 feet NAVD88 regardless of the opening height at the Mill Creek dike. For the ten foot opening at the Chequessett Neck Road dike, Mill Creek dike sluice height openings greater than 3 feet result in water surface elevations of greater than 6 feet NAVD88 in Mill Creek. Therefore, alternatives that could be considered for managing water levels within Mill Creek may include a maximum 3 foot sluice opening at Chequessett Neck Road with no dike at Mill Creek, or a dike at Mill Creek that would allow for managed water levels when the sluice opening at the Chequessett Neck Road dike is increased to opening sizes greater than 3 feet. The Mill Creek sluice/slide gate could also be closed completely and only allow flow out of the system.

Figure 6-31 presents a portion of the water surface elevation time series results in Mill Creek with a ten foot Chequessett Neck Road dike sluice opening and a three foot Mill Creek dike sluice opening. The horizontal axis presents time (in model simulation days) and the vertical axis presents water surface elevation (feet, NAVD88). The blue line presents the normal tidal conditions, the broken green line presents a 1-year or annual high tide event, and the red line presents a 100-year storm event. All results are shown for a location just upstream of the potential Mill Creek dike. For this alternative the peak water level during the 100-year storm surge event just exceeds the 6 feet NAVD88 limit (Table 6-1).

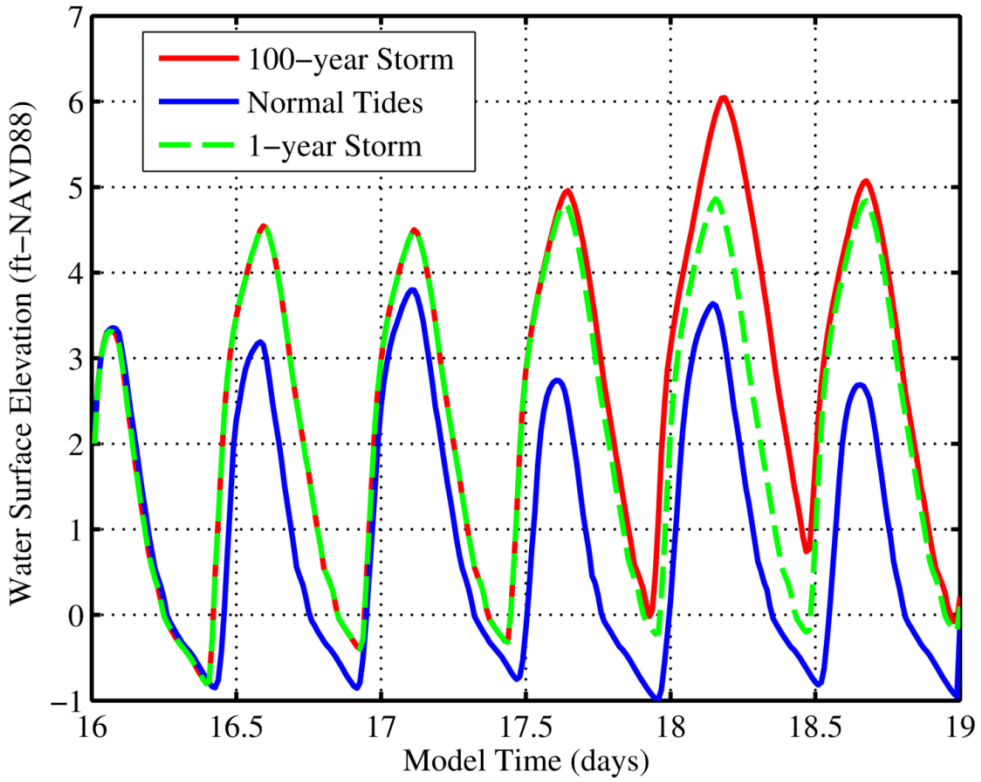

Figure 6-31. Water surface elevation for normal tide (blue line), 1-year storm (broken green line) and 100-year storm (red line) for a 10 foot sluice opening at Chequessett Neck Road and a 3 foot sluice opening at the potential Mill Creek dike.

Table 6-1. Mill Creek sub model water surface elevations tidal benchmarks for various sluice openings at the potential Mill Creek Dike.

		Mill Creek Dike											
		3' Sluice Opening at Chequesset Neck						10' Sluice Opening at Chequesset Neck					
		Increase Effective Opening Size ----->						Increase Effective Opening Size ----->					
Mill Creek Sub Basin (elevations in NAVD88, feet)	Wellfleet Harbor	1' opening	2' opening	3' opening	4' opening	5' opening	6' opening	1' opening	2' opening	3' opening	4' opening	5' opening	6' opening
Mean Low Water	-5.47	-0.11	-0.13	-0.14	-0.14	-0.14	-0.14	-0.1	-0.1	-0.11	-0.12	-0.12	-0.12
Mean Tide Level	-0.32	1.42	1.58	1.64	1.69	1.70	1.69	1.49	1.67	1.75	1.79	1.82	1.81
Mean High Water	4.84	2.94	3.29	3.42	3.51	3.54	3.52	3.07	3.44	3.61	3.69	3.75	3.74
Tide Range	10.31	3.05	3.42	3.56	3.65	3.68	3.66	3.17	3.54	3.72	3.81	3.87	3.86
Mean High Water Spring	6.22	3.45	3.91	4.14	4.26	4.34	4.36	3.64	4.22	4.52	4.72	4.83	4.92
Annual High Water	7.07	3.64	4.15	4.40	4.54	4.62	4.67	3.86	4.50	4.85	5.06	5.22	5.33
100-year Storm Event	9.31	4.23	4.88	5.23	5.43	5.53	5.59	4.66	5.5	6.04	6.39	6.61	6.73

Figure 6-32 shows contours of tidal benchmark levels (MLW, MHW, MHWS) and peak storm surge levels for 10 foot slide/sluice gate opening at Chequessett Neck Road, and a 3 foot slide/sluice gate opening at the proposed Mill Creek dike. This figure represents the maximum restoration level that could be attained while maintaining a maximum water surface elevation of less than 6 feet NAVD88 under the 100-year storm condition. The area between the blue (MLW) and green (MHW) lines represent the average intertidal area for this restored scenario.

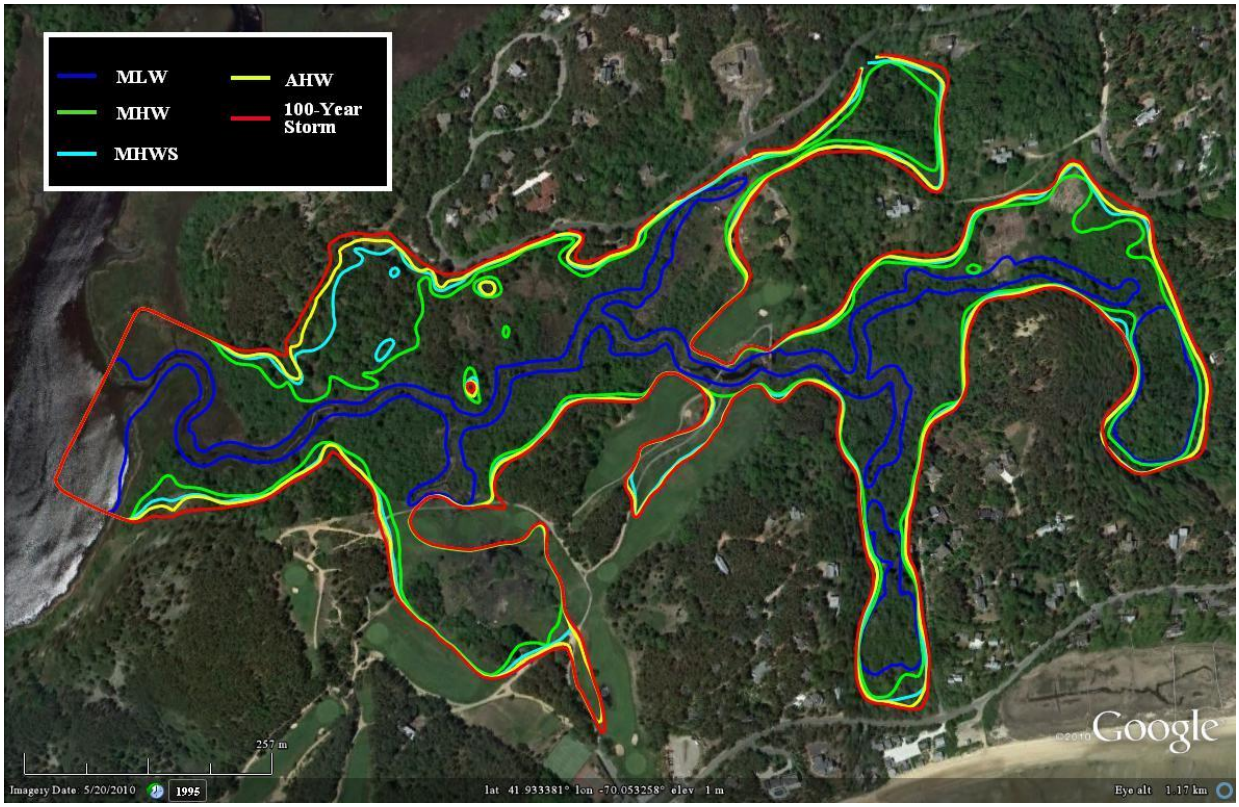

Figure 6-32. Contours of tidal benchmark water surface elevations and peak storm surge water levels for a 10 foot sluice opening at Chequessett Neck Road and a 3 foot sluice opening at Mill Creek.

As for the overall Herring River model, scenarios simulating sea level rise were also completed for the Mill Creek sub-basin model. Projected sea level rise over a 50-year time horizon (section 5.5.3) were also simulated for a ten foot opening at the Chequessett Neck Road dike and three foot opening in the Mill Creek dike. Predicted MHW levels for the sea level rise scenarios are presented in Table 6-2. Table 6-2 also presents the MHW levels for existing conditions and the fully open scenario for comparison. The alternative with a dike at Mill Creek and 10 foot sluice opening at Chequessett Neck Road predicts a slightly lower MHW level than the alternative with no dike at Mill Creek. Additional control introduced by the Mill Creek dike would allow for more precise management of the system under uncertain future conditions.

Table 6-2. Mean High Water levels within the Mill Creek sub-basin for various sea level rise projections. Model results present elevations in 50 years in feet, NAVD88.

Sea Level Rise Scenario	Wellfleet Harbor	Existing Conditions	Fully Open	Chequessett Neck Road 10 ft opening; Mill Creek 3 ft opening	Chequessett Neck Road 3 ft opening; No Mill Creek Dike
MHW, Low SLR Projection (50 years)	5.28	-0.10	4.54	3.70	3.91
MHW, Mid SLR Projection (50 years)	5.65	-0.03	4.67	3.77	3.99
MHW, High SLR Projection (50 years)	6.89	0.17	5.05	4.02	4.24

6.6.3 Freshwater Rainfall Storm Events

Another potential restoration option is to eliminate tidal exchange from the Mill Creek sub-basin (section 6.2.2). This alternative would essentially remove the Mill Creek sub-basin from the overall restoration effort. This would negate the need for any flood proofing mitigation within the sub-basin, but would also maintain degraded, freshwater conditions. Under this approach, the dike must be able to adequately drain freshwater rainfall events, such that the dike does not reduce the drainage ability of the Mill Creek system. As such, the model was used to simulate various discharge scenarios to determine how drainage may change for the proposed dike conditions. The alternative with a ten foot Chequessett Neck Road sluice opening and a 25 foot wide, three foot Mill Creek Dike slide/sluice gate opening and a one-way flap gate at the Mill Creek dike were evaluated for rainfall storm event scenarios. Three rainfall scenarios were developed for input into the model. These scenarios were based on a rainfall study lasting over half a year, cataloging all rainfall events (Nuttle, 1990). The first rainfall scenario simulated is a relatively low rainfall event, created by taking the mean of all rainfall events observed. The second rainfall scenario is based on the maximum rainfall event observed during the study period representing a moderate rainfall event. The final scenario is based on a prediction of a 100-year rainfall event (Nuttle, 1990), as determined by Nuttle. Table 6-3 presents the values used for the three rainfall scenarios, assumed to be evenly distributed over a 24 hour period.

Table 6-3. Rainfall scenarios (from Nuttle, 1990) used to simulate various discharge from the Mill Creek sub-basin.

Rainfall Scenario	Rainfall (in/day)
Low	1.1
Moderate	3.2
High (100-year)	6.8

All three rainfall scenarios were simulated assuming normal/spring tidal conditions in Wellfleet Harbor, a 165 foot opening width at Chequessett Neck Road with slide/sluice gate openings of 10 feet, and at 25 foot width at Mill Creek with slide/sluice gate openings of 3 feet, or a one-way flap gate only letting water out of the system. For comparison, existing conditions at Mill Creek with and without the rainfall are also presented. The flap gates implemented in the model only allow water to leave the Mill Creek basin, effectively allowing only freshwater runoff out of the Mill Creek sub-basin (as long as the water surface elevation in the Herring River is low enough to allow outflow from Mill Creek. Time series of water surface elevation in Mill Creek for the three rainfall scenarios (low, moderate, and high) are shown in Figures 6-33 through 6-35, respectively. Each figure shows four time series: the red line shows the water surface elevation with the proposed dike and slide sluice gate; the blue line shows the water surface elevation with the proposed dike and flap gate only allowing flow out; the green line shows the water surface elevation without a Mill Creek dike; the black broken line shows the water surface elevation with no rainfall or no dike at Mill Creek (baseline).

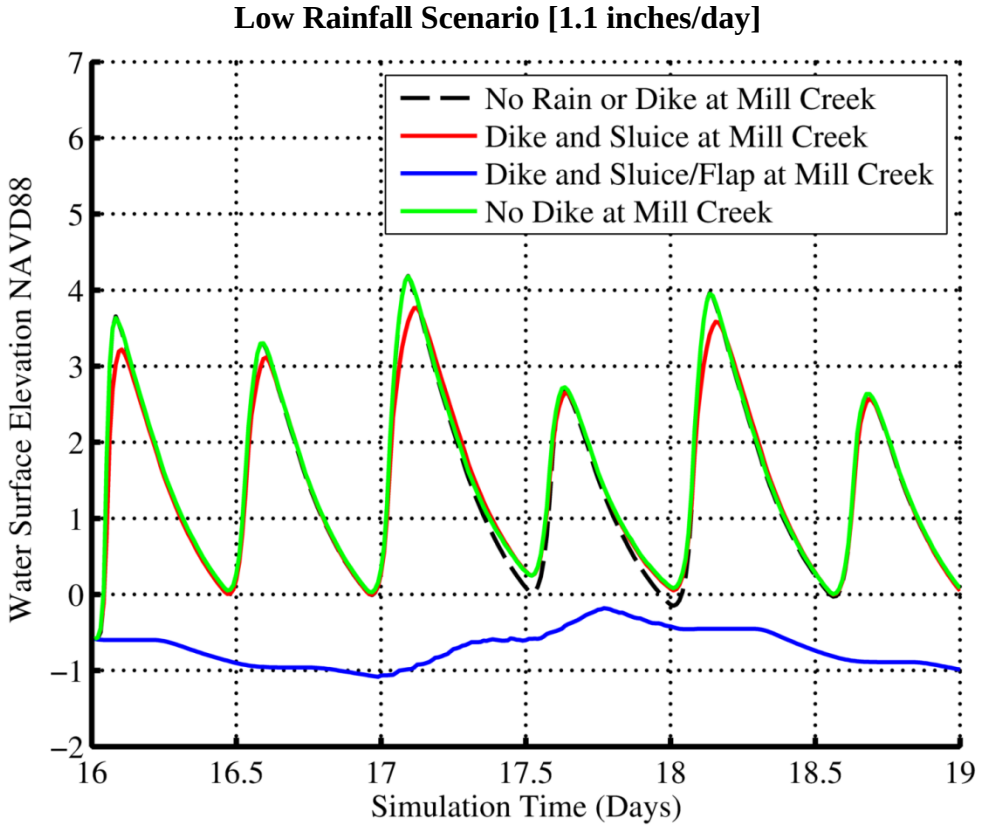

Figure 6-33. Water surface elevations in Mill Creek for a low rainfall event scenario. The red line is for a case with the dike with a slide/sluice gate, the blue for a dike one-way flap gate, the green with no Mill Creek dike, and black with no dike or rainfall.

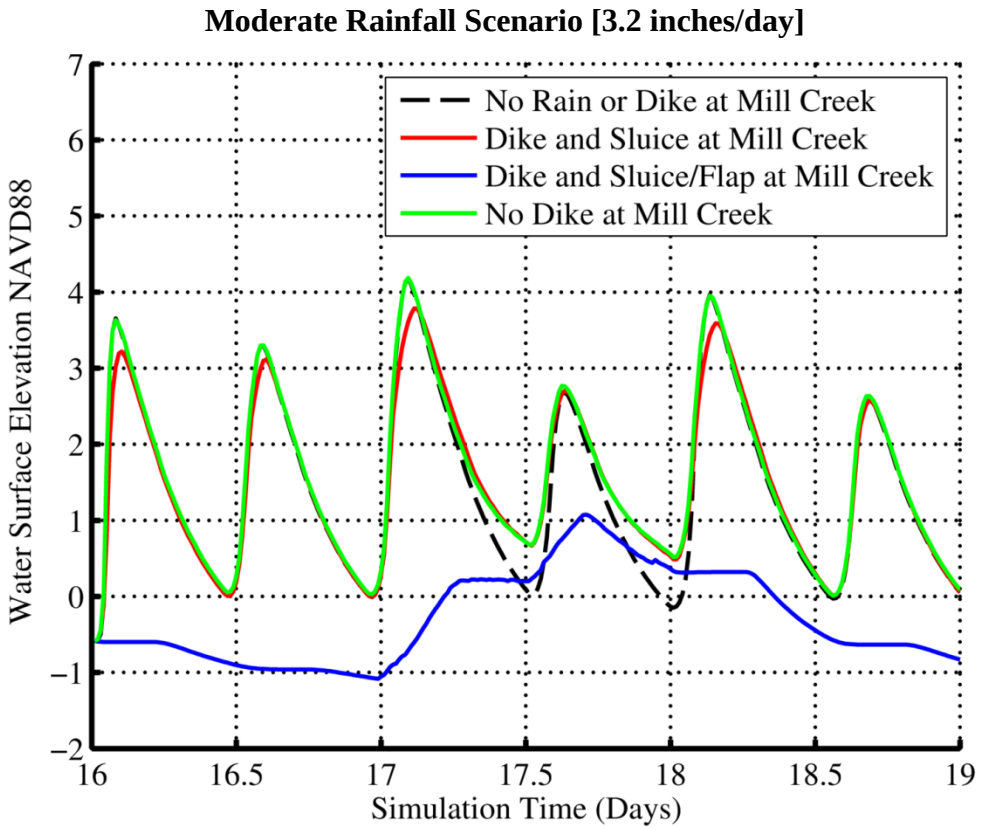

Figure 6-34. Water surface elevations in Mill Creek for a moderate rainfall event scenario. The red line is for a case with the dike with a slide/sluice gate, the blue for a dike one-way flap gate, the green with no Mill Creek dike, and black with no dike or rainfall.

The results show a decrease in the ability of the additional water to drain from the system, shown by the higher low tide elevations in the time series (green and red lines above black dashed line). However, the rainfall does not increase the water surface elevation level above the normal mean high water level within Mill Creek. In all cases, the impact of rainfall is smaller than the influence of the tides, which dominate the hydrodynamics of the system. Therefore, although the proposed dike and associated flow control structures will extend the time it takes the water to drain from the sub-basin, it does not result in higher water levels in the basin. The one-way flap gate (results shown by the blue line) restricts flow out of the system during the storm event and water backs up in the Mill Creek sub-basin. However, some water is allowed to drain out during low tides and the water surface elevation does not exceed 2 feet NAVD88 even in the high rainfall scenario.

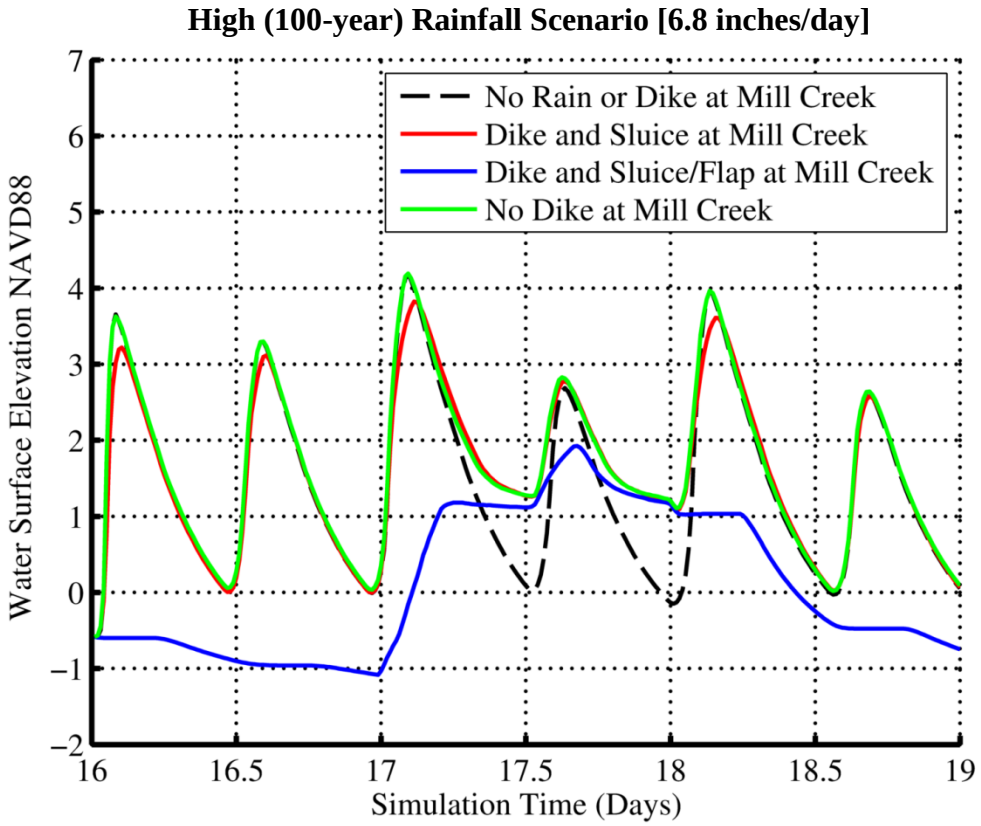

Figure 6-35. Water surface elevations in Mill Creek for a high rainfall event scenario. The red line is for a case with the dike with a slide/sluice gate, the blue for a dike one-way flap gate, the green with no Mill Creek dike, and black with no dike or rainfall.

6.6.4 CYCC Re-grading

Another potential component of the restoration alternatives under consideration for the Mill Creek sub-basin is a potential elevation and re-grading of the CYCC golf course. The proposed re-grading is geared towards reconfiguring the golf course holes at risk of potential flooding by increasing the elevation of selected areas within the sub-basin. The re-grading would also result in potential changes to the storage capacity of the of the Mill Creek sub-basin. Therefore, the Mill Creek sub-basin was also simulated with the proposed re-grading in place. Based on the engineering drawings provided by the HRRC, the topography of the Mill Creek sub-basin model domain was modified to represent the proposed re-grading. The modified grid, with the proposed CYCC re-grading, is presented in Figure 6-36.

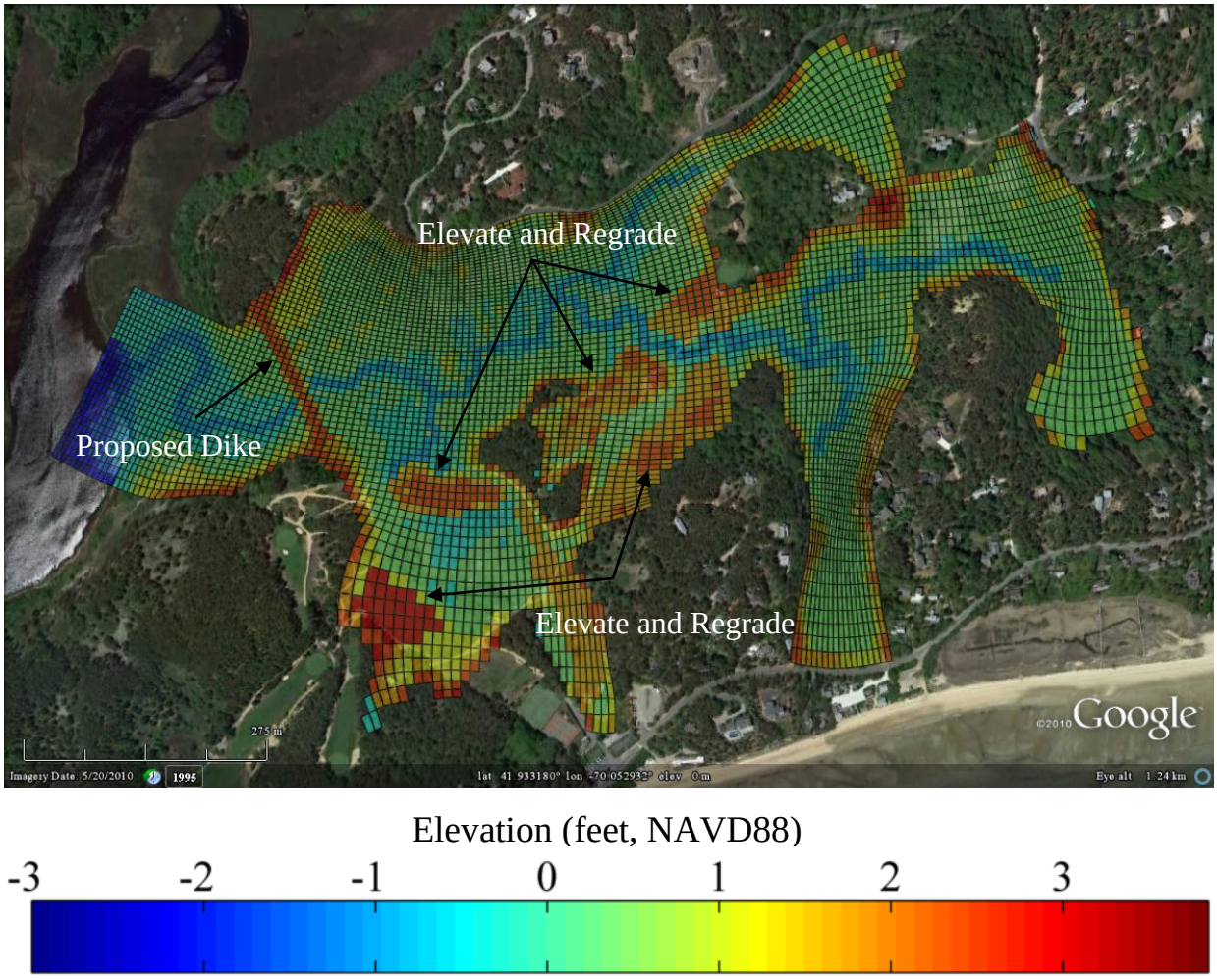

Figure 6-36. Mill Creek sub model domain with dike added and proposed re-graded golf course. Elevations shown in color (feet, NAVD88).

The re-graded CYCC golf course topography was then used to simulate normal tidal conditions, as well as storm events. The results of these simulations are summarized in Table 6-4. For the alternative with a 10 foot sluice/slide gate opening at Chequessett Neck Road and a 3 foot sluice opening at Mill Creek, a peak water surface elevation of approximately 6.4 feet occurs during a 100-year storm surge event for the re-graded Mill Creek sub-basin (a peak water surface elevation of 6.0 feet occurs for the existing topography). As such, the re-graded system removes some flood storage capacity from the basin. Therefore, for a 10' sluice/slide gate opening at Chequessett Neck Road, a reduced sluice opening should be considered at Mill Creek to maintain a maximum water level of less than or equal to 6 feet NAVD88 during the 100-year storm event. It is expected that the sluice openings at both Mill Creek and Chequessett Neck Road would be implemented using an adaptive management approach such that future conditions within the Mill Creek system could be adequately anticipated and managed.

Table 6-4. Water surface elevation levels within the Mill Creek sub-basin for the regraded golf course proposal. Model results present elevations in feet, NAVD88.

Tidal Benchmark	No Mill Creek Dike; Chequessett Neck Road 3' Opening (feet, NAVD88)	Mill Creek Dike 3' Opening; Chequessett Neck Road 10' Opening (feet, NAVD88)
Mean Low Water	-0.49	-0.47
Mean Tide Level	1.67	1.68
Mean High Water	3.82	3.83
Tide Range	4.31	4.30
Mean High Water Spring	4.60	4.77
Annual High Water	4.88	5.11
100-year Storm Event	5.75	6.36

6.6.5 Mill Creek Groundwater Impacts

Due to its close proximity to Wellfleet Harbor, groundwater levels in the Mill Creek sub-basin are likely influenced by the surface water levels in Wellfleet Harbor, as well as water levels in the Herring River and Mill Creek. It is anticipated that changes in Local Mean Sea Level (LMSL) in both Wellfleet Harbor and Mill Creek will result in changes to groundwater table elevations within the Mill Creek sub-basin. Therefore, due to either restoration efforts proposed for the larger Herring River Estuary or natural sea level rise, potential increases in LMSL may impact groundwater table elevations within the Mill Creek sub-basin. This section evaluates potential impacts to groundwater under the no action alternative for the proposed Herring River tidal restoration project. Under the no action alternative, the impact on groundwater elevation would be due to potential sea level rise changes in Wellfleet Harbor. The technical approach used to develop and calibrate a model of groundwater flow for the Mill Creek sub-basin is described below followed by a discussion of the model results. The approach represents a first-order approximation of the potential impact on groundwater elevation and is intended for planning purposes. The results provide estimates of changes in average water table elevations at sensitive receptors within the Mill Creek sub-basin and indicate areas where the water table elevation may increase (break out) to the land surface as a result of rising LMSL. The results of the analysis were constrained by the limited data that were available on the existing groundwater levels, recharge rates, freshwater inputs, and the soil constitution.

6.6.5.1 Technical Approach

The United States Army Corps of Engineers (USACE) provides guidance for incorporating the effects of sea level rise in the planning and design of civil engineering projects (USACE, 2009, 2011). This guidance has been applied in simulations of the Herring River hydrodynamic model to determine changes in surface water elevations that may result under the no action alternative for three potential sea level rise scenarios. As recommended by the USACE, these scenarios include: a "low" scenario that is based a projection of the observed historic rate of local sea level rise, an "intermediate" scenario that considers the possibility of accelerated sea level rise, and a

"high" scenario the considers increased acceleration resulting from the potential rapid loss of the Antarctic and Greenland ice sheets. Based on this guidance and hydrodynamic model results, projected sea level change in 50 years (2060) in Wellfleet Harbor and Mill Creek have been determined and used as input to a two-dimensional model of groundwater flow to evaluate potential changes in average water table elevations within the Mill Creek sub-basin under the no action alternative. The analysis assumes:

- Freshwater discharge into the Herring River system will remain similar under future conditions
- Rainfall conditions will remain similar under future conditions
- Subsidence is not included in the future projections, or assessed in a quantitative manner
- An increase in regional mean sea level does not significantly affect tidal hydrodynamics in Wellfleet Harbor other than to consistently increase the water level

6.6.5.2 Model Description

A two-dimensional model of groundwater flow was developed to simulate steady-state water table elevations within the Mill Creek sub-basin based on elementary hydrology (Singh, 1992). The water table elevation is influenced by the rate of recharge into the aquifer, as well as the elevation of surface water on the boundaries of the aquifer. Under steady-state conditions it is assumed the recharge rate and physical properties of the aquifer do not change, thus changes in the water table elevation depend primarily on changes in the surface water elevation at the aquifer boundaries. An increase in sea level on the boundary will cause a corresponding, but not necessarily uniform, increase in the water table elevation within the aquifer.

The law of conservation of mass is combined with Darcy's law for flow through a porous medium to develop governing equations for two-dimensional groundwater flow in an unconfined aquifer (Singh, 1992). The governing equations are the solved using the finite difference method with appropriate boundary conditions for surface water elevations in Wellfleet Harbor and Mill Creek. Figure 6-37 shows a finite difference cell representing a portion of the aquifer along with arrows representing the groundwater flux, *q*, on the cell faces.

Darcy's law for flow through a porous medium can be expressed as:

$$q_x = -K\frac{\partial h}{\partial x} \tag{6-1}$$

$$q_y = -K\frac{\partial h}{\partial y} \tag{6-2}$$

Where q_x and q_y are the horizontal groundwater flux in the x and y directions, respectively, K is a homogeneous and isotropic hydraulic conductivity, h is the water table elevation, and Δx and Δy represent the cell dimensions in the x and y directions, respectively. Under steady-state conditions, conservation of mass requires zero accumulation of water within the cell.

$$\sum inputs - \sum outputs = 0 \tag{6-3}$$

Considering the mass balance for the cell depicted in Figure 6-37, That is:

$$(q_x|_{x+\Delta x} - q_x|_x)\Delta y(h-z) + (q_y|_{y+\Delta y} - q_y|_y)\Delta x(h-z) + R\Delta x\Delta y = 0 \quad (6\text{-}4)$$

where R is a constant recharge rate and z is the elevation of the aquifer bottom which for simplicity is set at zero. Substituting (6-1) and (6-2) into (6-4), and dividing by the cell area and hydraulic conductivity, ΔxΔyK, the governing equation for unconfined steady-state ground water flow is obtained.

$$\frac{\partial}{\partial x}\left(h\frac{\partial h}{\partial x}\right) + \frac{\partial}{\partial y}\left(h\frac{\partial h}{\partial y}\right) = \frac{-R}{K} \quad (6\text{-}5)$$

Equation (6-5) is non-linear because of the unknown thickness of the unconfined aquifer, however making the substitution $u=h^2$ results in the linear partial differential equation:

$$\frac{\partial^2 u}{\partial x^2} + \frac{\partial^2 u}{\partial y^2} = \frac{-2R}{K} \quad (6\text{-}6)$$

To solve equation (6-6) for *u* the terms on the left hand side are replaced with 2nd order cell centered finite differences. For a grid cell at (i,j) equation (6) becomes:

$$\frac{u_{i+1,j} - 2u_{i,j} + u_{i-1,j}}{\Delta x^2} + \frac{u_{i,j+1} - 2u_{i,j} + u_{i,j-1}}{\Delta y^2} = \frac{-2R}{K} \quad (6\text{-}7)$$

Equation (6-7) represents a linear system of equations which are solved for $u_{i,j}$ using the iterative Gauss-Seidel method. Boundary conditions are applied by specifying values of h^2 at grid cells on the model boundary.

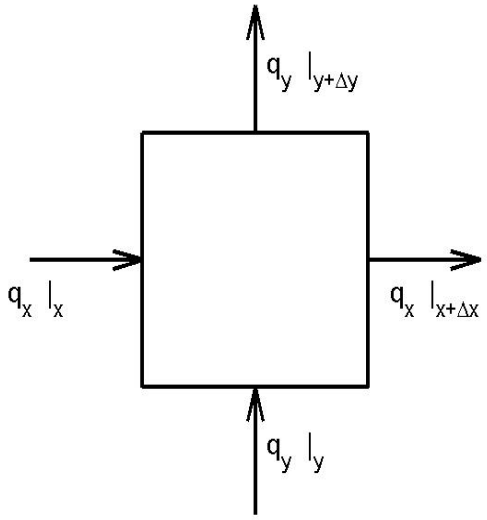

Figure 6-37. Finite difference representation of horizontal 2-D groundwater cell.

6.6.5.3 Model Configuration

A model grid was generated for the Mill Creek sub-basin consisting of approximately 10,000 square grid cells with a grid spacing of approximately 15 meters. Figure 6-38 shows the model grid and boundaries overlaid on an aerial photograph. Three different boundary conditions were applied in the model. A boundary condition representing LMSL in Wellfleet harbor was applied on the southern portion of the model domain extending along Mayo Beach up the Herring River to just downstream of the Chequessett Neck Road Dike (red line). A second boundary representing LMSL in Mill Creek/Herring River was defined along the east bank of the Herring River just upstream of the Chequesset Neck Road Dike and extending up the centerline of Mill Creek (blue line), and a third boundary was defined along the edge of the marsh plane extending around the remainder of the boundary (green line). Water table elevation on the third boundary was set at the either the predicted LMSL in Mill Creek or the land elevation, whichever was greater. The marsh plain boundary was defined this way under the assumption that water table could not rise higher than the marsh surface unless the surface was below LMSL. This could result in an over prediction of the water table elevation near the boundary in cases where the water table is below the marsh surface; however, this boundary is generally far enough away from the area of interest that any error associated with the potential over-prediction should be small. LMSL values used on the boundaries are listed in Table 6-5 and were determined from the larger Herring River modeling effort (Woods Hole Group). The aquifer saturated thickness was set by assuming the aquifer has a flat bottom at a depth of 15 meters below existing MSL. This simplifying assumption is based on observations of depth to saltwater in the area of interest (Fitterman, et al., 1989).

Table 6-5. LMSL on boundaries of groundwater model (feet, NAVD88).

	Wellfleet Harbor	Mill Creek
Existing conditions	-0.98	-0.85
Low sea level rise	-0.56	-0.82
Intermediate sea level rise	-0.16	-0.75
High sea level rise	1.05	-0.59

6.6.5.4 Model Calibration

Water table elevations observed in 1989 (Nuttle, 1990) were used to ground truth and calibrate the model. These data were collected at ten observation wells located within the Mill Creek sub-basin, as shown in Figure 6-39. A representative mean water table elevation at each location was determined by averaging the weekly data collected during the spring and early summer of 1989 (March 17th through July 28th). Average spring-time water table elevations were used to calibrate the model because during that time of the year the water table is generally higher, and the model should be a bit more conservative. Calibration was accomplished by adjusting the ratio of recharge rate to hydraulic conductivity (R/K) until model results best matched the observed average water table elevations. The average observed water table elevations and modeled water table elevations are listed in Table 6-6. The overall performance of the model is quantified with two measures of absolute error:

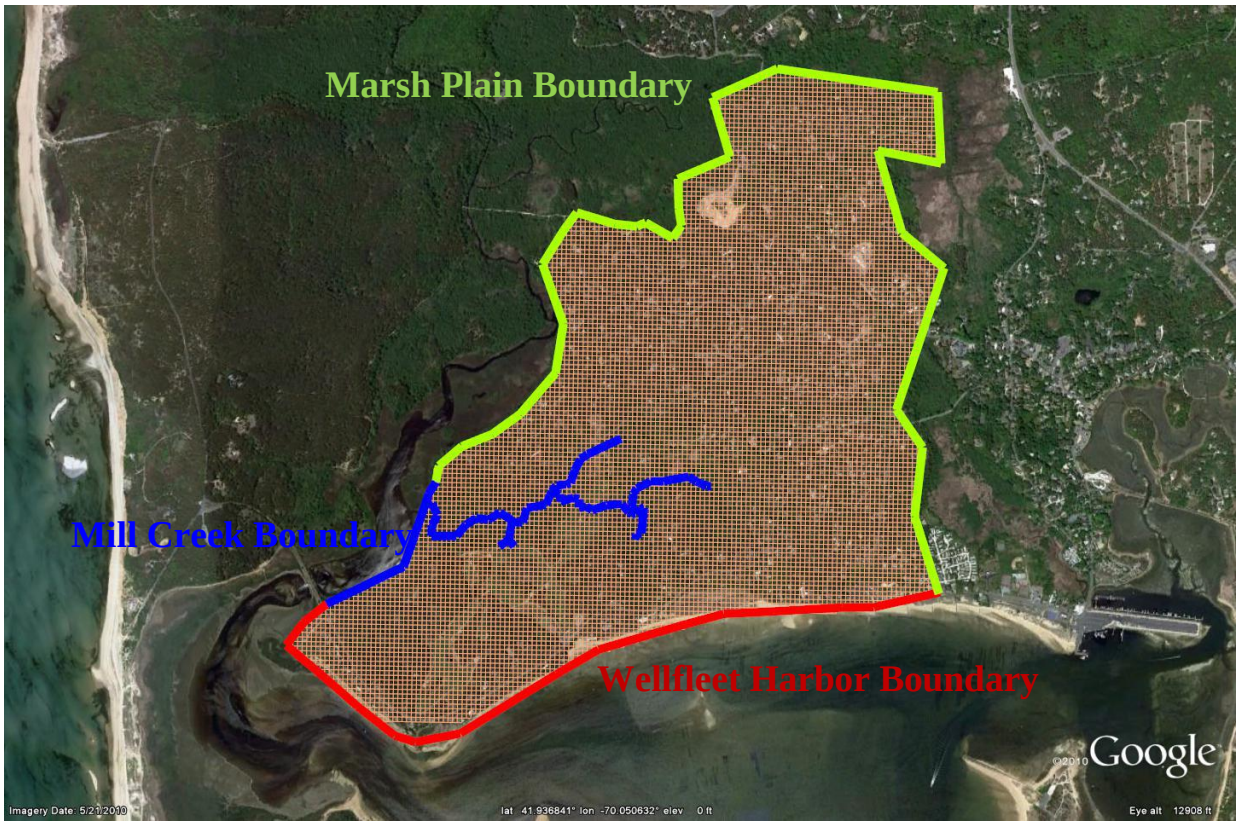

Figure 6-38. Groundwater model finite difference grid and boundaries: Wellfleet Harbor (red), Mill Creek boundary (blue), and marsh plain boundary (green) line.

$$Bias = \frac{\sum_{1}^{n}\left(h_{\mathrm{mod}} - h_{obs}\right)}{n} \tag{6-8}$$

$$RMSE = \sqrt{\frac{\sum_{1}^{n}\left(h_{\mathrm{mod}} - h_{obs}\right)^{2}}{n}} \tag{6-9}$$

Where h_{mod} and h_{obs} are the modeled and observed water table elevations respectively, and n is the number of observation wells. The bias provides a measure of how close on average the modeled results are to the observed data. A positive value indicates that the model is over-predicting the observations, while a negative value indicates that the model is under-predicting the observations. A bias of zero indicates that on average the model reproduces the observations. The RMSE is an average of the magnitude of the error at each observation well. RMSE is always positive with smaller values indicating better model performance. Both the bias and RMSE are measures of absolute error having the same units of the measured quantity from which they are computed. The resulting bias for the ground water model is 0.0005 feet, and the RMSE is 0.15 feet. A relative measure of error can be determined by considering variation in observed mean water table elevation within the observation area. The highest and lowest mean

water table elevations, 0.94 ft and -0.75 ft, were observed at wells IIC and IIIA, respectively. Based on this range the relative RMSE error is less than 9% of the observed range and the relative bias is insignificant. This indicates that the model is reasonably accurate in reproducing observed mean water table elevation within the Mill Creek sub-basin.

Table 6-6. Average water table elevations at the Mill Creek sub-basin observation wells (feet, NAVD88).

	IA	IIA	IIIA	IVA	IB	IIB	IIIB	IC	IIC	IIIC
Observed	-0.63	-0.72	-0.75	-0.26	-0.49	0.90	-0.24	-0.31	0.94	0.87
Modeled	*-0.78*	*-0.86*	*-0.75*	*-0.50*	*-0.34*	*-0.37*	*0.17*	*-0.52*	*2.37*	*1.1*

Figure 6-39. Location of observation wells in the Mill Creek sub-basin (Nuttle, 1990).

6.6.5.5 Model Results

The calibrated model was used to simulate the three sea level rise scenarios using the LMSL values listed in Table 6-5. The water table elevation output was then compared to the simulated existing water table elevation to determine the changes expected as a result of sea level rise. Model output was also compared to land surface elevation from the 2006 photogrammetry data set to identify areas where there is potential for sea level rise to cause the groundwater to break out of the land surface. Figure 6-40 presents the existing areas within the Mill Creek sub-basin that are currently surface water (e.g., Mill Creek) and areas that experience ponding or groundwater breakout and may currently be draining. It is likely that these areas currently

become flooded during heavier rainfall events since the groundwater is currently close to penetrating the ground elevation. Similarly, surface water and groundwater areas where the predicted water table elevation is greater than the land surface elevation (groundwater break out areas) are indicated by polygons in Figures 6-41 through 6-43 for the low, intermediate, and high sea level rise scenarios, respectively. The polygons do not necessarily indicate areas where ponding water is expected as once the water breaks through the land surface it may drain; however, these zones indicate areas where it is predicted that the groundwater may break out of the land surface. These areas may runoff resulting in a reduction in the water table elevation in the immediate vicinity. Further, there are a number of small streams and drainage ditches in the area, which are evident in the aerial photography but not resolved by the photogrammetry data. These conveyance channels are not considered by the groundwater model, although they likely provide an outlet for groundwater and a corresponding depression in the nearby water table. However, without proper drainage, the model is predicting that these low-lying areas will experience groundwater breakout and may be prone to flooding and/or ponding during rainfall events as well.

Figure 6-40. Surface water areas and groundwater breakout areas, existing conditions.

Figure 6-41. Surface water areas and groundwater breakout areas, low sea level rise scenario.

Figure 6-42. Surface water areas and groundwater breakout areas, intermediate sea level rise scenario.

Figure 6-43. Surface water areas and groundwater breakout areas, high sea level rise scenario.

In general, a larger increase in water table elevation is expected at locations closer to Wellfleet Harbor, while a smaller increase is expected at locations near Mill Creek. This can be expected considering that LMSL is expected to increase more in Wellfleet Harbor than in Mill Creek due to the asymmetrical tidal restriction imposed by the existing flap gates in the Chequessett Neck Road dike.

6.7 POTENTIAL CHANNEL VEGETATIVE CHANGES

The 2007 water surface elevation observations show a nearly complete attenuation of the tide within Pole Dike Creek (downstream of the Pole Dike Road Culvert) under existing conditions. Calibration of the model to these observations required the specification of a relatively high roughness length value (0.2 meters) for lower reach of Pole Dike Creek (between Pole Dike Road and High Toss Road), as presented in Chapter 5. This roughness length is nearly an order of magnitude greater than calibrated roughness length values specified for other streams in the model. This suggests that the lower reach of Pole Dike Creek may be blocked by an anomalous restriction (e.g. vegetation, caved bank, debris) preventing unimpeded tidal propagation into the Upper Pole Dike sub-basin. Although the exact source of the significant tidal attenuation is unknown, it may be feasible that the restriction may be either naturally or manually removed as the Herring River system is restored. For example, heavily forested areas with overgrown vegetation may transition into more typical marsh communities once tidal waters and salinity are reintroduced. If this change does occur during the restoration process, the Upper Pole Dike sub-basin maybe overly attenuated as a result of the high roughness length values applied in the

lower Pole Dike Creek region. To determine the impact that removal of restrictions may have on the results of the restoration alternative simulations, an additional simulation of normal tides was conducted with roughness length values for lower Pole Dike Creek reduced to a more typical value (0.033 meters). The results from this simulation were then compared to the alternative simulation using the calibrated roughness length values. Figure 6-44 shows a comparison of the water surface elevation time series in the Upper Pole Dike sub-basin for the restoration alternative with a total opening width of 165 ft at the Chequessett Neck Road Dike and slide/sluice gates open 3 feet. The red line shows the water surface elevation for the simulation using the calibrated roughness length values, the blue line shows the water surface elevation for the simulation with the lowered roughness length values, and the black dashed line shows the water surface elevation for existing conditions. The comparison shows that lowering the roughness length has very little effect on the water levels in the Upper Pole Dike sub-basin under the restored conditions. This can be explained by considering that the restoration alternative causes an approximately 1.5 foot increase in the mean water level allowing a significantly larger proportion of water to flow over the marsh plain where the roughness length was already set to lower roughness values and where water did not flow under existing conditions. As a larger volume of water flows over the marsh plain restrictions within the creek banks have a diminishing impact on the overall water levels.

The model calibration and verification was accomplished using observed data from the existing system in which conveyance is restricted to be within a number of relatively small channels, especially in the upper reaches of the system. Although the model has been shown to accurately simulate water levels during existing conditions when there is little flow over the former marsh plains, there is increased uncertainty in model results for the restoration alternatives because the frictional characteristics of vegetation in the former marsh plains is generally unknown. Also restoration activities may involve alteration of frictional characteristics as vegetation naturally reverts to a restored state. This uncertainty may be reduced in the future as monitoring and adaptive management of the system provide data that can be used to refine the model for the large currently non-tidal, former marsh plains.

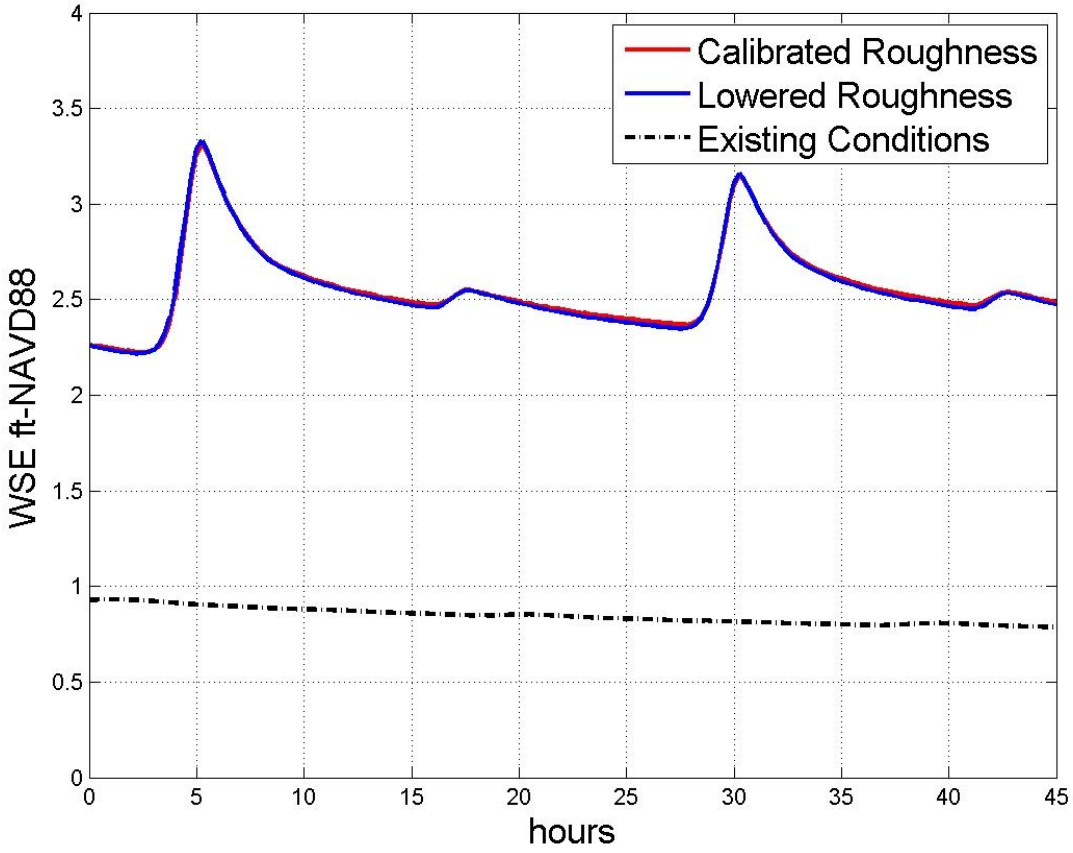

Figure 6-44. Water Surface elevation in the Upper Pole Dike Creek Sub-basin.

6.8 SUMMARY

This chapter presented a series of alternatives that were geared towards gaining a better understanding of system response to potential modifications and determine adaptive management steps and restoration endpoints. The results of this chapter were used to assist in defining specific restoration alternatives that are further analyzed and detailed in the next chapter. A summary of the key results from these series of alternatives that helped define the ultimate restoration alternatives is presented below.

- A range of potential opening widths at Chequessett Neck Road was simulated to determine the water surface elevations, tidal ranges, and salinity levels throughout the Herring River system. The results indicated that a 100 foot opening would optimize the water surface elevations and tidal range within the Herring River system, while a 165 foot opening would optimize the salinity penetration into the system. Although wider openings continued to let more tidal water and salt into the system, the changes were minimal and therefore there was a diminishing level of return in a restoration sense. As such, a 165 foot opening width was determined to be the largest width required to optimize restoration at Chequessett Neck Road.

- After determination of the optimal dike opening width, simulations for various opening heights (assumed to be controlled by slide/sluice gate structures in the new dike opening) that (1) evaluated target endpoints for restoration (based on limiting water surface elevations that could be accepted during storm conditions throughout the system) and (2) provided opening sizes that could be used as initial set points in the adaptive management process were simulated. The results indicated that:

    - A uniform 3' slide (sluice) gate opening across the entire 165' dike opening would limit the 100-year storm event water surface elevation to less than 6.0 feet NAVD88 throughout the system.

    - A uniform 10' slide (sluice) gate opening, which is fully vertically open, limits the 100-year storm event water surface elevation to less than 7.5 feet NAVD88 throughout the system.

Based on these series of alternatives, specific recommended alternatives were selected for the new dike opening at Chequessett Neck Road that represented specific restoration endpoints. These restoration endpoints would be accomplished through an adaptive management approach that would allow for controlled advancement towards the endpoints. Specifically, the following three alternatives were defined:

1. A new Chequessett Neck Road dike with a 165' wide opening and a future targeted maximum 100-year tide of 6 feet NAVD88 in the Lower Herring River (achieved with an approximate 3 foot slide [sluice] gate opening). Golf course re-grading and other flood proofing would be required in the Mill Creek sub-basin for this alternative. Several segments of low lying roads would also require elevation and regarding. Restoration would be significant through most of the system, but would not be maximized since the lower infrastructure elevations in the Mill Creek sub-basin would limit the maximum water surface elevation allowed in the system as a whole.

2. A new Chequessett Neck Road dike with a 165' wide opening and a future targeted maximum 100-year tide of 7.5 feet NAVD88 in the Lower Herring River (achieved with a 10' slide [sluice] gate opening) with a new dike at Mill Creek *eliminating* tidal exchange. A new proposed dike at the entrance to Mill Creek with a one-way flap gate flow control structure would be installed to eliminate the tidal exchange into the Mill Creek. This would allow freshwater flow out of the Mill Creek basin, but no tidal water into the Mill Creek basin. As such, this alternative would maximize restoration throughout the Herring River system, but the Mill Creek sub-basin would remain a non-tidal system. No re-grading or flood proofing in the Mill Creek sub-basin would be proposed, but flood mitigation would be required in other sub-basins.

3. A new Chequessett Neck Road dike with a 165' wide opening and a future targeted maximum 100-year tide of 7.5 feet NAVD88 in the Lower Herring River (achieved with a 10' slide [sluice] gate opening) with a new dike at Mill Creek *limiting* tidal exchange. This alternative would maximize restoration throughout the entire system; however, a new dike at the entrance to Mill Creek with appropriate flow control structure(s) would be installed to limit the tidal exchange into the Mill Creek producing similar water levels

as the 3' slide/sluice gate opening alternative. Flood proofing and mitigation would be needed throughout the Herring River flood plain.

Results for these specific alternatives are further presented and discussed in Chapter 7, along with the Mill Creek sub-basin components described below. Since the Mill Creek sub-basin is a critical element of each of these defined alternatives, the final alternatives were further detailed through assessment of the Mill Creek sub-basin. The development of potential tidal control measures at the entrance to the Mill Creek sub-basin followed a similar approach to the modeling and assessment of an opening at the Chequessett Neck Road dike. This included (1) optimization of an opening width at a new Mill Creek dike; (2) potential opening heights of a flow control structure to allow limited water into Mill Creek sub-basin; (3) simulations of a re-graded CYCC golf course; (4) evaluation of the Mill Creek sub-basin completely blocked from tidal exchange and the effect on freshwater outflow, and (5) a preliminary assessment of potential groundwater impacts in the Mill Creek sub-basin relative to both sea level rise and the restoration effort. These results indicated that:

- A 25 foot opening in a new dike at the entrance to Mill Creek would optimize restoration in the Mill Creek sub-basin with the optimized opening at Chequessett Neck dike.

- Alternatives that could be considered for managing water levels within Mill Creek may include a maximum 3 foot sluice opening at Chequessett Neck Road with no dike at Mill Creek, or a dike at Mill Creek that would allow for managed water levels when the sluice opening at the Chequessett Neck Road dike is increased to opening sizes greater than 3 feet. The Mill Creek sluice/slide gate could also be closed completely and only allow flow out of the system.

Additional recommendations, corresponding to the overall restoration effort, include:

- Removal of the High Toss Road culvert and replacement with either an open channel, or an open channel and complete removal of the existing causeway.

- Monitoring of upstream culverts, specifically the culverts at Pole Dike Road and Old County Road. As the restoration processes advances, these culverts may need to be replaced with larger culverts. However, since the effect on water surface elevation is relatively small, especially in the early stages of the restoration, these culverts do not need to be replaced during the initial restoration effort. Monitoring of water surface elevations and salinities during the adaptive management process should be conducted to determine the potential influence of these anthropogenic structures.

7.0 FINAL ALTERNATIVE ASSESSMENT

The alternative simulation processes, as discussed in Chapter 6, was used to narrow the potential restoration alternatives to a set of final alternatives (section 6.8). This chapter presents model results and analyses of these final alternatives, including both adaptive management stages and defined restoration endpoints. The results presented throughout this chapter comprise a set of standardized output that is available for each final alternative simulation. The report does not present all the data that are generated from the model runs; rather provides a summary, examples, and some key findings from the model results. Comprehensive standardized data output was provided to the HRRC for utilization in development of the Environmental Impact Statement (EIS).

This chapter also presents a preliminary sediment transport assessment. The methods and results presented represent first-order qualitative and quantitative assessment of potential sediment transport in the Herring River estuary. This assessment does not determine actual sediment movement but rather areas where there is potential for erosion or deposition. However, the analysis does provide reasonable results that can be utilized to help guide the adaptive management restoration approach.

7.1 SUB-BASIN DEFINITION

In order to discuss the detailed model results, which outputs data (water surface elevations, velocities, salinity, etc.) at over 85,000 locations throughout the Herring River estuary, the Herring River system was divided into specific sub-basins. Figure 7-1 shows the delineation of these specific sub-basins, and provides the approximate acreage within each sub-basin. The sub-basin division was based on evaluating physical parameters output (water surface elevation and salinity) from the model at various points throughout the model. When there was a significant change in these parameters across a geographical area, the areas were divided to represent a sub-basin. For example, water surface elevation changes significantly enough between upper and lower Bound Brook, that a sub-basin division was created for this region. The model results presented within each sub-basin represent an average value taken from a number of points within that particular sub-basin.

The Herring River East and Pole Dike Creek East sub-basin remain non-tidal for all restoration alternatives, although in large storm conditions with greater opening scenarios, tidal water does reach these sub-basins. The upper ponds in the system (east of the Herring River East sub-basin) remain non-tidal for all conditions. As such, these sub-basins are not included in the EIS impact analysis or discussed throughout this report.

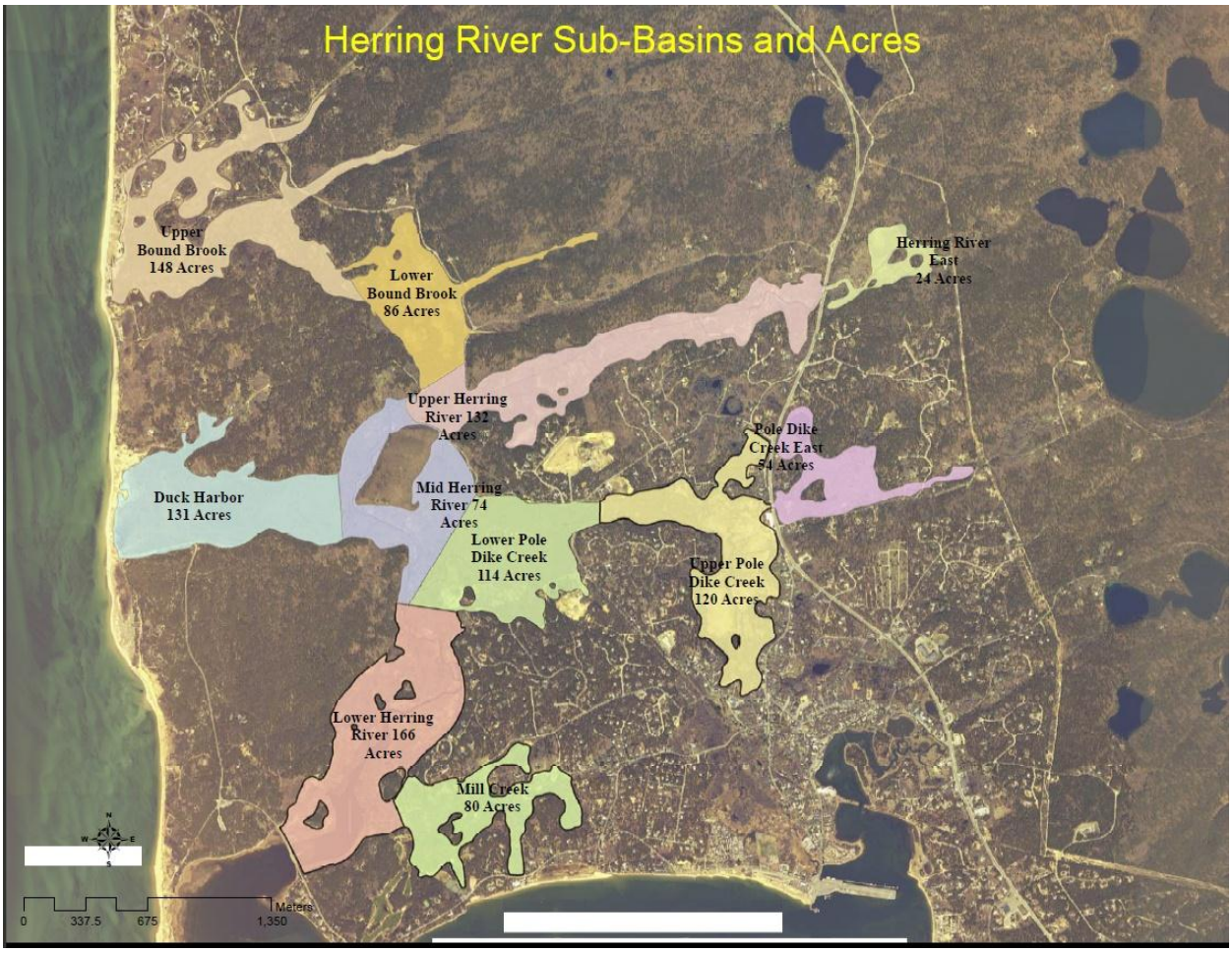

Figure 7-1. Sub-basin definition, delineation, and approximate acreage within each sub-basin for the Herring River estuary (graphic courtesy of the HRRC).

7.2 TIDAL BENCHMARKS AND SALINITY LEVELS

Water surface elevations and salinity throughout the Herring River system were evaluated using the results of the hydrodynamic model. Water surface elevation results from the alternative simulations were presented in three specific ways:

- Tables that present relevant tidal benchmarks (Mean Low Water, Mean High Water, Mean High Water Spring, Annual High Water), the 100- year storm water level, and potential future sea level rise scenarios for restoration endpoint alternatives. These water surface elevation values were provided for each sub-basin (section 7.1).

- Graphical aerial overviews and geo-rectified bounds of the water surface elevation level for each specific tidal benchmark.

- Interactive Google© Earth files that provide both the tables and water surface elevation shape files for each of the simulated water levels.

The salinity results from the model were also presented in two specific ways:

- For each specific sub-basin, the mean and maximum salinity is provided in a table as determined during the model simulation. These salinity values are an average value within that sub-basin and provide a regional value of salinity. Salinity distributions vary throughout each sub-basin. These salinity values should be assessed along with the salinity values presented at specific marsh receptors (section 7.5) throughout the estuary to provide an estimate of the salinity values.

- Graphical aerial overviews showing the estimated maximum salinity penetration at a snapshot in time for each simulated scenario.

Table 7-1 presents an example of the tabular results (in this case for the Lower Herring River sub-basin) that are available for each sub-basin. The table shows the physical parameter (i.e., tidal benchmark, salinity level) in the first column and the various scenarios in the first row. The water surface elevation data are all presented in feet relative to the NAVD88 datum, while salinities are presented in practical salinity units (psu). The numeric difference between psu and ppt is small and both indicate ocean salinity. The modern oceanographic definition of salinity is the Practical Salinity Scale of 1978. It yields a practical salinity from new equations, smooth expansions of conductivity ratio, which were carefully fit to the real salinity of diluted North Atlantic seawater. The numeric unit is psu (practical salinity unit) and is distinct from the previous physical quantity ppt (kg salt per kg water in parts per thousand); however the difference between the two is insignificant. The various scenarios include:

- Wellfleet Harbor – The tidal benchmark elevations in Wellfleet Harbor determined from observed water surface elevation data. For example, the Mean High Water elevation in Wellfleet Harbor is 4.84 feet NAVD88. These set of values are the same in every sub-basin table. Salinity values were set to the average observed value of approximately 30 psu in the Harbor based on salinity observations for all alternatives. While a variable salinity value was used in calibration, the average salinity value was selected for the all existing conditions and alternative cases so that comparisons between alternatives could be more easily conducted.

- Existing Conditions – The tidal benchmark elevations and salinity levels in the sub-basins currently, as provided by the calibrated hydrodynamic model.

- Fully Open – The tidal benchmark elevation and salinity levels in the sub-basins for the scenario that removed all anthropogenic structures (as presented in section 6.1).

- A range of sluice/slide gate openings associated with the proposed 165’ dike opening, including the restoration endpoints (3’ and 10’ opening heights as defined in Chapter 6). These results are intended to be used to help guide the adaptive management program, as

well as provide results for assessing the potential impacts for the proposed restoration endpoints.

Table 7-1. Tidal benchmarks and salinity levels in Lower Herring River sub-basin for a range of sluice/slide gate openings.

				Chequesset Neck New Dike Opening (165' Opening)							
				Increase Sluice/Gate Opening Height(s) ---------->							
Lower Herring River Sub Basin (elevations in NAVD88, feet) (salinity in psu)	Wellfleet Harbor	Existing Conditions	Fully Open	1/3 gates 1' open	1/3 gates 2' open	2/3 gates 1' open	1' opening	3' opening	5' opening	7' opening	10' opening
Mean Low Water	-5.47	-2.20	-2.72	-1.52	-2.56	-2.62	-2.73	-2.42	-2.38	-2.36	-2.36
Mean Tide Level	-0.32	-0.98	0.96	0.22	0.06	0.06	0.25	0.83	0.95	1.01	0.97
Mean High Water	4.84	0.24	4.64	1.96	2.68	2.74	3.23	4.07	4.28	4.38	4.30
Tide Range	10.31	2.44	7.36	3.48	5.24	5.36	5.96	6.49	6.66	6.74	6.66
Mean High Water Spring	6.22	0.36	6.22	2.34	3.30	3.38	3.79	4.80	5.23	5.44	5.59
Annual High Water	7.07	0.43	6.75	2.60	3.52	3.56	3.95	5.10	5.61	5.86	6.08
100-year Storm Event	9.31	0.91	8.78	3.26	3.98	4.00	4.48	5.97	6.70	7.10	7.48
MHW, Low SLR Projection (50 years)	5.28	0.30	4.76	N/A	N/A	N/A	N/A	4.03	N/A	N/A	4.40
MHW, Mid SLR Projection (50 years)	5.65	0.34	4.87	N/A	N/A	N/A	N/A	4.10	N/A	N/A	4.49
MHW, High SLR Projection (50 years)	6.89	0.50	5.22	N/A	N/A	N/A	N/A	4.30	N/A	N/A	4.78
Mean Salinity (Dike^)	30*	26.1	28.7	27.0	27.7	27.8	27.8	28.5	28.6	28.6	28.7
Maximum Salinity (Dike^)	30*	29.9	30.0	30.0	30.0	30.0	30.0	30.0	30.0	30.0	30.0
Mean Salinity (Dog Leg)	30*	1.4	27.1	12.4	16.3	16.8	19.7	25.9	26.9	27.2	27.2
Maximum Salinity (Dog Leg)	30*	14.7	30.0	27.4	29.4	29.6	29.7	30.0	30.0	30.0	30.0

* = Salinity in Model within Wellfleet Harbor

^ = Just upstream of Dike

The Mean High Water (MHW) benchmark associated with the sea level rise scenarios was only computed for existing conditions, fully open, and the restoration endpoints only. Adaptive management openings were not simulated for expected 50-year sea level rise since these opening sizes are only intended to be temporary on the pathway to the restoration endpoints. These tables provide a significant amount of information, and details for each sub-basin are not presented herein for brevity; however, some other key items of note, include:

- The table for the Mill Creek sub-basin includes additional scenario results for the inclusion of a dike at the entrance to Mill Creek. These results include increased opening heights at the Mill Creek dike associated with both a 3' and 10' opening height at Chequessett Neck Road dike. There are also scenarios presented with the re-graded CYCC.

- Sub-basins upstream of High Toss Road include simulation results for cases with the upstream infrastructure (culverts) removed and in place. This includes removal of all the culverts in the upper portions of the system. In general, results are similar for both with and without the infrastructure in place. However, with the infrastructure removed, the upper portions of the system, which even under larger openings have minimal tidal range, tend to drain more efficiently. This results in a reduced MLW and MHW elevation. This improved drainage is beneficial for reducing areas of ponding and stagnant water throughout the upper portions of the estuary.

- As discussed in section 6.1, the fully open scenario included the removal of historical road crossing and railroad embankments allowing for improved flow both on ebbing and flooding tides throughout the system. The new dike opening height scenarios only included modifications to the existing infrastructure (culverts) and not removal of historical embankments. As such, there are some differences between the fully open and the maximum restoration case (e.g., 10' opening height). Specifically, the fully open case, which shows lower water surface elevations in the upper sub-basins, can more effectively drain water out of the system in addition to allowing more water into the system.

Figure 7-2, 7-3, and 7-4 provides examples of the graphical aerial overviews and geo-rectified bounds of the water surface elevation tidal benchmarks. Figure 7-2 presents the Mean Low Water (blue line) and Mean High Water (green line) elevations for existing conditions. The limited tidal range under current conditions is clearly depicted in this graphic, as a vast majority of the system is non-tidal, and the overall intertidal area is minimal, even just upstream of the dike. Figure 7-3 presents the MLW (blue line) and MHW (green line) elevations for the 3 foot opening height restoration endpoint. There is a significant increase in intertidal area and a return to historical tidal conditions for a majority of the system. Figure 7-4 shows a comparison of the Mean High Water Spring (MHWS) elevations for existing conditions (red) and the 3 foot opening height restoration endpoint (yellow). The comparison illustrates the difference expected in water levels during a mean high spring tide condition for the two scenarios. Similar comparisons, and subsequently various calculations (e.g., acres of intertidal area), can be evaluated using the interactive shape files for all alternatives.

From a salinity perspective, the maximum salinity penetration under normal tidal conditions for existing conditions is shown in Figure 7-5, while the salinity penetration for the 3 foot height opening at the proposed Chequessett Neck Road dike is shown in Figure 7-6. The colorbar corresponds to salinity levels in psu. Under existing conditions, the salt water does not propagate beyond High Toss Road, while for the proposed 3 foot height opening, salt water advances into a significant portion of the upper sub-basins.

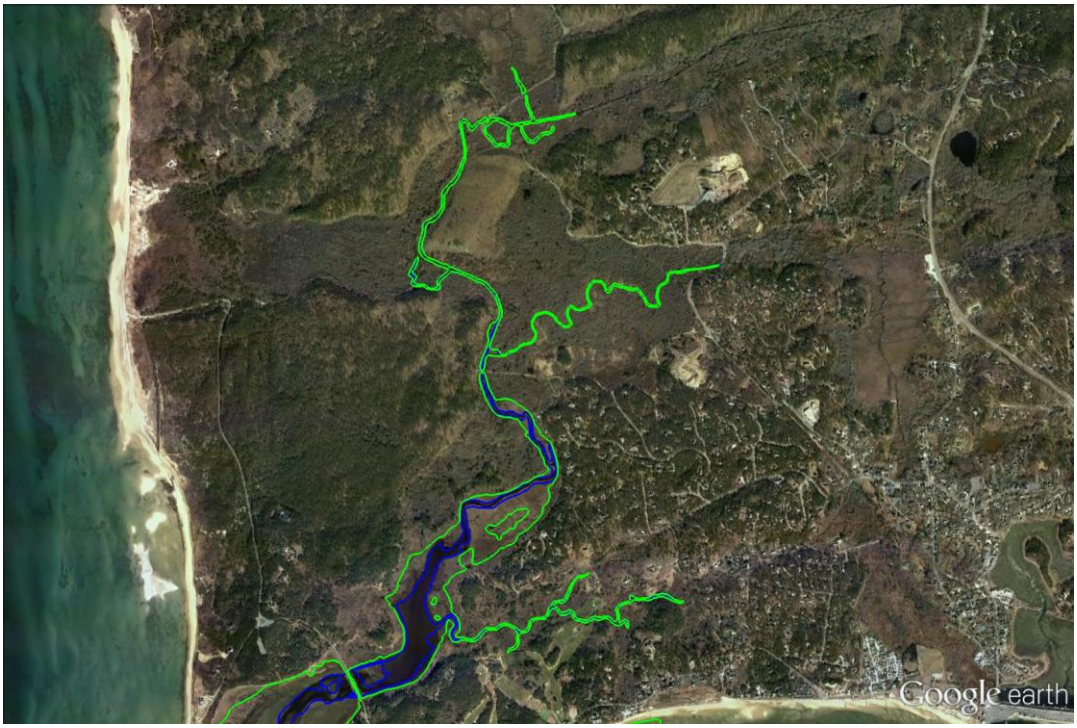

Figure 7-2. Mean High Water (green line) and Mean Low Water (blue line) elevations for existing conditions in Herring River.

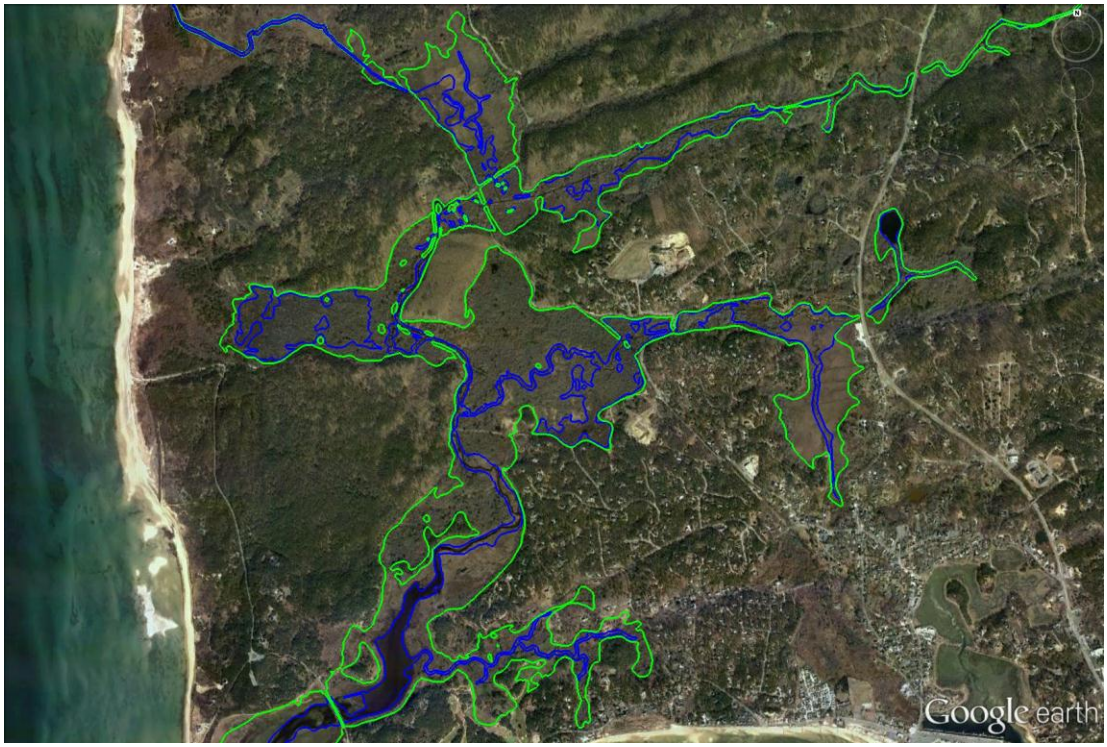

Figure 7-3. Mean High Water (green line) and Mean Low Water (blue line) elevations in Herring River for a 3 foot opening height at proposed Chequessett Neck Road dike.

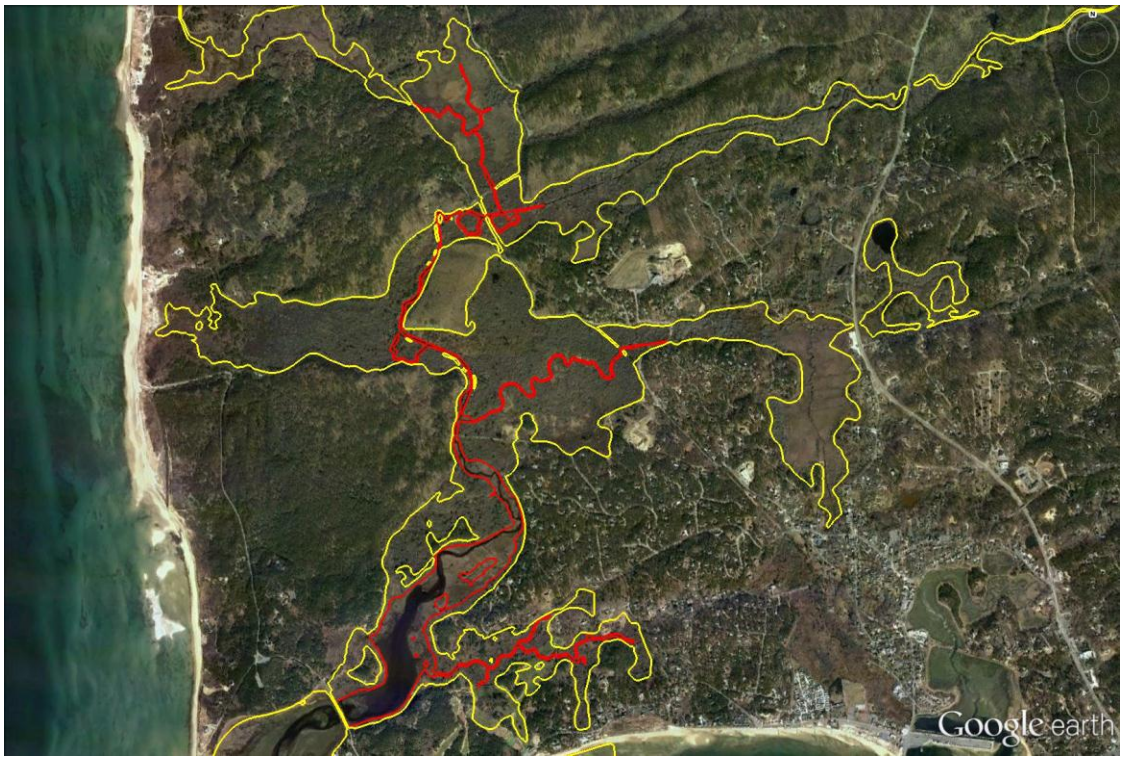

Figure 7-4. Mean High Water Spring contour for existing conditions (red line) and for a 3 foot sluice/slide gate opening at proposed Chequessett Neck Road dike (yellow line).

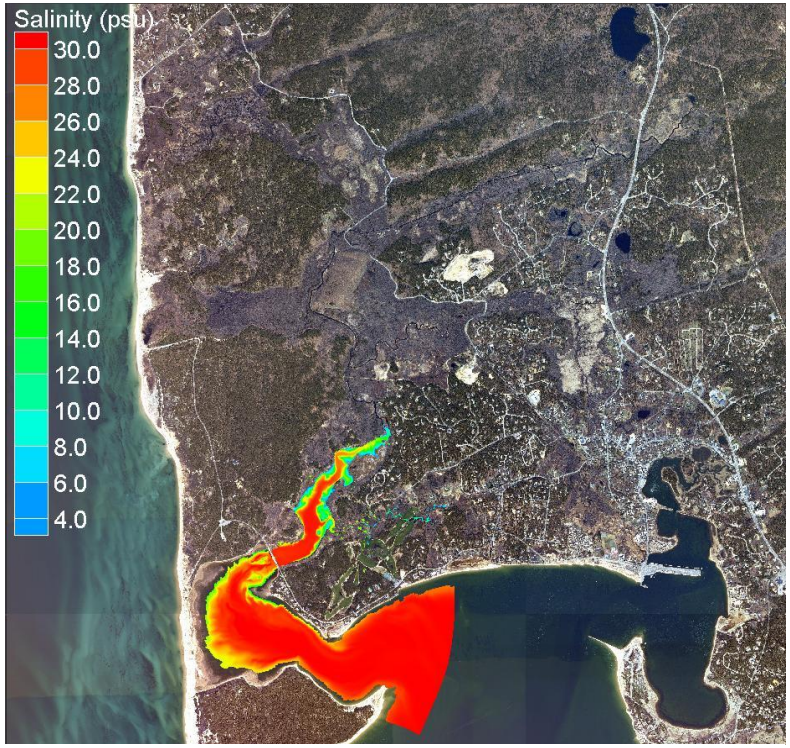

Figure 7-5. Maximum salinity penetration during normal tidal conditions for existing conditions.

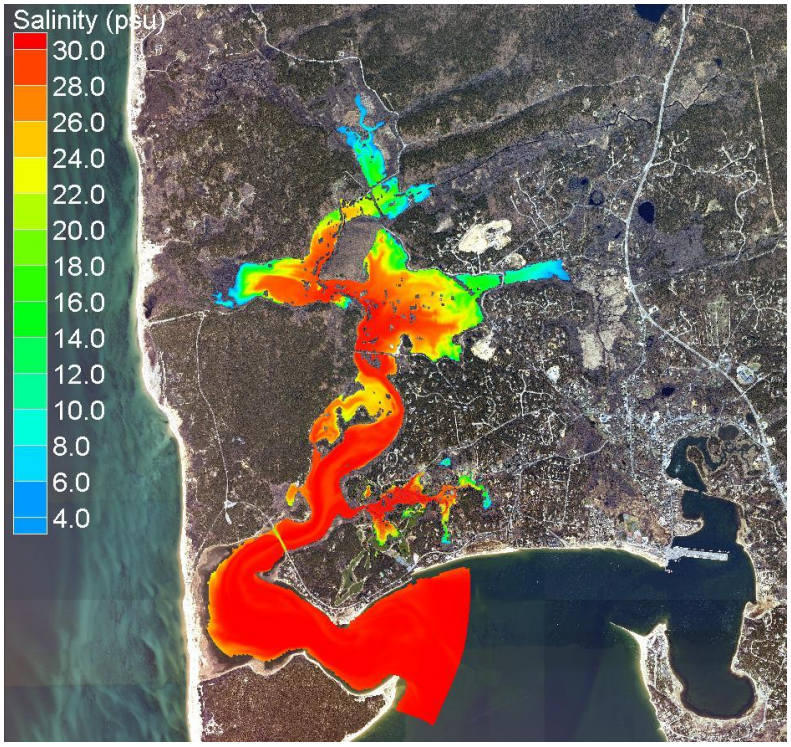

Figure 7-6. Maximum salinity penetration during normal tidal conditions for 3 foot height opening at proposed Chequessett Neck Road dike.

7.3 TIDAL FLUSHING

Residence time can be interpreted as the average amount of time that a parcel of water spends in an embayment (Knauss, 1978) or the time required to flush the volume of water in an embayment assuming a well-mixed, steady-state system. For this study, residence time is computed using the following formula by Zimmerman (1988):

$$\text{Residence Time} = \frac{\text{Volume of water to be flushed (mean tide level)}}{\text{Tidal Prism}_{\text{flood}}} \times T_{M_2}$$

where $T_{M2} = 12.42$ hours

This was calculated for each flood tide during the calibration study, and the results were then averaged. All of the information required for the residence time calculation was output from the numerical model. Water volume is provided for the mean-tide level (MTL) from the model; however, the volumes of the upper freshwater ponds in the system are not included in this volume since these are non-tidal and are not expected to be flushed by tidal processes.

As stated above, residence time indicates the average time that a parcel of water spends in a water body. Residence time, therefore, indicates how quickly a water body is flushed. If the embayment volume is small or if flow rate is large, residence times will be relatively small, which suggests the embayment is being flushed quickly. Lower residence times generally correspond to higher water quality; however, water quality also is dependent upon pollutant/nutrient loading, naturally occurring chemical breakdown processes, and the rate of the quality of water outside the embayment.

For example, the rate of pollutant/nutrient loading and the quality of water outside the embayment both must be evaluated in conjunction with residence time to obtain a clear picture of water quality. Efficient tidal flushing (low residence time) is not necessarily an absolute indication of high water quality if pollutants and nutrients are loaded into the embayment faster than can be flushed out of the embayment. Neither are high residence times an indicator of poor water quality if the water being flushed contains relatively small concentration of pollutants. Advanced understanding of water quality can be obtained from the calibrated hydrodynamic model by extending the model to include pollutant/nutrient dispersion and mixing or through particle tracking simulations. However, the residence time provided herein is valuable for planning purposes, and can be used in conjunction with nutrient loading information to assess water quality.

Two types of residence times are provided: system residence times and local residence times. Results from the calibrated model were used to calculate the system and local residence times. The system residence time of a Herring River area was based on the tidal exchange with Wellfleet Harbor, while the local residence time was based on the tidal exchange with an adjacent basin of water (e.g., Mill Creek to Lower Herring River). For instance, the system residence time of Mill Creek indicates the time required to flush the water to Wellfleet Harbor, whereas the local residence time indicates how long it takes to flush Mill Creek with new water from Lower Herring River. Residence times were computed for 1) the entire estuary system

(excluding the freshwater ponds), 2) Mill Creek (with no dike or regrading), and 3) the Herring River system upstream (above) High Toss Road. Table 7-2 presents the system residence times. The system residence times are based on the entire volume of the system, and are computed for existing conditions, a 3 foot sluice/slide opening at the proposed Chequessett Neck Road dike, and a 10 foot sluice/slide opening at the proposed Chequessett Neck Road dike.

Table 7-2. Volumes and *system* residence times for Herring River.

Basin / Sub-basin	Simulation Case	Volume (m^3) at MTL	Residence Time (hours)
Entire System	Existing Conditions	4,130,000	13.6
	3' Sluice Opening	4,780,000	12.9
	10' Sluice Opening	4,920,000	12.8
Mill Creek	Existing Conditions	35,600	12,553
	3' Sluice Opening	87,960	504
	10' Sluice Opening	97,730	424
System above High Toss Rd.	Existing Conditions	1,800,000	4,801
	3' Sluice Opening	2,140,000	191
	10' Sluice Opening	2,240,000	144

The system residence times shown in Table 7-2 indicate that on a whole the system is relatively well flushed; however the sub-basins of the system exchange water with Wellfleet Harbor less rapidly. For example, the system above High Toss Road takes approximately 200 days to fully flush with Wellfleet Harbor under existing conditions. Depending on the nutrient/pollutant loading, these more remote portions of the System may have reduced water quality. A long system residence time is not a direct indicator of poor water quality though. When a system residence time is high, it is important to compute the local residence time for each sub-basin. A local residence time is the time it takes a parcel of water to leave a particular sub-basin area and mix with the adjacent water body. Table 7-3 lists the local residence times.

Table 7-3. Volumes and *local* residence times for Herring River.

Basin / Sub-basin	Simulation Case	Volume (m^3) at MTL	Residence Time (hours)
Entire System	Existing Conditions	4,130,000	13.6
	3' Sluice Opening	4,780,000	12.9
	10' Sluice Opening	4,920,000	12.8
Mill Creek	Existing Conditions	35,600	108
	3' Sluice Opening	87,960	10.8
	10' Sluice Opening	97,730	10.0
System above High Toss Rd.	Existing Conditions	1,800,000	2086
	3' Sluice Opening	2,140,000	100
	10' Sluice Opening	2,240,000	78

The local residence times in Table 7-3 are lower that the system residence times presented in Table 7-2. For instance, the local residence time for Mill Creek is less than 5 days, while the system residence time is over 500 days. This indicates that Mill Creek exchanges water rapidly with the Lower Herring River, but not so rapidly with Wellfleet Harbor. Therefore, if water quality in Lower Herring River is generally acceptable, than water quality in Mill Creek may be acceptable as well.

The proposed opening at Chequessett Neck Road results in substantially improved flushing within the system, specifically in the sub-basins of Lower Herring River, where existing tidal exchange is minimal. Table 7-4 summarizes the percent improvement in tidal flushing for the system for the 3' and 10' openings. The improved opening size is particularly effective at flushing the extents of the system beyond High Toss Road.

Table 7-4. Tidal flushing improvements due to the proposed opening at Chequessett Neck Road.

Basin / Sub-basin	Simulation Case	Decrease in Residence Time (Percent)
Entire System	3′ Sluice Opening	5%
	10′ Sluice Opening	6%
Mill Creek	3′ Sluice Opening	90%
	10′ Sluice Opening	91%
System above High Toss Rd.	3′ Sluice Opening	95%
	10′ Sluice Opening	96%

7.4 LOW-LYING INFRASTRUCTURE

The existing Herring River marsh plain, which historically would have been regularly inundated with tidal water, contains numerous low-lying infrastructure (e.g., roadways, properties, etc.), as well as other critical locations (e.g., CYCC golf course holes) throughout the system. These sensitive receptors may potentially be influenced by the restoration and changes to the water surface elevations.

Table 7-5 shows an example of the potential flooding at High Toss Road under various alternatives. When High Toss Road remains dry for a given scenario, it is indicated as dry in the corresponding cell. Once the sensitive receptor is inundated with water, the water surface elevation is provided in the cell. For example, in Table 7-5, the low point surveyed at High Toss Road is between 3.1 to 3.3 feet NAVD88. During a 100-year storm event, with a 1 foot height opening, High Toss Road will be overtopped and the water surface elevation would reach approximately 4.2 feet NAVD88.

Table 7-5. Tidal benchmarks at High Toss Road sensitive receptor for a range of sluice/slide gate openings.

High Toss Road (low point in road 3.1-3.3 ft NAVD88) (elevations in NAVD88, feet)		Chequesset Neck New Dike Opening (165' Opening) — Increase Sluice/Gate Opening Height(s) --------->									
	Wellfleet Harbor	Existing Conditions	Fully Open	1/3 gates 1' open	1/3 gates 2' open	2/3 gates 1' open	1' opening	3' opening	5' opening	7' opening	10' opening
Mean Low Water	-5.47	dry	dry	dry	dry	dry	dry	dry	dry	dry	dry
Mean High Water	4.84	dry	4.2	dry	dry	dry	dry	3.72	3.89	3.96	3.93
Mean High Water Spring	6.22	dry	5.57	dry	dry	dry	3.49	4.39	4.79	4.97	5.08
Annual High Water	7.07	dry	6.12	dry	dry	3.32	3.63	4.92	5.21	5.43	5.59
100-year Storm Event	9.31	dry	7.98	dry	3.65	3.67	4.16	5.58	6.27	6.66	7.01
MHW, Low SLR Projection (50 years)	5.28	dry	4.31	N/A	N/A	N/A	N/A	3.92	N/A	N/A	4.22
MHW, Mid SLR Projection (50 years)	5.65	dry	4.4	N/A	N/A	N/A	N/A	3.97	N/A	N/A	4.30
MHW, High SLR Projection (50 years)	6.89	dry	4.7	N/A	N/A	N/A	N/A	4.15	N/A	N/A	4.55

7.5 MARSH RECEPTORS

Under existing conditions, nearly all of these former marsh areas are currently non-tidal. As such, no existing data are available that observed the wetting and drying processes of these marsh plains. As discussed, the model uses a well-tested and robust wetting and drying scheme that was applied to determine the water surface elevations throughout the marsh plains. Water surface elevations and salinity values were evaluated at specific locations throughout the marsh plain, as shown in Figure 7-7. Additional metrics, hydroperiod, percent of tides wetting, and a classification letter were also determined at each marsh receptor location. These locations can be used to assess the relative changes, and potential ecological changes that may occur throughout the Herring River system. The model results for the marsh receptor location are presented as:

- Tables that present relevant tidal benchmarks (Mean High Water and Mean High Water Spring) critical for marsh vegetation delineation, mean and maximum salinity levels, hydroperiod (the length of time [in hours] a point stays wet once it has gotten wet), and percent wetting (the percentage of high tides that wet that point). The tables also provide a classification letters, which are defined as:
    - A = a location that always stays dry
    - B = a location that only gets wet during spring tides
    - C = a location that wets during normal tides
    - D = remains wet, but has some tidal influence and may dry during spring tides
    - E = a location that remains sub-tidal
- Interactive Google© Earth files that provide the tables at each marsh receptor location.

Figure 7-7. Location of marsh receptors throughout the Herring River system.

Table 7-6 shows an example of a marsh receptor table for a point (LHR-F) in Lower Herring River. When the marsh receptor remains dry for a given scenario, it is indicated as dry in the corresponding cell. If a point becomes sub-tidal, or permanently ponded, the hydroperiod is set to infinity.

Although useful, hydroperiod and percent wetting may not be the best indicators for ecological change within a complicated topography and system such as Herring River. Hydroperiod and percent wetting should be used in concert to get a general sense of what is going on in a region. When evaluating a single point, such as a marsh receptor, the pathways of flow to each receptor point vary based on opening sizes and amount of water getting in and out. Therefore, the hydroperiod and percent wetting don't always follow a systematic pattern due to complicated flow and topographic features. Table 7-7 provides ranges of hydroperiod and percent wetting that can be used to provide general approximations of the physical characteristics of a marsh receptor location. Assessment of each marsh receptor is not straightforward and must be carefully evaluated in concert with the time varying water surface elevations and salinity propagation into the specific marsh areas.

Table 7-6. Model results for marsh receptor location LHR-F located in the Lower Herring River sub-basin for a range of sluice/slide gate openings.

			Chequesset Neck New Dike Opening (165' Opening)							
			Increase Sluice/Gate Opening Height(s) ---------->							
Marsh Receptor LHR-F (approximate elevation 1.7 ft NAVD88) (elevations in NAVD88, feet)	Existing Conditions	Fully Open	1/3 gates 1' open	1/3 gates 2' open	2/3 gates 1' open	1' opening	3' opening	5' opening	7' opening	10' opening
Hydroperiod (hours)	0	5.5	1.5	3.3	3.3	4.3	5.2	5.4	5.4	5.4
Percent Wetting (%)	0%	100%	31%	83%	85%	100%	100%	100%	100%	100%
Mean High Water	dry	4.38	1.77	2.55	2.62	3.11	3.88	4.06	4.15	4.12
Mean High Water Spring	dry	5.80	2.22	3.18	3.26	3.64	4.56	4.98	5.19	5.30
Classification	A	C	B	B	B	C	C	C	C	C
Mean Salinity (psu)	21.9	25.8	22	16.1	15.8	16.2	21.9	23.8	23.8	24.6
Maximum Salinity (psu)	22.3	28.3	22.7	23	23	23.8	26.7	28.1	28.2	28.2

Table 7-7. Hydroperiod and percent wetting ranges and approximate descriptions of expected processes.

Hydroperiod Range	% Wetting	Description
0	0	Dry all the time
0-1	0-10	Dry except during the highest spring tide(s)
1-2	5-40	Probably getting wet during some spring tides only and draining well
	40-90	Getting wet during normal and spring tides, draining well
2-4	5-40	Probably getting wet during most spring tides only and draining well, shallow depth
	40-90	Getting wet during normal and spring tides, draining well, shallow depth
4-6	5-40	Probably getting wet during all tides and draining well, significant depth
	40-90	Getting wet during normal and spring tides, draining well, significant depth
6-12	5-40	Probably getting wet during spring tides and experiencing difficulty draining
	40-90	Probably getting wet during all tides and experiencing difficulty draining
12+	Any	Flooded

7.6 PONDING

Simulations of the adaptive management steps and restoration endpoints revealed there were certain areas within the system that were prone to ponding of water with the introduction of the increased tidal exchange. These areas, shown in Figure 7-8, are generally due to subsidence that has occurred over the century of marsh degradation, or caused due to poor drainage pathways. Areas A, B, C, and D in Figure 7-8 are potentially prone to ponding due to limited drainage capacity and/or pathways. For example, although the Duck Harbor area (B) adequately floods during a rising tide that overtops higher elevation topography, there are minimal low-lying channels from Duck Harbor to the main Herring River channel that inhibit the ebbing capacity of the region. This is also the case in area C. In other cases, the existence of downstream subsided areas limit the drainage capacity of an area due to excess water contained in the system. This is typically the case for areas A, D, and G. Other locations, such as E, F, and G, are prone to ponding simply due to the topographic nature of the regions, which have subsided over the past century.

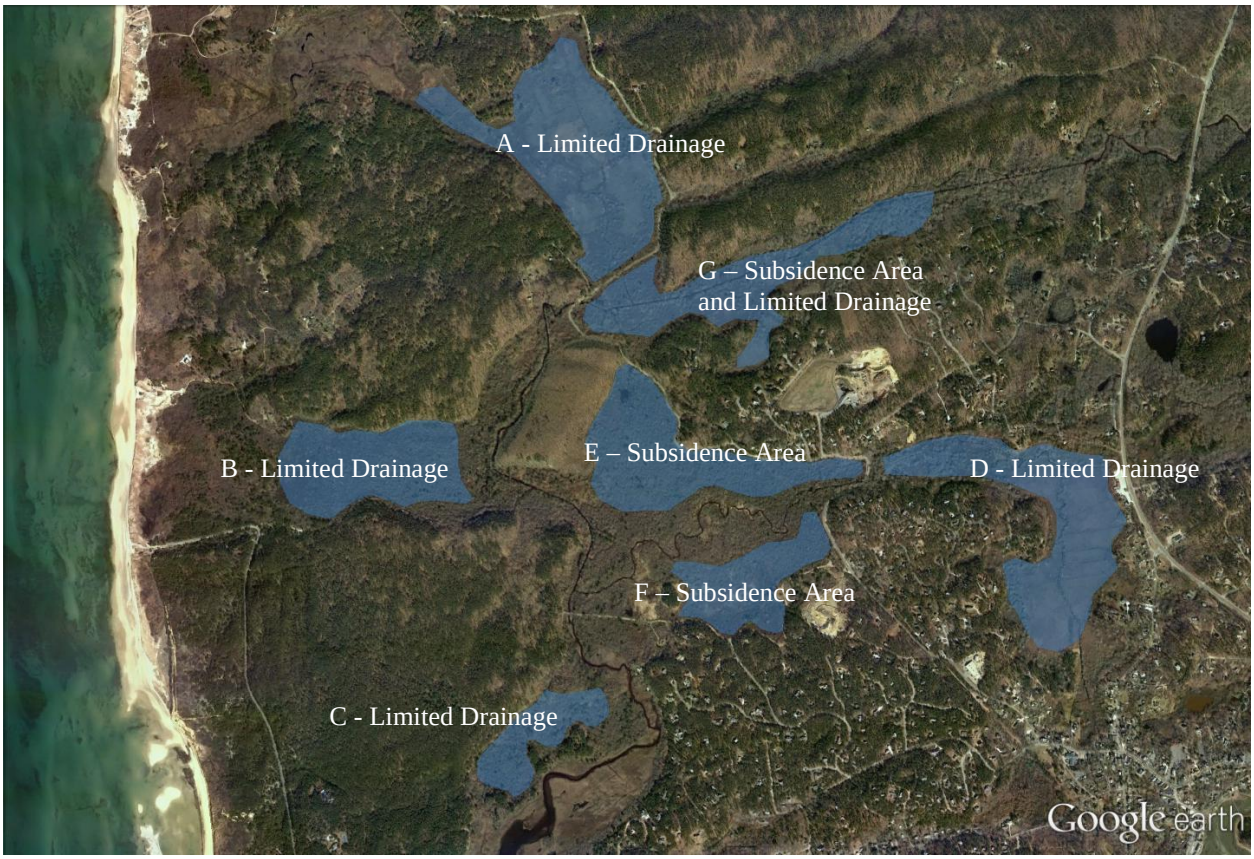

Figure 7-8. Location of potential ponding areas within the system.

Although these potential ponding areas appear in the hydrodynamic model for restoration endpoint simulations (3 foot and 10 foot height openings), it is unclear whether this will actually occur during the restoration process. The hydrodynamic model is using the existing bathymetry to simulate future restoration endpoints. However, due to the adaptive management approach

that is intended to be applied to the system (smaller incremental openings over time), it is likely that this topography will be modified as the system responds to increased tidal exchange. For example, it is expected that additional sediment will be transported into the system (section 7.7) and be deposited in the lower velocity zones of the subsided areas. Additionally, existing channels leading to limited drainage areas will be naturally widened and deepened due to the increased tidal flux during the restoration process. Other adaptive management actions may also be undertaken to facilitate accretion of subsided areas. Therefore, the areas indicated in Figure 7-8 are not likely to experience long-term ponding with appropriate adaptive management and monitoring. In addition, additional manual effort (e.g., channel creation to help increase tidal flux between Duck Harbor and the main Herring River channel) also could be used to expedite the restoration process. It is not expected that these areas will experience significant ponding in the future; however, the areas are presented here to help guide the adaptive management approach and potential monitoring efforts.

7.7 SEDIMENT MOBILIZATION AND TRANSPORT

Sediment transport processes are an important aspect of the overall restoration project. Considering the relative importance of sediment transport processes with respect to tidal restoration (e.g., accretion of sediment on subsided marsh plains), as well as concerns of potential impacts to shellfish aquaculture in Wellfleet Harbor, potential changes to sediment transport within the Herring River system is an important aspect the proposed restoration project. As such, this section presents (1) a qualitative assessment of the local sediment dynamics based on existing data and previous studies, and (2) the methodology and results of an analytical sediment transport analysis in the Herring River system utilizing time-varying results from the two-dimensional hydrodynamic model and sediment data collected throughout the existing system. The second approach provides a quantitative assessment of sediment transport potential and its spatial distribution. Sediment transport potential is estimated for normal tidal conditions and also for tidal flood condition representative of the 1-percent annual chance storm surge event. Results of the sediment transport analysis are used to indicate areas of potential erosion and deposition. These results can be used to project sediment transport pathways in the existing system and illustrate how sediment transport pathways may change due to potential tidal restoration alternatives.

The methods and results presented in this section represent first-order qualitative and quantitative assessment of potential sediment transport in the Herring River estuary. This assessment does not determine actual sediment movement but rather areas where there is potential for erosion or deposition. Furthermore, sediment transport causes changes in morphology that are not considered in this analysis. Changes in the morphology can have an effect on the hydrodynamics which in turn affects the sediment transport. The determination of actual rates of erosion and accretion and changes in morphology would require a more sophisticated analysis and modeling effort. Although this could be done by applying the sediment transport capabilities of EFDC and collection of additional sediment coring data to calibrate and validate the sediment transport module, the potential sediment transport approach presented herein provides sufficient information for evaluating potential changes to the sediment dynamics of the Herring River System. A fully numerical evaluation of the sediment transport dynamics within the system would also require prohibitive computational costs considering typical time scales for morphological change are on the order of decades or more. Therefore, considering the many

factors that influence sediment transport and the fact that restoration plans for the Herring River include adaptive management of the system, Woods Hole Group believes the analytical assessment presented here provides reasonable results for the assessment of environmental impacts and address the potential changes to sediment dynamics of the system.

7.7.1 Qualitative Sediment Analysis and Background

A preliminary sediment transport analysis by Woods Hole Group was completed to:

- Compile and review existing data, reports and studies;
- Perform a qualitative assessment of local sediment dynamics, and
- Identify areas of concern/data gaps and recommend next steps for additional sediment transport assessment as appropriate.

The results of this first level sedimentation analysis are summarized in this section.

7.7.1.1 Existing data, reports, and studies

- Spaulding & Grilli (2001, 2005) report and data – Spaulding & Grilli (2001) reported measurements of sea level, water temperature, salinity, and dissolved oxygen at one location upstream and one location downstream of the Chequessett Neck Dike from June to October 2000. Two shorter term (12.4 hours) measurements of currents, sea level, salinity, temperature at numerous locations were also reported. Additionally, the Spaulding & Grilli (2001) work included: sediment samples and topographical measurements; a numerical model of the tidal hydrodynamics, which assumes a horizontal sea level within the Herring River and a representation of the flow through the Dike based on standard hydraulic formulas; and a numerical model of the salinity distribution within the Herring River, based on a balance between downstream freshwater discharge and upstream transport of salt by means of longitudinal tidal dispersion.

  The primary conclusion, as relevant to sediment transport was that the onshore transport of sand through the existing Dike structure occurs during flood tide because of strong flood currents, while ebb currents are insufficient to re-suspend sediment. This process was cited to explain the existence of the flood tide delta upstream of the Dike.

  Spaulding and Grilli (2001) seafloor samples indicate coarse sediments (90-99% sand and 1-10% percent gravel) at eight sites and finer sediments (52-85% sand and 15-48% percent silt and clay) at the remaining four sites, which were located in deeper water than the sites with coarser sediments. The tidal calculations indicate that if the culverts through the Dike were widened, the tidal velocities upstream of the Dike would remain too small to transport sediment (< 20 cm/s), and that transport of fine sediments (silt and clay) would occur only during storms, with dispersal both up- and downstream of the Dike.

  Spaulding & Grilli (2001) reported measurements of sediment size distribution upstream of Chequessett Neck Dike. These measurements indicate that the surficial sediments are

dominated by sand, with smaller amounts of gravel and silt and clay (Figure 7-9). The measurements indicate a statistically significant (at 95% confidence) increase in the sand fraction with increasing distance upstream of the dike, although the corresponding required decrease in fractions of gravel and of silt and clay are not statistically significant at 95% confidence.

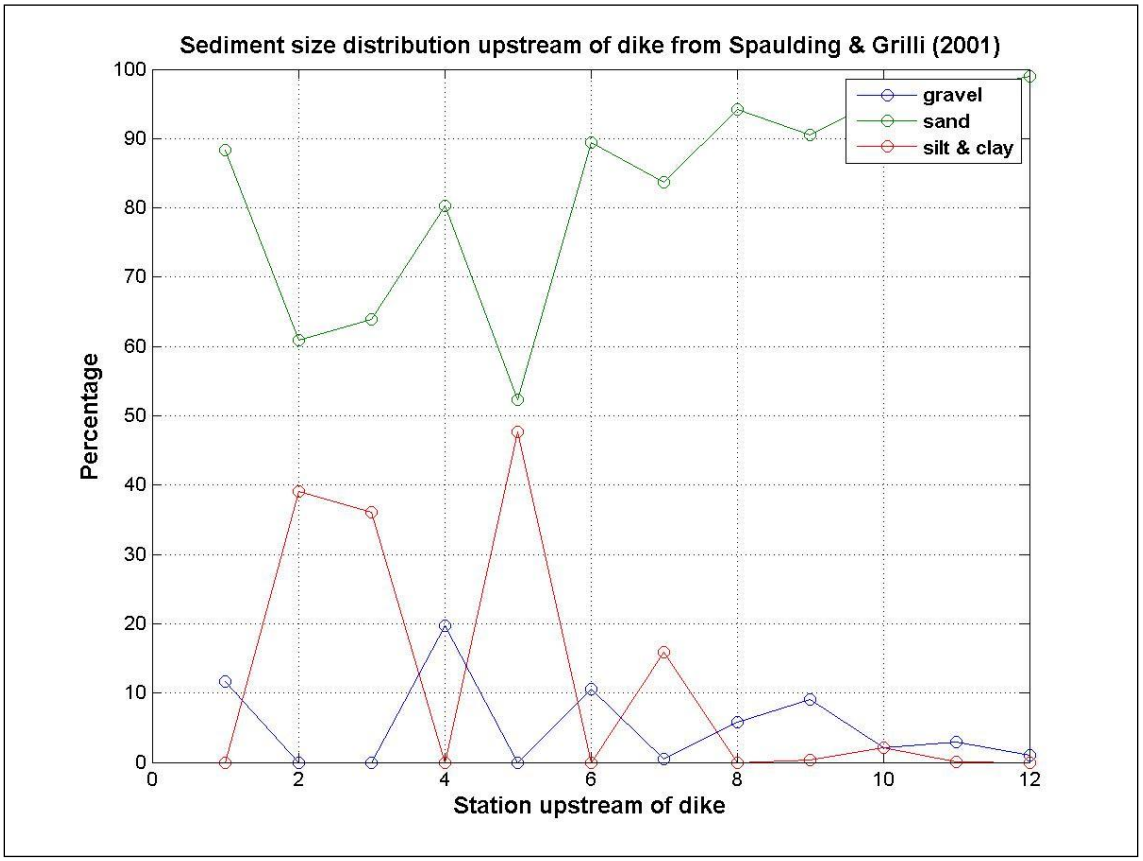

Figure 7-9. Surficial sediment grain size distribution upstream of Chequessett Neck Dike from Spaulding & Grilli (2001) measurements and analysis.

- Dougherty (2004) report - Dougherty (2004) used a diverse set of information to determine whether opening the Chequessett Neck Dike would affect the stability or the sedimentation in the area seaward of the dike. Source materials for Dougherty's analysis included numerical hydrodynamic simulations reported by Spaulding & Grilli (2001), pre-existing maps and aerial photographs, and knowledge of the geological history and processes. The overall conclusion is that opening the dike would not affect either the stability of the area downstream of the dike or the sedimentation seaward of the dike. Specific conclusions related to the stability of the area downstream of the dike included: (1) stability of the area downstream of the dike depends more on the sand supply, littoral drift, and sea-level rise in Cape Cod Bay than on the Herring River flows and sediment; (2) the area downstream of the dike influences the Herring River, instead of the opposite, as evidenced by the deflection of the River, the formation of the area downstream of the dike, and the wide mudflats indicating low flow velocities downstream of the dike; and

(3) the sediment spit ('The Gut") is unlikely to breach and form a permanent inlet because of the extensive marsh backing the barrier beach, although temporary wash overs might occur during storms and close quickly as a result of natural post-storm processes (Dougherty also noted that foot traffic across the dune system of the Gut has worsened erosion and increased the possibility of wash overs).

The specific conclusions related to sedimentation seaward of the Dike are a reiteration of the Spaulding & Grilli (2001) conclusions and an analysis based on maps and aerial photographs. This work indicates that if the Chequessett Neck Dike were removed the only changes in sedimentation would be proximal to the dike, with little influence on shellfish grants on Egg Island.

- Harvey (2010) thesis and surface sediment samples - Harvey (2010) reported on collection and analysis of surficial (top 2cm) sediment samples from up and downstream of the Chequessett Neck Dike and from Mayo Beach. These samples indicate predominantly sand with smaller amounts of gravel, silt and clay, with no systematic variation of the sediment size distribution with distance upstream of the Chequessett Neck Dike (Figure 7-10). The mean sediment diameter has no systematic dependence on distance upstream from the dike (Figure 7-10) and averages approximately 300 microns. Harvey (2010) inferred (from the surficial sediment data and from results from prior studies and knowledge of geological processes) that reducing the flow constrictions at the dike would not increase sedimentation or transport of organic material (including fecal coliform bacteria) downstream of the dike. Harvey (2010) also suggested that greater threats to shellfish production downstream of the Dike might come from sediment and organic matter originating below the Dike, in part associated with vegetation dieback. Harvey (2010) further suggested that Hatches Harbor in Provincetown, MA is a similar system to Herring River, and cited work by Portnoy, et al. (2003) that showed increased sedimentation upstream of an improved (opened) hydraulic structure in Hatches Harbor.

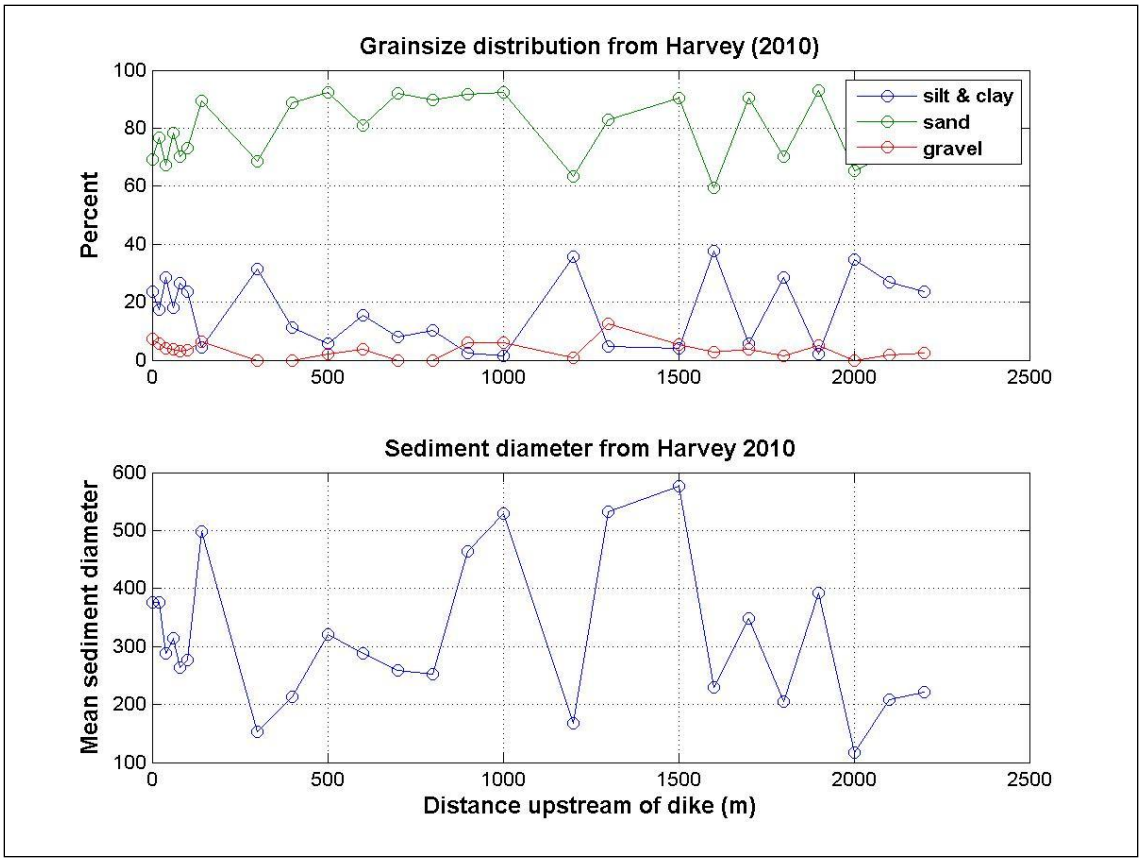

Figure 7-10. Surficial sediment grain size distribution upstream of Chequessett Neck Dike from Harvey (2010) measurements and analysis.

- National Park Service (NPS) grain size analysis and organic matter at aquaculture sites in Wellfleet Harbor - Measurements obtained by the National Park Service at the aquaculture sites in Wellfleet Harbor indicate small (always less than 3%) concentrations of organic matter. The corresponding grain size analysis indicates relatively large mean sediment diameter (300 to 600 microns) at all aquaculture sites (Figure 7-11).

- National Park Service Soil Cores (Summer 2009) - The National Park Service collected soil cores in June of 2009. Grain size data were available for nine (9) cores, which are presented in Table 7-8. Cores ranged in depth from 5 cm to 100 cm, and represented a range of grain size distributions. As with prior data sets (see below sections), the dominant grain size just upstream from the dike (Core #5) is a fine to medium sand. Figure 7-12 illustrates a section of the sandy material that was characteristic of Core #5. Overall, the fraction of silt and clay material (retained or smaller than #200 sieve) is relatively small. Figure 7-13 illustrates a sample of the fine material from Core #7.

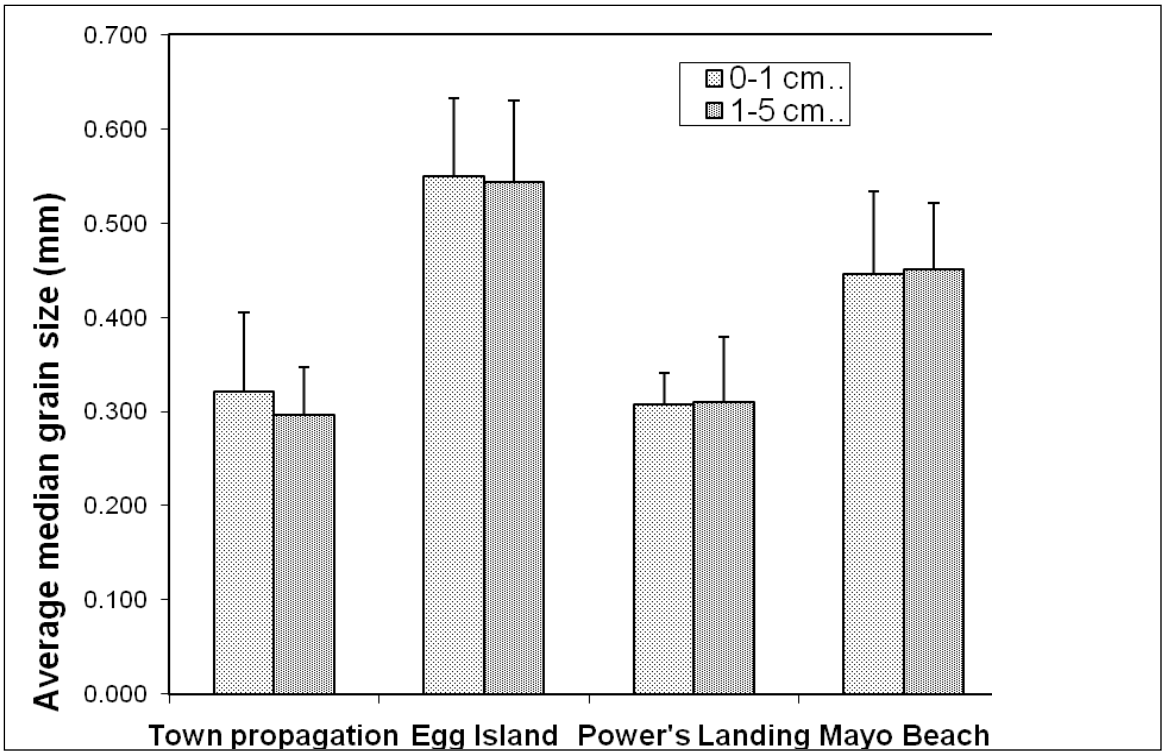

Figure 7-11. Surficial sediment grain size analysis at aquaculture sites based on NPS data.

Table 7-8. National Park Service Core Grain Size Data from June 2009.

		Percent Retained By Size Class (Sieve #)										
		>1"	#4	#5	#10	#18	#35	#60	#120	#200	<75um	
Core	Depth (cm)	>256 mm	4.76 mm	4 mm	2 mm	1 mm	0.5 mm	0.25 mm	.125 mm	.074 mm	<.075 mm	Notes
5	0-30	0.0%	4.3%	0.0%	3.8%	15.2%	32.8%	33.3%	7.8%	0.6%	0.7%	Just inside dike
7	10-60	0.0%	17.1%	0.6%	3.7%	12.2%	28.8%	21.3%	10.5%	4.2%	1.6%	River edge
10	0-5	0.0%	17.3%	2.9%	8.0%	8.6%	12.9%	14.6%	34.5%	0.4%	0.3%	Submerged @ low tide
15	0-25	0.0%	1.1%	0.2%	2.6%	14.5%	48.9%	24.6%	7.1%	0.5%	0.2%	Egg Island
18	0-100	0.0%	19.8%	2.1%	5.6%	10.2%	23.9%	26.9%	8.4%	1.6%	1.4%	Creek edge @ High Toss culvert
19	0-50	0.0%	68.5%	4.9%	9.2%	6.9%	4.2%	2.8%	1.6%	0.9%	0.9%	Near river edge
28	0-30	0.0%	1.0%	0.1%	0.6%	8.1%	34.0%	41.5%	13.7%	0.8%	0.3%	Sand spit near Old Saw
29	0-50	0.0%	34.4%	1.5%	5.7%	11.1%	20.6%	16.9%	6.6%	1.5%	1.4%	Phragmites edge
32	0-50	0.0%	16.5%	2.1%	5.4%	10.3%	24.2%	26.8%	11.3%	1.8%	1.4%	

Figure 7-12. Sample of sandy material from Core #5.

Figure 7-13. Sample of fine sediment from Core #7.

- National Park Service synoptic measurements of total suspended solids (ongoing) - The National Park Service (NPS) measured total suspended solids (TSS) from water samples at mid-depth during ebbing tide at 11 fixed locations on 32 occasions during the period 2005 to 2009 (these observations continue to be conducted). The time series plots of these measurements indicate substantial variability of TSS, ranging from a low of 1 mg/l

to more than 2035 mg/l (Figure 7-14). Although the NPS TSS measurements do not indicate any visible, consistent spatial structure, a correlation analysis was conducted to further investigate the spatial structure. In simplified terms, the correlation analysis attempted to quantify spatial trends in the data. Results from the analysis are shown by Figure 7-15, which relates the correlation of TSS values to separation distance between measurement locations. High values would indicate a coherent spatial structure in suspended sediment concentrations (e.g., continuous trend of high levels at a particular location). If there was a meaningful spatial structure, the dots on Figure 7-14 would trend consistently from high to low from left to right on the graph.

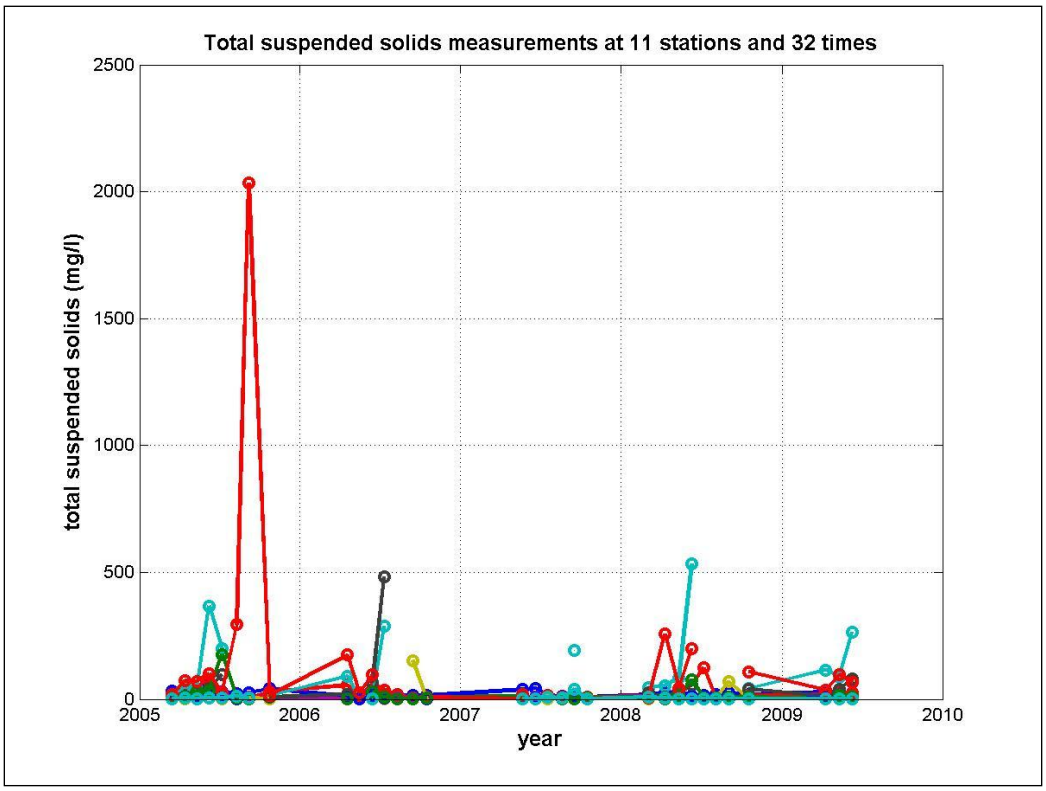

Figure 7-14. Synoptic measurements of total suspended solids (TSS) obtained by the National Parks Service at 11 fixed locations and 32 times during the period 2005 to 2009.

Instead of indicating a good correlation, the results showed that the squared correlation coefficients (r2) based on measurements at some pairs of sample locations are inconsistent. The pair-wise squared correlation coefficients (r2), based on the 14 times when samples were obtained simultaneously at all 11 locations, have no consistent dependence on the separation distance between the sample pair locations (Figure 7-15). The correlations between sample pairs indicate no organized dependence on location within the channel network. A supplemental spatial empirical orthogonal functions also was conducted (not shown), and did not indicate a spatial structure with any coherent dependence on location within the channel network. The lack of spatial coherence of the synoptic TSS measurements is likely a result of the fact that tidal velocities under the existing conditions in the Herring River are too small to re-suspend seafloor sediments at

most locations (Spaulding & Grilli, 2001), suggesting that TSS is dominated by exceedingly fine materials with small settling velocities and large spatial variability in seabed distribution and water column concentrations.

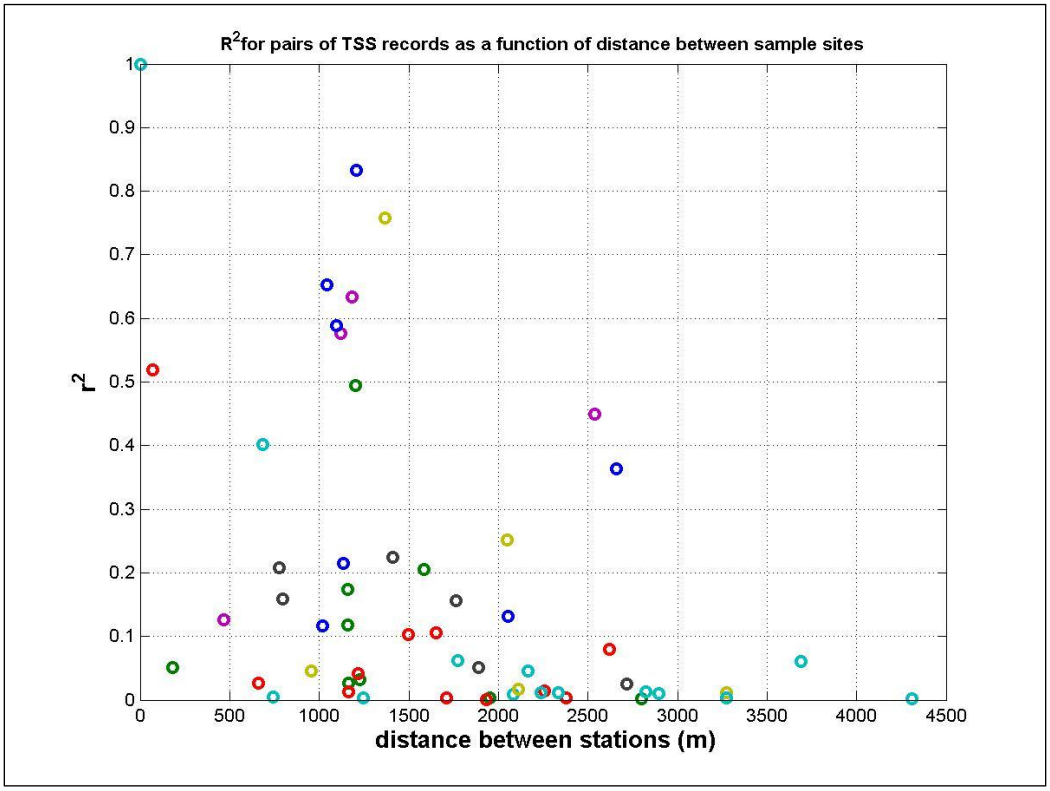

Figure 7-15. Squared correlation coefficient r^2 as a function of distance between pair-wise samples for all 14 times at which samples were obtained at all 11 locations.

- National Park Service continuous measurements of turbidity (ongoing) - In addition to the TSS, the National Park Service (NPS) also collects continuous measurements of turbidity at two locations: Dogleg and Old Saw. The turbidity measurements are highly variable, ranging from zero to more than 1700 nephelometric turbidity units (NTU) (Figure 7-16). More detailed analysis showed the turbidity measurements at the two sites were not significantly correlated with each other at 95% confidence. Figure 7-16 also shows that neither turbidity time series was correlated with rainfall (Figure 7-16). Addition analysis showed that neither of the continuous turbidity measurements is significantly correlated at 95% confidence with the synoptic measurements of total suspended solids (TSS) at any of the eleven TSS sample locations. The continuous turbidity measurements are characterized by large changes over short time periods (Figure 7-16). Wild-point editing (removal of all points more than four standard deviations from the mean) results in time series with far less variability, but even after editing the series at the two locations remain uncorrelated with each other or with the TSS measurements (at 95% confidence).

A spectral analysis of the measurements also was conducted to determine if the turbidity measurements revealed periodic trends over time. The spectra of turbidity measurements (Figure 7-17) indicated significant spectral peaks at diurnal (daily) and semi-diurnal (twice daily) frequencies as well as for harmonics of the semi-diurnal frequency (multiples of the twice daily frequency). These peaks were attributable to along-channel channel tidal currents (i.e., advection or re-suspension of suspended sediments by tidally forced velocities). More quantitative interpretation of the continuous turbidity measurements is problematic because of the lack of correlation between the turbidity and TSS measurements and the lack of correlation between the turbidity measurements at the two sites.

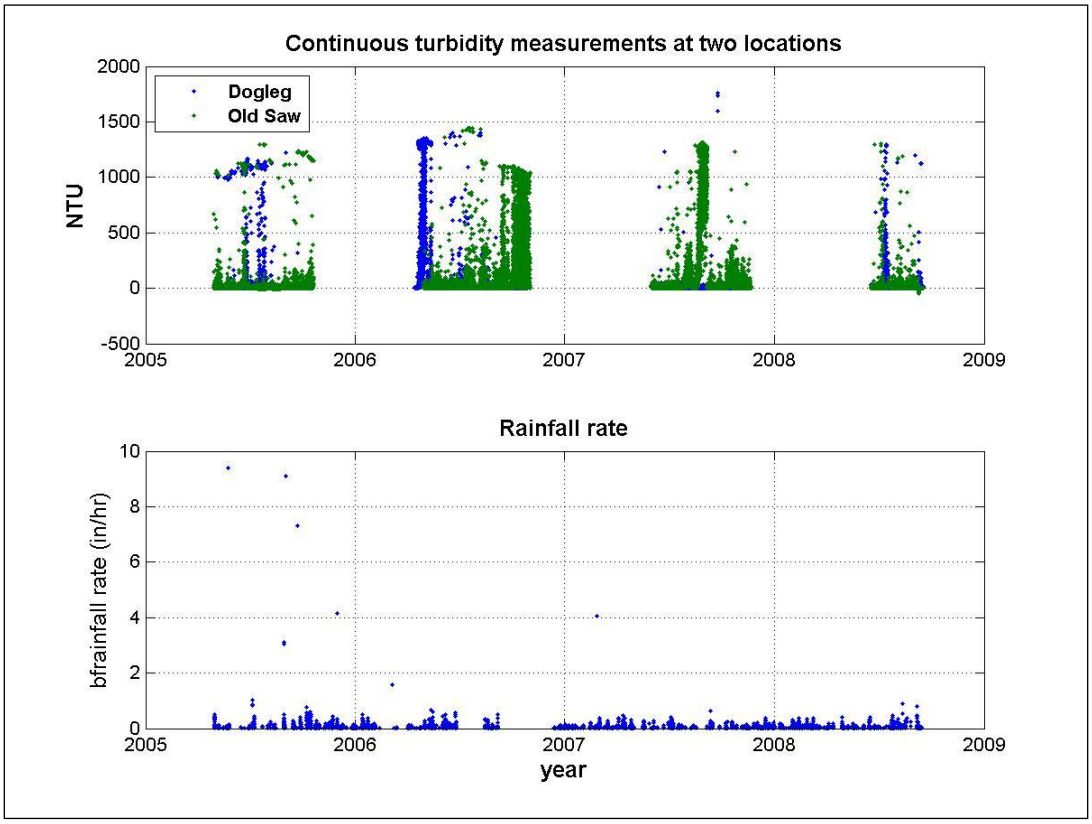

Figure 7-16. NPS continuous turbidity measurements at Dogleg and Old Saw locations (top panel) and rainfall rate measured at a nearby location (bottom panel).

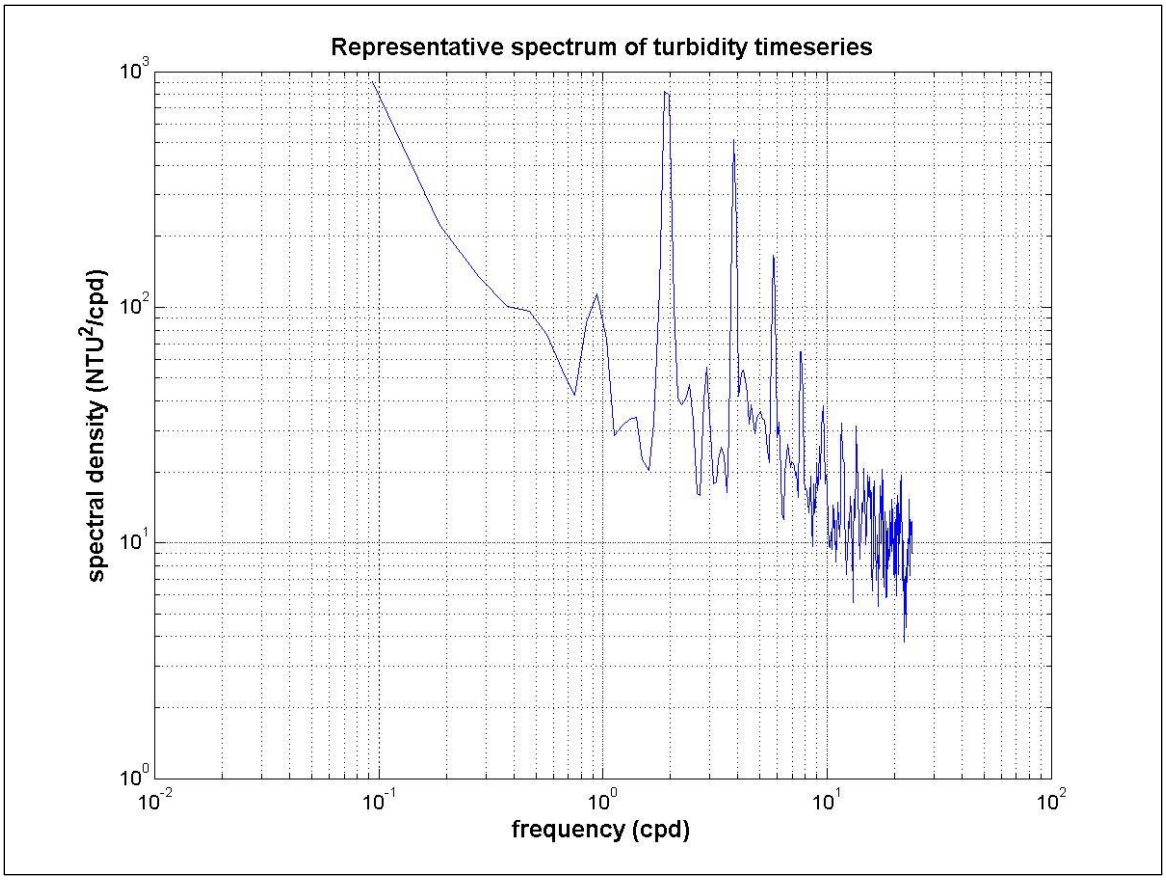

Figure 7-17. Spectrum of first 8192 wild-pointed turbidity measurements at the Dogleg measurement site. Peaks correspond primarily to daily and twice daily tidal activities.

7.7.1.2 Qualitative Assessment of the Sediment Dynamics

The measurements and analyses reported by Spaulding & Grilli (2001) and by Harvey (2010) indicate that the seabed sediment upstream of the Chequessett Neck Dike is predominantly (approximately 80%) sand, with a smaller amount (approximately 20%) of silt and clay and an even smaller amount of gravel. The mean sediment diameter upstream of the Dike is approximately 300 microns, or 0.3 mm which is characteristic of fine to medium sand. The data analysis and computations of Spaulding & Grilli (2001) indicate that under existing conditions the tidal velocities are too small to move the sand-sized particles, except in the vicinity of the Dike where flows through the single culvert open during flooding tides are relatively strong. The measurements and analysis of Spaulding & Grilli (2001) indicate that under existing conditions the flux of sediment is upriver. The reason that the net sediment transport is directed upstream is that the quantity $\langle u^3 \rangle$, where u is the along-channel velocity, is positive upstream at the Dike. In hydrodynamics, this quantity (the cube of the along channel velocity) is a proxy for the direction of the sediment flux. Since the flow rate (Q) must average to nearly zero over a tidal cycle (to ensure that the tidally averaged volume of water in the Herring River system remains constant), the change in area of flow caused by the gated entrance results in a change in the velocity (u). By continuity, the velocity, u is equal to Q/A, where A is the cross-sectional area of the flow. Because of the existing gate and weir system in the culverts at the Dike, the flow during flood

tide is predominantly through one culvert, while the flow during ebb is through three culverts. Thus the cross-sectional area A through the culverts is roughly three times larger during ebb than during flood, and consequently the velocity u, and the cubed velocity proxy, is much larger during flood than during ebb.

The conclusions are that the sediment flux must be upstream at the Dike under existing conditions, and that the flow is sufficient to move the predominantly coarse sediment only in the vicinity of the Dike. These conclusions are consistent with observations of a flood-tide delta just upstream of the Dike (Figure 7-18). According to the standard Shields diagram, the shear velocity (square root of boundary shear stress divided by fluid density) for initial motion of the 300-micron particles that dominate the seabed (assuming a plane seabed) is approximately 0.014 m/s, corresponding roughly to a depth-averaged velocity of 0.3 m/s (assuming a bottom drag coefficient of 0.0025).

Woods Hole Group has two-dimensional (depth-averaged) simulations of the Herring River system and portions of Wellfleet Harbor based on the Environmental Fluid Dynamics Code (EFDC), as presented herein. Velocities were output at six stations from the model with increasing distance upstream in the Herring River (see Figure 7-19). There are two analysis sites at the Dike (one just downstream and one just upstream). Woods Hole Group executed computations for three cases: existing conditions, a 30-m opening at the Dike, and a full opening (no obstruction) at the present location of the Dike to provide an initial semi-quantitative assessment of sediment transport throughout the system. Although the EFDC model results have not been analyzed completely for sediment transport purposes, results to date are sufficient for a qualitative and semi-quantitative analysis. Figure 7-20 presents the root mean square tidal velocities for the three evaluated scenarios as a function of station location (Figure 7-19). For existing conditions (blue line), tidal velocities increase through the dike at stations 3 and 4 (capable of moving sediment) and then decrease substantially in the system (stations 5 and 6). For the 30 m opening (green line), the tidal velocities are larger than the existing condition through the dike (stations 3 and 4) as the volumetric flow and cross-sectional area are increased, but are still cause a tidal restriction such that the velocity also rises. Tidal velocities upstream of the dike (stations 5 and 6) are also larger as the flow is larger than existing conditions. For the fully open scenario (red line), the tidal velocities through the inlet are lower since the cross-sectional area is large enough to eliminate the constriction; however, tidal velocities upstream of the dike (stations 5 and 6) are larger due to the increased volumetric flow and consistent cross-sectional area.

Figure 7-18. Photograph of the Chequessett Neck Dike showing a flood tidal delta. Reproduced from Harvey (2010).

The EFDC simulations also indicate that the maximum tidal velocities, with a 30-m opening at the dike, are easily sufficient to move the dominant sand near the dike and just sufficient for sediment motion upstream and downstream. With the full opening, modeled velocities are just sufficient to move sediment downstream and near the dike and easily sufficient to move sediment upstream of the dike.

The quantity $\langle u_{parallel}^3 \rangle$, where $u_{parallel}$ is the velocity parallel to the channel (in the direction of the principal axes of the velocity), is a useful proxy for indication of the direction of the sediment flux. Figure 7-21 shows the upstream sediment flux proxy as a function of station. A positive flux denotes transport upstream (toward the head) of the Herring River system, while a negative flux indicates transport downstream. The computations indicate downstream sediment flux in the Herring River, upstream of the Dike, for both the 30-m opening and fully open scenarios (Figure 7-21). The simulations for the 30-m opening indicate upstream flux in the immediate vicinity of the Dike, reducing to negative (downstream) values well seaward of the Dike. The simulations for the fully open case indicate nearly zero flux at and downstream of the Dike. Thus, the simulations for both the 30-m and fully open scenarios indicate downstream flux upstream of the Dike and a convergence of flux, corresponding to sediment accretion, in the vicinity of the Dike. The simulations for both cases indicate a weak seaward sediment flux downstream of the Dike.

Figure 7-19. Location of velocity information extracted from the model. Site selected for analysis indicated by red circles.

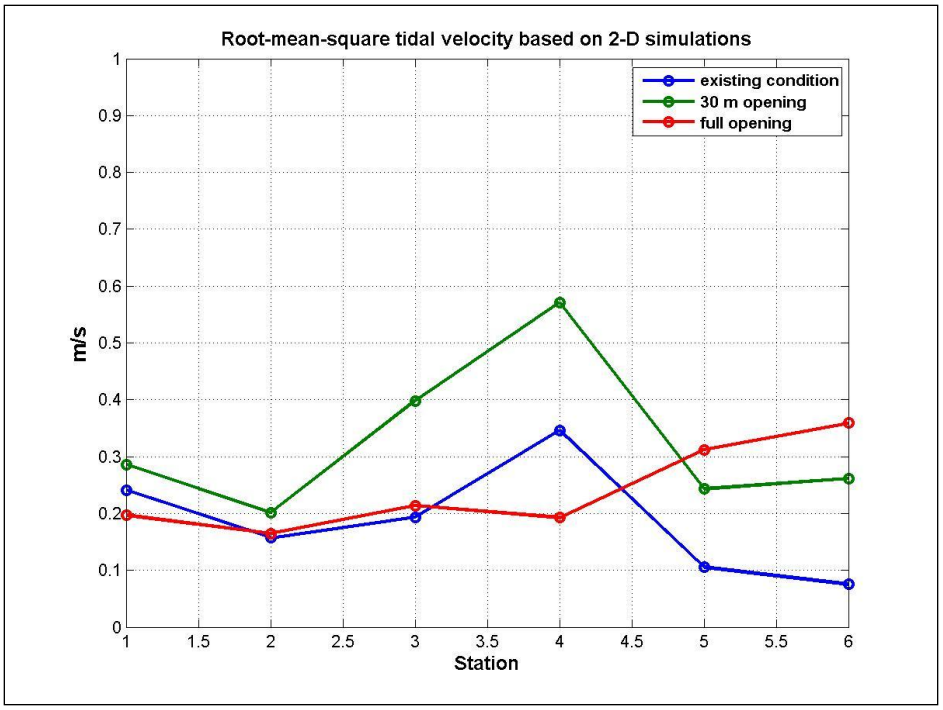

Figure 7-20. Root mean square tidal velocities at selected stations based on EFDC simulations for three dike scenarios. The blue line presents existing conditions at the dike, the green line presents a 30 meter dike opening, and the red line presents fully open conditions at the dike.

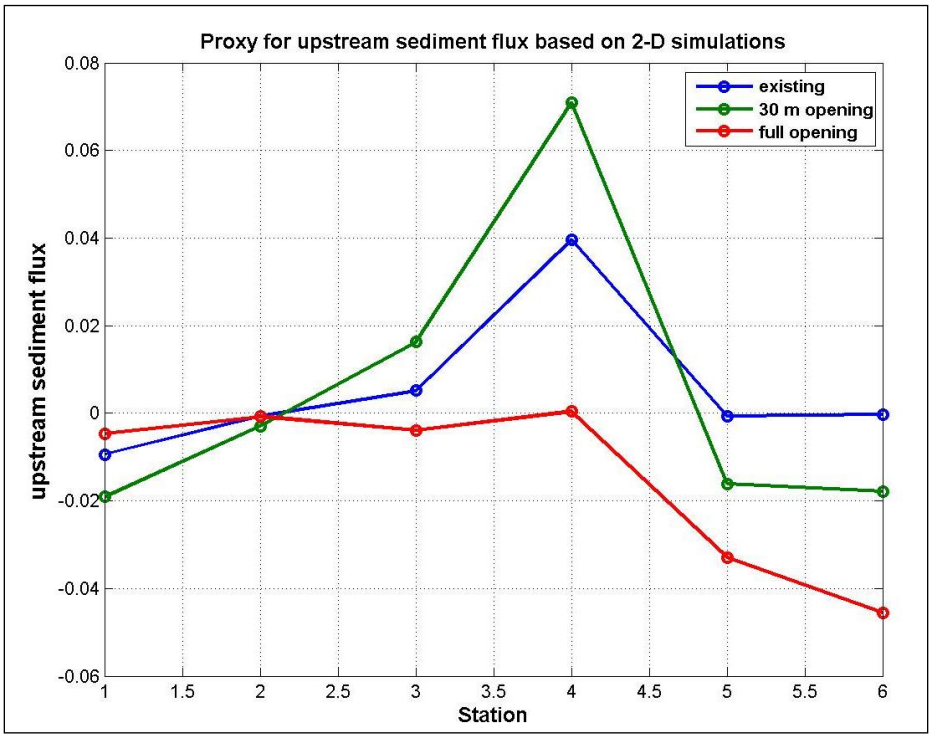

Figure 7-21. Proxy for upstream sediment flux based on EFDC simulations. Positive flux is upstream in the Herring River system.

In summary, the qualitative sediment transport analysis allowed for the following conclusions:

- Current velocities for existing conditions are sufficient to initiate sediment movement, but only in the vicinity of the dike during normal conditions.
    - Fine-grained silt sized particles can be transported within the system.
    - Sand sized particles can only be transported in the near vicinity of the dike for the existing configuration.
    - Net transport at the dike for existing conditions is into the River as supported by the first level calculations and demonstrated by the presence of the flood tidal delta. This is typical of a flood dominant system. This flood-dominant process is accentuated by the existing structure at the Herring River dike, which confines the cross-section to one culvert during the flood tides.
    - Storm events can move sediment upstream of the dike, but only within a limited area due to the restriction to tidal flows caused by the dike.

- Preliminary model results indicate opening the dike may alter the current sediment transport patterns:
    - Velocities are significant enough under normal conditions to initiate movement of sediment
    - Results indicate the possibility for increased sediment transport within the system and that under normal conditions this may tend to move more sand downstream toward the dike.
    - Results indicate a continued trend of upstream sediment transport at the dike, which creates the potential for increased sediment accumulation upstream from the dike, as there could be a convergence of sediment exporting the system with sediment input to the system immediately upstream from the dike.
    - Model simulations suggest a slight seaward transport of sediment downstream from the improved dike opening.

This preliminary, qualitative sediment transport analysis, as well as the review of existing data and studies, revealed the potential for altered sediment transport patterns in the Herring River system if the dike is improved. Based on the relevance of the sediment transport regime to the future health of the marsh, valuable nearby shellfish resources, and overall stability of the coastal beach system, a more detailed sediment transport evaluation was warranted. However, Woods Hole Group did not believe that a fully numerical approach was warranted at this time; rather, an analytical modeling approach, based on the results of the hydrodynamic model and the existing sediment data collected throughout the system was recommended. This recommended approach for the quantitative sediment transport analysis is detailed below.

7.7.2 Characterization of sediments

The analytical sediment transport analysis requires characterization the sediment in the existing system. Understanding the spatial distribution of bottom sediments in the existing system is important in determining how sediment moves in the existing system, as well as how it might move in a more tidally restored system. Grain size data from sediment samples collected between Mayo Beach and High Toss Road (as presented in Section 7.7.1) were used to

characterize sediments in the Herring River estuary. Three sources of sediment grain size data were identified for use in the assessment. These include:

- Surface samples collected for an earlier hydrodynamic modeling study conducted by Spaulding and Grilli (2001)
- Sediment cores collected by the National Park Service in 2009
- Surface samples collected by Harvey (2010)

Surficial sediment samples described by Spaulding and Grilli (2001) were diver collected at 12 locations within the estuary shown in Figure 7-22. Grain size distributions for these samples were determined using standard sieve-pipette methods at the University of Rhode Island, Geosciences Department. The National Park Service collected sediment cores and performed sieve analyses on 9 sediment cores samples at the locations shown in Figure 7-23. Harvey (2010) collected a large number of samples of the top 2 cm of sediment along shore-normal transects at Mayo Beach and in the area just downstream of the dike, as well as samples from the main river channel between Chequessett Neck Road and High Toss Road. Grain size analyses for 285 of these samples were conducted at Wellesley College using laser particle diffraction techniques. The locations of these samples are shown in Figure 7-24. A review of the sediment data and how they vary throughout the existing system is given in the preliminary sedimentation was presented in section 7.7.1.

In preparation for the analytical sediment transport analysis the median grain size (d_{50}) was determined graphically from the grain size distribution of each sample. The median grain size values were then interpolated to the Herring River hydrodynamic model domain grid using an inverse distance weighted interpolation scheme. The interpolated values are shown as colored contours in Figure 7-25. Median grain sizes in the area of interest range from 75 μm to 750 μm representing Wentworth classes of very fine to coarse sand. Only one sample grain size distribution is available for the portion of the estuary above High Toss Road. Values of d_{50} in the area above High Toss Road have been primarily extrapolated from the data below High Toss Road. Although, the sediment transport modeling results could likely be improved with more detailed sediment data upstream of High Toss Road, it is also expected that a majority of the sediment transport changes that will occur in the Herring River system will occur downstream of High Toss Road.

Figure 7-22. Location of surfical sediment samples from Spaulding-Grilli (2001).

Figure 7-23. Locations sediment cores taken by the National Park Service.

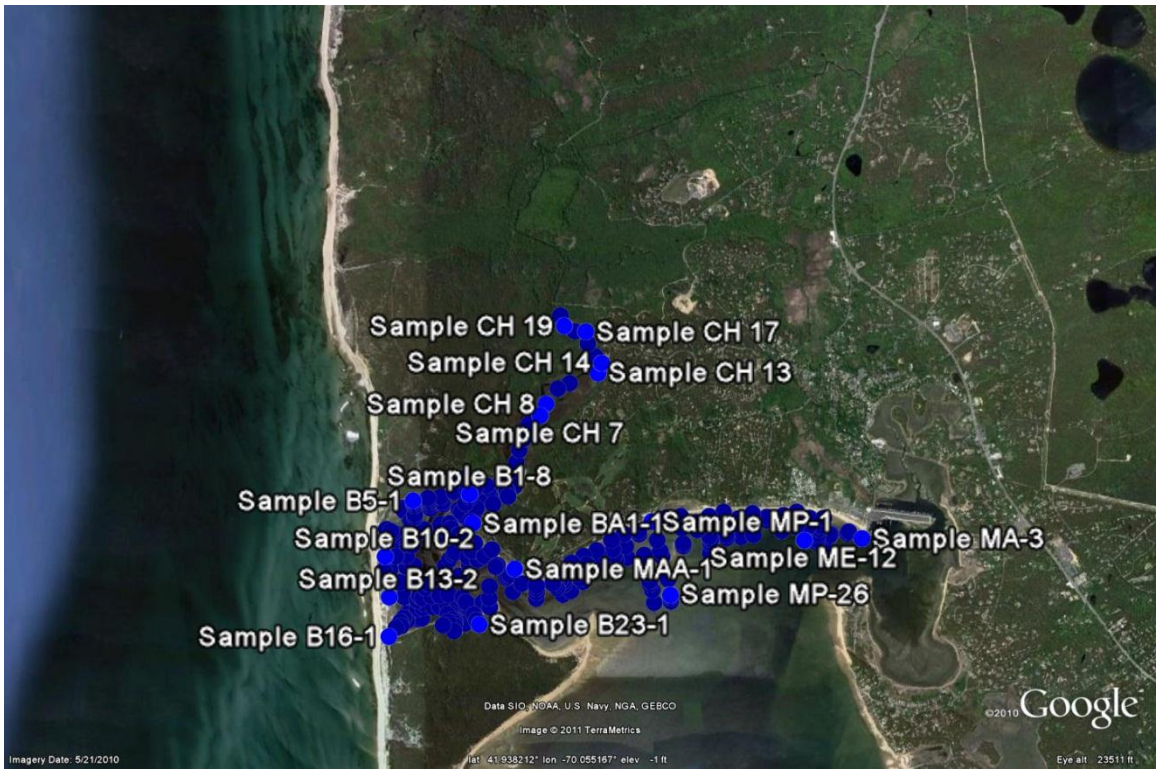

Figure 7-24. Location of surfical sediment samples from Harvey (2010)

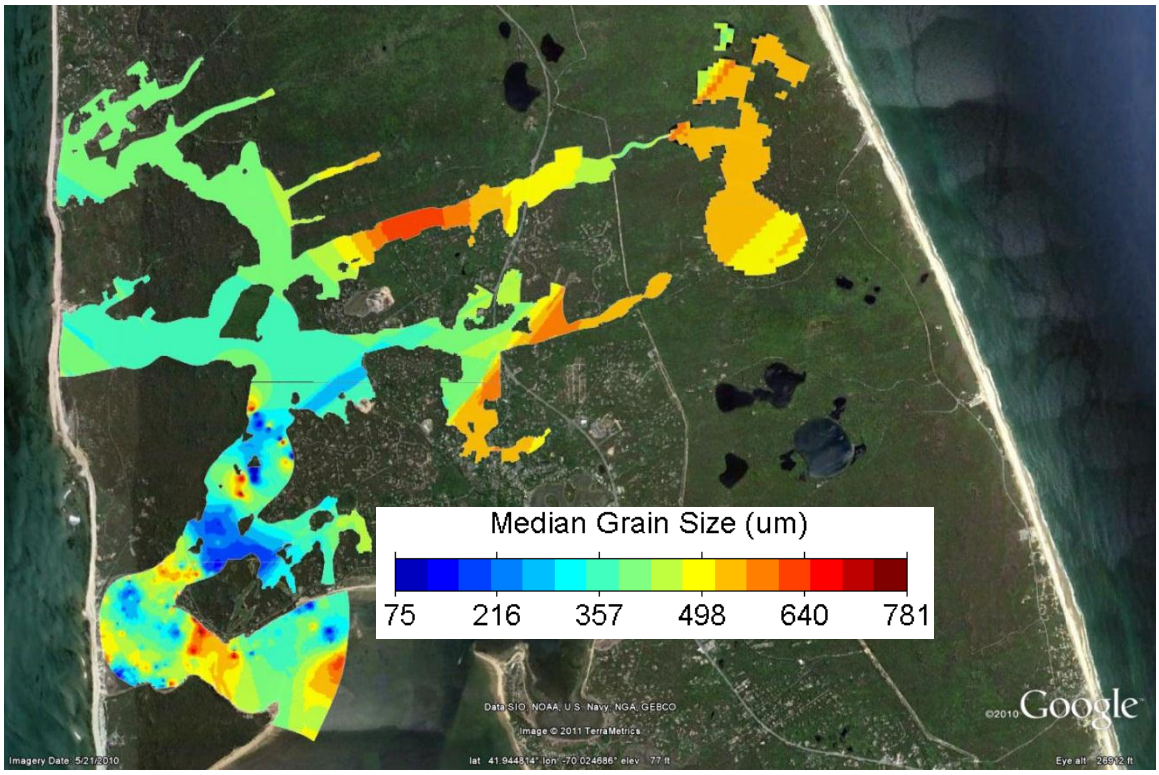

Figure 7-25. Median Grain Size (d_{50}) interpolated to EFDC model grid.

7.7.3 Sediment Transport Theory

The analytical sediment transport model employed for this analysis is based on the established concept that sediments begin to move when sufficient stress is applied to the estuary bottom (bed). Typically, a mild, steady flow over a bed of cohesionless grains will not result in sediment transport (Fredsoe and Deigaard, 1992). However, when subjected to a large enough flow, the driving forces impacting sediment grains exceed the stabilizing forces, and sediment will begin to move. Through dimensional analysis, Shields (1936) derived an expression that identifies the point where bed stress equals bed resistance. The threshold of particle motion is based on a ratio between the driving forces (drag, lift, and buoyant forces) and stabilizing forces (friction and gravitational forces) as seen in Figure 7-26. The Shields parameter (ψ) results from equating the driving and stabilizing forces. For a flat bed:

$$\psi = \frac{\tau_b}{(s-1)\,\rho g\, d_{50}} \tag{7-1}$$

where,

τ_b = bottom shear stress

ρ = density of the water

s = relative density of sediment (≈2.65 for natural sediment)

g = acceleration due to gravity

d_{50} = grain diameter at which 50% of the sediment is finer by weight.

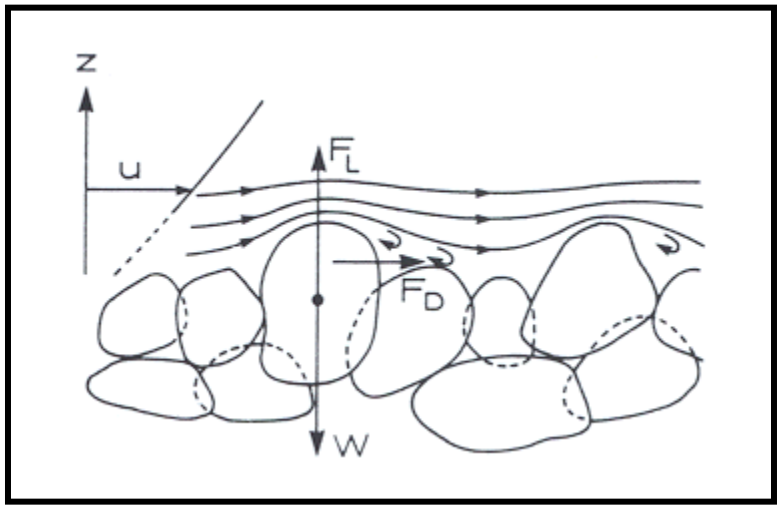

Figure 7-26. Forces acting on grains resting on the estuary bed (Fredsoe and Deigaard, 1992). F_L = lifting force, F_D = drag force, and W = grain weight.

Bottom shear stress (τ_b) is determined from the 2-D hydrodynamic model output of depth and depth averaged current velocity using the logarithmic law of the wall assuming hydraulically rough flow (Kundu and Cohen, 2004). The logarithmic law of the wall expresses the vertical velocity profile as:

$$u = \frac{u_*}{\kappa} \ln\left(\frac{y}{y_0}\right) \tag{7-2}$$

with the friction velocity (u_*) defined as,

$$u_* = \sqrt{\frac{\tau_b}{\rho}} \tag{7-3}$$

and the depth averaged velocity (u_{ave}) defined as,

$$u_{ave} = \frac{1}{h}\int_{y_0}^{h} u dy \tag{7-4}$$

Where,

u = vertical velocity profile

y = vertical coordinate

y_0 = roughness length (y at which u appears to go to zero)

h = water column depth

κ = the Von Karman constant (≈0.41)

Substituting the law of the wall (7-1) in to the definition for depth averaged velocity (7-2) and integrating yields an expression for the depth averaged current velocity in terms of the friction velocity, depth, and roughness length.

$$u_{ave} = \frac{u_*}{\kappa}\left[\ln\left(\frac{h}{y_0}\right) + \frac{y_0}{h} - 1\right] \tag{7-5}$$

Substituting the definition friction velocity (7-2) into (7-5) and rearranging yields an expression for bottom shear stress as a function of the depth averaged current velocity, depth and roughness length.

$$\tau_b = \rho\left(\frac{\kappa u_{ave}}{\ln\left(\frac{h}{y_0}\right) - 1 + \frac{y_0}{h}}\right)^2 \tag{7-6}$$

Once the bottom stress and Shields parameter have been calculated at points of interest, the resulting values are compared to a critical Shields parameter (Ψ_{cr}) to determine if sediment mobilization occurs. The critical value of ψ for the initiation of sediment motion is found by using a methodology to determine the threshold Shields' Criterion, ψ_{cr} (Soulsby, 1997):

$$\psi_{cr} = \frac{0.30}{1+1.2D_*} + 0.055\left[1 - e^{-0.020D_*}\right] \tag{7-7}$$

where D_* is the dimensionless grain size given by:

$$D_* = \left[\frac{g(s-1)}{\nu^2}\right]^{1/3} d_{50} \tag{7-8}$$

where ν is the kinematic viscosity of water.

At locations where the Shields parameter, as determined from Equation (7-1), is greater than the critical Shields parameter, as determined from Equation (7-7), initiation of sediment movement is expected and erosion may occur. Conversely, where the Shields parameter is less than the critical Shields parameter sediment is not expected to move and deposition is possible.

7.7.4 Sediment Transport Potential

Using the criterion presented above, the sediment transport potential was determined for normal tidal conditions and a 100 year extreme storm surge event. Each scenario was simulated for the No Action Alternative, and the restoration alternative with a 165 feet wide culvert span at Chequessett Neck Road with sluice openings of 3 feet. The sediment transport potential is quantified by computing the Shield's parameter in each model grid cell from the flow velocity and depth at 15 minute intervals during the model simulations. The Shield's parameters are then compared to the critical Shields parameters for the sediment size in each model grid cell. The difference between the Shields parameter and the critical Shields parameter is expressed as a percentage of the critical Shields parameter. Values greater than zero indicate the initiation of sediment movement while values less than zero indicate potential deposition. The results are presented using a color scale which transitions smoothly from blue to green indicating decreasing potential for deposition, then from yellow to red indicating increasing potential for erosion. The results indicate areas where the flow has potential to initiate sediment movement. This analysis determines when and where sediment movement can be expected, but it does not track the actual movement of sediment particles. However, general sediment transport pathways can be deduced from the results by considering the mechanisms through which sediments are moved. Once sediment movement is initiated it can be transported by the current. To deduce

sediment transport pathways it is necessary to consider the temporal and spatial variations in sediment transport potential, as well as the direction and duration of the tidal currents. Therefore, the results are presented as series of snapshots with the phase of the tide indicated to differentiate between flood and ebb tidal currents.

For this analysis it is useful to consider three general classes of sediment based on the mode of sediment transport that might be expected. These include: bed load, suspended load, and transport of fines. Bed load consists of sediment particles rolling, sliding, or saltating (i.e. skipping along the bottom while impacting other particles and causing them to move as well). Bed load is typically made up of coarser heaver sediment and sand particles. Suspended load consists of sediment particles that become entrained in the water column during times of high bottom stress but then settle to the bottom when the current velocity and turbulence are reduced (primarily sand particles). For our purposes, suspended load will generally remain in suspension for time scales that approximate a tidal period or less. The mechanism for transport of fines is similar to suspended load, however, fines remain in suspension of time scales significantly greater than a tidal period allowing them to travel large distances (e.g., non-cohesive muds and silts). Furthermore, it is useful to consider the Herring River Estuary system as a series of three separate basins based on the flow regime. These are: the area seaward of Chequessett Neck Road (Chequessett Neck Road), the lower Herring River (i.e. between the Chequessett Neck Road and High Toss Road, and the upper Herring River (i.e. all tributaries and sub-basins upstream of High Toss Road).

7.7.4.1 Normal Tidal Conditions, Existing Conditions

Results from the hydrodynamic model simulation of normal tides for existing conditions were used to determine the sediment transport potential. Figures 7-27 thru 7-31 show instantaneous snapshots the sediment transport potential as it evolves through a normal tidal cycle. A time series of the water surface elevation (tide) output from just below Chequessett Neck Road is included in each figure. A red dot on the time series indicates the time at which the sediment transport potential snapshot was computed. Figure 7-27 shows a snapshot at slack high tide. At this time, initiation of sediment movement is not expected anywhere in the system except in a small area near the existing sluice gate in the Chequessett Neck Road Dike. This is expected since the water velocities will be at their lowest point during the tidal cycle (i.e., water depth is at the deepest and velocities are near zero at a reversing tide). At this point in the tidal cycle, any sediment suspended in the water column would be able to settle to the bottom throughout most of the estuary.

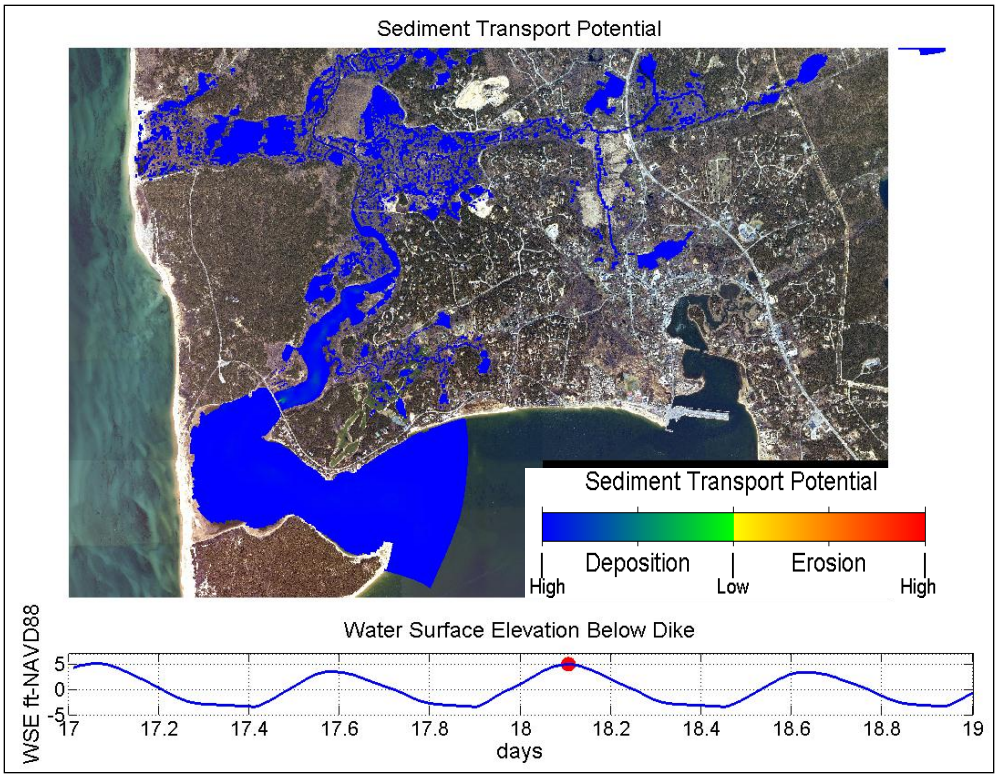

Figure 7-27. Sediment transport potential for existing conditions during a normal high tide; deposition is possible throughout the system.

Figure 7-28 shows the time during the following ebb tide when sediment motion is first initialized in the area downstream of the dike. There is no significant sediment movement in the areas upstream of the dike. Approximately an hour later, the maximum areal extent of possible incipient motion occurs as shown in Figure 7-29, again with no significant movement upstream of the dike. At this time during the tidal cycle, some bed load is expected to slowly be transported (saltated) toward the harbor, while suspended sediment and fines are becoming entrained into the water column.

Shortly thereafter, the tide reverses direction (flooding tide) in the area downstream of the dike. As shown in Figure 7-30, the tide is beginning to flood into the Herring River and initiation of sediment movement and erosion is no longer expected. Some of the coarser fraction of suspended sediment may settle to the bottom (likely in a similar location where it was initially located), while the remainder of the suspended sediment and the fines remain in suspension as the current changes direction.

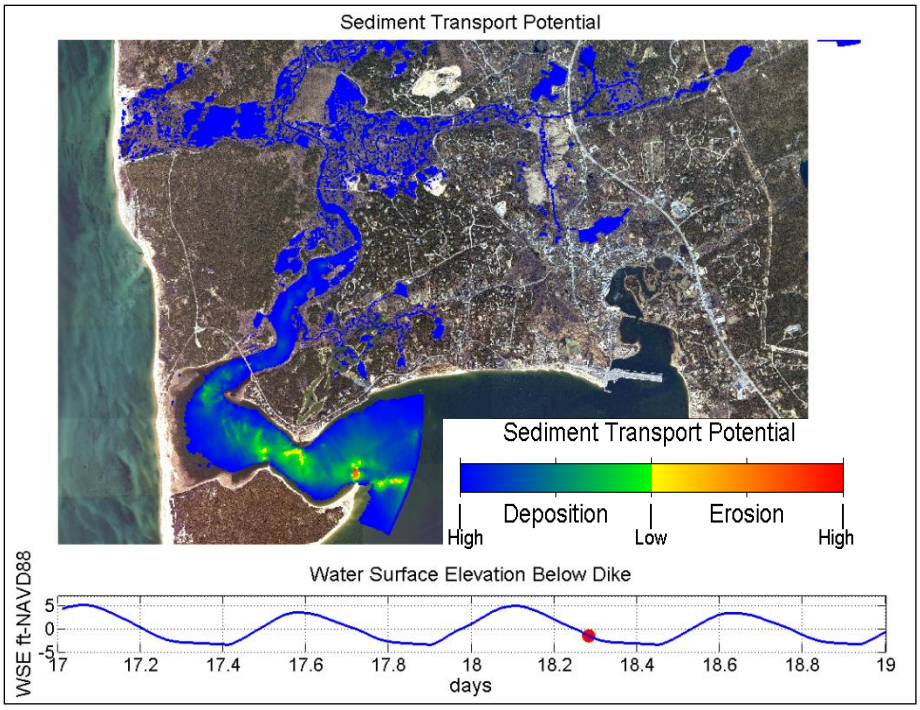

Figure 7-28. Sediment transport potential for existing conditions during a normal ebbing tide; sediment mobilization is initialized.

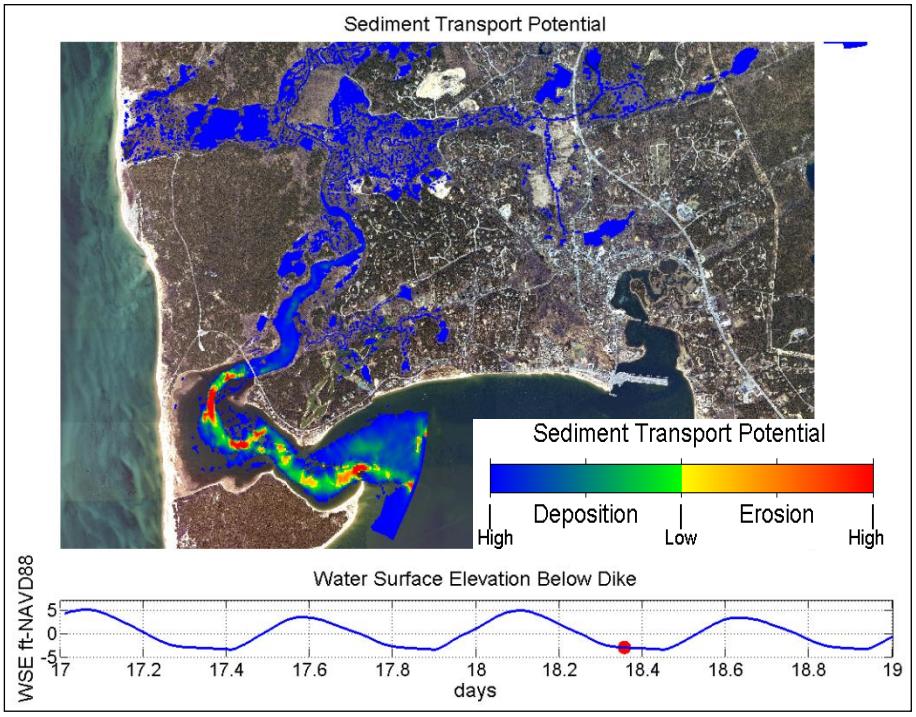

Figure 7-29. Sediment transport potential for existing conditions during a normal late-ebbing tide; maximum area of sediment mobilization occurs due to the shallow water depths.

Figure 7-31 shows the sediment transport potential during a flood tide. During a flooding tide, the increasing water depth results in incremental decreases in the bottom stress. As a result, significant entrainment of bottom sediments downstream of the dike is not expected during the remainder of the tidal cycle. However, the flood tide currents are still relatively strong and turbulent during the flooding tide and thus continue to carry suspended load and fines upstream. Subsequently, during the slack high tide (Figure 7-27), suspended load can settle after being transported upstream during the flood tide. The general trend of upstream sediment transport under existing conditions is exhibited by the large flood tidal shoal that has developed just upstream of the Chequessett Neck Road dike.

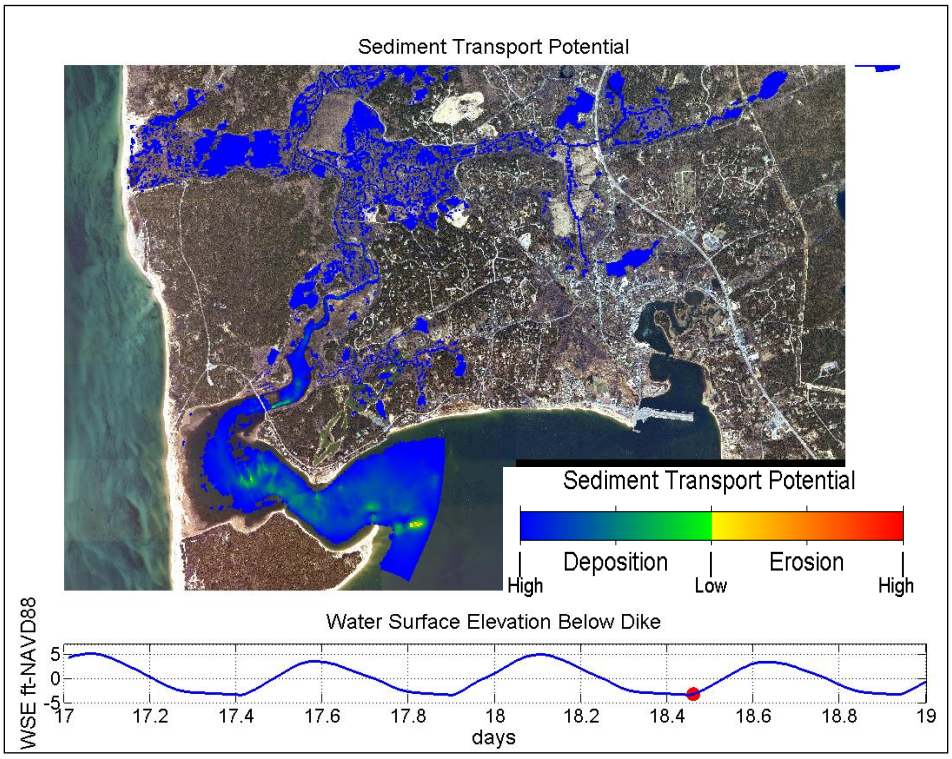

Figure 7-30. Sediment transport potential for existing conditions during a normal low slack tide; the current begins to change direction.

In addition, under existing conditions, increased tidal asymmetry imposed by Chequessett Neck Road dike reduces the total volume of water and suspended sediment that can physically be transported into the lower Herring River. Any suspended sediment that does pass through the sluice gate will quickly settle out because flood tide currents in the lower Herring River are severely reduced by the dike (again, supported by existence of the large flood tide shoal in that is present in the existing system). The dike also causes a significant reduction in the flood tide current velocity in the area downstream of the dike. This reduction in current velocity likely deposits a portion of suspended sediment in the upper region of the area downstream of the dike during the relatively long slack flood tide. This may be expected to change during restoration alternatives that increase the opening of the dike. Fine-grained material that becomes mobilized most likely remain entrained and ultimately become mixed with water in Wellfleet Harbor during the ebb tide. Although some fines may settle to the bottom in vegetation near the fringes

of the system during high tide, it is likely that most fines make their way out of the estuary and into the larger Wellfleet Harbor and Cape Cod Bay.

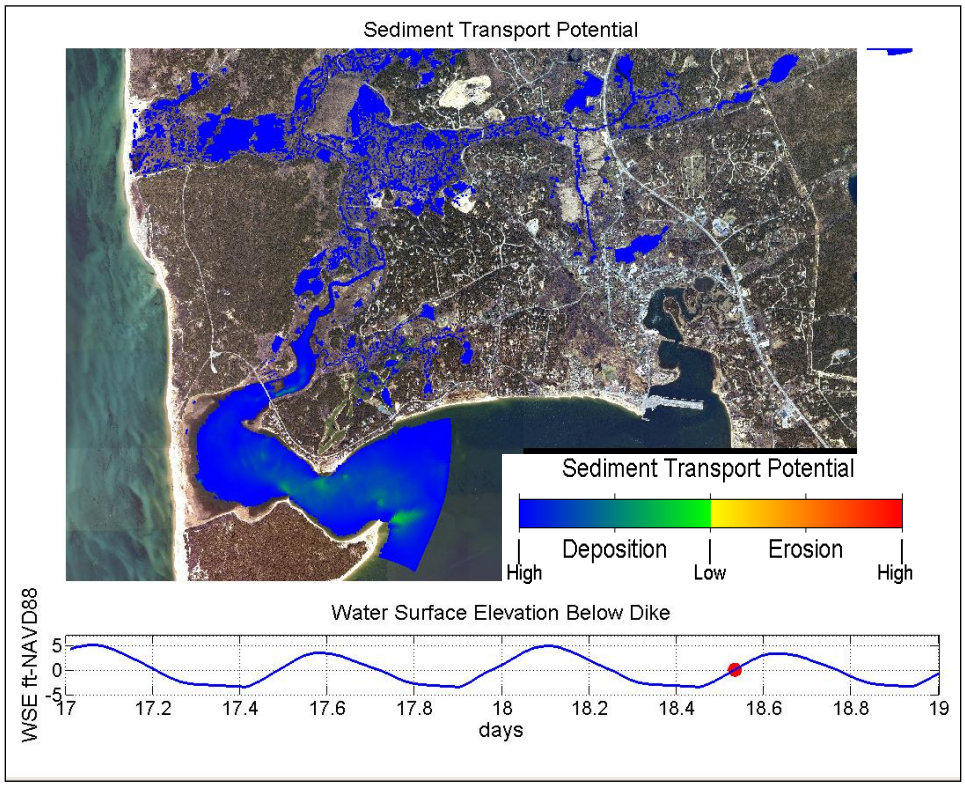

Figure 7-31. Sediment transport potential for existing conditions during a normal mid-flood tide; suspended sediment is transported up the river if it can make it through the existing dike opening.

7.7.4.2 Normal tidal conditions, 3 foot sluice opening with new dike

Hydrodynamic model results of normal tides for a new 165 foot dike opening with a 3 foot sluice opening were also used to compute sediment transport potential. Figures 7-32 through 7-36 show a series of snapshots of the sediment transport potential as it evolves through a normal tidal cycle. A time series of the water surface elevation output from just below Chequessett Neck Road is included in each figure. A red dot on the time series indicates the time at which the sediment transport potential snapshot was computed. Under these conditions, there is more significant sediment mobilization upstream of the Chequessett Neck Road dike due to the increase tidal flux passing through the new dike opening. This produces a widening of the tidal channels and creeks throughout the system, as shown by the erosional areas in the channels indicated in the snapshots by the red and yellow zones. The areas downstream of the dike also show some increased erosional areas due to the increased tidal flus into and out of the Herring River system.

Figure 7-32 shows the sediment transport potential when it is high tide near Chequessett Neck Road. At this point in the tidal cycle, due to the phase lag in the system, water is still flooding

into the upper portions of the estuary and there is some potential for upstream estuary sediment mobilization and transport in Mill Creek and the upper Herring River. As the tide approaches slack high throughout the estuary, suspended sediment can potentially deposit in the depositional zones (blue areas) shown in the system. Figure 7-33 shows a snapshot of the sediment transport just as the ebbing tide begins to initiate sediment mobilization. Initially the greatest potential for sediment movement is in lower Herring River just above Chequessett Neck Road. As the water level in the Wellfleet Harbor continues to lower and ebb velocities increase, the area of potential sediment mobilization increases to include the area downstream of the dike and a larger area in the Lower Herring River.

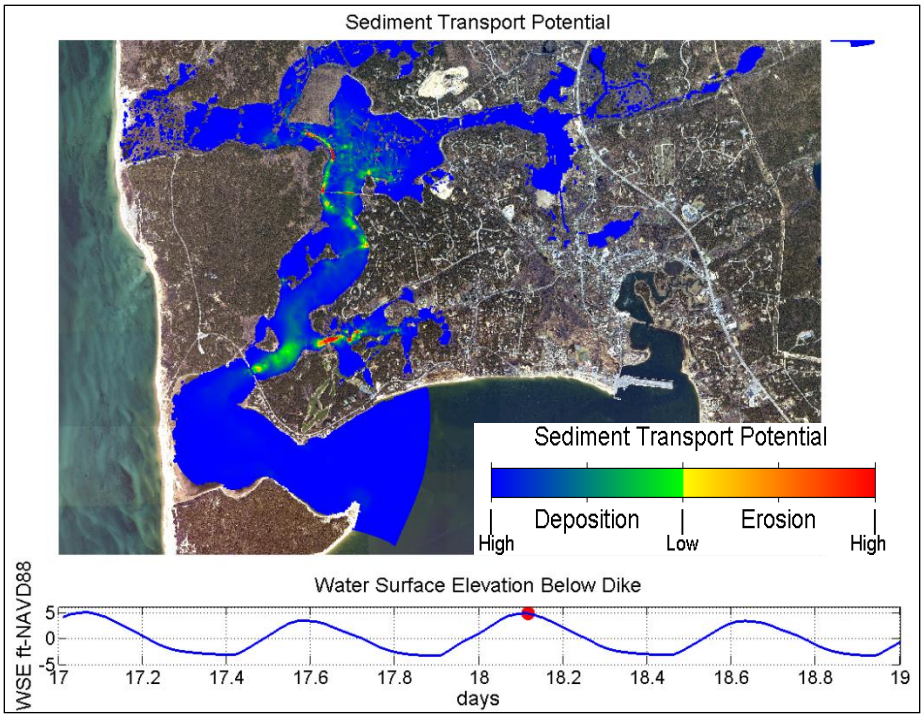

Figure 7-32. Sediment transport potential for 3 foot opening during a normal high tide; deposition is possible in the upper portions of the system in the blue zones.

Figure 7-34 shows the greatest area of potential mobilization of sediment, which occurs towards the end of an ebb tide. At this point in the tidal cycle, the current is flowing toward the harbor and any mobilized sediment would also be moving toward the harbor. However, as shown Figure 7-35, the tide changes direction relatively quickly and suspended sediment would begin to be transported upstream. Bedload traveling seaward stops and some of the heavier suspended sediment particles may be deposited on the bottom, but sediment remaining in suspension would be transported back up estuary with the next flood tide. As the flood flow increases, the area just upstream of the Chequessett Neck Road Dike becomes potentially mobilized again, with transport upstream, as shown in Figure 7-36. Any suspended sediment entering this area would likely pass through the dike and lower Herring River and become deposited farther up in the estuary during the following high tide slack (Figure 7-32).

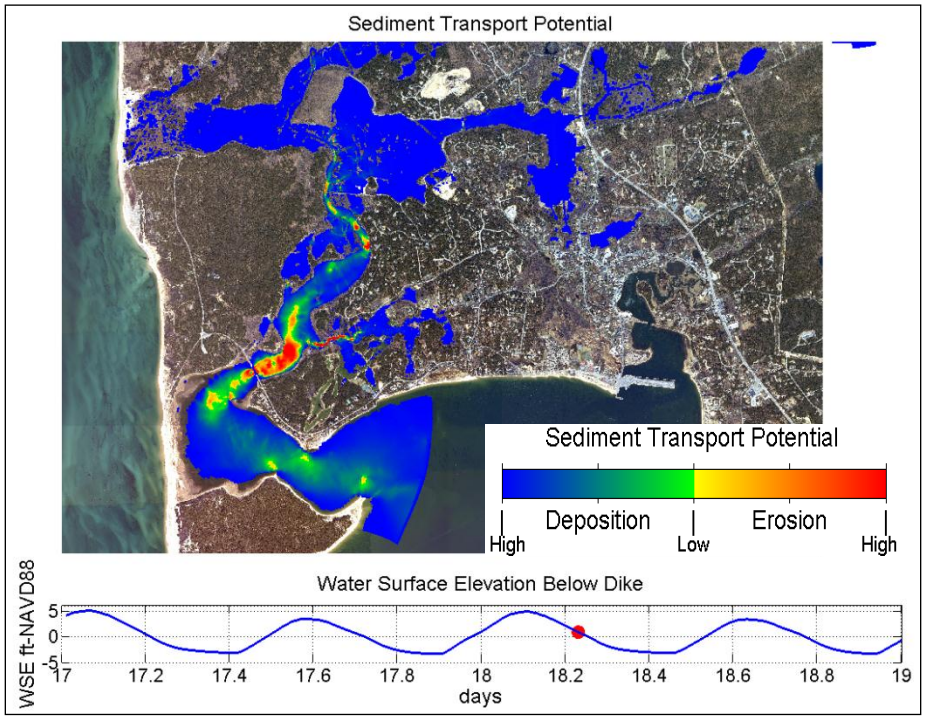

Figure 7-33. Sediment transport potential for 3 foot opening during an ebbing tide; sediment mobilization begins in the lower Herring River.

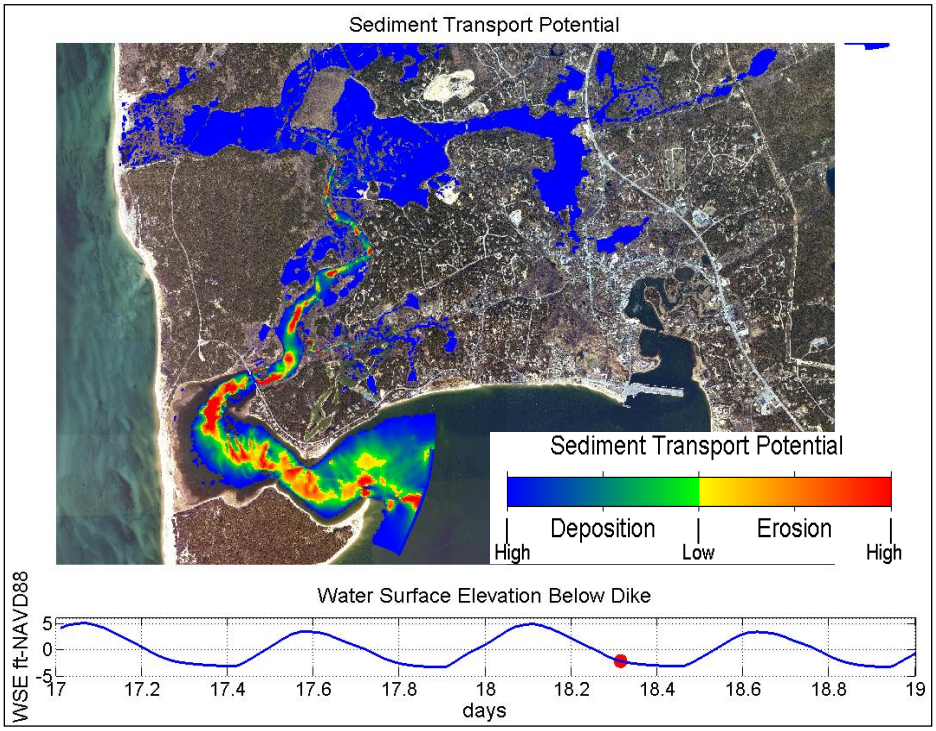

Figure 7-34. Sediment transport potential for 3 foot opening during a late ebbing tide; maximum area of potential transport occurs.

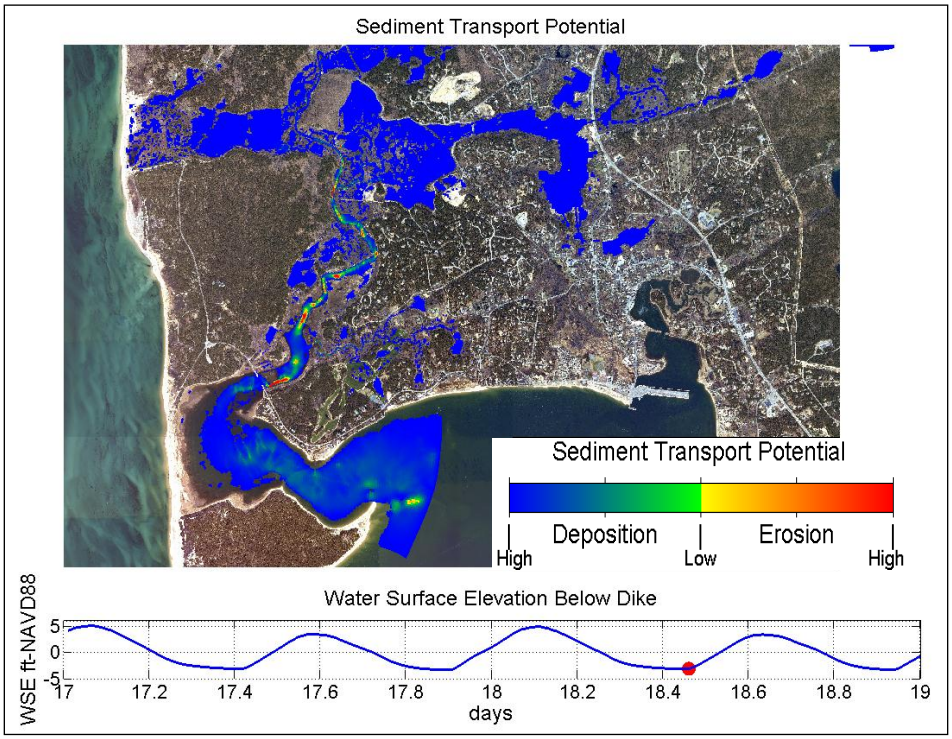

Figure 7-35. Sediment transport potential for 3 foot opening at low tide; tidal reversal in Wellfleet Harbor.

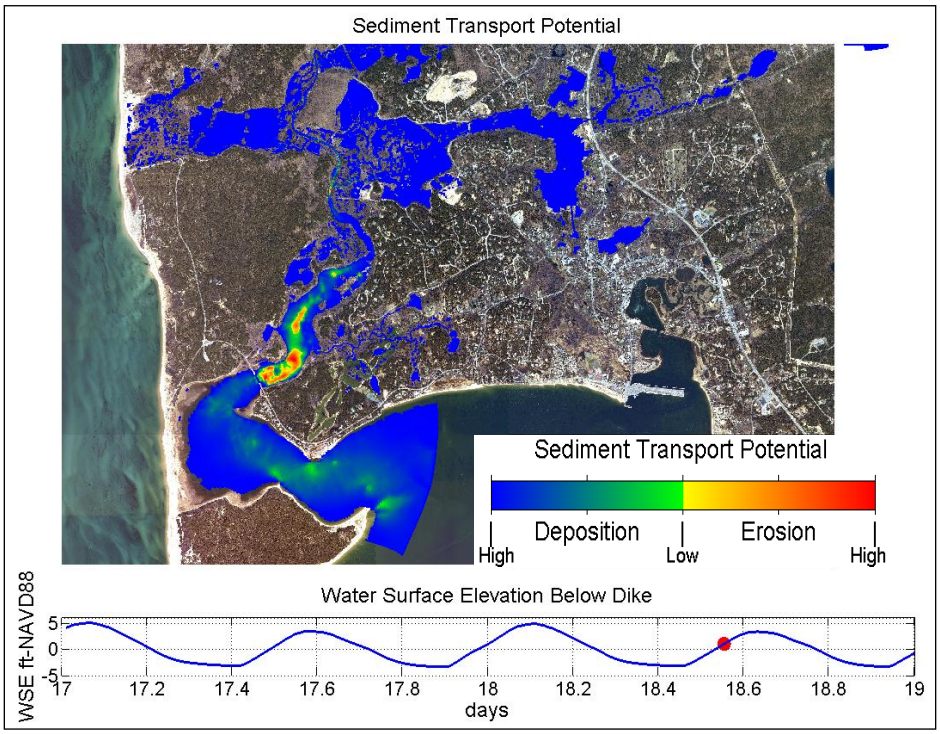

Figure 7-36. Sediment transport potential for 3 foot opening during flooding tide; upstream transport occurs in the lower Herring River.

Areas of potential sediment mobilization were quantified to provide a means for comparison of the alternatives. The total area of potential mobilization was computed by summing the area where the sediment transport potential indicates mobilization at least once during the normal tides simulations. Separate totals were computed for the areas above and below Chequessett Neck Road. The results are presented in Table 7-9. This analysis does not directly quantify the movement of sediment. Therefore, it cannot determine areas or volumes of potential erosion. However, because erosion can only occur in areas where sediment is mobilized the areas listed in Table 7-9 can be taken as a highly conservative upper limit on the potential area of erosion. The areas of deposition, which are much larger than the erosional areas, are not shown in the table, since their change is simple reduced by the increased erosional areas.

When compared to existing conditions, the 3 foot opening shows similar pathways for sediment transport in the areas downstream of the dike. Generally, bed load is expected to move slightly seaward or remain in the same location, while a majority of the suspended sediment will ultimately be transported farther upstream into the estuary. For the 3 foot opening conditions, this general process is expected to increase, with potential bed load transport extending from the lower Herring River to the area downstream of the dike, while and increased sediment load of suspended sediments would make their way upstream past Chequessett Neck Road during flood tides. Over time, these processes would likely lead to a coarsening of the sediment in the area downstream of the dike, particularly in the area near the new proposed Chequessett Neck Road dike.

Table 7-9. Total area of potential sediment mobilization (erosional area) during normal tides (in acres).

	No Action Alternative	3 foot opening	10 foot opening
Above Chequessett Neck Road dike	0.1	41.8	57.5
Below Chequessett Neck Road dike	55.7	102.2	98.1

Under existing conditions, there is minimal sediment transport occurring in the Herring River system (upstream of the dike); however, with the new dike opening, potential sediment transport in the lower Herring River during both the flood and ebb tides will begin to occur. Initially, this is likely to lead to some transport of fine-grained material out of the lower Herring River that will not easily settle and be transported into Cape Cod Bay and possibly dispersed within Wellfleet Harbor. In addition, a significant portion of this material would be transported into the subsided, upper portions of the estuary due to asymmetry in the tidal current and trapping by vegetation. The upper Herring River remains primarily a depositional environment with the exception of the area near High Toss Road during the flooding tide. Considering the greater volume of sediment that is able to enter the upper Herring River, it is likely that 3 foot opening will lead to significant deposition of suspended sediment and fines in the upper estuary, specifically in lower lying areas that have historically subsided.

7.7.4.3 100-year Storm Surge, Existing Conditions

Existing conditions hydrodynamic model results from the simulation of a 100-year storm surge event were used to compute sediment transport potential. Figures 7-37 through 7-41 show a series of snapshots of the sediment transport potential as it evolves through a tidal cycle that coincides with the peak of the storm surge. Figure 7-37 shows the sediment transport potential just as the storm tide begins to enter the area just downstream of the dike. At this time, there is a large area of potential transport in the area just downstream of the dike and sediment would be mobilized and transported upstream towards and potentially beyond Chequessett Neck Road (if the material can make it past the existing dike).

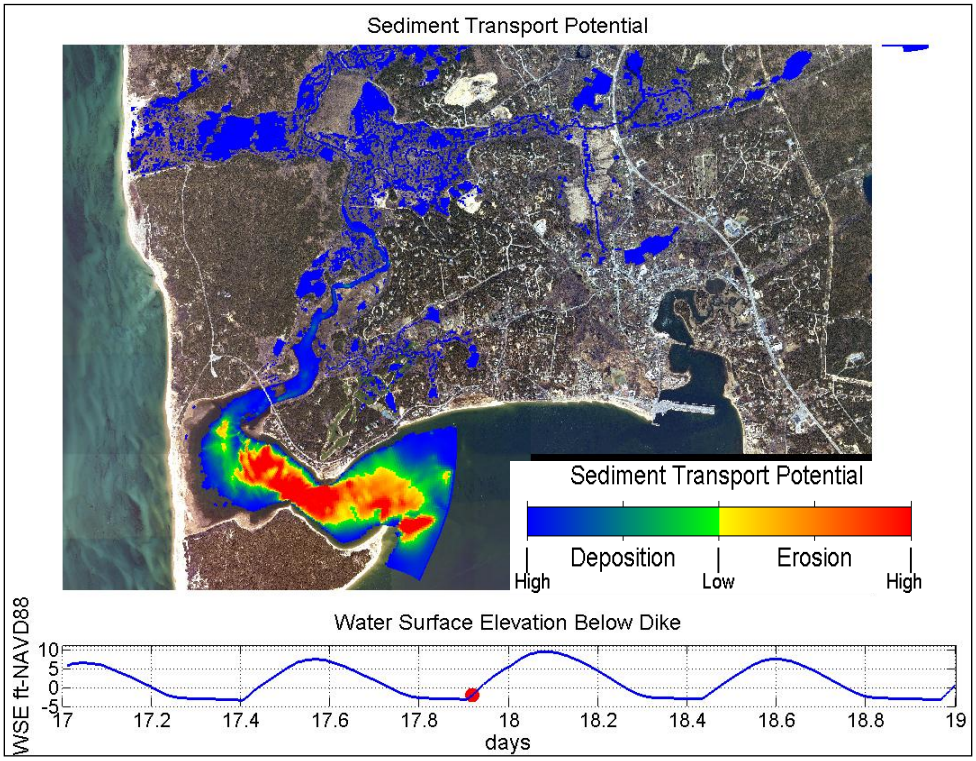

Figure 7-37. Sediment transport potential for existing conditions at the start of a 100-year storm surge.

Figures 7-38 through 7-40 show the sediment transport potential within the Herring River system during the passage of the 100-year storm. During these three snapshots, there is potential deposition throughout the entire system due to the increased water depth throughout. Sediment transport that was initiated during the initial influx of storm water carries sediment upstream into the system and this suspended sediment would begin to settle and deposit in the upstream portions of the system. However, it is likely that under existing conditions a significant amount of material does not make it past the existing dike. As such, only a small fraction of suspended sediment would likely travel through the sluice gate and be deposited in the lower Herring River.

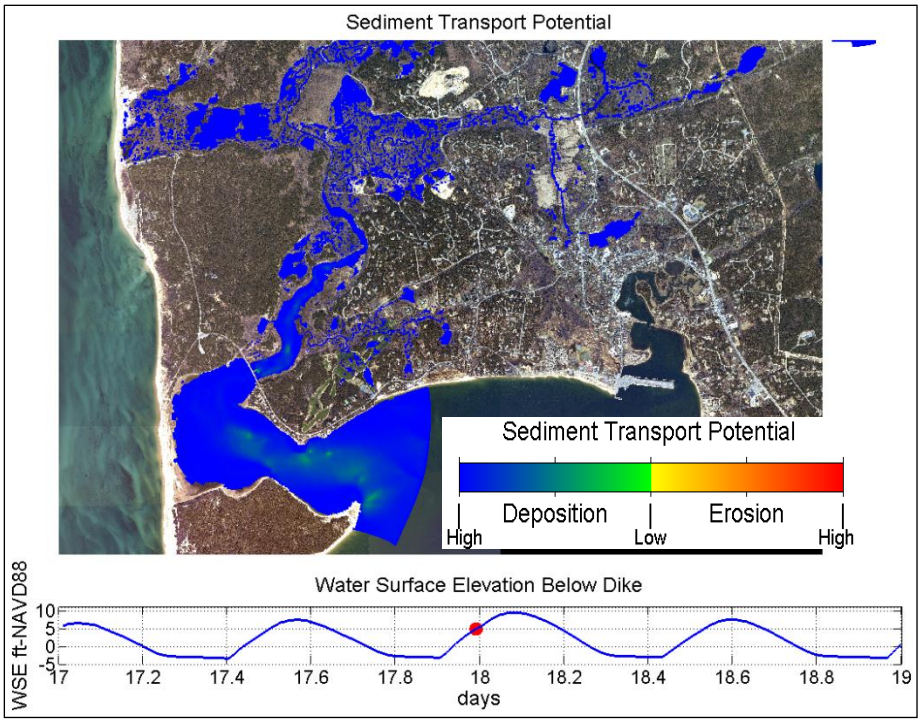

Figure 7-38. Sediment transport potential for existing conditions during the passage of the 100-year storm surge.

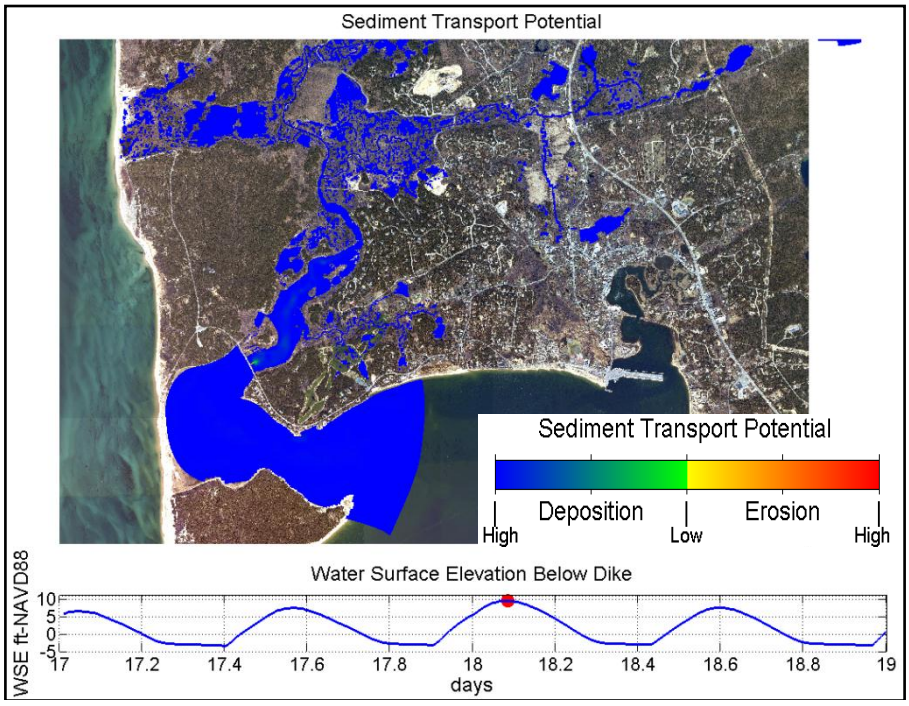

Figure 7-39. Sediment transport potential for existing conditions during the passage of the 100-year storm surge.

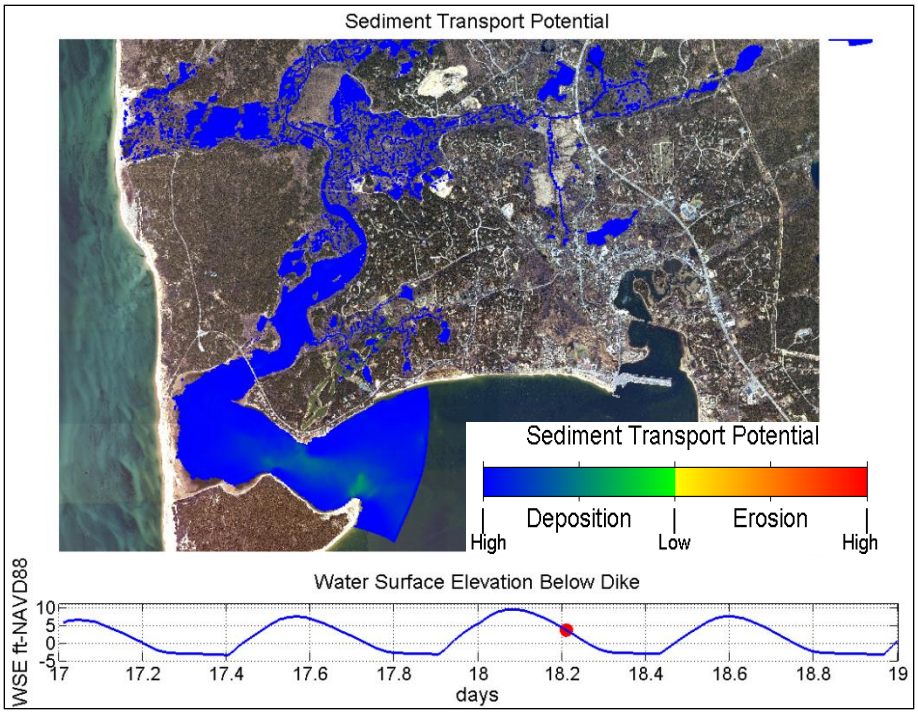

Figure 7-40. Sediment transport potential for existing conditions during the passage of the 100-year storm surge.

As the surge recedes, the transport potential again shows possible mobilization in the area downstream of the dike (Figure 7-41). However, it is likely that this material may have already been scoured during the incoming storm surge and will not be scoured significantly more during the receding storm. This erosional area appears in the analytical model since this approach does not include a dynamic bed (e.g., the topography and bathymetry remains fixed). As such, the model indicates there may be erosion in this area when in reality this area had already been significantly deepened during the initial influx of the storm tide and may not erode significantly more. Overall, the storm surge is not expected to cause significant mobilization of sediment in the lower or upper Herring River. Although more suspended sediment would be carried above Chequessett Neck Road than during normal tidal conditions. The area just downstream of the dike shows the greatest potential mobilization, which may occur in both directions (upstream and downstream). The results show a larger area of potential mobilization during the rising surge suggesting a net up estuary transport bed load and coarser suspended sediment. Fines entrained during the surge would likely make their way out of the system and ultimately become dispersed in Cape Cod Bay.

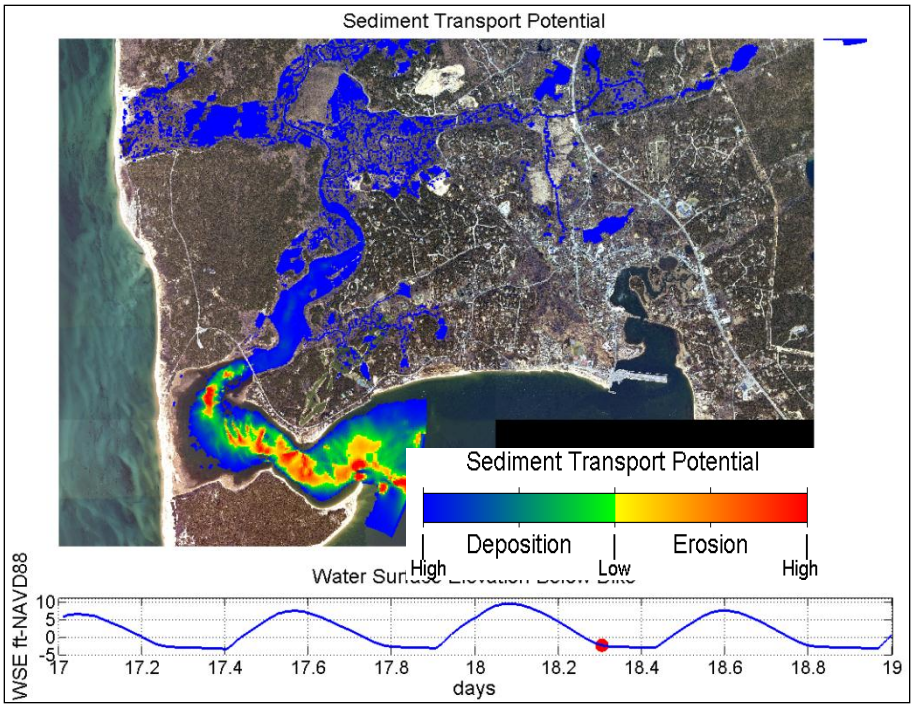

Figure 7-41. Sediment transport potential for existing conditions as the 100-year storm surge recedes.

7.7.4.4 100-year Storm Surge, 3 foot sluice opening with new dike

Hydrodynamic model results from the simulation of a 100-year storm surge event for 3 foot opening were used to compute sediment transport potential as well. Figures 7-42 thru 7-46 show a series of snapshots of the sediment transport potential as it evolves through the passage of a 100-year storm surge. Figure 7-42 shows the sediment transport potential as the storm tide begins to enter the area just downstream of the dike. At this time, flow is still ebbing from the upper Herring River and low tide is occurring in the lower Herring River just above Chequessett Neck Road. Potential for upstream sediment transport occurs in the area downstream of the dike. Figure 7-43 shows the storm surge starting to fully enter the Herring River system and suspended sediments are transported upstream while sediment initialization ceases in the area downstream of the dike. In the lower Herring River, additional sediment is mobilized as the storm surge propagates into the system. Suspended sediments entering the area from the area downstream of the dike would remain suspended as they are transported into Mill Creek and the upper Herring River. Figure 7-44 shows the sediment transport potential as the surge peaks in Wellfleet Harbor. At this stage, the surge is still flowing into the upper portions of the Herring River estuary, and a large area near High Toss Road has started to mobilize/erode. Sediments mobilized in the lower Herring River and lower portion of the upper Herring River will potentially be deposited farther up in the estuary. Figure 7-45 shows the sediment transport potential as the surge begins to recede in Wellfleet Harbor. At this time the peak surge is occurring in the upper Herring River and deposition of all the mobilized sediments will be occurring throughout most of the estuary.

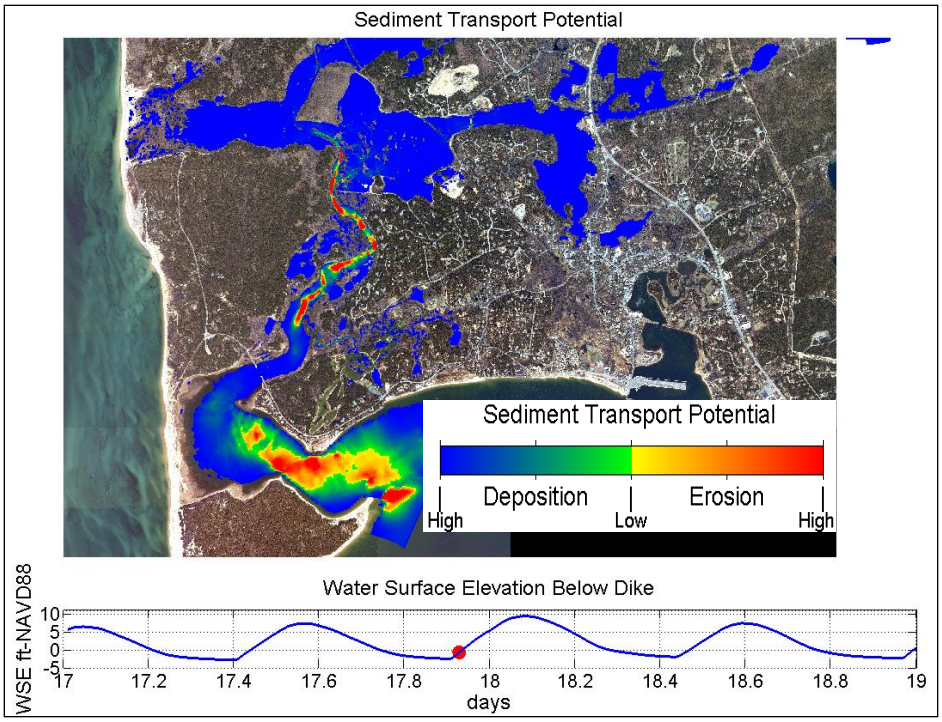

Figure 7-42. Sediment transport potential for 3 foot opening opening at the beginning of the 100-year storm surge.

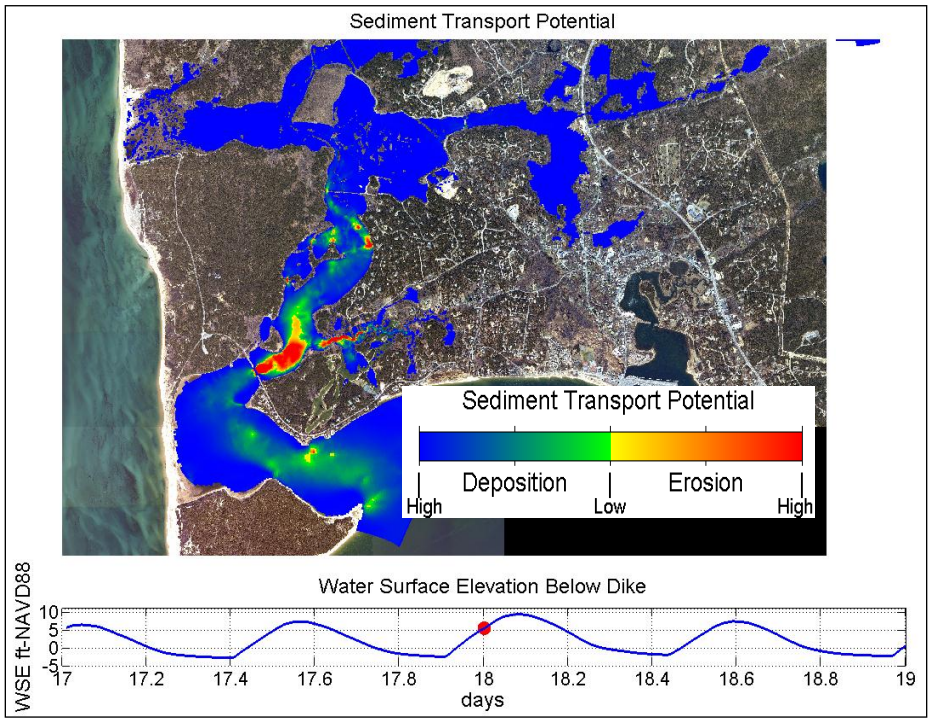

Figure 7-43. Sediment transport potential for 3 foot opening opening at mid-flood for the 100-year storm surge.

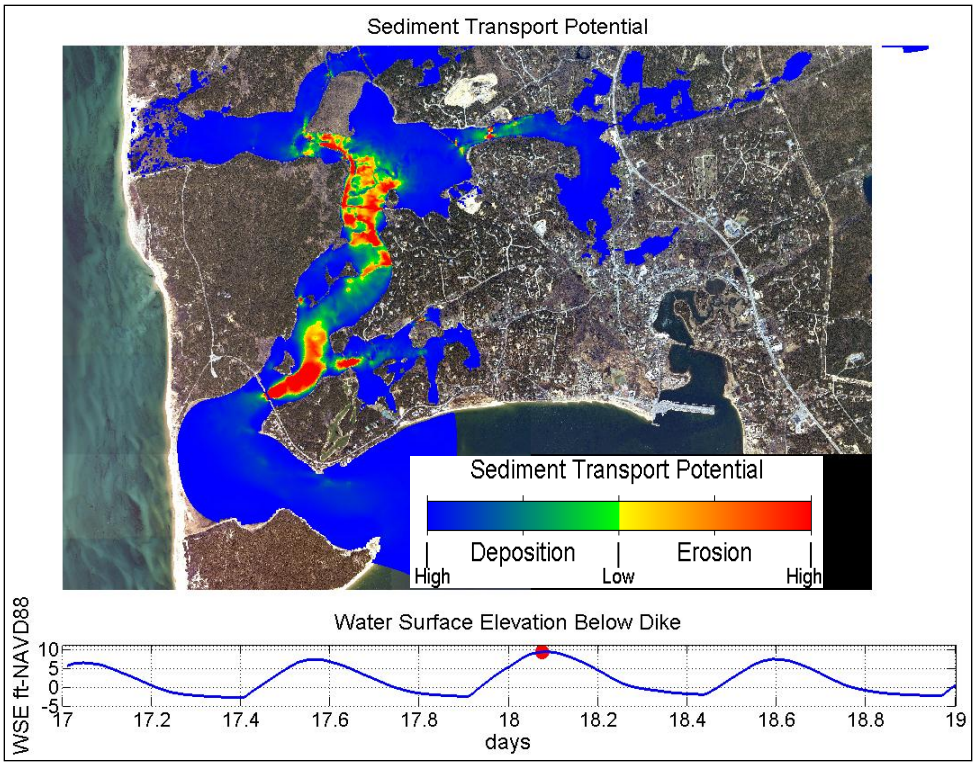

Figure 7-44. Sediment transport potential for 3 foot opening opening as the 100- year surge peaks in the area just downstream of the dike.

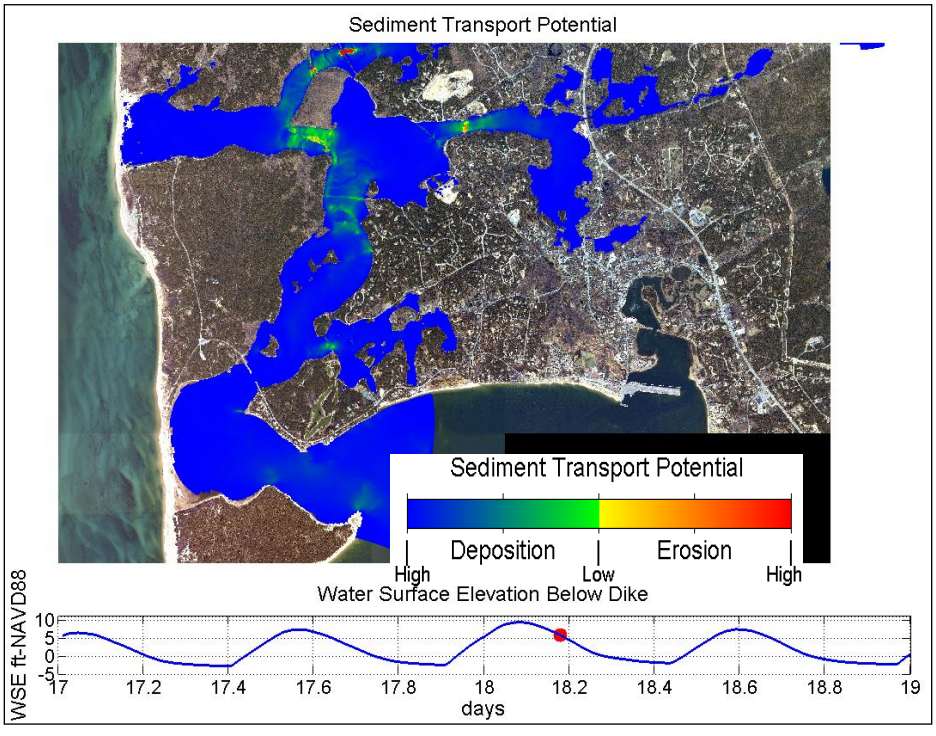

Figure 7-45. Sediment transport potential for 3 foot opening opening as the 100- year surge peaks in the upper estuary.

Figure 7-46 shows time with the greatest area of potential mobilization as the surge recedes. At this time significant seaward mobilization is occurring in the lower Herring River and the area downstream of the dike. However, it is likely that this material may have already been scoured during the incoming storm surge and will not be scoured significantly more during the receding storm. As for existing conditions, this erosional area appears in the analytical model since this approach does not include a dynamic bed (e.g., the topography and bathymetry remains fixed). As such, the model indicates there may be erosion in this area when in reality this area had already been significantly deepened during the initial influx of the storm tide and may not erode significantly more. Overall, the storm surge delivers a significant amount of sediment upstream into the system; significantly more than during normal tidal conditions.

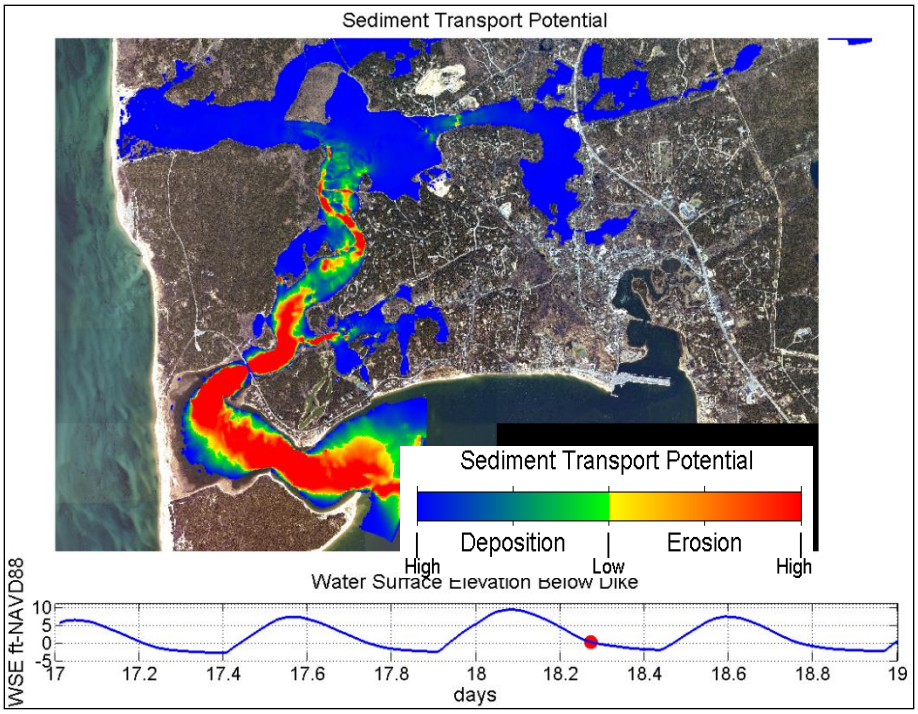

Figure 7-46. Sediment transport potential for 3 foot opening opening as the 100-year storm surge recedes.

Areas of potential sediment mobilization were quantified to provide a preliminary means of comparing the alternatives. The total area of potential mobilization during the 100-year storm surge was computed by summing the area in which the sediment transport potential indicates mobilization at least once during the simulation. Separate totals were computed for the areas above and below Chequessett Neck Road. The results are presented in Table 7-10. This analysis does not directly quantify the movement of sediment. Therefore, it cannot determine areas or volumes of potential erosion. However, because erosion can only occur in areas where sediment is mobilized the areas listed in Table 7-10 can be taken as a highly conservative upper limit on the potential area of erosion.

Table 7-10. Total area of potential sediment mobilization during 100-year storm surge (in acres).

	No Action Alternative	3 foot opening	10 foot opening
Above Chequessett Neck Road Dike	0.1	132	217
Below Chequessett Neck Road Dike	153	217	230

Qualitatively, sediment transport pathways in the area downstream of the dike are similar for both existing conditions and the restoration alternatives. However, because the Chequessett Neck Road dike severely restricts flow in the upstream reaches for existing conditions, a significantly smaller volume of water enters the estuary during the 100-year storm surge when comparing current conditions to proposed restorations. For existing conditions, there is practically no sediment mobilization above Chequessett Neck Road even during the 100-year storm surge. However, there will be a moderate increase of suspended sediment entering the lower Herring River and being deposited during a storm event when compared to normal tidal conditions. For the 3 foot opening, storm surge simulations indicate a significant mobilization of sediment in both the lower Herring River, as well as in the lower portion of the upper Herring River near High Toss Road. Significantly greater mobilization and erosion exists at the area near High Toss Road as the storm surge floods into the upper estuary and transports sediment upstream into depositional areas (primarily subsided regions). Downstream of High Toss Road, it is likely that bed load will be moved in both directions resulting in little net movement. Some sediment suspended during the flooding storm tide will likely deposit in areas of the estuary that are not typically flooded during normal conditions. As the surge recedes fines that are not deposited in the upper estuary will proceed toward the dike. Some of this sediment may make it into Wellfleet Harbor and become dispersed before following tide brings it back into the estuary or it is carried into Cape Cod Bay.

7.7.5 Additional Sediment Transport Considerations

Sediment transport processes are expected to change when the Herring River system is restored. In addition to the analysis presented within this section, some additional considerations related to sediment transport include:

- Since the proposed restoration will be progressed through an adaptive management approach, the results presented herein for the 3 foot sluice opening at the new dike represent a more drastic change than will occur in reality. It is expected that the changes to the sediment transport regime will occur over smaller incremental steps (via incremental opening of the sluice/slide gates) with the end goal (after a number of years) being the 3 foot opening. As such, the sediment transport changes and amount of sediment transported will be less than is indicated in the modeling, which represents a significant opening size immediately after construction of a new dike. In addition, results from a 10 foot sluice opening are not presented since the topography and bathymetry of the system are expected to change significantly as the system adapts to the incrementally larger dike openings through time. With the adaptive management approach, the changes

in the topography will be so significant that the quantitative results of the 10 foot sluice opening simulations using existing topography may have reduced accuracy.

- To further illustrate the net upstream sediment transport that is expected to occur once the new dike is in place and is initially opened, the pathway of a suspended sediment particle was tracked through a complete tidal cycle. Figure 7-47 shows the results of the suspended particle tracking that was initially mobilized in the High Toss Road region. The color of each dot represents the age of the suspended particle, progressing from blue (start of tracking) to red (end of tracking and 1 complete tidal cycle). The suspended particle is transported downstream during the ebb tide, but then returns upstream during the flood tide and settles in a position further upstream than where it originally started. If mobilized on the subsequent tide, it would be transported further upstream over the next full tidal cycle until it deposits in an area that is always depositional throughout the entire tidal cycle.

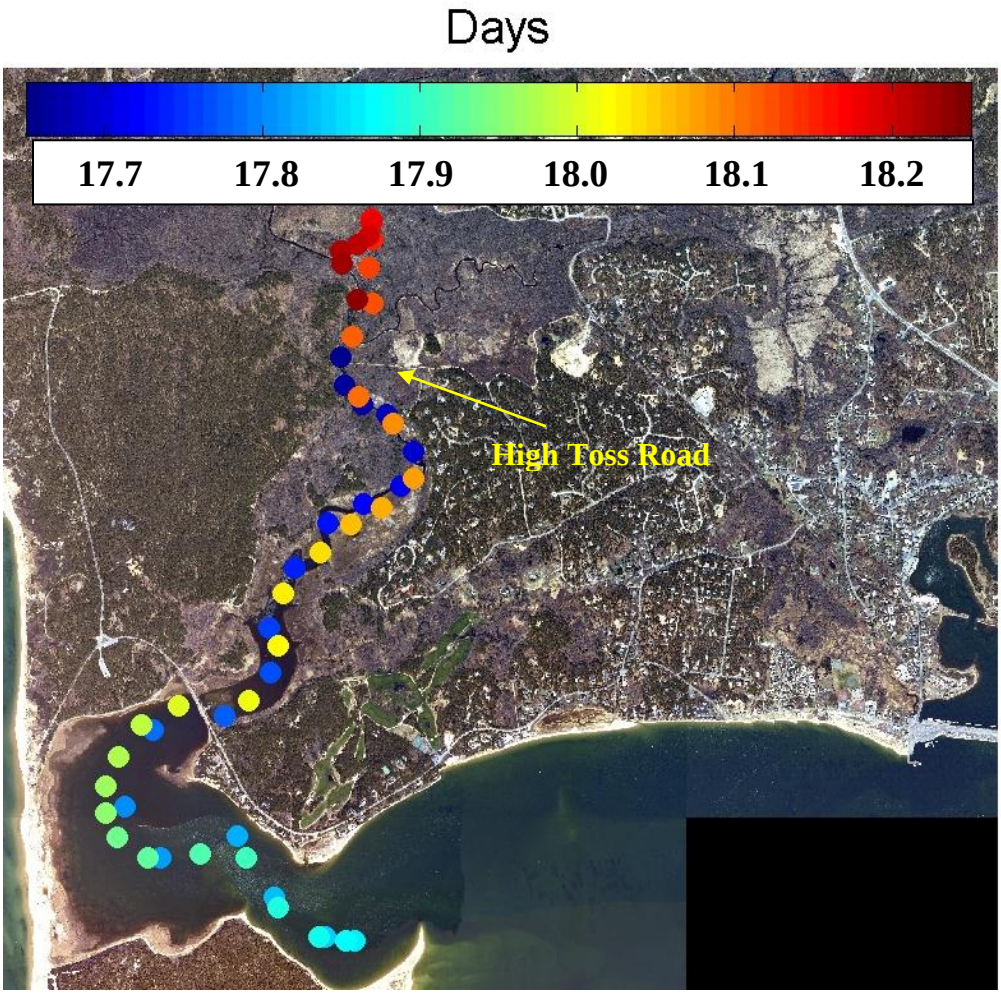

Figure 7-47. Suspended sediment particle tracking through a complete tidal cycle. The particle was initialized at High Toss Road during an ebb tide.

- Significant and valuable shellfish aquaculture exist in Wellfleet Harbor and there are concerns that the proposed restoration may result in smothering of these resources areas with sediment discharged from the Herring River system due to the increased tidal exchange. It is expected that when the system is initially opened, some fine grain material will be likely transported downstream into the Wellfleet Harbor area. Over the long-term however, sediment will be transported upstream into the Herring River system. In addition, the amount of sediment deposited in the Wellfleet Harbor area is not expected to be significant. The adaptive management approach of the proposed opening at the Chequessett Neck Road dike will limit the total amount of material mobilized and a significant portion of the fine grained material may stay in suspension to areas seaward of Wellfleet Harbor. Additionally, the total volume of sediment mobilized from within the Herring River system is small compared to the area of Wellfleet Harbor. For example, if it is assumed that (1) all sluices are immediately opened to 3 feet (e.g., no adaptive management), (2) all sediment mobilized is transported downstream and deposited in Wellfleet Harbor, and (3) the depth of erosion for all mobilized areas is 1 foot, then the total thickness of sediment deposited in Wellfleet Harbor would be less than 1 cm (approximately 0.76 cm). As such, even using conservative assumptions, the potential sediment deposition thickness is minimal.

8.0 REFERENCES

Akcelik, V., B. Jaramaz, and O. Ghattas. 2001. Nearly Orthogonal Two-Dimensional Grid Generation with Aspect Ratio Control. J. Comp. Phys. 171, 805-821.

Beskenis, J.L. and R.M. Nuzzo. 1984. Herring River Survey, August 15-17, 1984. Massachusetts Division of Water Pollution Control (MDWPC), #13,700-38-50-7-84-C.R. 35 p.

Brunner, G.W. 2002. HEC-RAS River Analysis System Hydraulic Reference Manual. Hydraulic Engineering Center, Davis CA.

Chow, V. T. 1959. Open-Channel Hydraulics. The McGraw-Hill Book Company, Inc.

Dougherty, Amy J. 2004. Sedimentation Concerns Associated with the Proposed Restoration of the Herring River Marsh, Wellfleet, MA. Report to Cape Cod National Seashore, Town of Wellfleet and Association of Women Geoscientists. 63 p.

Fitterman, D.V., G.A. Brooks, and S.L. Snyder. 1989. Geophysical Investigation of Depth to Saltwater near the Herring River (Cape Cod National Seashore), Wellfleet, Massachusetts, U.S. Geological Survey Open-File Report 89-677.

Fitterman, D.V., K.F. Denehy. 1991, Verification of Geophysically Determined Depths to Saltwater near the Herring River (Cape Cod National Seashore), Wellfleet, Massachusetts, U.S. Geological Survey Open-File Report 91-321.

Fredsoe, J. and R. Deigaard. 1992. Mechanics of Coastal Sediment Transport. World Scientific, New Jersey, 392 pp.

Hamrick, J. M. 1992. A Three-Dimensional Environmental Fluid Dynamics Computer Code: Theoretical and Computational Aspects. The College of William and Mary, Virginia Institute of Marine Science. Special Report 317, 63 pp.

Hamrick, J. M. 1994. Linking Hydrodynamic and Diogeochemical Transport Models for Estuarine and Coastal Waters. *Estuarine and Coastal Modeling, Proceedings of the 3rd International Conference*, M. L. Spaulding *et al*, Eds., American Society of Civil Engineers, New York, 591-608.

Hamrick, J.M. 1996. A User's Manual for the Environmental fluid Dynamics Computer Code. The College of William and Mary, Virginia Institute of Marine Science. Special Report 331, 185 pp.

Harvey, T. Y. 2010. The Herring River Tidal Restoration Project from a Scientific and Social Perspective: A Baseline Study and Analysis of Sedimentological Parameters in the Herring River Estuary, Cape Cod National Seashore, Wellfleet, MA. Unpublished undergraduate honors thesis, Wellesley College, Wellesley, MA.

IPCC, 2007. Climate Change 2007: The Physical Science Basis, Contrigutions of Working Group I to the Fougrh assessment Report of the Intergovernm,ental Panel on Climate Change. Solomon, S., D. Qin, M. Manning, Z. Chen, M. Marquis, K.B. Averty, M.Tignor and H.L. Miller (eds.). Cambridge University Press. Cambridge, United Kingdo, and New York, NY, USA 996 pp.

Knauss, John A. 1978. Introduction to Physical Oceanography. New Jersey: Prentice-Hall, Inc.

Leendertse, J. J. 1987. Aspects of SIMSYS2D A System for Two Dimensional Flow Computations. Prepared for USGS.

Martin, L. 2004. Salt Marsh Restoration at Herring River: An Assessment of Potential Salt Water Intrusion in Areas Adjacent to Herring River and Mill Creek, Cape Cod National Seashore. Technical Report NPS/NRWRD/NRTR-2004/319.

Martin, L. 2007. Identification of Private Wells Adjacent to the Herring River Flood Plain that Could be Affected by Restoration of Tidal Flow, Memorandum to John Portnoy September 4, 2007.

Masterson, J.P. 2004. Simulated Interaction Between Freshwater and Saltwater and Effects of Ground-water Pumping and Sea-level change, Lower Cape Cod Aquifer System, Massachusetts: U.S. Geological Survey Scientific Investigations Report 2004-5014, 72 p.

Masterson, J.P. and J.W. Portnoy. J.W. 2005. Potential Changes in Ground-water Flow and Their Effects on the Ecology and Water Resources of the Cape Cod National Seashore, Massachusetts, U.S. Geological Survey General Information Product 13 June 2005.

NRC, 1987. National Research Council Responding to Changes in Sea level: Engineering Implications. National Academy Press, Washington, D.C.

Nuttle W.K. 1990. Extreme Values of Discharge for Mill Creek and Options to Control Flooding from the Herring River, Report to National Park Service Cape Cod National Seashore.

Portnoy, J.W. 1984. Salt Marsh Diling and Nuisance Mosquito Production on Cape Cod, Massachusetts. J. Amer. Mosq. Cont. Assoc. 44:560-564.

Portnoy, J.W., C.T. Roman, and M.A. Soukup. 1986. Hydrologic and Chemical Impacts of Diking and Drainage of a Small Estuary (Cape Cod National Seashore): Effects on Wildlife and Fisheries, Manuscript Submitted for Publication in the Proceedings of "A Symposium on Waterfowl and Wetlands Management in the Coastal Zone of the Atlantic Flyway." Wilmington, DE. September 16-19, 1986, 254-265.

Portnoy, J.W. and A.E. Giblin. 1997. Effects of Historic Tidal Restrictions on Salt Marsh Sediment Chemistry, Biogeochemistry, 36:275-303.

Portnoy, J.W. 1999. Salt Marsh Diking and Restoration: Biogeochemical Implications of Altered Wetland Hydrology, Environmental Management, 24:111-120.

Portnoy, J. W., C. T. Roman, S. M. Smith, and E. Gwilliam, 2003. Estuarine Habitat Restoration at Cape Cod National Seashore: the Hatches Harbor Prototype. Park Science, 22, 51-58.

Portnoy, J.W. and J.R. Allen. 2006. Effects of Tidal Restrictions and Potential Benefits of Tidal Restoration on Fecal Coliform and Shellfish-water Quality, J. Shellfish Research, 25:609-617.

Roman, C. T. 1987. An Evaluation of Alternatives for Estuarine Restoration Management: The Herring River Ecosystem (Cape Cod National Seashore). Technical Report. National Park Service Cooperative Research Unit, Rutgers University, New Brunswick, New Jersey

Roman, C.T., R.W. Garvine, and J.W. Portnoy. 1995. Hydrologic Modeling as a Predictive Basis for Ecological Restoration of Salt Marshes, Environmental Management, 19:559-566.

Ryskin, G. and L. G. Leal. 1983. Orthogonal Mapping. *J. Comp. Phys.*, 50, 71-100.

Shields, I.A. 1936. Application of similarity principles and turbulence research to bed-load movement (in German). Mitteilunden der Presoss. Versuchsanst. Fur Wasserbau and Schiffbau, Berlin, No. 26.

Singh, V. P., 1992. Elementary Hydrology. Prentice-Hall Inc., Upper Saddle River, NJ.

Smagorinsky, J. 1963. General circulation experiments with the primitive equations, I. The basic experiment. *Mon. Weather Rev.*, 91, 99-164.

Soulsby, Richard. 1997. Dynamics of Marine Sands. Thomas Telford, Publications, London, England.

Spaulding, M.L. and A. Grilli. 2001. Hydrodynamic and Salinity Modeling for Estuarine Habitat Restoration at Herring River, Wellfleet, Massachusetts. The University of Rhode Island, submitted to the National Park Service.

Spaulding, M.L. and A, Grilli. 2005. Simulations of Wide Sluice Gate Restoration Option for Herring River. Report to NPS. 12 p.

U.S. Army Corps of Engineers. 1988. Tidal Flood Profiles New England Coastline, September 1988.

U.S. Environmental Protection Agency. 1990. Technical Guidance Manual for Performing Waste Load Allocations, Book III Estuaries, Part 2, Application of Estuarine Waste Load Allocation Models. EPA 823-R-92-003.

USACE. 2009. Water Resource Policies and Authorities Incorporating Sea-level Change Considerations in Civil Works Programs. Department of the Army, U.S. Army Corps of Engineers, Washington DC 20314-1000. Engineering Circular No. 1165-2-211.

USACE, 2011. Sea-level Change Considerations for Civil Works Programs. Department of the Army, U.S. Army Corps of Engineers, Washington DC 20314-1000. Engineering Circular No. 1165-2-212.

Woods Hole Group 2006, Review of "Hydrodynamic and salinity modeling for estuarine habitat restoration at Herring River, Wellfleet, Massachusetts" Final Report, Prepared for Conservation Law Foundation 13 p.

Zimmerman, J.T.F. 1988. Hydrodynamics of Estuaries. Boca Raton, FL: CRC Press, Inc.

Woods Hole Group, Inc.
81 Technology Park Drive
East Falmouth, MA 02536

Tel: (508) 540-8080
Fax: (508) 540-1001
Web: www.woodsholegroup.com

Houston Office
10615 Shadow Wood Drive, Ste 100
Houston, TX 77043-2844
Tel: (713) 468-5075
Fax: (713) 468-1115

Delaware Office
100 Carlson Way, Suite 9
Capital City Business Park
Dover, DE 19901-2365
Tel: (302) 734-1434
Fax: (302) 734-1434

Woods Hole Group do Brasil
Servicos em Oceanografia
Rua Luiz Paulistano, 430 ap 102
Recreio dos Bandeirantes
Rio De Janeiro – RJ 22795-455
Tel 1: 55 21 2135 3671
Tel 2: 55 21 2135 3647